Anthropization of a semiarid Mediterranean multi-layer aquifer system (Campo de Cartagena, SE Spain) : hydrodynamic, geochemical and isotopic approaches

Paul Baudron

THÈSE
Pour obtenir le grade de

Docteur de
Systèmes intégrées en Biologie, Agronomie, Géosciences, Hydrosciences et Environnement

Spécialité : Eaux Continentales et Sociétés

Présentée et soutenue publiquement par

Paul BAUDRON

le 11 juillet 2013

Anthropisation d'un système aquifère multicouche méditerranéen (Campo de Cartagena, SE Espagne). Approches hydrodynamique, géochimique et isotopique.

Travail réalisé à :
-IRD, UMR G-EAU, Montpellier,
- IGME, Murcie, Espagne
- INUAMA, Univ. Murcie, Espagne

Devant le jury :

Mr Juan José Duran Valsero	Directeur, Direction de la recherche et de prospective scientifique, IGME	Rapporteur
Mr José Benavente Herrera	Professeur, Université de Grenade	Rapporteur et Président du jury
Mr Christian Leduc	Directeur de recherche, IRD	Co-directeur de thèse
Mr Florent Barbecot	Professeur, Université du Québec à Montréal	Examinateur
Mr Séverin Pistre	Professeur, Université de Montpellier 2	Examinateur

Preface

The present research was conducted within the framework of the project “Modelación Hidrológica en Zonas Semiáridas”, funded by the Ministry of Agriculture and Water (Consejería de Agricultura y Agua) of the Región of Murcia and coordinated by the Euromediterranean Water Institute Foundation (F-IEA). It was part of the sub-project “Investigación Hidrogeológica en Zonas Semiáridas” carried out by the Institute of Water and Environment (INUAMA) of the University of Murcia. This research was also partly conducted within the “CARTAG-EAU” project funded by the French “SICMED-MISTRALS” initiative. Additional financial support was provided by F-IEA through two projects called “Estimación de la Descarga Submarina al Mar Menor mediante isótopos del Ra-Rn” and “Caracterización de los acuíferos del Campo de Cartagena mediante técnicas isotópicas” that allowed complementary analyses.

Scientific and management activities were supervised by my advisers Dr. José Luis García Aróstegui at the Murcia office of the Geological Survey of Spain (IGME), Dr. Christian Leduc at the Institute for Research and Development (IRD) as a researcher of the G-EAU Research Unit in Montpellier, France, and Dr. Melchor Senent at the aforementioned INUAMA of the University of Murcia. The first year of this PhD corresponds to the definition of research axes, setup of field site, contact with project partners, building of collaboration agreements, writing of project proposals and organization of fieldwork. In addition, a large fieldwork task was performed, even if not all results are included in this manuscript.

Because of the high level of equipment and knowledge needed for the three main chapters of this thesis, their realization was based on partnerships with a series of institutions, detailed in the introduction, whose researchers played a key advisory role.

Acknowledgements

First, I would like to thank my advisers Melchor Senent Alonso, Jose Luis García Aróstegui and Christian Leduc for offering me the opportunity to develop these investigations in semiarid hydrogeology. This thesis would never have been possible without their unconditional logistical, scientific and moral support, together with their confidence in my decisions conducting this thesis. I would need a full page, not a few lines, to describe not only their contribution to my training, but also all the nice moments we shared.

Most experiments would not have been possible without the financial support of the IEA, and the interest of his director Francisco Cabezas Calvo-Rubio whom I would like to acknowledge specifically.

The experiments developed in this project were conducted together with the following institutions that I would like to thank: Univ. of Murcia (INUAMA), Univ. of Paris XI-Orsay (UMR IDES), Univ. of Aix-Marseille (UMR CEREGE), Polytechnical Univ. of Cartagena (UPCT), Univ. of Avignon (UMR EMMAH) and IRD (UMR HSM).

First, I would like to highlight the role of Florent Barbecot (IDES, now Univ. of Montreal), whose guidance was determinant for the realization of the isotopic tracing in groundwater. This chapter was also notably enhanced through scientific discussions with Christelle Marlin (IDES), Yves Travi (EMMAH), Jean-Denis Taupin (HSM) and Marina Gillon (EMMAH). The Random Forest investigation was guided by Francisco Alonso Sarria (INUAMA), whose expertise and ideas were fundamental. The investigation of submarine groundwater discharge was the fruit of a large collaboration with Christelle Claude (CEREGE), Javier Gilabert (UPCT), Olivier Radakovitch (CEREGE), Sabine Cockenpot (CEREGE), Francisco Lopez Castejón (UPCT) and Adriano Mayer (EMMAH). David Martinez Vicente (IEA) contributed to most of these works. I also would like to thank Eilon Adar (Univ. Ben Gurion, Israel) for his welcome in Israel and the intense work we conducted on the Mixing Cell Model, although it is not included in this thesis.

The kind support of Joëlle Lopez, José Plácido Mendez Perez and Charo Sauria for administrative work was indispensable. Christine Legrand was incredibly smart regarding my absent-mindedness regarding administrative aspects.

Acknowledgements

Field work in Murcia was conducted with the assistance of Juan Guerra (IEA). I am thankful to the researchers, technicians and students of the following institutions, who performed laboratory analysis: Nicolas Patris and Sandra VanExter at HSM (stable isotopes of water, inorganic ions), Aurélie Noret and Gael Monvoisin at IDES (^{13}C and ^{14}C), Milanka Babic at EMMAH (Br/Cl and ^{3}H), Sabine Cockenpot at CEREGE (^{222}Rn, ^{223}Ra, ^{224}Ra, ^{226}Ra), and the UPCT team (continuous nitrate analyses, electrical conductivity, chlorophyll and turbidity inside the Mar Menor Lagoon, inorganic ions in groundwater).

I greatly appreciated the nice atmosphere in Murcia with all the team. In addition to David Martinez-Vicente with whom I shared so much, I would like to thank Francisco Gomariz Castillo, Toñi Morales, Angel Perni, Charo Sauria, Francisco Pellicer, Paqui Guerrero, Angel Garcia, María Antonieta Fernandez. In Montpellier, I appreciated the friendly team spirit between PhD students, especially Marina Alazard, with whom I enjoyed sharing both hard and happy moments; without forgetting Carla Manciati, Ahmed Salem, Andrew Ogilvie and the communicative nice mood of Maxime Thibon. I enjoyed the atmosphere in Orsay. To cite some, Aurélie Noret and her great cakes, Gael Monvoisin and his nice music, Pierre Lepape, Sebastien Leilbrandt, Senda Zarrouck, Stérenn Ramond, Céléstine Delbard, Delphine Jouvin…

Great thanks to my family and friends, who supported me during these years, with my repetitive "I can't come, I have to work". Conducting this thesis was a very special moment for me, and it would not have been possible without their support and patience. Some of you even directly participated in this work, like Chema and Belén, who accompanied me at field work or Adrien and Golshanak who hosted me, in incredible conditions, during long weeks in Montpellier. These years counted with the great atmosphere in "Bacon Bridge", the nice mood of the Caravaca people, the support from the Chevreuse valley people, the great times with the Granada people (and the kids), the Berlin people… Thanks to all.

.

Table of contents

List of Figures

List of Tables

Abstract

The Campo de Cartagena area in the Murcia region (SE Spain) is an emblematic case and an extreme illustration of the hydrological and environmental changes caused by the intensive use of groundwater for agriculture in semiarid Mediterranean areas. Historically called “the Desert of Murcia”, it now represents one the most productive agricultural areas of the country. In the absence of surface water, the agricultural development was based on the use of groundwater from the underlying multi-layer aquifer system, leading to the overexploitation of the deeper layers, while irrigation return flow and the subsequent increased recharge rates caused the increase of water table levels in the unconfined aquifer. In addition, a large number of boreholes of the area are screened in several aquifers and allow an artificial connection between different groundwater masses. Moreover, as a consequence of the water table increase in the shallow aquifer, a permanent flow appeared in the last kilometres of the surface watershed. Together with the uncontrolled release of brines from private groundwater desalination, it induced a permanent surface flow of water to the main outlet of the system, the Mar Menor lagoon. In this context, understanding the complex evolution of the whole system and how the hydric balance is affected is a hard task.

Three main aspects are treated in this dissertation, following three research focuses: i) the review of existing data, and the development of a statistical tool for optimizing large geochemical datasets in multi-layer aquifer systems, ii) the quantitative and qualitative assessment of the evolution of recharge rates as a consequence of the development of agriculture with the help of environmental tracers and iii) the study of submarine groundwater discharge in the context of a highly anthropized watershed with radon and radium isotopes.

The first research focus represented a wide bibliographic task in order to collect nearly all information on the evolution of the aquifers (e.g. archaeological reports, old newspapers, first reports from the Spanish Geological survey IGME, modern measurements and water analyses). The evolution along one century of the multi-layer aquifer system could be partly reconstituted, highlighting the inversion of the vertical hydraulic gradient between the upper aquifers and the decrease of water table levels by more than 500 m in the last century for the deepest aquifer level. As well, the new inventory of tubewells showed that many previous

studies misinterpreted the piezometric and geochemical time-series by mistaking aquifer corresponding to each tubewell. This difficult assessment of the origin of groundwater samples in large datasets from complex multi-layer aquifers as in the Campo de Cartagena was identified as a major limitation for a reliable interpretation of geochemical results.

A method was therefore developed based on a supervised classification method, the Random Forest (RF) machine learning technique, to identify the layer from where groundwater samples were extracted. The classification rules were based on the major ion content of water samples. Despite the availability of 40 years of chemical and water table time series, only a limited fraction of the sampled tubewells included a reliable determination of the borehole design and, consequently, of the aquifer layer being exploited. Added difficulty was the very similar compositions of water samples extracted from different aquifer layers. Moreover, not all groundwater samples included the same geochemical variables. Despite the difficulty of such a background, the Random Forest classification reached an accuracy over 90%. These results were much better than the Linear Discriminant Analysis (LDA) and Decision Trees (CART) supervised classification methods. From a total of 1549 samples, 805 (52%) came from one unique identified aquifer, 409 (26%) proceeded from a possible blend of waters from several aquifers and 335 (22%) were of unknown origin. Only 468 of the 805 unique-aquifer samples included all the chemical variables that were needed to calibrate and validate the models. Finally, 107 groundwater samples of unknown origin and featuring a complete set of variables could be classified.

The second research axis was motivated by the difficulty to update the hydric balance of the multi-layer aquifer when irrigation return flow represents an additional source of recharge, added to the limited rainfall infiltration. Environmental tracers (^{14}C, ^{13}C, ^{2}H, ^{18}O, ^{3}H) were combined to high-resolution temperature loggings to investigate the long-term evolution of recharge in the Campo de Cartagena aquifer system once identified in situ the depth of origin of groundwater.

Despite the complex background, this methodology allowed a reliable interpretation of environmental tracers and provided a better understanding of the groundwater flow patterns. The tritium method did not give good quantitative results because of the high variability of the recharge signal but remained an excellent indicator of recent recharge. Nonetheless, both pre-anthropization and post-anthropization recharge regime could be identified and quantified

by radiocarbon. Before the development of agriculture, recharge varied from 17 $mm.a^{-1}$ in the mountain ranges to 6 $mm.a^{-1}$ in the plain, for a mean annual rainfall is over 300 mm. In response to the increase of agricultural activity, recharge fluxes to the plain were amplified and nowadays reach up to 210 $mm.a^{-1}$ in irrigated areas. These values are strengthened by global water budget and local unsaturated zone studies.

The third research axis consisted in quantifying submarine groundwater discharge (SGD) with radionuclides in this uncommon context where additional sources of radionuclides were supposed to be carried by the surface water network. In order to quantify SGD and decipher the influence of the different water sources on the Mar Menor, a radon (^{222}Rn) and radium (^{223}Ra, ^{224}Ra) survey was combined with the hydrodynamic modeling of the lagoon.

The areas of influence of the plume of radionuclides from the river were identified, the main areas of SGD were located and a location for a submarine emissary was proposed. Groundwater from underlying sediments was selected as the best representative SGD end member, compared to groundwater sampled from piezometers. Mass balances in winter and summer seasons provided yearly SGD fluxes of water of 7.2-15.9 10^8 $m^3.a^{-1}$ (^{222}Rn), 21.9-44.7 10^8 $m^3.a^{-1}$ (^{224}Ra) and 6.9 10^8 $m^3.a^{-1}$ (^{223}Ra, measured in winter only). The difference between values for ^{222}Rn was explained by the different temperature and wind conditions. Water level effect, rather than tidal pumping, was identified as the main driver for recirculated saline groundwater, while fresh submarine groundwater discharge from the aquifer was about 1% of total SGD.

As the this case study is an extreme case of anthropization, these results present a wide interest that is not limited to the Murcia region or the Campo de Cartagena aquifer. Around the semiarid Mediterranean Sea, most hydrosystems have been heavily disturbed by human activities and many aquifers are already overexploited. The methods developed in this thesis might also be used in other Mediterranean sites where groundwater exploitation seems to follow a continuous and inevitable increase.

Résumé

Situé au SE de l'Espagne, le Campo de Cartagena est un cas emblématique extrême des changements hydrologiques et environnementaux causés par l'utilisation intensive des eaux souterraines pour l'agriculture dans les zones semi-arides du pourtour méditerranéen. Historiquement appelée « le désert de Murcie », cette région est aujourd'hui l'une des zones agricoles les plus productives du pays. En l'absence de ressources en eau de surface, le développement agricole s'est basé sur l'utilisation des eaux souterraines, entraînant la surexploitation des horizons les plus profonds de l'aquifère multicouche, tandis que l'augmentation de la recharge liée au retour d'irrigation cause une remontée des niveaux dans la nappe superficielle libre. Un grand nombre de forages multi-crépinés permettent une connexion artificielle entre les différents aquifères, et donc un possible transfert de contaminants d'origine agricole depuis la nappe superficielle vers les nappes profondes. Suite à la montée des niveaux piézométriques dans la nappe superficielle, un débit permanent est maintenant observé dans les derniers kilomètres du réseau hydrographique. S'y ajoutent les rejets incontrôlés de saumures issues d'usines privées de désalinisation d'eau souterraine, aboutissant eux aussi à l'exutoire du système, la lagune de la Mer Mineure. Dans ce contexte, comprendre la complexité de l'évolution du bilan hydrique est un enjeu scientifique majeur.

Trois principaux aspects sont traités dans cette thèse, suivant trois axes de recherche : i) la réinterprétation de données historiques, hydrogéologiques ou non, afin de reconstituer l'évolution récente du système, accompagnée de la mise en oeuvre d'un outil statistique pour déterminer l'origine d'échantillons géochimiques ; ii) l'étude quantitative de l'évolution de la recharge et des processus de mélange, en conséquence du développement agricole, à l'aide de traceurs environnementaux et iii) l'étude de la décharge sous-marine d'eau souterraine et la localisation des perturbations anthropiques depuis le réseau hydrique de surface en combinant le radon et le radium avec une modélisation hydrodynamique de la lagune.

Le premier axe de recherche a comporté une large tâche bibliographique pour rassembler toutes les informations sur l'évolution des aquifères, issues de sources aussi variées que des études archéologiques, des journaux anciens, les premiers rapports de l'Institut Géologique Espagnol (IGME) mais également des analyses, mesures et observations récentes. L'évolution du système aquifère multicouche au cours du siècle passé a ainsi été

partiellement reconstituée, mettant en évidence l'inversion des gradients hydrauliques entre les trois premiers aquifères et une baisse de plus de 500 m dans la nappe la plus profonde.

En complément, un nouvel inventaire des forages basés sur la révision des données techniques disponibles et sur des enquêtes de terrain a montré qu'un nombre important d'études antérieures a pu mal interpréter les chroniques de piézométrie et de géochimie. En effet, les déterminations de l'aquifère correspondant à chaque forage sont, lorsqu'elles existent, souvent en partie erronées. Malgré la disponibilité de 40 ans de chroniques piézométriques et géochimiques, il est rare de trouver les descriptions techniques complètes des forages, ce qui limite les possibilités d'interprétation. Ainsi, sur un total de 1549 échantillons, 805 (52%) ont révélé correspondre à un aquifère unique, 409 (26%) provenir d'un mélange entre plusieurs aquifères tandis que 335 (22%) étaient d'origine inconnue. Dans ce contexte, la difficile détermination de l'origine des échantillons d'eau souterraine provenant de bases de données officielles représente une difficulté majeure pour une interprétation fiable des données géochimiques et piézométriques.

Une méthode reposant sur la méthode d'apprentissage automatique Random Forest a donc été mise en œuvre afin d'identifier l'aquifère d'origine d'échantillons d'eau souterraine. Bien que communément utilisée dans d'autres domaines comme la médecine ou la télédétection, cette méthode n'avait encore jamais été employée en hydrogéologie. Elle appartient à la famille des méthodes de classification supervisées, qui permettent d'identifier l'origine d'un échantillon inconnu, une fois calé un modèle à partir d'échantillons d'apprentissage. Les règles de classification du modèle sont basées sur la composition en ions majeurs des échantillons d'apprentissage, malgré les difficultés d'application de cette approche dans ce contexte caractérisé par i) la forte similarité de la composition chimique des échantillons représentatifs des différents aquifères et ii) la forte disparité des éléments chimiques analysés dans chaque échantillon. En l'occurrence, seulement 468 des 805 échantillons représentatifs d'un unique aquifère possédaient les déterminations nécessaires pour le calage et la validation du modèle. Dans ce contexte difficile, le modèle Random Forest a atteint un taux d'exactitude de 90%, bien supérieur aux autres méthodes de classification supervisée que sont l'Analyse Discriminante Linéaire (LDA) ou les arbres de décision (CART). Ce résultat a même été amélioré jusqu'à près de 95% grâce à l'identification et l'élimination des échantillons les moins fiables et des variables les moins

utiles. Finalement, 107 échantillons d'origine inconnue présentant toutes les variables nécessaires ont été classifiés.

Le deuxième axe de recherche a été motivé par la difficulté d'actualiser le bilan hydrique du système aquifère, où le retour d'irrigation s'ajoute à l'infiltration des précipitations comme source de recharge de la nappe superficielle. Des traceurs environnementaux (^{14}C, ^{13}C, ^{2}H, ^{18}O, ^{3}H) ont été employés pour caractériser l'évolution à long terme de la recharge des nappes supérieures et les principaux processus de mélanges. L'échantillonnage géochimique a été complété par des profils de température de haute résolution réalisés au sein des forages, avant et durant le pompage. Ils ont démontré leur utilité pour identifier in situ la profondeur d'origine des eaux souterraines. De plus, ils ont apporté de précieuses informations sur les processus de mélange au sein des forages, mettant notamment en évidence les échanges entre différentes masses d'eau lorsque le forage est au repos.

L'analyse des ions majeurs a confirmé les résultats de la révision des données anciennes : la très proche minéralisation des trois nappes supérieures et la forte variabilité en solides dissous dans des eaux du Quaternaire. Néanmoins, les isotopes stables de l'eau ont permis de différencier les eaux de la nappe supérieure ($\delta^{18}O > -5.5‰$ vs VSMOW) de celles des nappes profondes ($\delta^{18}O < -5.5‰$ vs VSMOW). Ils ont également permis de mettre en évidence des effets d'évaporation, d'altitude et de fluctuations climatiques. La combinaison des différents traceurs géochimiques a ensuite permis de développer l'étude des processus de mélange à une échelle locale (à l'intérieur du forage) ou régionale (au sein des aquifères).

La forte variabilité du tritium dans les eaux d'irrigation (entre 0 et 80 UT), et donc dans le signal de recharge, n'a pas permis de quantifier précisément les temps de résidence des eaux modernes. L'identification des échantillons correspondant à une recharge ancienne (pré-anthropisation) ou à une recharge moderne (post-anthropisation) est basée sur le radiocarbone, une fois appliqué un coefficient de correction des temps de résidence dans les deux gammes d'âge. Finalement, des taux de recharge de 17 $mm.an^{-1}$ dans les zones montagneuse et de moins de 10 $mm.an^{-1}$ en plaine ont été calculés pour la phase pré-anthropisation. Puis, en réponse à la mise en place de l'activité agricole dans la plaine, des flux de recharge atteignant aujourd'hui jusqu'à 210 $mm.an^{-1}$ y ont été mis en évidence.

Le troisième axe de recherche est la quantification de la décharge sous-marine d'eau souterraine (SGD) vers la lagune de la Mer Mineure à l'aide des isotopes du radon (^{222}Rn) et du radium (^{223}Ra, ^{224}Ra). Basée sur le bilan des flux entrants et sortants dans la lagune, cette méthode s'utilise généralement dans des contextes où les activités des sources autres que les eaux souterraines sont négligeables par rapport à ces dernières, et ont donc un faible impact sur le bilan et sur la distribution spatio-temporelle des traceurs. Or, le contexte du Campo de Cartagena est inhabituel du fait de l'apport de grandes quantités de ces traceurs via le réseau de surface de la Rambla del Albujón et des rejets sauvages. Les mesures de traceurs ont donc été combinées à une modélisation hydrodynamique de la lagune pour comprendre l'impact de ces apports.

En comparant les valeurs mesurées et modélisées, la principale zone d'influence du panache de radionucléïdes de la rambla a pu être identifiée, restant la majorité du temps à une faible distance de la côte. Les principales zones de SGD ont également été localisées, dans des secteurs où les hautes valeurs mesurées ne pouvaient pas être justifiées par le panache de la rambla. De même, des rejets de saumure ont été localisés dans zones très restreintes à hautes activités observées sporadiquement.

Une difficulté récurrente dans la réalisation de ce type de bilan est la détermination de la composition de l'eau souterraine douce issue de la nappe. La grande majorité des auteurs considère arbitrairement une valeur moyenne à partir d'échantillons prélevés dans des piézomètres proches de la frange côtière. Néanmoins, dans ce travail, un calcul simple a démontré que l'eau porale des sédiments couvrant le fond de la lagune avait une composition nettement plus représentative, permettant donc un calcul de SGD plus fiable. Finalement, les bilans de masse en été et en hiver aboutissent à des flux de SGD de l'ordre de 7.2 à15.9 10^8 $m^3.an^{-1}$ (^{222}Rn), 21.9-44.7 10^8 $m^3.an^{-1}$ (^{224}Ra) et 6.9 10^8 $m^3.an^{-1}$ (^{223}Ra, mesuré en hiver seulement). La différence entre les deux valeurs obtenues avec ^{222}Rn a été expliquée par des conditions météorologiques différentes (température et vent). L'effet de la variation du niveau de la mer, plus que l'effet des marées généralement considéré, a été identifié comme le moteur de la recirculation d'eau salée, tandis que la décharge d'eau douce souterraine issue de la nappe a été évaluée à 1% des SGD totales.

Cette étude d'un cas extrême d'anthropisation présente un large intérêt bien au-delà du système aquifère multicouche du Campo de Cartagena ou de la région de Murcie. En effet,

sur le pourtour méditerranéen semi-aride, la plupart des hydrosystèmes sont lourdement impactés par les activités humaines et de nombreux aquifères sont d'ores et déjà surexploités. Les méthodes mises en place dans cette thèse pourront ainsi être appliquées dans d'autres sites méditerranéens où l'exploitation de l'eau souterraine suit une évolution comparable, continue et apparemment inexorable.

Resumen

Localizado en el sureste de España, el Campo de Cartagena es un caso paradigmático de modificaciones hidrológicas y ambientales relacionadas con el uso intensivo de aguas subterráneas para regadío en zonas semiáridas del Mediterráneo. Históricamente calificada como "el desierto de Murcia", esta región se ha convertido en una de las zonas agrícolas más productivas del país. Teniendo en cuenta la ausencia de recursos hídricos superficiales, el desarrollo agrícola se ha basado desde su inicio en el uso de las aguas subterráneas. A medida que se incrementaban las necesidades de agua para regadío, se perforaban tramos cada vez más profundos del acuífero multicapas, y, paralelamente se producía un aumento de la recarga por retorno de riego con la consiguiente subida de los niveles piezométricos en el acuífero superior. El gran número de sondeos ranurados en todos los tramos permeables atravesados permite una conexión artificial entre los distintos acuíferos, y por lo tanto una posible transferencia de contaminantes de origen agrícola desde el acuífero superior hacía los más profundos. A raíz de la subida de los niveles en el acuífero superior, un caudal permanente ha aparecido en el curso bajo de la red hidrográfica (fundamentalmente rambla del Albujón), al que se suman los rechazos de desaladoras privadas de agua subterránea, confluyendo todo ello en la laguna del Mar Menor. En este contexto, la comprensión de la compleja evolución del sistema hídrico es un reto científico de primer orden.

En esta Tesis Doctoral se han tratado tres aspectos principales o ejes de investigación: i) la reinterpretación de datos históricos de diferente índole para reconstruir la evolución reciente del sistema hídrico, acompañada por el desarrollo de una herramienta estadística para determinar el origen de muestras hidrogeoquímicas; ii) el estudio mediante trazadores ambientales de la evolución de la recarga a los acuíferos y de los procesos de mezcla como consecuencia del desarrollo agrícola, y iii) el estudio de la descarga submarina de agua subterránea y la localización de perturbaciones antrópicas desde la red hídrica de superficie mediante el empleo combinado de radón y radio, y la modelización hidrodinámica de la laguna.

El primer eje de investigación ha supuesto una importante tarea bibliográfica de recopilación de todo tipo de información acerca de la evolución de los acuíferos, procediendo de fuentes tan variadas como estudios arqueológicos, hemerotecas (años 1850 a 1950),

fondos documentales históricos del IGME, así como análisis químicos, medidas y observaciones recientes. La evolución del sistema acuífero multicapa pudo ser parcialmente reconstituida, evidenciando la inversión de los gradientes hidráulicos verticales entre los tres primeros acuíferos y una bajada de más de 500 m en el acuífero más profundo.

En complemento, un nuevo inventario de los sondeos basado en la revisión de datos técnicos disponibles y en encuestas de campo ha mostrado que un importante número de estudios anteriores ha podido malinterpretar algunas evoluciones piezométricas e hidrogeoquímicas. De hecho, las determinaciones del acuífero de procedencia de las aguas de cada sondeo son, cuando existen dado el carácter privado de los sondeos, a menudo parcialmente erróneas. A pesar de la disponibilidad de más de 40 años de crónicas piezométricas e hidrogeoquímicas, se encuentran pocas veces las descripciones técnicas de los sondeos, lo que limita las posibilidades de interpretación. Como resultado, de un total de 1549 muestras, 805 (el 52%) revelaron proceder de un acuífero único, 409 (el 26%) proceder de una mezcla entre varios niveles acuíferos mientras 335 (el 22%) tenían un origen desconocido. En este contexto, la difícil determinación del origen de las muestras de agua subterránea procediendo de bases de datos oficiales representa una dificultad de mayor orden para una interpretación fiable de los datos químicos del agua y de los niveles piezométricos. Una metodología basada en el método de aprendizaje automático Random Forest, más empleada en otros campos de la ciencia como la medicina o teledetección, ha sido desarrollada para identificar el acuífero de origen de muestras de agua subterránea. Este método nunca había sido empleado en hidrogeología. Se trata de un método de clasificación supervisado que permite identificar el origen de una muestra desconocida una vez calibrado un modelo a partir de muestras de aprendizaje. Las reglas de clasificación del modelo se basan en la composición en iones mayoritarios de las muestras de aprendizaje, a pesar de las dificultades de aplicación de este método en un contexto caracterizado por: i) la fuerte similaridad de la composición química de las muestras representativas de los diferentes acuíferos y ii) la fuerte disparidad de los elementos químicos analizados en cada muestra. En este caso, solamente 468 de las 805 muestras representativas de un único acuífero poseían las determinaciones necesarias para el calibrado y la validación del modelo. En este difícil contexto, el modelo Random Forest alcanzó una exactitud del 90%, muy superior a otros métodos de clasificación supervisada que son el Análisis discriminante lineal (LDA) o los árboles de clasificación (CART). Estos resultados aún se pudieron mejorar hasta casi un 95%

gracias a la identificación y la eliminación de las muestras menos fiables y de las variables menos útiles. Finalmente, se clasificaron 107 muestras de origen desconocido que presentaban todas las variables necesarias.

El segundo eje de investigación estuvo motivado por la dificultad de actualizar el balance hídrico del sistema acuífero, donde el incierto retorno de riego se suma a la infiltración de las precipitaciones como fuente de recarga del acuífero superficial. En este caso se emplearon trazadores ambientales (^{14}C, ^{13}C, ^{2}H, ^{18}O, ^{3}H) con el objetivo de caracterizar la evolución a largo plazo de la recarga de los acuíferos y de los principales procesos de mezcla. El muestreo hidrogeoquímico fue completado con perfiles de temperatura de alta resolución realizados dentro de los mismos sondeos, antes de y durante el bombeo. Éstos últimos demostraron su utilidad para la identificación in situ de la profundidad de origen de las aguas subterráneas, y, además, aportaron información sustancial sobre los procesos de mezclas en el seno de los sondeos, con especial foco en los intercambios entre varias masas de agua cuando el sondeo está en reposo.

La interpretación de los iones mayoritarios ha confirmado, en líneas generales, los resultados de la revisión de datos antiguos, es decir una mineralización muy parecida en los tres primeros acuíferos y una alta variabilidad en el total de sólidos disueltos en las aguas del Cuaternario. Sin embargo, los isótopos estables del agua permiten diferenciar las aguas del acuífero superior ($\delta^{18}O > -5.5‰$ vs VSMOW) de las de los acuíferos profundos. También pueden observarse los efectos de evaporación, de altitud y las fluctuaciones climáticas. La combinación de distintos trazadores geoquímicos ha permitido desarrollar el estudio de los procesos de mezcla a escala local (interior del sondeo) y regional (dentro de los acuíferos).

Dada la alta variabilidad del tritio en las aguas de riego (entre 0 y 80 UT), y en la señal de recarga, no se ha logrado una cuantificación precisa de los tiempos de residencia de las aguas modernas. La identificación de las muestras correspondientes a una recarga antigua (pre-antropización), o a una recarga moderna (post-antropización), se ha basado en el radiocarbono, una vez aplicado un coeficiente de corrección de los tiempos de residencia en ambas gamas de edad. Finalmente, se han obtenido una tasas de recarga para la fase pre-antropización de 17 mm/año en las zonas más elevadas e inferiores a 10 mm/año en la zona de llanura. Como respuesta al desarrollo de la actividad agrícola en la llanura, las tasas de recarga obtenidas presentan valores muy superiores a los anteriores, unos 210 mm/año.

El tercer eje de investigación ha consistido en la cuantificación de la descarga submarina de agua subterránea (SGD) hacía la laguna del Mar Menor mediante la aplicación de isótopos del radón (^{222}Rn) y radio (^{223}Ra, ^{224}Ra), basados en el balance de los flujos de entrada y salida de la laguna. Este método se utiliza generalmente en contextos donde las actividades de fuentes distintas de las aguas subterráneas son despreciables frente a esas, y por lo tanto tienen un impacto limitado en el balance y en la distribución espacio-temporal de los trazadores. Sin embargo, el contexto del Campo de Cartagena no es habitual dadas las aportaciones de grandes cantidades de esos trazadores a través de la red de superficie de la Rambla del Albujón y de los importantes entradas de salmueras procedentes del rechazo de desaladoras de aguas subterráneas. Las medidas de trazadores se combinaron con una modelización hidrodinámica de la laguna para comprender el impacto de tales aportaciones.

La comparación de los valores medidos y los modelizados, ha permitido discriminar la zona de influencia de la pluma de radionúclidos de la rambla, y su ubicación principalmente cercana al borde costero. Las principales zonas de SGD han sido también localizadas en sectores donde no se pueden justificar valores muy altos asociados a la pluma de la rambla. Del mismo modo, se han podido localizar los rechazos de salmueras en zonas muy restringidas en las que se midieron altas actividades observadas esporádicamente.

Una dificultad recurrente en la realización de este tipo de balances radón/radio es la determinación de la composición del agua subterránea "dulce" originada por el acuífero. La gran mayoría de los autores considera arbitrariamente un valor medio a partir de muestras extraídas en sondeos próximos a la zona costera. Sin embargo, en esta investigación, un cálculo simple ha demostrado que el agua contenida en los poros de los sedimentos que cubren el fondo de la laguna tenían una composición mucho más representativa, permitiendo así un cálculo de SGD mucho mas fiable. Finalmente, los balances de masa en verano y en invierno proporcionan flujos de SGD del orden de 7.2 a 15.9 10^8 m^3.año^{-1} (^{222}Rn), 21.9 a 44.7 10^8 m^3.año^{-1} (^{224}Ra) y 6.9 10^8 m^3.año^{-1} (^{223}Ra, medido en invierno solo). La diferencia entre ambos valores obtenidos con ^{222}Rn se explica con condiciones meteorológicas diferentes (temperatura y viento). El efecto de la variación del nivel de mar, más que el efecto de marea generalmente considerado, fue identificado como el motor de la recirculación de agua salada, mientras la descarga de agua subterránea dulce originada por el acuífero fue evaluado en un 1% de las SGD totales.

Finalmente, cabe destacar que el estudio de este caso extremo de antropización presenta un interés mucho más allá del sistema acuífero multicapa del Campo de Cartagena. Efectivamente, en el área mediterránea semiárida, un importante número de acuíferos presentan explotación intensiva y creciente con fuertes modificaciones de flujos hídricos. Los métodos implementados en esta Tesis podrán ser aplicados en otros ámbitos mediterráneos donde la explotación del agua subterránea sigue una evolución comparable, continua y aparentemente inexorable.

Chapter 1

Introduction

1.1 Groundwater in arid and semiarid Mediterranean

As a large part of the Mediterranean basin is under arid or semiarid climate, large volumes of water are needed to supply industrial, human and agricultural needs (e.g. Alcamo et al., 2007; Iglesias et al., 2007). During the last decades, the large increase in population, the rise of living standards, the development of irrigated agriculture, and new activities (especially tourism) have drastically modified the water uses (e.g. Cudennec et al., 2007). Anthropogenic long-term changes are very important (e.g. Servat et al., 2003), either in terms of water requirements, or through changes in geography and land cover (Kundzewicz et al., 2007; Rosenzweig et al., 2007).

In addition, the Mediterranean region is considered as one of the areas most vulnerable to global change, under hazard of decreasing rainfall, increasing temperature and intensification of the recurrence of extreme climatic events (IPCC, 2007). According to the Plan Bleu (Margat & Treyer, 2004), 60% of the world's water-poorest population (i.e. with less than 1000 m^3 per capita per year) lives in the Mediterranean basin, especially in its southern and eastern parts. Therefore, improving the identification of the main hydrological processes, and their variability and changes, is essential for a better management of the water resources, and for the day-to-day life of millions of people.

During the last century, most Mediterranean countries followed a similar pathway regarding their agricultural, industrial and urban water supply, although irrigated agriculture concentrates most of the demand (Margat and Treyer, 2004). Initially, the first resource to be exploited was surface water, concentrated into networks of public hydraulic infrastructures, i.e. mostly dams and irrigation networks, and later inter-basin water transfer channels. Rapidly, in parallel with the irregular availability of surface water at the seasonal and interannual scale, the continuous increase in water demand required additional sources of water.

By contrast to surface water, even when stored in large dams, groundwater provides a relative inter-annual stability of the resource. Despite the often low renewal rate (e.g. Scanlon et al., 2008), groundwater soon started to play a complementary role, by securing the water supply and complementing the limited surface water resources. Indeed, it even created new

opportunities by allowing irrigation in areas that would never have been cultivated or by allowing agricultural practices of higher added value requiring larger volumes of water.

In its present state, the Mediterranean region illustrates well the large range of natural and anthropogenic stresses affecting groundwater resources (e.g. Cudennec et al., 2007). In most Mediterranean countries, the development of groundwater exploitation has been based partly or mainly on private initiative with little or no regional planning. Human-induced perturbations strongly affect the natural dynamics of groundwater flow in both quantitative and qualitative aspects (Kass et al., 2005). They often induce extremely dynamic reactions compared to climatic effects. Examples are numerous in Spain (e.g. Pulido-Bosch et al., 2012), Morocco (e.g. Ben Kabbour et al., 2005), Tunisia (e.g. Ben Hamouda et al., 2011), Turkey (e.g. Guler et al., 2012) or Middle-East (e.g. Vengosh et al., 2005). Intensive withdrawals can lead to groundwater depletion (e.g. up to 200 m in 30 years in Molina et al., 2011), while irrigation flow may cause increased recharge to unconfined aquifers and the subsequent modification of groundwater chemistry (Kass et al., 2005). Surface hydrology can also be affected (intermittent rivers running completely dry or turning to a permanent flow, wetland appearing or disappearing; etc.). Understanding the quantitative and qualitative impacts of the agricultural exploitation of the aquifers is therefore an important scientific stake.

1.2 Campo de Cartagena, a natural laboratory

In Spain, intensive exploitation affects 77 aquifers, and currently represents more than 700 10^6 m^3a^{-1} (Custodio, 2002). In the same way as in many other semiarid countries, most part of the extracted groundwater (75%) is for irrigated agriculture. As a consequence of the new water availability, areas that were historically called “deserts” represent nowadays some of the most productive agricultural areas of the country (Pulido-Bosch et al., 2000; García-Aróstegui, 2012). The most acute situation is found on the southeastern side of the Peninsula, more precisely in Murcia, where numerous aquifers have been affected by the intensive exploitation of groundwater for several decades (Molina et al., 2009).

In particular, the Campo de Cartagena area is an emblematic, and extreme, example of hydrological and environmental changes caused by the intensive use of groundwater for agriculture in semiarid Mediterranean areas. Because of the absence of surface water and an

increasing demand of water for irrigation, the agricultural development of the area was historically based on the use of groundwater. The exploitation of the Campo de Cartagena multi-layer aquifer system started with the shallow one and progressively reached the deepest ones, leading to overexploitation. A large number of the boreholes of the area are screened in several aquifers, allowing an artificial connection between different groundwater masses of different chemistry (Jimenez Martinez et al., 2011). Indeed, a complete technical description of these boreholes (e.g. depth, contributing aquifer-s) is not always available. Since 1980, the arrival of external surface water from the Tagus-Segura water transfer channel (TTS) modified even more the hydric fluxes in the Campo de Cartagena. It lowered the withdrawals of the shallow unconfined aquifer and provided additional volumes for irrigation, with the corresponding charge of agrocontaminants (e.g. up to 450 mg/l of nitrate). As a consequence, water table levels in the shallow aquifer increased and a permanent flow appeared in the last kilometers of the surface watershed. Together with the uncontrolled release of brines from groundwater desalination, this induced a permanent surface flow of water to the main outlet of the system, the Mar Menor lagoon.

1.3 Specific approaches

Thus, the Campo de Cartagena area is a good illustration of various forms of the anthropization of groundwater resources and constitutes an appropriate laboratory for the study of transient states in coastal Mediterranean aquifers. It provides the opportunity to develop specific investigations adapted to such an anthropized context, following three main axes that correspond to chapters 4, 5 and 6.The first one refers to a detailed analysis of the existing historical information; including a novel approach for the identification of the aquifer(s) corresponding to boreholes lacking data on their design. The second approach corresponds to a Quantitative and qualitative assessment of the evolution of recharge as a consequence of the set-up of agriculture, using environmental tracers combined with high resolution temperature profiles. The third one presents the quantification of submarine groundwater discharge in the context of a highly anthropized watershed coupling radon and radium isotopes with hydrodynamic modeling.

1.3.1 Review of historical information

Any study centred on unsteady-state systems has to start with the review of historical data (land-use, climatology, water table level, hydrogeochemistry, etc). Its analysis can provide precious information on the state of evolution of the system. In addition, it offers the possibility to cross various types of information to validate hypotheses. It is the basic step before any further interpretation, and has to cross all types of information, even not hydrological data, together with hydrochemical and piezometric data.

In complex multi-layer groundwater systems like Campo de Cartagena, the correct assessment of the aquifer reflected by a borehole, i.e. the basic driving condition for a reliable interpretation of geochemical and hydrodynamic results (Mayo, 2010) might become a hard task. In addition to badly designed boreholes that directly allow a communication between several aquifer layers, the cement ring of old boreholes initially well-designed might be in bad conservation states and allow such communication. In most case there is even no available information on the tubewell design. As a consequence, despite the large quantities of geochemical and piezometric data available, only those corresponding to fully documented tubewells should be used for investigation.

To face this critical limitation, a possibility would be to investigate one by one every undocumented borehole; for example, using inside borehole geophysical material. Nonetheless, it is very costly and time consuming as it requires taking out the pump and all connections before using the geophysical devices, among others. Moreover, it requires the authorization of the owner.

Hence, there is a need for a tool that could provide an automatic and accurate estimate of the aquifer layer from which a water sample has been extracted. A possibility is to base this tool on geochemical criteria. Such a method would have to deal with additional difficulties as similar water types, temporal changes in the origin of groundwater, or having different ions analyzed in different samples. Moreover, it should be applicable with common major ion geochemistry.

In this context, I collected and reviewed all kind of information that could provide a new insight on the long-term evolution of the Campo de Cartagena along the last century. In addition, I approached the team of Dr. Francisco Alonso Sarriá (INUAMA, Univ. Murcia),

who proposed to test a supervised classification method for automatically assessing the belonging of a sample to a set of previously identified classes, a method that they had successfully implemented to remote sensing. I was responsible for the building of a geochemical dataset based on the review of more than 1000 boreholes in the area, confirmed by a review in field of the most important ones. This dataset was then inserted into a series of statistical models of their construction. Step by step, we worked together in order to assess the most reliable model and elaborate the most efficient strategy. These works have been synthesized in a paper under revision by Journal of Hydrology (Baudron et al., 2013a) and presented at an international congress (Baudron et al., 2012a).

1.3.2 Evolution of recharge conditions and rates: isotopic approach.

Beyond the hydrological processes that show a strong variability in time and space, groundwater recharge may be the most considerably affected by modifications in land use and land cover (e.g. Leduc et al., 2001; Scanlon et al., 2006). In semiarid Mediterranean, rainfall mostly occurs during strong and violent storm event, inducing important runoff and limited recharge on the land. On the other hand, despite water saving technologies like drip irrigation, artificial recharge by irrigation return-flow may occur and significantly increase the recharge of shallow aquifers. The quantitative assessment of the related additional water inflow to the aquifer is then a fundamental task for updating the regional water budget and defining a sustainable management of the water resource.

Environmental tracers have been used for multiple topics in Mediterranean hydrology and hydrogeology. They provide information for understanding rainfall processes (e.g. Cruz San Julian et al., 1992; Celle-Jeanton, 2001; Fernandez-Chacon et al., 2010), groundwater flow (e.g. Celle-Jeanton et al., 2009), exchange between aquifers (Adar et al., 1992) or between aquifers and hydrographic network (e.g. Burnett et al., 2003). Regarding recharge assessment, environmental tracers are widely used for estimating recharge at integrated scale in time and space in semiarid areas (e.g. Le Gal La Salle et al., 2001; Klaus et al., 2008). Recent reviews on processes and techniques were proposed by Scanlon et al. (2006) and Herczeg and Leaney (2011). Studies using environmental tracers in groundwater to assess the recent evolution of recharge in semiarid areas as a consequence of changes in land use were mostly developed in the last decade, with applications, among others, in Niger (e.g. Favreau

et al., 2002), Ivory Coast (Adiaffi et al., 2009), or China (e.g. Currell et al., 2010). Nevertheless, only a limited number of studies worldwide focused on the direct impact of irrigation on recharge (e.g. Horst et al., 2008; Qin et al., 2011) applying environmental tracers in groundwater.

In addition, the use of environmental tracers in complex multi-aquifer systems faces the difficulty of in situ identification of irreproachable sampling points, because of possible artificial mixing of water from the different layers. Assessing whether groundwater samples are representative of regional aquifer conditions or might result from local inside-borehole perturbations is a basic step before any interpretation. This tricky stage is rarely mentioned in the scientific literature. Several authors discussed the origin of a sample from long-screened boreholes by theoretical and modelling approaches (Lacombe et al., 1995; Elci et al., 2003) or with experimental approaches (Martin-Hayden, 2005; Mayo, 2010). Excepting authors like Barbecot et al. (2000), this topic has not been studied in details, and no in situ methodology exists.

In this investigation, despite the increase in the number of groundwater samples reliably usable for a geochemical study provided by section 4.7, the high homogeneity in the geochemical composition of the different aquifers did not allow to trace recharge, mineralization and mixing processes. I contacted with the IDES team from Univ. Paris Sud) to propose a collaboration using radiocarbon and tritium as complementary tracers to understand the evolution of recharge conditions since the set-up of agriculture and the mixings of water from different horizons. Once selected the most reliable sampling points, and found the first part of financial founding for the experiment, I organized the sampling campaign and performed part of the lab work (crystallization of dissolved inorganic carbon) at the IDES laboratory. The interpretation of the results was then discussed with Dr. Barbecot (IDES), Pr. Yves Travi (UAPV) and Dr. Jean-Denis Taupin (UM2), among others. Two scientific publications were extracted from of this chapter, one is published in Hydrological Processes (Baudron et al., 2013b) and the other one has been accepted in Radiocarbon (Baudron et al., 2013c). In addition, partial results were presented in four international congresses (Baudron et al., 2011; 2012b, c, d).

1.3.3 Submarine Groundwater Discharge

Another illustration of the impact of increasing anthropogenic pressure on Mediterranean aquifer systems is the modification of hydrology and ecology of coastal areas by modifying submarine groundwater discharge (SGD) (e.g. Burnett et al., 2003; Moore and Arnold, 1996). In the Mediterranean Sea, such processes are a particular source of concern in wetlands (e.g. Rodellas et al., 2012) and lagoons (e.g. Gattacceca et al., 2011). SGD assessment is therefore a critical need for water resources management.

A series of methodologies were used in the last decades to locate and quantify SGD. One is a simple Darcy's calculation of groundwater flow through the aquifer (e.g. Senent et al., 2009). Another one consists in direct measurements of groundwater seepage rates using a manual "seepage meter" (e.g. Israelsen and Reeve, 1944; Cable et al., 1997), i.e. a chamber inserted into the sediments and connected to a plastic bag. Submarine groundwater discharge can also be calculated from water balances of aquifers (e.g. Oberdorfer et al., 1996) or surface water masses (e.g. Martinez-Alvarez et al., 2012). Numerical modeling methods are also developed (e.g. Smith and Turner, 2001).

Another possibility is to use natural tracers. The radon and radium approaches rely on a global mass balance of the studied water masses, as pioneered by Moore (1996) or Cable et al. (1996). The interest is based on the simple field implementation and on the spatio-temporal integration. Along the last decade, numerous authors successfully applied this method in many places worldwide (e.g. Burnett et al., 2001; Mulligan and Charette, 2006) and to a lesser extend in the Mediterranean (Garcia-Solsona et al., 2010; Gattacceca et al., 2011; Rodellas et al., 2012; Weinstein et al., 2007).

The most sensitive part of the mass-balance method lies in a precise determination of the discharge rates and the radionuclide activities of the different end-members. Such calculation is particularly sensitive i) to the composition of discharging groundwater and ii) to the assessment of inputs from surface water.

The behaviour of radon and radium in coastal aquifers is complex (e.g. Burnett et al., 2003). No specific rule exist for assessing the composition of discharging groundwater, although it has a direct impact on the calculated SGD values. The discharge processes are not

always well known, and the use of mean values as representative for a complex system is not completely satisfying.

Surface water fluxes often represent limited inputs of radionuclides. Nonetheless, in highly anthropized watersheds, surface water tributaries may carry unexpected high quantities of radon and radium to coastal lagoons. In such cases, their precise assessment remains a fundamental task for deciphering the influence on the tracer distribution in water masses and on the radionuclide mass-balance. This task is even more difficult when surface-water hydrodynamics is very reactive, inducing a fast dispersion of the tracers due to strong waves or tides (e.g. Ferrarin et al., 2008; Santos et al., 2009a; Liu et al., 2011). Nonetheless, their precise localization and sampling is not always an easy task, especially where artificial submarine emissary are present.

Once reviewed the different methods for its quantification, the radon and radium method appeared to be the most adapted to the complex and large scale system of the Mar Menor. In addition, a hydrodynamic modelling of the lagoon seemed to be a good methodology to follow the dispersion of radionuclides into Mar Menor. Therefore, I approached the CEREGE team, who completed just before such a survey in the Venice Lagoon, to discuss the feasibility of such a radionuclide investigation in the Mar Menor. I also contacted the Department of Chemical & Environmental Engineering at UPCT, specialists of surface hydrodynamics in the Mar Menor lagoon. They joined the project, provided and sailed the boat for sampling and leaded a modelling task of the hydrodynamics of the lagoon. The acceptance of two project proposals by the IEA foundation, in addition to the support from the aforementioned CARTAG-EAU project, allowed performing the three campaigns, for which I organized all logistic aspects (definition and planning of the experiments, travels, accommodation, vehicles, administrative authorizations etc). I collaborated to all field analysis, while laboratory analysis was performed by the CEREGE team (Dr. Christelle Claude, Dr. Olivier Radakovitch, Sabine Cockenpot) and University of Avignon (Dr Adriano Mayer). Hydrodynamic modelling was performed by Francisco Lopez Castejon and Dr Javier Gilabert, after we elaborated the strategy together. The interpretation of the data was performed by myself in direct collaboration with the different member of the project. A scientific publication will soon be submitted to Estuarine, Coastal and Shelf Science (Baudron et al., 2013d). In addition, results were presented in two international congresses (Baudron et al., 2011b, c).

Chapter 2

Study area

2.1 Geomorphology, climate and economy

The Campo de Cartagena is located in the South of the region of Murcia (Figure 1), in southeast Spain. It is characterized by a wide plain with a slight tilt southeastwards, rounded by small mountains, except on its eastern side where its borders are defined by the Mediterranean Sea and the Mar Menor lagoon.

The altitude of the mountainous relieves that separate the Campo de Cartagena from the Murcia plain culminates a 1065 m asl in the western part and progressively decreases to the east. In the Southeastern part, several peaks reach up to 551 m asl, at the 2 small mountains located eastern from Fuente Alamo culminate at 292 and 305 m asl. In the central part, the plain is interrupted by several hills, standing out the Cabezo Gordo (312 m asl) and the Carmoli (117 m asl), as detailed in section 2.2.

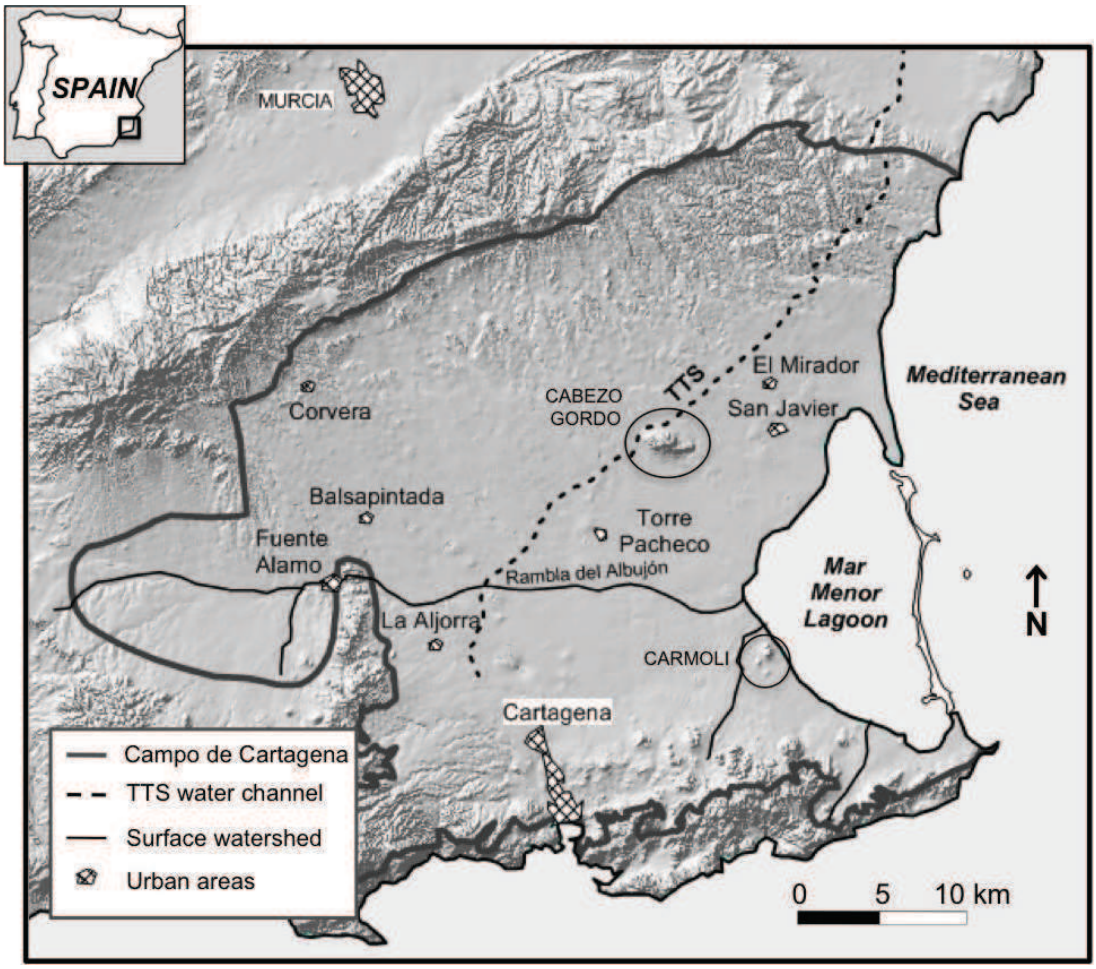

Figure 1 : General map of the study area. Black circles highlight the main hills that interrupt the plain.

The region is characterised by a semiarid Mediterranean climate, with mean annual temperatures ranging from 14 °C to 17 °C (Conesa, 1990). The mean annual rainfall is 300 mm, with most precipitation concentrated into short-episodic storm events in autumn and spring. No permanent watercourse exists and the area is drained by several ephemeral streams.

Despite the semiarid climate and the absence of surfacewater, the regional economy relies on agro-industry, which is the primary land use (one third of the total surface area). Developed during the 20th century, irrigated agriculture converted this area in one of the most productive agricultural areas in Europe. It was mostly based on the use of groundwater, supported since the early 1980s with the arrival of water from the Tagus-Segura water transfer channel (TTS) that carries water from the centre of Spain at a distance of 450 km.

2.2 Multi-layer aquifer system

The Campo de Cartagena multi-aquifer system is one of the main groundwater resources of the Mediterranean basin (Margat and Treyer, 2004). It is composed of five aquifers, i.e. four sedimentary aquifers and the basement, all intensively exploited by agriculture.

The upper productive layer is a shallow unconfined Quaternary aquifer (Figure 3) composed of sand, silt, clay, conglomerate, caliche and sandstone (Jiménez-Martínez et al., 2012). Below the Quaternary aquifer and separated by thick aquitard layers, three confined aquifers exist at increasing depths: the Pliocene sandstone; two Miocene formations: limestone (Messinian), sandy limestone and conglomerate (Tortonian).

The impermeable subtract of the system corresponds to the Mesozoic and Paleozoic basement representative of the Internal Betic Zone, inside which locally appears a fifth aquifer, constituted by metamorphic limestone locally named “marble” (Triassic). Several outcrops of andesitic volcanic domes of Tortonian age are also found.

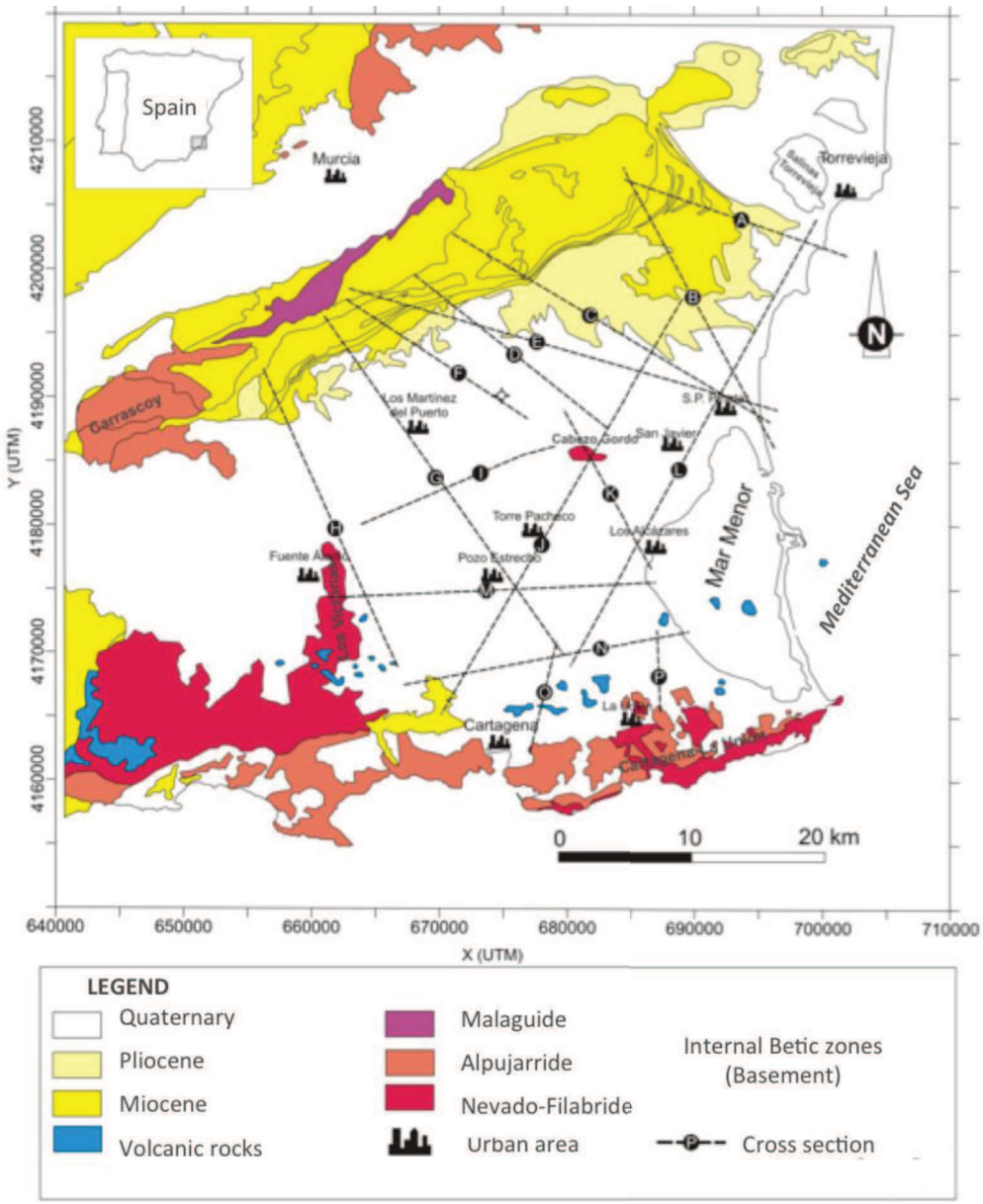

Figure 2: Geological map the location of the cross section "E" of Figure 3, adapted from García-Aróstegui et al. (2012)

As aforementioned, intensive irrigated agriculture covers more than one third of the surface area, with a total water demand close to 200.10^6 $m^3.a^{-1}$ (CARM, 2000). Irrigation water comes from various sources: i) groundwater from the multi-aquifer system (mainly Messinian and Quaternary, then Pliocene and Triassic, more rarely from Tortonian), ii) remote water transferred through the TTS channel, iii) private brackish groundwater desalination plants, iv) public seawater desalination plants and v) sewage water treatment plants.

More than 90% of the total volume is provided by the three first sources (CARM, 2000) and their relative contribution is basically driven by the availability of source ii), while sources i) and iii) act as buffers to reach the needed volume of irrigation water at the optimal salinity for crops.

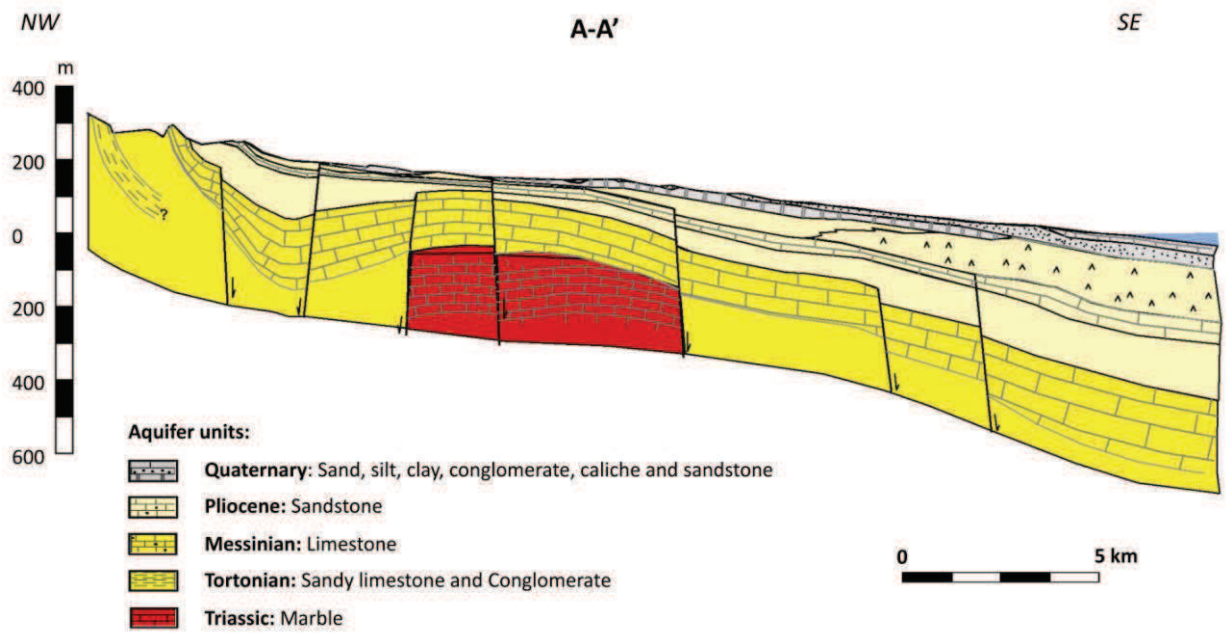

Figure 3: Geological cross-section "E" from Figure 2, adapted from IGME (1994).

A main peculiarity of the area is the existence of an unknown number of small brackish groundwater desalination plants (source iii) used to lower the elevated salinity of groundwater (Lorenzen et al., 2012) before irrigating. Despite the lack of precise data, a rough estimation of the volume of brines can be made by considering reverse osmosis to have an efficiency of 75% (usually observed) and 5% of the irrigation water to come from groundwater desalination (based on field observation).

The total volume of brines would then reach an order of magnitude of $3.5.10^6$ $m^3.a^{-1}$ comparable with the 5.10^6 $m^3.a^{-1}$ of surface water inputs to the lagoon proposed by Senent et al. (2009). The final destination of these brines is uncertain, and a matter of interest, since part is supposed to be released to the Quaternary aquifer, to the Mar Menor lagoon directly or through the network of temporary rivers that drains the watershed.

Natural recharge to the multi-layer aquifer system is small and depends on the respective outcrop areas of each aquifer. The Quaternary aquifer is also recharged by the

irrigation return flow, complex combination of multiple sources of surface and ground waters. Farmers mix the different sources of water and store them in open air water reservoirs before their application to crops. The mixing proportions between groundwater and TTS water mainly depend on the availability of TTS water.

Close to 2000 boreholes are officially numbered (Figure 1). Many of them are screened in several aquifers, allowing an artificial connection between the different water masses (Jimenez Martinez et al., 2011), and possibly complicating the recharge patterns. In most cases, the technical description of the borehole is not available, and the precise depths of screens are unknown. Such boreholes presumed to host artificial connection between different aquifers are called hereafter "doubtful".

2.3 Mar Menor lagoon

The main surface outlet of the watershed is the Mar Menor lagoon (135 km^2), one of the largest coastal lagoons of the Mediterranean Sea (Figure 47). It represents a volume of 605 10^6 m^3 with a mean depth of 4.5 m, with a maximum depth close to 6.5 m. Water temperature in the depth ranges between 7.8 °C in winter and 30.2 °C in summer (Lopez-Castejon, personal communication) in coherence with the atmospheric temperature variations.

The Mar Menor is separated from the Mediterranean Sea on its eastern side by a 22 km long narrow sandy bar system (La Manga; width between 100 and 1200 m) tied to four volcanic outcrops. Other volcanic outcrops in the lagoon form three small islands. Three inlets connect the lagoon with the Mediterranean Sea (Figure 47), although the main water exchange occurs through the central one, the Estacio channel that was dredged in 1973 to make it navigable.

Due to the scarcity of precipitations (300 $mm.a^{-1}$), which mainly occur during storm events, the limited surface runoff does not compensate the high evaporation of the lagoon, requiring a net inflow from the Mediterranean Sea of about 130 10^6 $m^3.a^{-1}$ (Cabezas et al., 2009). The lagoon is therefore hypersaline, around 64 mS/cm. Calculated renewal time ranges from 0.66 to 1.2 year (Ruzafa, 1998; Gilabert. 2008; Cabezas, 2009; Martínez-Álvarez et al., 2011). Water circulation can be very dynamic and is mainly controlled by wind and atmospheric pressure (Arévalo, 1998).

Despite a weak stratification in the early morning, the water column can be considered homogeneous (Lopez-Castejón, personal communication). Still, local stratification can be found in some areas close to the inlets and affected by the Mediterranean Sea water. Variations of the water level in the lagoon are limited to a few centimetres of amplitude, and are controlled by both tidal cycles and non-tidal phenomena like the variations of the atmospheric pressure.

Some authors suggested the existence of faults systems under the lagoon (Montenat, 1973; Lillo Carpio et al., 1979) or at its western limits (Rodriguez Estrella, 2004). However, García-Aróstegui et al. (2012) recently reviewed the existing information and did not identify such faults systems along the lagoon. In the absence of further indication, the Quaternary aquifer is assumed to fully underly the lagoon.

2.4 Surface hydrology

Similarly to other semiarid areas of SE Spain and of the Mediterranean, a network of ephemeral streams called "ramblas" drains the area, transferring rainwater only during the sporadic rainfall events. The main stream is the Rambla del Albujón. Flowing E-W, it constitutes the axial drainage of the Campo de Cartagena; its watershed (556 km^2) has a shoreline of about 40 km long (García-Pintado et al., 2007), and covers almost half of the Quaternary aquifer surface area. It also artificially concentrates water from neighbouring watersheds that used to flow directly to the lagoon.

Since the 1980s', a permanent flow has appeared in the last kilometres of the river bed; it represents nowadays around 5.10^6 $m^3.a^{-1}$ (IEA, 2011). This is explained by the natural drainage of the Quaternary aquifer, whose water table level has risen in response to the increased irrigation return flow. In addition, a high number of agricultural drains and artificial releases now increase the Rambla del Albujón flow. Artificial releases are mostly brines from private desalination plants and discharge of the Los Alcázares sewage water treatment plant.

Mean data from a 2.5 year survey (IEA, 2011) shows that two underground pipes (R2 and R3 in Figure 4), that cannot be related to any origin, discharge respectively 0.8 10^6 $m^3.a^{-1}$ and 2.4 10^6 $m^3.a^{-1}$ of water to the Rambla del Albujón.

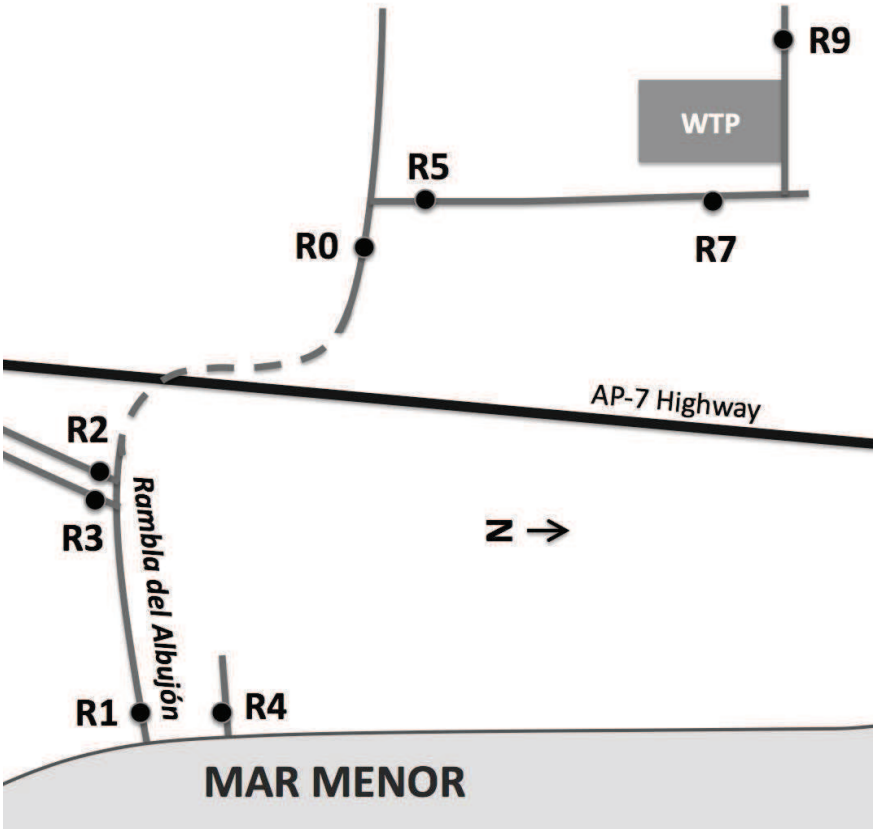

Figure 4: Key locations in the Rambla del Albujón surface water network. Discontinuous line indicates discontinuous presence of water. WTP is the Los Alcázares urban water treatment plant. Schematical figure not to scale

A few tenths of meters downstream, the mouth of the rambla (R1) discharges 7.7 10^6 $m^3.a^{-1}$ to the lagoon (IEA, 2011). On an annual basis, the contribution of R2+R3 therefore represents 41% of the total discharge of this rambla.

This ratio is much lower during the rainy events (IEA, 2011). It illustrates an additional complication for SGD assessment (see Chapter 6), as high radionuclide activities (initially issued from groundwater) may be carried by surface water to the lagoon through both aquifer drainage and brines release. A few tenths of meters away from R1, R4 discharges 2.9 10^6 $m^3.a^{-1}$ (IEA, 2011) supposed to come from the drainage of the Quaternary aquifer (Velasco et al., 2006).

.

Chapter 3

Data

3.1 Introduction

This chapter aims at presenting an overview of official geochemical and water table level data that was available previously to this investigation, provided by the Spanish Geological Survey of Spain (IGME). It also briefly describes the main data collected during this investigation.

3.2 Data from official networks

3.2.1 Geochemistry

Close to 40 years of groundwater sampling represent a large dataset of more than 1200 geochemical analysis that account for the 5 aquifers of the Campo de Cartagena multi-aquifer system. Most samples were analyzed for major ions only, but a number of them also give information on Cu (>400 samples), B or Cr (>200 samples), beyond others.

The spatial repartition of the sampled tubewells is heterogeneous and the number of hydrochemical data is highly changing depending on the studied tubewell (Figure 5). As further explained in section 4.4, that presents the results of the new inventory of boreholes, most of the sampled points did not come with a precise assessment of the corresponding aquifer, that might even be several; or when it exists, this information is not always detailed enough.

The temporal repartition of the sample is also highly variable. Despite a mean total number of samples close to 50 per year for the whole area, the number of samples from the IGME dataset is highly dependent on the year of sampling (Figure 6). It varies from 1 or 2 samples (1991 and 1975, respectively) to more than 150 samples in 1989 and 2001.

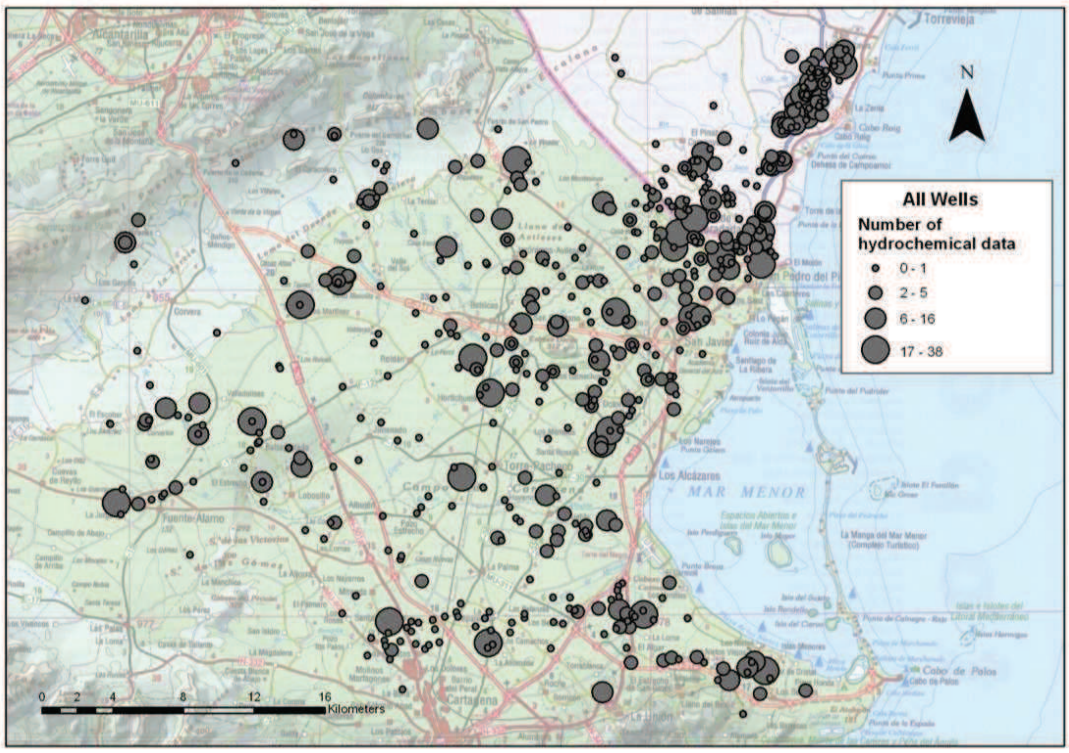

Figure 5: Map of the registred tubewells indicating the number of hydrochemical data. Figure made in 2010.

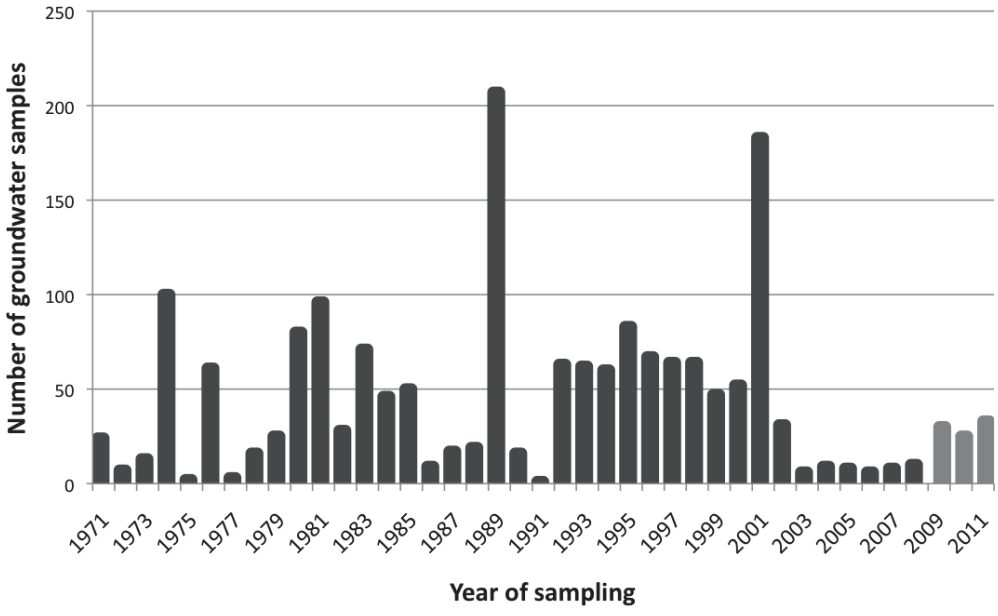

Figure 6 : Evolution of the number of groundwater samples. Columns in grey include sampling for the present investigation.

3.2.2 Water table levels

As well as for the hydrochemical survey, the IGME database features more than 40 years of water table measurements in the Campo de Cartagena, summing 7334 measurements in 1134 tubewells. More than 2/3 of the tubewells featuring water table data were measured only once. A total of 74 tubewells present data spread over more than 1 year, and are considered as times series. The spatial repartition of these tubewells (Figure 7) is not homogeneous in the study area, as they are mostly centered in the northern part. Similarly to the official geochemical database, the determination of the aquifer(s) represented by these tubewells is not always unquestionable, and it limits notably the number of tubewells whose data can be reliably interpreted.

An interesting point is the highly variable density of measurement depending on the year of observation (Figure 8). At the beginning of the water table survey, up to 280 tubewells were sampled each year (1973). This number decreased to 150 approximately in the two following years and then remained around a mean value of 25, except some peaks as in 1995 when close to 100 tubewells had their water table level measured. As further detailed in section 4.4, the precise assessment of the aquifer of combination of aquifers to which these tubewells correspond is not always an easy task.

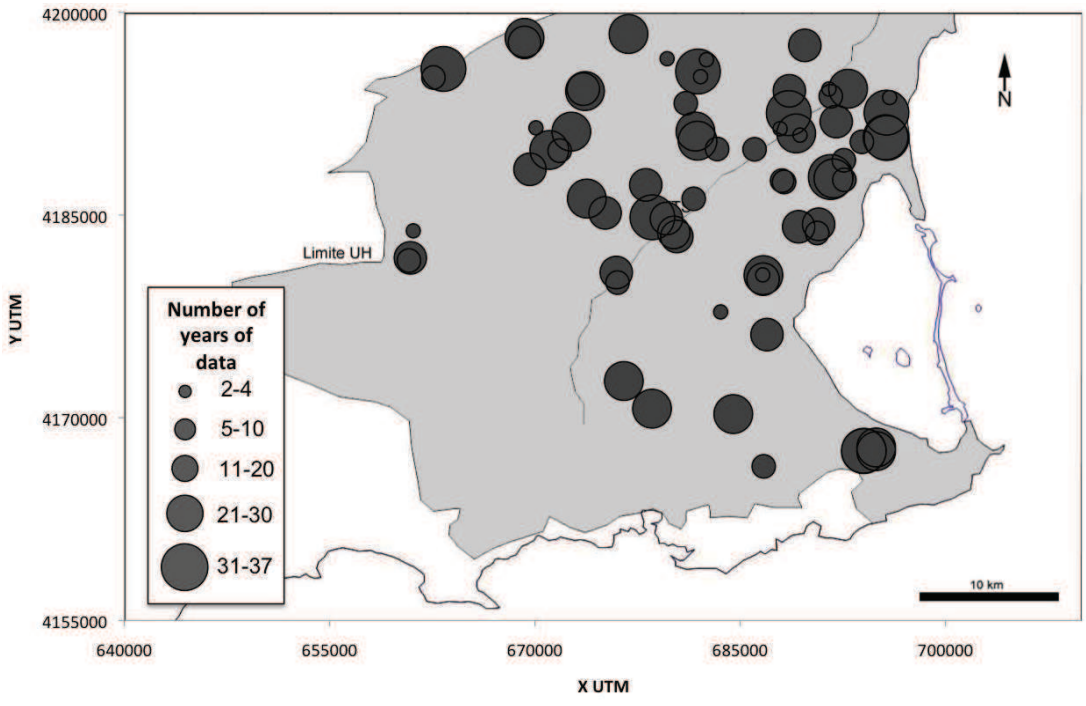

Figure 7 : Map of tubewells with water table data covering more than 1 year.

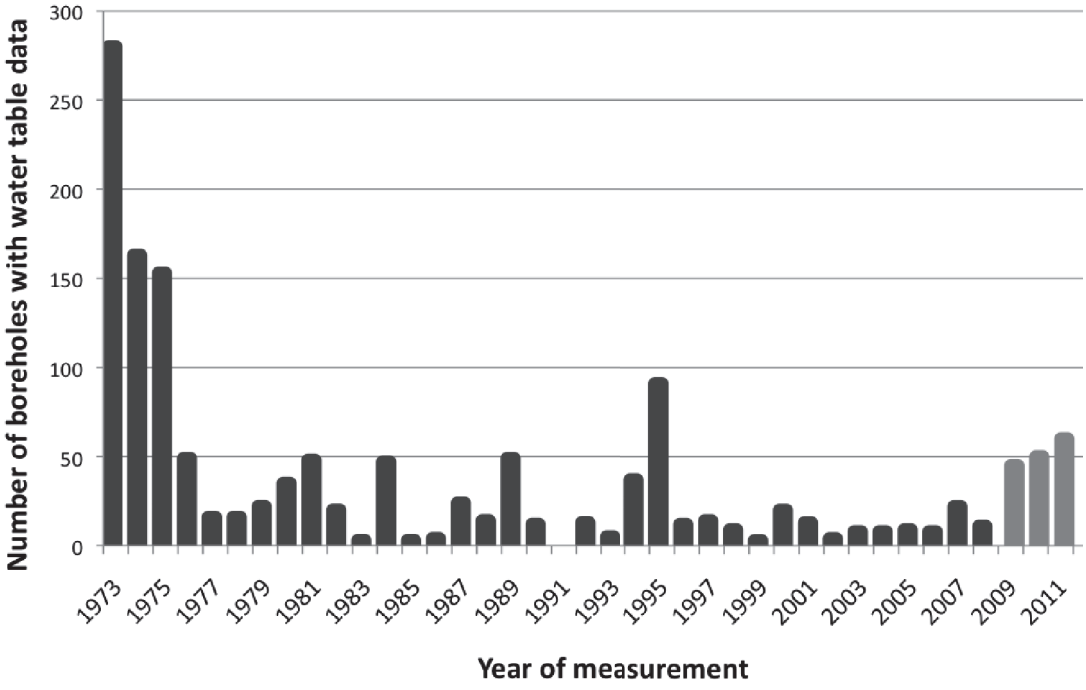

Figure 8 : Evolution of the number of boreholes with at least one water table measurement. Columns in grey include measurement performed during the present investigation.

3.3 Data collected during this investigation

3.3.1 Precipitation

A monthly sampling of stable isotopes of water was performed in a network of pluviometers in the Campo de Cartagena. The device consisted in a 19 cm diameter funnel installed at a height between 1.5 and 2 m (depending on the possibilities of the site), connected with a tube to a 15 l plastic can that was inserted at 50 cm in the soil (Figure 9) and covered by a white tap (although in black color in Figure 9) in order to avoid evaporation. All connections were hermetically sealed.

Five devices were installed in the Campo de Cartagena, taking advantage of the precise data and the protection against vandalism offered by automated weather stations from the SIAM (Sistema de Informacion Agraria) network of the Food and Agriculture Research and Development Institute of Murcia (IMIDA). Sampling started in September 2009.

Figure 9 : Details of the sampling device for the analysis of stable isotopes in precipitation. The black tap was finally painted in white.

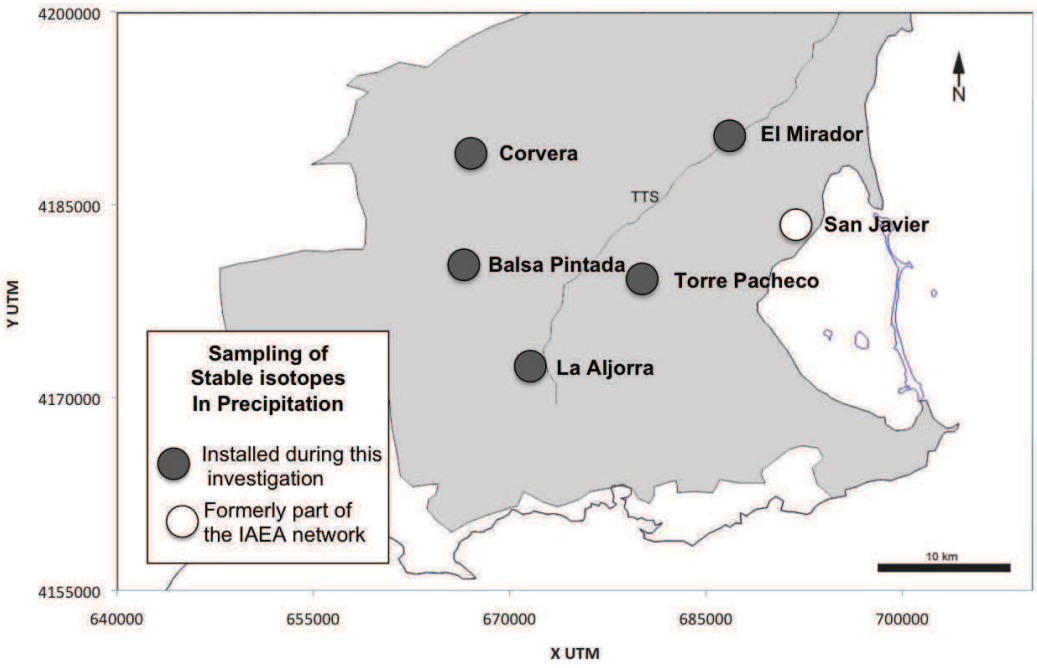

Figure 10 : Location of the sampling devices for stable isotopes in precipitation

3.3.2 Borehole inventory

The first task of this investigation was linked to the difficulty of assessment of reliable boreholes representative for each one of the 5 aquifers and for the different possible mixings.

Once reviewed all the available information (see section 4.4) the field review of 475 boreholes was conducted. Basic step before any interpretation of existing geochemical and piezometric data, it was also a requirement before any new sampling campaigns could be performed. Since the available data had not been updated since almost forty years (date of the last inventory), the owners of the well were rarely the same as in the inventory data, when available. Moreover, data on the localization of the boreholes (schematic maps, coordinates) was scarse and generally not precise enough. This task was spread over more than one year and partly realized with the contribution of Juan Guerra from IEA and Clemente Trujillo from IGME.

Finally, 70% of the boreholes (331) could be found (Figure 11), although half of them were abandoned, in bad conditions or even destroyed due to the construction of urban areas and golf resorts. The owner could be identified in close to 200 cases, and sampling was possible in 124 tubewells. Only a tenth of these boreholes were eligible for the water table survey of deep aquifers, due to the electrical and hydraulic equipment installed inside the boreholes, but more than 50 contributed to the design of a new piezometric network of the Quaternary aquifer.

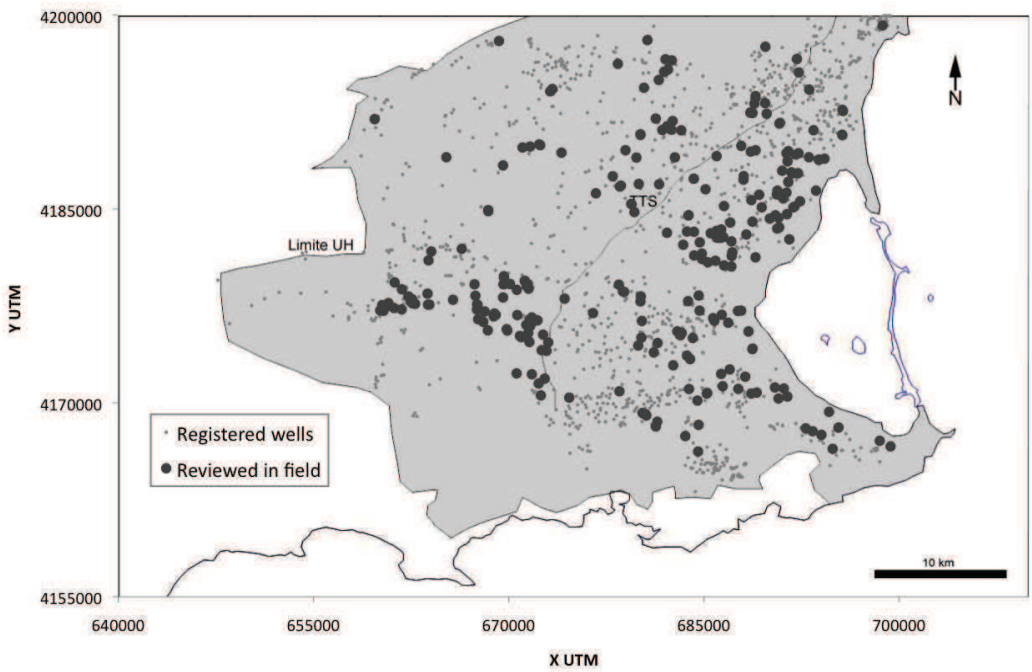

Figure 11 : Location of the registered boreholes and those whose characteristics were updated after the field review.

3.3.3 Groundwater

3.3.3.1 Environmental tracers

Groundwater samples were collected along several sampling campaigns between 2010 and 2012, together with the measurement of the main physic-chemical parameters (temperature, pH, electrical conductivity, dissolved oxygen) and the in-field analysis of the most unstable ions (alkalinity, nitrite, ammonium) by titer determination. Several tracers were considered, depending on the sub-project in which the samples were integrated. The number of samples for each tracer and each campaign is detailed in Table 1.

Table 1 : Number of groundwater samples collected for each environmental tracer for several sampling campaigns between 2010 and 2012. The data from a campaign performed between Univ. of Granada and IGME in 2009 are also indicated. Values between brackets correspond to partial measurements. Tracers with an asterisk are still being analysed.

Tracer	May/Jun 2009	Feb. 2010	Jun. 2010	Nov. 2010	Feb. 2011	Jul. 2011	Jan. 2012
Geochemistry	33 (9)	34	15	6	24	7	7
$\delta^{18}O$ - $\delta^{2}H$	42	36	23	6	24	7	7
^{222}Rn				6		7	7
$^{224\text{-}226\text{-}228}Ra$				6		7	7
^{223}Ra							7
$\delta^{13}C$ - $A^{14}C$					22		
^{3}H					24		
SF_6* - CFC*					12		
Noble gases*					12		

3.3.3.2 Water table levels

A series of boreholes was selected out of the new borehole inventory and used as a base for a new water table levels network, together with ones recently constructed by the Segura Basin Authority (CHS). This survey was performed monthly during the hydrological years 2009-2010 and 2010-2011.

In total, it counted with more than 50 tubewells and dug wells corresponding to the Quaternary aquifer, together with a tenth of deep boreholes reaching confined aquifers and derived from the CHS network.

Every time it was possible to collect a sample (i.e. half of the time), the main physic-chemical parameters aforementioned were measured. In addition, seven automated levellogers were installed in the aforementioned boreholes. Two of them were installed in the "Séneca" Quaternary boreholes (Figure 13) and provide a vertical profile at the discharge zone of the Quaternary aquifer to the lagoon as they are screened at a depth of 80 m and 8 m respectively.

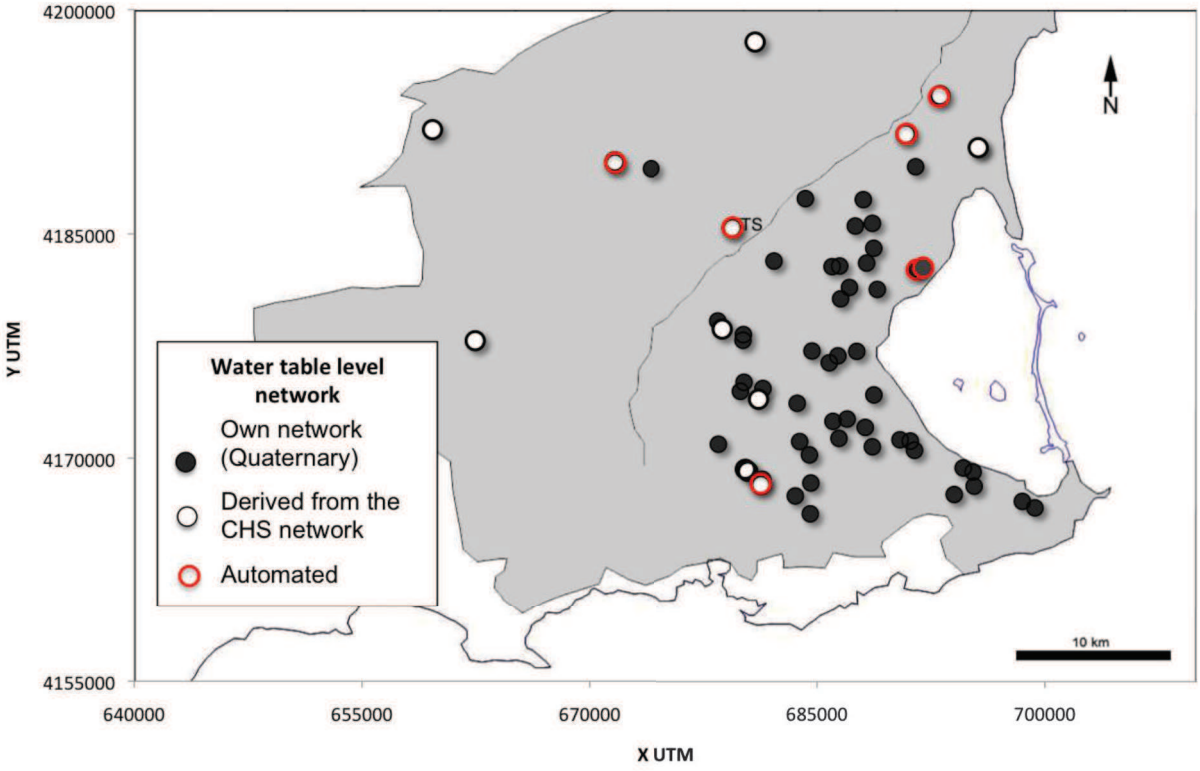

Figure 12 : Location of the water table level network of this investigation, including automated boreholes.

3.3.3.3 Temperature and conductivity logging

Temperature and conductivity loggings were performed monthly in a series of tubewells during the two hydric years 2009-2010 and 2010-2011, using a conventional material (temperature resolution of 0.1°C). Four of them were located at close distance (<1 km) from the rambla and four others were located along the border of the Mar Menor.

In addition, ten boreholes were surveyed with a home-made high resolution temperature sensor (0.01°C) during the February 2011 sampling campaigns for environmental isotopes.

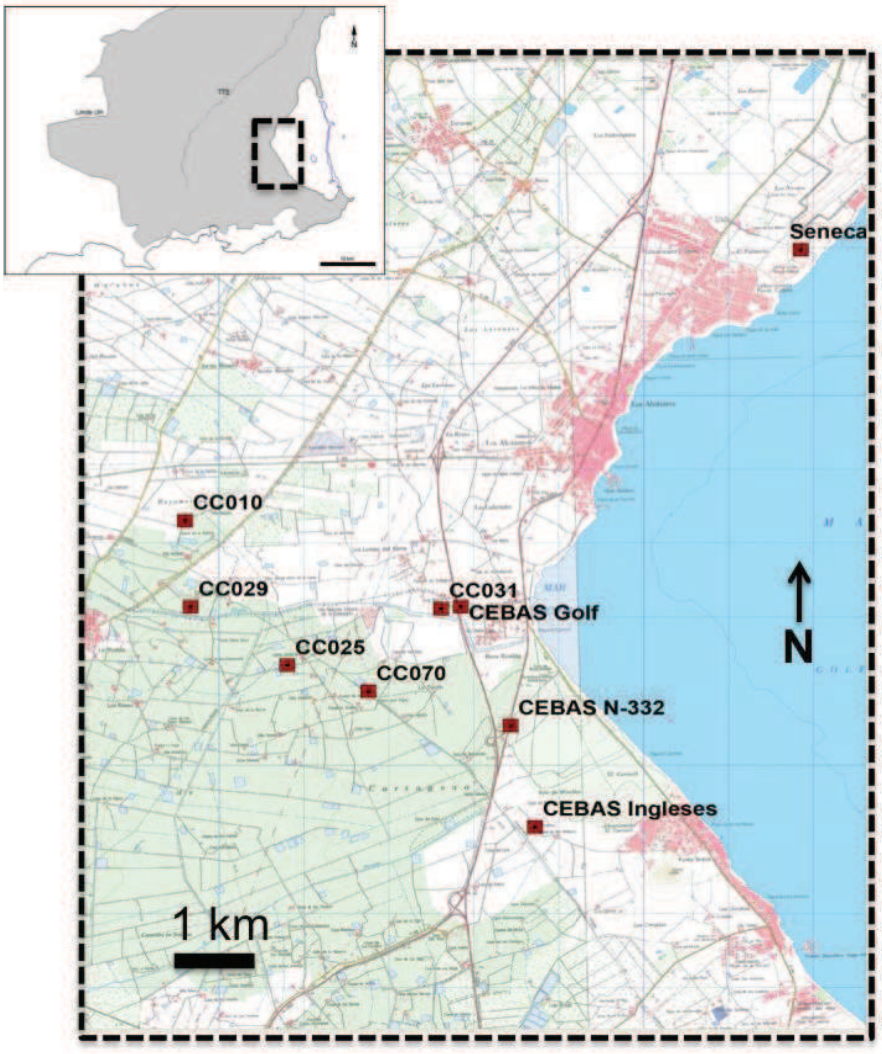

Figure 13 : Location of the monthly loggings for electrical conductivity and temperature

3.3.4 Surface water

During the hydrological years 2009-2010 and 2010-2011, the discharge of surface water was measured monthly in the key points of the Rambla del Albujón watershed indicated in Figure 4. Physic-chemical parameters were measured and a sample for stable isotopes of water was collected, although these samples have not been analysed at the moment. The same protocol was applied monthly to the TTS water transfer channel.

The measurements in the Rambla del Albujón watershed were repeated during the November 2010, July 2011 and January 2012 surveys, together with the sampling of surface water for ^{222}Rn, ^{223}Ra and ^{224}Ra. The number of tracers analysed in each case in detailed in Table 2.

Table 2 : Number of measurement and surface water samples collected in the Rambla del Albujón watershed during the monthly campaigns and the three SGD campaigns.

Tracer	Hydrol. years 2009-2010 2010-2011	Nov. 2010	Jul. 2011	Jan. 2012
Physic-chemical param.	Monthly	1	15	25
$\delta^{18}O$ - $\delta^{2}H$	Monthly	1	15	25
^{222}Rn		1	15	25
$^{224\text{-}226\text{-}228}Ra$		1	1	3
^{223}Ra				3

3.3.5 Mar Menor and Mediterranean Sea

A number of environmental tracers was measured and sampled in the Mar Menor lagoon and the Mediterranean Sea during three surveys performed by boat in November 2010, July 2011 and January 2012 (Figure 14). In addition, a 24h survey was performed from the port of Los Urrutias in July 2011. The detail of tracers analysed in each case is given in Table 3.

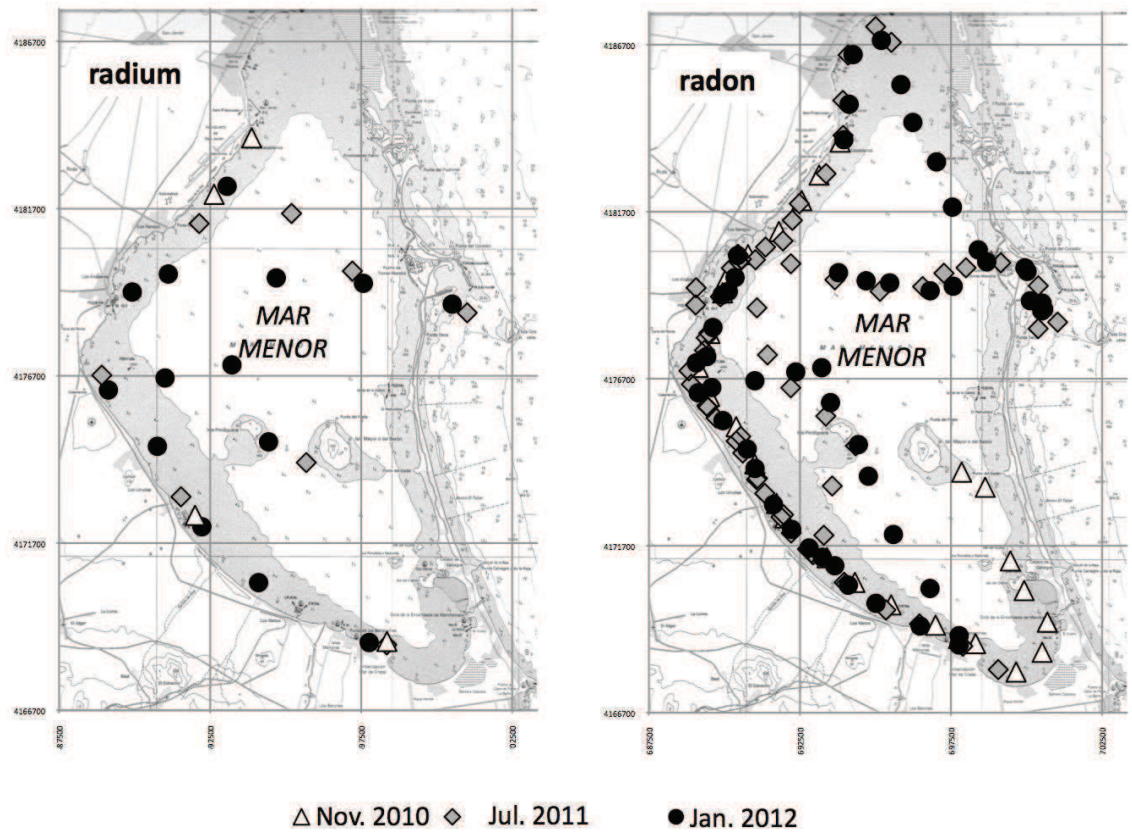

Figure 14 : Samples collected or analysed in Mar Menor and Mediterranean Sea for radium (left) and radon (right) radionuclides.

Table 3 : Number of measurements of radon and radium radionuclides, physic-chemical parameters and other tracers in Mar Menor and the Mediterranean Sea (between brackets). Asterisks mean continuous measurements.

Tracer	Nov. 2010	Jul. 2011	Jan. 2012	24h survey
^{222}Rn	35	59 (4)	50 (7)	84
$^{224\text{-}226\text{-}228}$Ra	4	8 (1)	14 (1)	
^{223}Ra			14	
E.C., Temp.	*	*	*	84
Nitrate	*	*	*	14
Chlorophyl	*	*	*	
Turbidity	*	*	*	

Chapter 4

New interpretations of historical information

4.1 Introduction

Understanding the behavior and the evolution of a hydrogeological system in transient state requires a global overview of the processes that are taking place. This is generally not a simple task, as it requires searching, synthesizing and crossing all measurements and all data that can be found, even in datasets and archives that have apparently nothing to see with hydrogeology. In addition, in multi-layer aquifers like Campo de Cartagena, where long-screened boreholes are common, the basic steps before the analysis of official time series is a reliable assessment of the origin of groundwater samples, in order to avoid misinterpretation.

This chapter starts with the description of the dataset used in this investigation, before describing the construction of a 3D geological model. Then, it develops the new interpretation of the historical information concerning the evolution of the Campo de Cartagena multi-layer aquifer system along the last 150 years. It includes various sources such as old newspapers (up to 150 years), old hydrogeological studies (up to 100 years) and more recent (i.e. the last 40 years) time series of the water-table levels and geochemical surveys conducted by IGME. Indeed, a method is proposed for identifying the aquifer of origin of unknown samples out of a geochemical database.

4.2 3D Geological model

The geometrical characterization of a geological object is fundamental, not only for the mining industry or for structural geology, but also for identifying the spatial extent of aquifers and the possible variations of their hydrodynamic characteristics. This is a pre-requisite for the reliability of numerical flow and transport models.

One of the initial objectives of this thesis was to build a groundwater flow model representative for the Campo de Cartagena multi-later aquifer system. A large effort was therefore dedicated to the geometrical analysis of the aquifers of the area and the integration into a 3D geological model.

Different sources were exploited: geological cross-sections and additional information from the new geological maps of the area (IGME, 2005); reinterpretation of the data from the main references regarding geometrical aspects (ITGE, 1989) and the recent review by Jiménez-Martínez et al. (2012); information from INC boreholes; stratigraphic columns from

the new boreholes of the Segura Basin Authority (Confederación Hidrográfica del Segura, CHS); reports on deep injection of brines from desalination (Ramos 2003; Ramos y Sánchez, 2003); boreholes from oil and gas exploration; investigations for CO_2 storage; reports on geothermal energy (IGME, 1982); geophysical investigations (seismics, gravimetry, SEV etc) and boreholes drilled within a parallel project (Séneca 08225/PI/08).

Finally, this information was integrated with the marine geology data from IGME (1990), including: bathymetry, isopachs of the Plio-Quaternary (top of the Messinian) and of the Betic basement (including the Triassic formations). Figure 15 and Figure 16 show an example of the final results.

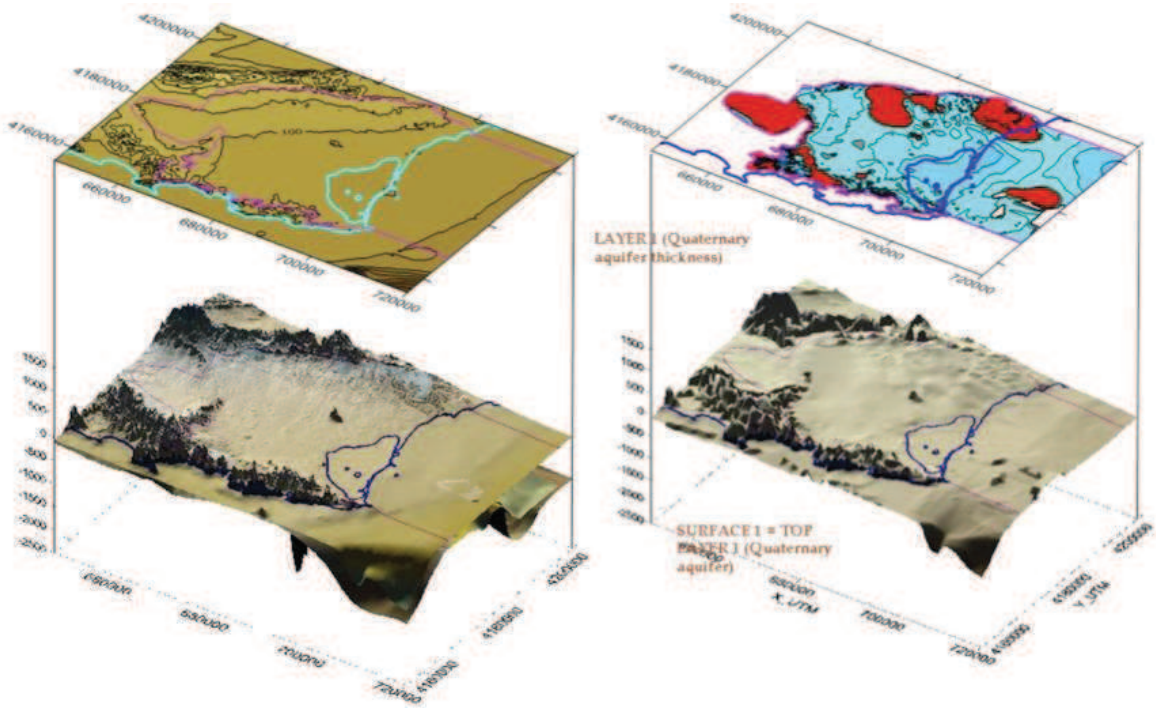

Figure 15: Map of isohypses and 3D representation of the surface (left). Isopachs and 3D representation of the base of the Quaternary aquifer (right).

In fact, it was not possible to run the groundwater flow model during the PhD time but the time consuming task of building the 3D geological model constitutes a significant progress for the present work and for further projects. In addition, it provides useful physical indications on the boundaries of the aquifer system.

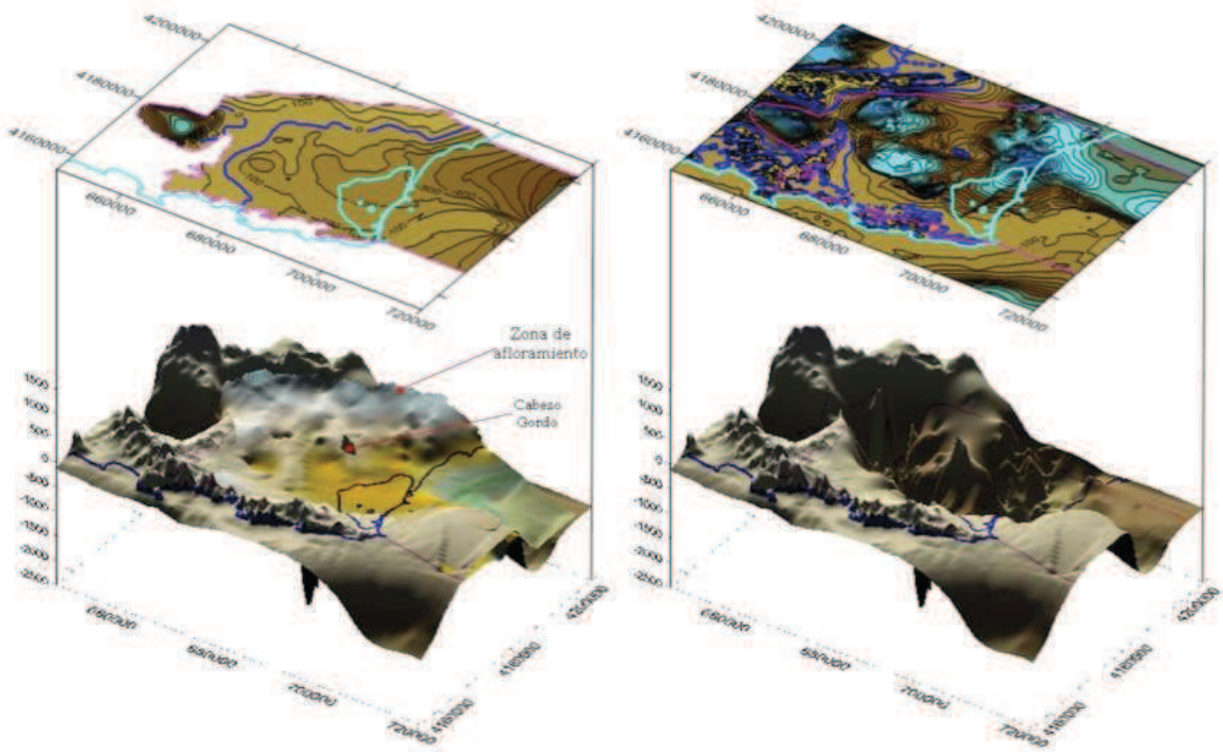

Figure 16: Map of isohypses and 3D representation of the top of the Messinian aquifer (left) and of the Betic basement (right).

While elaborating the geological model, many problems appeared. For example, no criteria was found to limit the Pliocene aquifer to the western border of Mar Menor, although this possibility was proposed in previous studies (e.g. Rodríguez-Estrella, 2004). Its limit would be located along the eastern border of Mar Menor (La Manga), since the existing geological data from the continental platform did not indicate its presence further to the east.

As well, the existing geological data in the continental platform indicates the eastern limit for the Messinian aquifer to be located in the marine zone, 11 km further below the Mediterranean Sea. The extent of the Tortonian aquifer remains also hard to assess because of the important and frequent lateral changes in facies. There is no information on possible deeper aquifers, as deep boreholes (up to 1000 m) for CO_2 and brines storage did not detect any Aquitanian-Burdigalian aquifer formations.

4.3 One century of groundwater exploitation

The first reports mentioning the importance of the Campo de Cartagena area are almost contemporary with the creation of the Spanish Geological Survey (IGME) in 1849. Historical

information reveals a clear link between the mining and metallurgical industry (Cartagena-La Union Mountains) and agriculture on the land. This is explained not only by the experience in drilling and the available equipment, but also by the sources of direct private investment.

In the middle of the XIXth century, various authors mentioned the existence of an artesian basin in the Campo de Cartagena area (e.g. Peñuelas, 1851). In the early XXth century, several publications encouraged drilling artesian boreholes (e.g. Mesa y Ramos, 1909), motivated by mining investigations (Villasante, 1913; Guardiola, 1927) and by reports from IGME (Dupuy de Lome et al. 1917; Marin, 1925). The first hydrogeological report of the hydrogeology of the Campo de Cartagena (Rubio, 1928) described the "artesian basin" and mentioned the existence of a large number of artesian boreholes, reaching depths above 200 m in some cases (Figure 17).

The first artesian borehole was performed in 1915 by Sánchez Madrid close to Los Alcázares, with a total depth of 205 m. Most probably, it reached the Messinian aquifer. Then, in the 1920s, a large number of artesian boreholes were drilled. Artesianism seems to have ended in the Messinian in the beginning of the 1930s, but the name "artesian well" remains in the cultural tradition.

Although only little information is available regarding hydrogeological aspects of the Campo de Cartagena in the 1930s, 1940s and 1950s, indirect data can be obtained from the Campo de Cartagena Association of Irrigators, founded in 1952. In addition, Román (1996) reviewed several aspects of land use and exploitation and analysed the historical evolution of hydraulic technology and extraction systems along the XIXth and XXth centuries.

In the early 1960s, IGME pointed out the need to extend the irrigated areas of Spain and initiated a series of systematic and exhaustive hydrogeological studies focussed on groundwater exploitation. The first investigations were conducted in the Region of Murcia together with the Instituto Nacional de Colonización (INC) and the Region of Murcia (Excma. Diputación Provincial de Murcia). The results highlighted the existence of a large number of wells and boreholes in the area (Trigueros et al., 1962). Between 1961 and 1962, INC financed the drilling of at least 18 boreholes in the Campo de Cartagena, with maximum depths of 400 m (INC, 1962).

Figure 17: Historical document from Rubio (1928) including a) theoretical sketch of the artesianism in the basin, b) map of extent, c) stratigraphic column in the Barrionuevo borehole (San Javier) and d) interpretative cross section.

In the 1970s were performed the investigations leading to the Plan Nacional de Investigación de Aguas Subterráneas (PIAS). This ambitious program synthesized the state of the art about the aquifers of the country. The report corresponding to the Campo de Cartagena (IGME-IRYDA, 1978) was exclusively based on data collected during the 1970s investigations, without any reference to previous study or previous data. As most studies published later supposed that no data existed before the PIAS programme, important information like artesianism that was not cited in PIAS was never cited again.

In the 1980s various groundwater investigations were realized by IGME. The report "Las aguas subterráneas del Campo de Cartagena" (IGME, 1994) remained as the major reference until the recent studies by CARM (2000).

4.4 Boreholes inventory

More than 40 years of groundwater survey by IGME provides a large quantity of geochemical and piezometric data, covering a large spatio-temporal range. But most boreholes were drilled by private owners on their own initiative and, because of the lack of technical information for most of them, the origin of groundwater samples and the significance of water table measurements are usually highly questionable. Identifying representative boreholes for each aquifer layer, which is a basic step for any hydrogeological study, is a difficult task here.

In order to determine the aquifer(s) corresponding to each sample, all available information about close to 2000 tubewells was collected and reviewed. Most data came from the last inventory of wells by IGME, started in 1973 and partly updated at the beginning of the 1980s. Complementary partial inventories (e.g. Conesa-García, 1990) were added, as well as technical reports provided by well owners and drilling companies. The review of the data was based on the following criteria: total depth, depths of the screens, presence of a cement ring, age and state of conservation of the tubewells, and the water table evolution (when available).

Based on these criteria, an Aquifer Reliability (AR) index was established to weight the reliability of the aquifer assessment for each tubewell. Three levels were defined: A (high reliability), B (medium reliability) and C (low reliability). "A" class was assigned when more than two different informations were present and uniformly indicated whether a unique

aquifer of origin or a potential mixing between aquifers. “B” class was assigned when only two informations were coherent. “C” class was assigned when only one information was available. This index did not take into account any chemical or water table data. Indeed, this review highlighted that some previous hydrogeological studies had partially inappropriate aquifer assessment, leading to hazardous interpretations. In order to check the descriptions, the 475 boreholes belonging to one of the three A, B, C classes were checked in the field. An example of the results is given by Table 4.

Table 4: Example of the results of the boreholes inventory. The asterisks indicate tubewells where the review did not confirm the official aquifer assessment.

Tubewell ID	Aquifer (Official)	Aquifer(s) (Review)	AR Index
263880001	Quaternary	No information*	C
273750016	Tortonian	No information*	C
273760008	Pliocene	Quaternary+Pliocene*	A
273760009	Pliocene	Pliocene+Messinian*	A
273760019	Quaternary	Quaternary	B
273760064	Messinian	Messinian	C
273760079	Tortonian	No information*	C
273760083	Messinian	No information*	C
273770020	Messinian	Messinian	C
273770026	Messinian	Messinian	B
273780003	Messinian	Messinian	B
273780013	Quaternary	Quaternary	B
273780014	Messinian	Quaternary+Pliocene+Messinian*	B
273780029	Messinian	Messinian	C
273780061	Messinian	Quaternary+Pliocene+Messinian*	A

Although this review represents a crucial advance for identifying representative boreholes, a large number of them remain not identified. Out of a total of 1845 boreholes, 290 were identified as corresponding to a single identified aquifer layer, 377 to a potential mixing between several aquifer layers by intra-borehole flow (e.g. Ma et al., 2011) and 1178 boreholes remained of unknown origin.

The corresponding numbers of boreholes with at least one piezometric data were and 125, 51 and 9, respectively. As well, boreholes with at least one geochemical analysis were 154, 142 and 334, respectively.

4.5 Water table evolution

Investigating a groundwater system in transient state supposes an effort of reconstitution of its presumed steady state. In highly anthropized areas like Campo de Cartagena, a key task is to understand and evaluate the modifications occurred as a consequence of intensive agriculture. To this end, data collected by IGME since 40 years was combined with historical data presented in section 4.3 in order to reconstitute groundwater levels all along the exploitation period, i.e. the last century.

A good example is the western part of the Campo de Cartagena around the town of Fuente Alamo. This area does not receive water from the TTS and it is settled on the Triassic and Quaternary aquifers. As the Triassic water quality is adapted to an agricultural use and the transmissivity of this formation allows a high pumping, it is intensively exploited. According to IGME data, in the last five years, levels have been quite stable: around 350 m below sea level (Figure 18). This case is exceptional at the Mediterranean scale, as such levels cannot correspond to a natural state. The analysis of IGME data reveals a continuous decrease of the water table level, from sea level since the early 1980s to 350 m below sea level in 2012, i.e. more than 10 m per year. Although no older IGME data is available, the review of INC reports reveals that water table levels were around 70 m above sea level in the mid-1960s. The Quaternary aquifer levels were stable in the 1970s, and similar to the present state, i.e. around 115 m above sea level.

The estimation of the water table levels in the 1920s was based on several archaeological reports like Gómez et al. (2012) and Berrocal Caparrós et al. (1999) and on the specificity of the town of Fuente Alamo. As indicated by its name ("Poplar spring"), the settlement of this town was conditioned by a permanent surface flow in the rambla that reveals gaining conditions. In this area the Quaternary sediments underlying the stream form a thin cover of low permeability (Gómez et al., 2012) that borders the lower topographic outcrop of the Triassic aquifer. The most logical source for water would therefore be the discharge of Triassic groundwater into the foothill and then into the Quaternary sediments, as described by Lillo Carpio (1978) in other places of the area. This assumption is supported by two points i) the absence of springs originating directly from the Quaternary aquifer in the Campo de Cartagena and ii) the good quality of the water, that was used for drinking supply in Fuente Alamo (Gómez et al., 2012), while the Quaternary groundwater in the close

surroundings had an important salinity (Gómez et al., 2012). Therefore, the water table level from the Triassic aquifer (Figure 18) at the beginning of intensive groundwater exploitation (1920) was probably close to the level of the Rambla in Fuente Alamo. A very close level was assessed for the Quaternary aquifer, as local old dug wells indicated levels close to the one of the rambla.

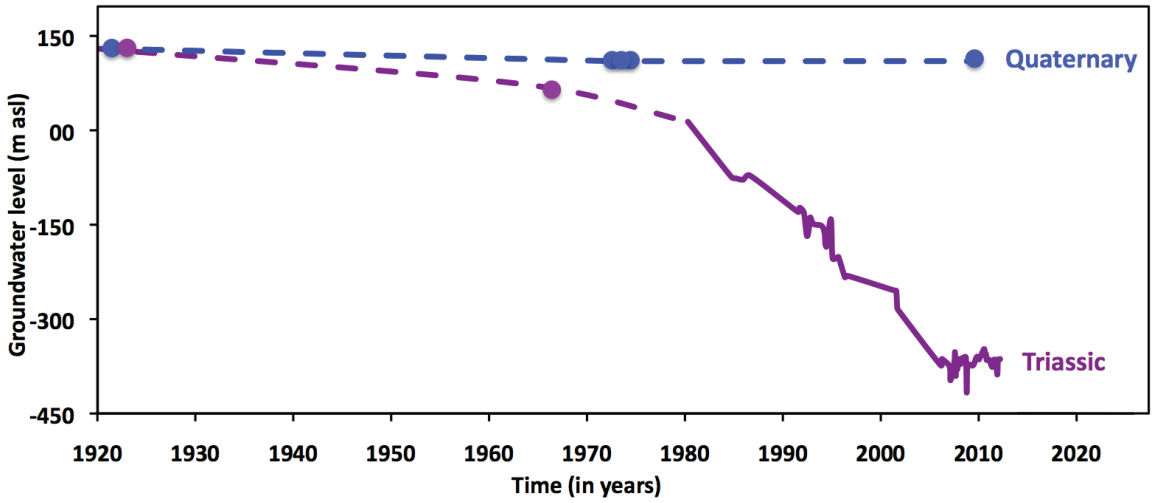

Figure 18: Long-term variations of groundwater levels in the western area. Dots correspond to punctual values obtained from the present reconstitution. Discontinuous lines correspond to reconstructed evolution.

Another notable illustration of the consequence of anthropization is found in the southeastern part of the Campo de Cartagena, a few kilometres away from the coast line. For the last 10 years of piezometric data (2000-2010), groundwater levels have been quite stable in this area (Figure 19) : they are often 15-18 m amsl (Quaternary), 15-23 m bmsl (Pliocene) and 51-86 m bmsl (Messinian). Despite the low heads in the confined levels, there is no evidence of sea-water intrusion yet. The piezometric measurements by IGME, started in the mid-70's, show that the present stability follows a gradual groundwater recovery, linked with the TTS implementation as an external source of water in the early 80's.

In the same area, the interpretation of the observations of artesian boreholes at the beginning of the XXth century allows estimating groundwater heads at this period: about 25 m amsl in the Pliocene aquifer and 45 m amsl in the Messinian aquifer. Surprinsingly, the hydraulic heads decrease with the depth of the formation (i.e. highest level in the Quaternary, followed by the Pliocene and followed by the Messinian), which is the opposite of the situation one century ago. The vertical hydraulic gradients between layers have been inverted

and the flow between aquifers through long-screened boreholes has occurred in both directions, downwards or upwards, corresponding to these two distinct phases. This case highlights the need of reconstituting long time series for a more realistic interpretation of the system evolution.

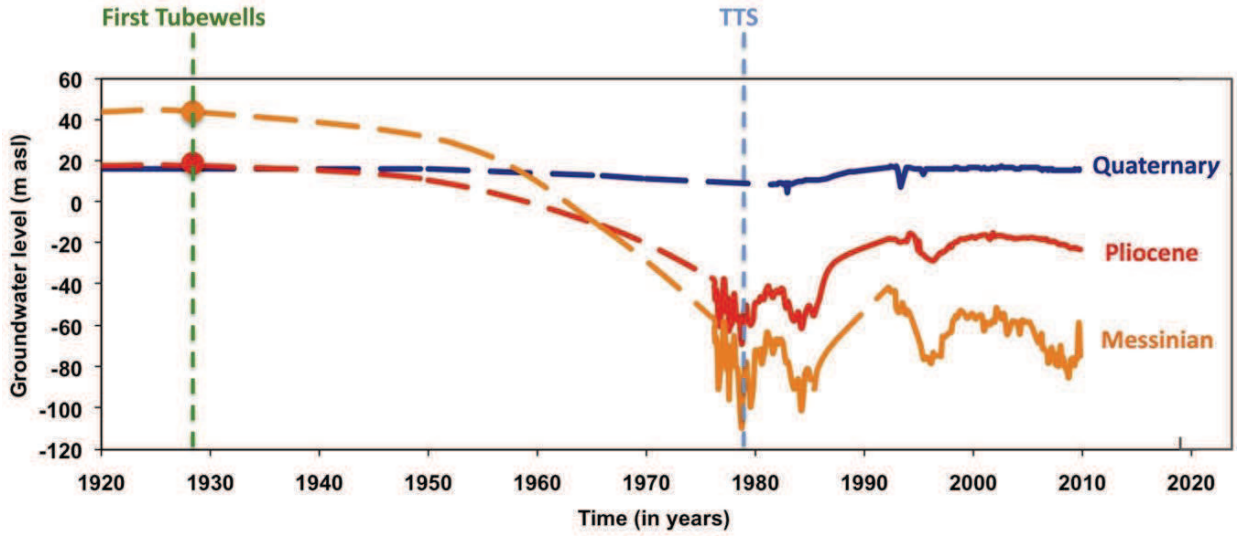

Figure 19: Long-term variations of groundwater levels in the mid-northern coastal area. Dots correspond to punctual values obtained from the present reconstitution. Discontinuous lines correspond to reconstructed evolution.

4.6 Geochemistry

Geochemical data was collected from a wide variety of sources. More than 80% came from the official groundwater quality surveys performed between the early 1970s and early 2000s by IGME. Complementary data was provided by the Confederación Hidrográfica del Segura (CHS), in several sampling campaigns from 2005 to 2008 and from 2010 to present. Additional geochemical data came from research projects conducted by the Universities of Granada (2009, unpublished data), the University of Murcia (2009 and 2011, unpublished data) and the IDES laboratory of the University Paris Sud (2011, unpublished data). Data from unpublished IGME reports and groundwater analysis kindly eased in the field by wells owners during the fieldwork of this investigation was also included. The final dataset is composed by 1,549 groundwater samples (Table 5) collected in 497 boreholes over a wide range of years, sampling conditions, analytical methods and aquifers. Information about the borehole design was only available for 296 (15%) of the boreholes.

Table 5: Summary of the groundwater samples included in the dataset. Values between brackets correspond to complete Cl^-, SO_4^{2-}, HCO_3^-, NO_3^-, Ca^{2+}, Na^+, Mg^{2+}, K^+ and SiO_2 geochemical data

COMPLETE GEOCHEMICAL DATASET		Number of samples	Number of tubewells
All samples	**TOTAL**	**1549 (761)**	**497**
BOREHOLE INFORMATION			
Samples from one only aquifer	Quaternary	392	62
	Pliocene	78	20
	Messinian	238	61
	Tortonian	29	5
	Triassic	68	6
	sub-total	**805 (468)**	**154**
Mixing of different layers	**sub-total**	**409 (182)**	**142**
No data on aquifers	**sub-total**	**335 (111)**	**201**

In addition to the Piper diagram (Figure 20), various graphical and multivariate statistical techniques were applied to samples of each aquifer in order to facilitate the water classification: Stiff pattern diagram, Schoeller semi-logarithmic diagram, hierarchical cluster analysis (HCA) and principal components analysis (PCA). Nonetheless, this did not help to identify clear trends that would reflect spatio-temporal phenomenons, distinct mineralisation processes or mixing patterns. As a consequence, only a very limited use can be made out of the major ion geochemistry.

From the 1549 groundwater samples, 1014 have an absolute Ionic Balance Error (IBE) below 5%, 131 have a IBE above 5% and the IBE calculation is not possible because of the lack of chemical elements in 404 samples. Based on the 805 samples from one single aquifer, the geochemical water-type of each aquifer was assessed. The Piper diagram for samples with high and medium degree of reliability (AR=A and AR=B) is presented in Figure 20. The Tortonian and Triassic aquifers are well differentiated, with Mg-Na-HCO3 and Ca-SO4

water types, respectively. Nonetheless, the Quaternary, Pliocene and Messinian aquifer are all included in the same Na-Ca-Cl to mixed-Cl water type.

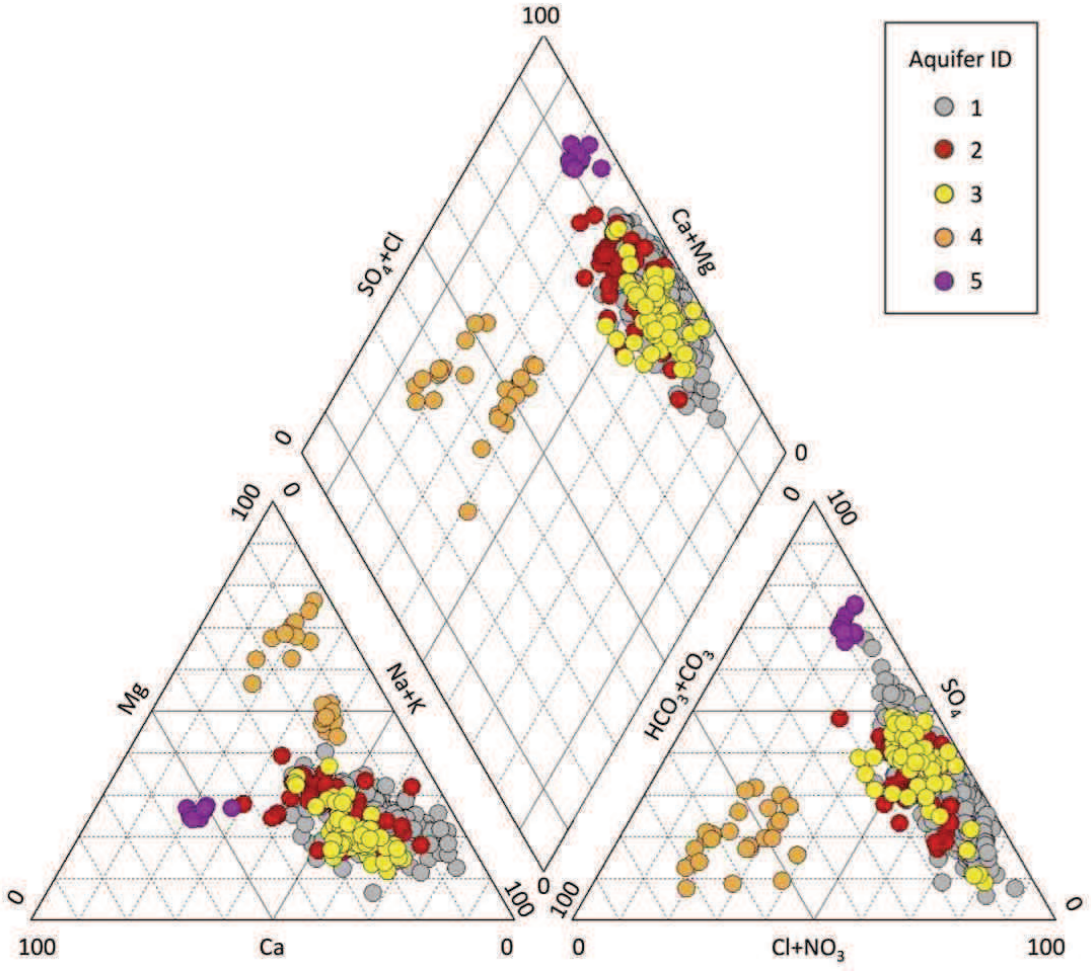

Figure 20: Piper diagram for the samples from single identified aquifer tubewells with AR=A. 1=Quaternary, 2=Pliocene, 3=Messinian, 4=Tortonian, 5=Triassic.

This similarity between water types in the three upper aquifers is a strong limitation to the geochemical differentiation. This could be partly explained by: i) the likeness of the aquifer sediments, responsible for a similar mineralization of groundwater (confirmed by similar saturation rates); ii) the inside-borehole mixings between water masses (Jiménez-Martínez et al., 2011), which could have impacted the groundwater quality at a regional scale and iii), regarding the Quaternary aquifer, the irrigation return flow that mixes water coming from the lower layers into this upper one.

Only nitrate was identified as a qualitative indicator of recent recharge to the Quaternary aquifer, since concentrations up to 450 mg.l^{-1} were measured in the last decade in some Quaternary boreholes. Nonetheless, the concentrations are very variable in space and time, certainly influenced by the fact that nitrate measurements remain very sensitive to the redox conditions in the aquifers but also during and after sampling. An attempt was made (Jimenez-Martinez et al., 2010) to use nitrate as an indicator for local groundwater mixing through boreholes between the Quaternary and Pliocene aquifers, based on the observation of increasing nitrate contents in the Quaternary and Pliocene aquifers. Nonetheless, the borehole inventory presented in section 4.4 revealed that the boreholes considered as representative of the Pliocene aquifer in this 2010 study were actually long-screened, with communication between aquifers. Their interpretation is then questionable.

At a larger scale, once updated the geochemical dataset according to the new borehole inventory, no nitrate contents higher than 50 mg/l was found in any of the deep aquifers (Pliocene to Triassic). Still, values higher than 15 mg/l were found in 11% of the samples from the deep aquifers and are not evident to explain, as discussed in section 5.4.1.

4.7 Origin of groundwater samples

The new borehole inventory revealed that a limited number of boreholes featured enough information to assess the aquifer of origin of groundwater samples and the representativeness of piezometric measurement. In order to obtain a higher number of samples representative of each aquifer, a statistical method predicting the correct aquifer layer for any groundwater sample could be a solution.

Statistical methods have been widely used in hydrology and hydrogeology (e.g. Adams et al., 2001; Lambrakis et al., 2004; Cloutier et al., 2008; Daughney et al., 2012), generally as a tool to subdivide and classify large hydrogeochemical datasets to facilitate interpretation. They may also be used to estimate mixing proportions (e.g. Valder et al., 2012). The techniques most applied are the aforementioned PCA and HCA. However, these methods show several limitations, like the difficulties to define classes in highly homogeneous datasets and the subjectivity of the criteria defining the classes. In addition, PCA and HCA belong to unsupervised classification methods (Table 6). It means that they can be used to

create a set of classes out of the whole dataset, but they cannot assign samples to a set of a priori classes.

In contrast, in the supervised classification approach (Table 6), the prediction of the output class of any new sample is enabled by a set of decision rules (classification model) defined out of a set of labelled training samples. Indeed, there would be a possibility to identify the aquifer of origin of a groundwater sample based only on its geochemical composition with a supervised classification model, once calibrated with a previous dataset of samples from each one of these aquifers.

Table 6 : Overview of the relations between the main classification methods.

Unsupervised		Supervised		
PCA	HCA	LDA	CART	Neural networks
			RF	

Linear Discriminant Analysis (LDA) is a classical multivariate technique for supervised classification (Vaselli et al., 1997). However, traditional statistical methods have been proven inadequate to identify complex patterns and relationships that require more sophisticated procedures (De'ath and Fabricius, 2000). These new procedures include computer intensive machine learning techniques based on recursion, sampling and randomizations (Babovic, 2005; Prasad et al., 2006).

Approaches based on decision trees (Breiman et al., 1984) are among the most applied supervised classification methodologies. Random Forest (Breiman, 2001), is the one that have recently received most interest. It combines a large number of decision trees (usually 500 to 2000) to obtain a more accurate classification without overfitting the model to a specific dataset.

Studies using Decision Trees are found in remote sensing (e.g. Guhimre et al., 2010), medicine (e.g. Lempitsky et al., 2009), genetics (e.g. Cutler and Stevens, 2006), chemistry (e.g. Svetnik et al., 2004), ecology (e.g. Cutler et al., 2007, Peters et al., 2008, Elsenber, 2011) or soil sciences (e.g. Schmidt et al., 2008). LDA was applied to classify groundwater samples only in rare occasions (e.g. Lambrakis et al., 2004). Other machine learning methods as Neural Networks are more frequent in Hydrogeology (e.g. Kurtulus and Razack, 2007),

but they are more difficult to calibrate and were not used in the present study. Except the recent studies by Smith et al. (2010) on bacterial source tracking in lakes and Olson and Hawking (2012) on stream base-flow water chemistry, no study using Random Forest was found in Hydrogeology or for the analysis of hydro-geochemical datasets. The Random Forest classification method was therefore tested to determine the origin of groundwater samples from undocumented boreholes based on their geochemistry. Linear discriminant analysis and a simple classification tree were also used to compare results.

4.7.1 Methodology

4.7.1.1 Training dataset

The first step in building a supervised classification model is to collect and prepare a "learning" or "training" dataset to be analyzed. It is used to learn how the value of a qualitative variable, or « target variable » (here, the aquifer layer) is related to the values of a set of « predictor » variables (here, the geochemical ions).

The 805 samples from a single identified aquifer were used to calibrate the model. The model was then used to estimate the aquifer of origin of the 335 samples for which no design information was available and had a complete dataset. The geochemical ions (thereafter called variables) selected to perform the classification are the concentrations (expressed in mg/l) of Cl-, SO_4^{2-}, HCO_3^-, NO_3^-, Ca^{2+}, Na^+, Mg^{2+}, K^+ and SiO_2.

One of the problems encountered was that the nine concentrations were not measured in all the samples. Only 468 of the 805 labeled samples included all the nine variables needed to calibrate and validate the models. Minor and trace elements were not taken in consideration due to the very limited number of samples featuring their determination.

4.7.1.2 Models used

Once obtained and prepared the training dataset, several models were run to assess which one would provide the most accurate classification model in relation to the defined categories. Three models were run first: Linear discriminant analysis (LDA); Classification and regression trees (CART) and Random Forest (RF). After eliminating the less reliable samples, the RF model became RF1. Then, a number of samples assigned to one aquifer that

did not feature all variables were added to RF1, providing the RF2 model. These 5 models are detailed thereafter.

4.7.1.2.1 Linear Discriminant Analysis (LDA)

LDA (Vaselli et al., 1997) is one of the simplest methods for supervised classification. It is used to classify samples into mutually exclusive groups on the base of independent variables. This objective is attained by maximizing the between-group variance and minimizing the within-group variance. It is closely related to the unsupervised principal component analysis (PCA) in that they both look for linear combinations of variables that best explain the data. An important assumption of LDA is that the independent variables are normally distributed. If only two variables are available, the separators between the groups will become lines. If three variables are available, the separator is a plane. When the number of variables is higher than three, the separators become a hyper-plane.

4.7.1.2.2 Decision Trees

Decision trees are used to build a model by a recursive binary partition of a labeled dataset into increasingly homogeneous nodes (Figure 21). Homogeneity is measured with the Gini index (Breiman et al., 1984), defined as $G = \Sigma k\ p_k \cdot (1 - p_k)$, where p_k is the proportion of observations in the k^{th} class. This index is minimized when all observations belong to the same class. At each step the node with the highest G value is split; a an optimization is done to select the predictor variable and the numeric threshold, or group of values is the variable is categorical, that would produce the lowest G value in the subsequent nodes The splitting process continues until no further subdivision can reduce the Gini index (Cutler et al., 2007).

The final result should be a fully-grown classification tree whose lower nodes include cases belonging to just one class. However, the lower nodes are seldom, if ever, completely homogeneous. In this case, the predominant class is used to label the node, being the other cases classification errors. On the basis of these errors it is possible to prune the tree to allow a higher generalisation capacity. A typical pruned classification tree has 3 to 12 terminal nodes. This trained decision tree can then be used to classify an unlabeled dataset. Interpretation of classification trees increases in complexity as the number of terminal nodes increases (Cutler et al., 2007).

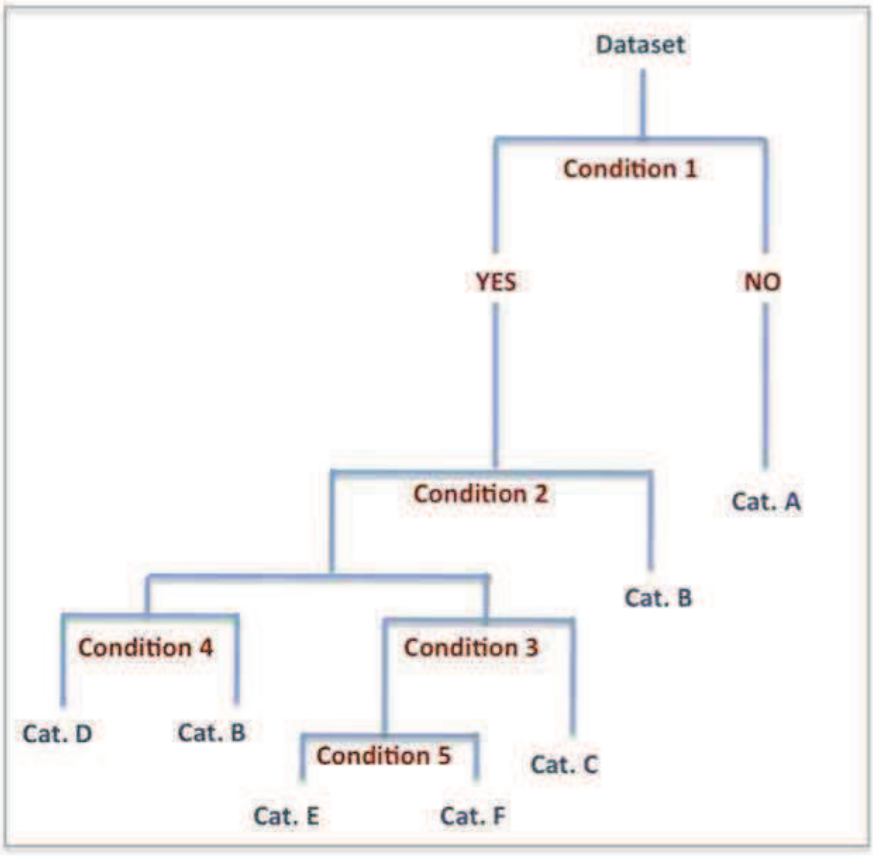

Figure 21: A decision tree

4.7.1.2.3 Ensemble Learning

The main problem of classifying with a unique tree is its high sensitivity to the input data, small modifications in the dataset can produce completely different models. Ensemble Learning techniques have recently received much interest as a tool to overcome this limitation of decision trees, to obtain better predictive performance.

Bagging (Breiman, 1994) is one of the most used ensemble learning methods. It generates independent trees by re-sampling the same dataset by bootstrapping. That is generating new datasets of the same size as the initial one by random sampling with replacement. Around 67% of the original observations occur at least once in each new generated dataset.

Observations not included in any of the new datasets are called "out-of-bag" observations. The trees obtained are not pruned and are used to classify the out-of-bag observations. As each initial observation is included inside the out-of-bag of several trees, its

class is estimated several times. The final estimation assigns each observation to the most "voted" class (Liaw and Wiener, 2002).

4.7.1.2.4 Random Forest (RF)

Random Forest (RF) is a bagging based method proposed by Breiman (2001). It generates a large number of trees (500 to 2,000) using bootstrapping (Figure 22); each tree is then trained using a randomized subset of the predictors. This somewhat anti-intuitive modification adds randomness to bagging and decreases the correlation between trees. Uncorrelation is a desiderable property in ensemble learning classifiers to guarantee that different results give sense to the voting system. Random Forest produces very good results compared to other machine learning based classification systems (Support Vector Machines or Neural Networks) or to other decision tree algorithms (Breiman, 2001; Liaw and Wiener, 2002).

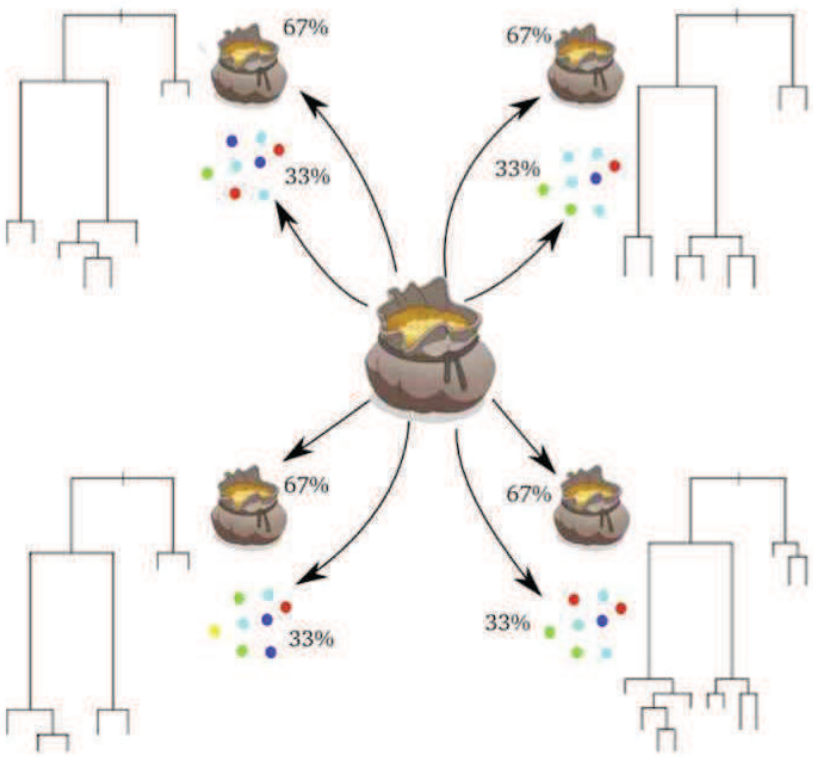

Figure 22: Illustration of Random Forest showing 4 new generated datasets originated by bootstrapping, and the corresponding classification trees. Around 67% of the original observations occur at least once in each new generated dataset and the other 33% are classified.

Random Forests do not overfit the model to the dataset since the classification error of one permutation can be overcome by the ensemble of permutations (Ghimire et al., 2010). This way the large number of trees reduces generalization error (Breiman, 2001; Pal, 2005; Prasad et al., 2006). Since the out-of-bag observations are not used in the fitting of the trees, the out-of-bag estimates can be used to perform a cross-validation accuracy estimation (Cutler et al., 2007).

One of the parameters that can be set up by the user is the number of variables included in each classification tree. Nevertheless, the method does not seem to be very sensitive to this value, which is by default the square root of the total number of variable used (Gislason et al., 2006).

Another user configurable parameter is the number of generated trees, although a higher number does not seem to provide a substantial increase in the classification accuracy (Liaw and Wiener, 2002). In general, random forests do remarkably well and require very little tuning (Hastie et al., 2003).

A disadvantage of Random Forest compared to the simple classification tree approach is that individual trees cannot be examined separately, thus becoming a “black box” approach (Prasad et al., 2006).

However, it does provide several metrics that help in interpretation. Variable importance is evaluated based on how much worse the prediction would be if the data for that predictor were permuted randomly. The resulting values can be used to compare relative importance among predictor variables. In this way, the procedure is much more interpretable than methods such as Neural Networks, and it has been called a “grey box” approach (Prasad et al., 2006).

4.7.1.2.5 Validation

Random Forest includes its own cross validation procedure (out-of-bag cross validation). While some authors consider it unnecessary to perform a separate cross-validation (Efron and Tibshirani, 1997; Breiman, 2001; Svetnik et al., 2004), others like Mitchell (2011) affirm that this internal cross validation can generate biases in the classification. Although it is computationally more intensive, it was preferred to perform a

separate leave-one-out cross validation to compare Random Forest results with other methods' (LDA and decision trees) with the same validation tool. The results of a cross-validation are organized in a confusion matrix (Table 7) where columns (*j*) correspond to real classes, and lines (*i*) show the model results. Each element of the n_{ij} matrix represents the number of observations corresponding to class *j* that were classified as class *i*.

Table 7: Mathematical illustration of a confusion matrix. Adapted from Congalton and Green (2008).

	j=columns (true class)						**row totals**
i=rows (model class)		**1**	**2**	**3**	…	**J**	***ni*+**
	1	*n*11	*n*12	*n*13	…	*n*1*J*	*n*1+
	2	*n*21	*n*22	*n*23	…	*n*2*J*	*n*2+
	3	*n*31	*n*32	*n*33	…	*n*3*J*	*n*3+
	…	…	…	…	…	…	…
	I	*nI*1	*nI*2	*nI*3	…	*nIJ*	*nI*+
tot. column	***n*+*j***	*n*+1	*n*+2	*n*+3	…	*n*+*J*	*n*

Several indices measuring the accuracy of the classification can be generated from the confusion matrix (Congalton and Green, 2008). The overall accuracy is the proportion of cases in the principal diagonal. The omission error of class *i* is the proportion of cases from class *i* not classified as such. The commission error of class *i* is the proportion of cases incorrectly classified as class *i*. Finally, the kappa index corrects the overall accuracy for random chance agreement as detailed in Congalton and Green (2008):

4.7.1.3 Formulation of tested models

A general schema of the methodology used in this study is shown in Figure 23. Five models were tested:

1. Linear Discriminant Analysis (LDA)

2. Classification Tree using the CART algorithm (CART)

3. Random Forest (RF0)

4. Random Forest eliminating unreliable samples (RF1)

5. Random Forest eliminating variables to increase accuracy (RF2)

Several algorithms to apply classification tress have been proposed. In this study the Classification and Regression Trees (CART) proposed by Breiman et al. (1984) was used.

Model RF1 was an attempt to increase the accuracy of the results by the detection and elimination of unreliable samples (Figure 20). Two strategies were applied. First, the ionic balance for each water sample was calculated to determine if errors in classification could be related with errors in the balance.

Secondly, the qualitative evaluation of the reliability of the aquifer assessment (AR) for each borehole was considered. As for the previous case, the aim was to assess whether unreliable ground water samples decreased the accuracy of the classifications.

The purpose of model RF2 was to deal with the decrease in accuracy observed when the number of variables reaches a certain threshold. This phenomenon is known as Hugues effect, or Curse of Dimensionality (Hugues, 1968). It can be attributed to a significant reduction of the sample density in the space of variables as the increase in the number of variables is not compensated by an increase in the sample size.

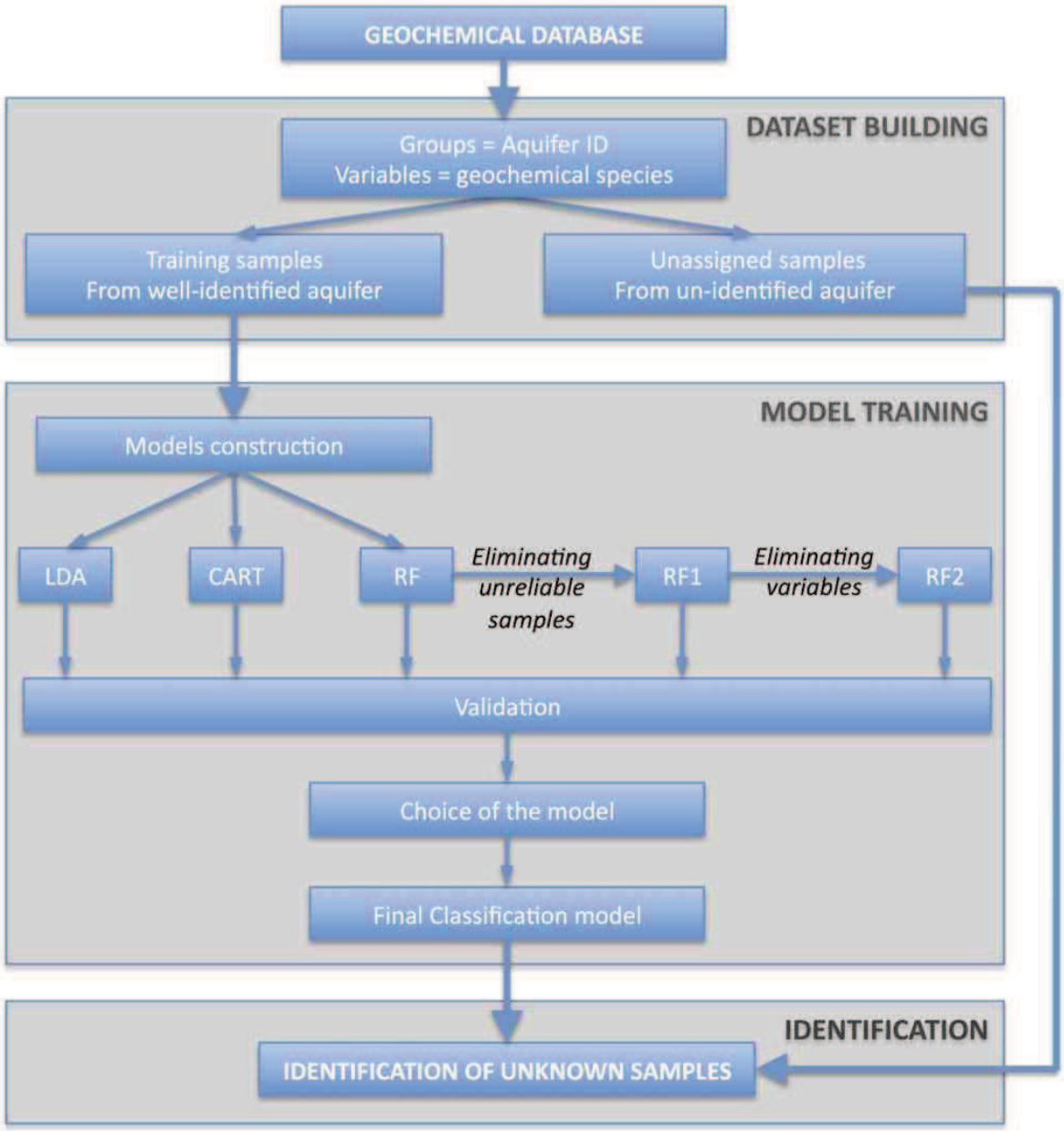

Figure 23: Methodological scheme

Several models were built to analyze this phenomenon and check its effects, starting with the simplest model, with only the most important variable, using Random Forest variable ordination. Then, the variable that most increased the accuracy of the model was added. The selection of this variable was not based on only one classification but on 50 different classifications of each new generated model, so that the random behavior of the Random Forest could be faced.

The corresponding distribution of accuracy parameters are obtained, in this case calculated using out-of-bag cross-validation instead of leave-one-out cross validation to save computing resources and because in this case different Random Forest results are being compared. Using a similar procedure, the other variables were progressively added. The expected result was a fast increase in accuracy when adding the first variables, followed by a stabilization or even a decrease in accuracy, due to the Hugues effect with the incorporation of the less important variables.

The work was carried out with the R programming language (R Development Core Team, 2010) using the R packages *rpart* (Therneau et al., 2011) and *randomforest* (Liaw and Wiener, 2002) that implement the CART and Random Forest algorithms, respectively.

4.7.2 Results and discussion

4.7.2.1 Linear Discriminant Analysis (LDA)

Table 8 shows the results of the LDA classification. Overall accuracy reaches 84.8% with a kappa index of 0.764. Despite of these significantly high values, omission and commission errors reach 100% for the Pliocene aquifer. This means that no sample from the Pliocene was classified as such and that all samples classified as Pliocene were incorrectly classified.

Table 8 : Confusion matrix of discriminant analysis

	Q	P	M	To	Tr
Quaternary	206	7	5	0	0
Pliocene	0	0	1	0	1
Messinian	26	22	130	1	2
Tortonian	1	1	0	24	0
Trias	0	0	4	0	37
Commission error	5.5	100	28.2	7.7	9.8
Omission error	11.6	100	7.1	4	7.5
κ=0.764 Overall accuracy=84.8%					

4.7.2.2 Classification and Regression Trees (CART)

According to the confusion matrix (Table 4), the results are quite good, with an overall accuracy of 88%. As for LDA, the omission error reaches 100% in the case of the Pliocene aquifer; however, the commission error was 0%, meaning that no sample was classified as Pliocene.

Table 9: Confusion matrix of Classification and Regression Trees

	Q	P	M	To	Tr
Quaternary	227	11	11	0	2
Pliocene	0	0	0	0	0
Messinian	5	18	127	2	2
Tortonian	1	1	1	23	0
Trias	0	0	1	0	36
Commission error	2.6	0	10	8	10
Omission error	9.56	100	17.64	11.54	2.7
κ=0.809 Overall accuracy=88%					

In the decision tree produced (: Classification tree generated by CARTFigure 24), each one of the 8 internal nodes is defined by a condition. The sample continues on the left branch if this condition is fulfilled and on the right branch if not. The 9 final nodes correspond to the 5 layers, except Pliocene which, as has been said, did not receive any observation. Another way to display the nodes is to use a binary axis. Figure 25 to Figure 27 illustrate and explain the main geochemical nodes of the classification tree obtained. They show how the first decision rules split the space of the variables into a set of different subregions corresponding to different aquifers.

In the space defined by NO_3^- and Ca^{2+} (Figure 25), a high number of Quaternary samples were correctly classified because of NO_3^- concentrations above 44 mg/l. The number of badly classified samples was 6 from the Pliocene aquifer, 6 from the Messinian and 2 from the Triassic aquifer. One possible explanation could be a mixing with Quaternary water with high contents in NO_3^-. As well, all samples with less than 44.0 mg/l of NO_3^- and less than

55.5 mg/l of Ca^{2+} are directly classified as Tortonian. These include 92% of the Tortonian samples and 3 samples coming from other aquifers, therefore wrongly classified. The samples with less than 44.0 mg/l of NO_3^- and more than 55.5 mg/l of Ca^{2+} generate two sub-trees that are analyzed in Figure 26 and Figure 27.

The first sub-tree involves samples with less than 44.0 mg/l of NO_3^- and Ca^{2+} between 55.5 mg/l and 277.5 mg/l (Figure 26). The definitive assignation (Messinian or Quaternary) of the samples is based on the Mg^{2+} and Cl^- contents. The second sub-tree (Figure 27) includes three variables: Cl^- on the abscissa, HCO_3^- on the ordinate and the threshold in Cl^-, highlighted by the size of the points. Figure 27 also shows how successful the classification in this part of the tree is, with only one error for the Triassic aquifer and three for the Pliocene, probably partly explained by the mixing process cited above. The confusion between Pliocene and Quaternary can be explained by Quaternary nitrate-rich (NO_3^- <44.0 mg/l) water entering the Pliocene through long-screened boreholes, and in some cases with high Cl^- as well. The confusion with the Messinian seems to be linked to the same problem, but it also has to be taken in account that both sample types are located in the same regions of the space of the variables.

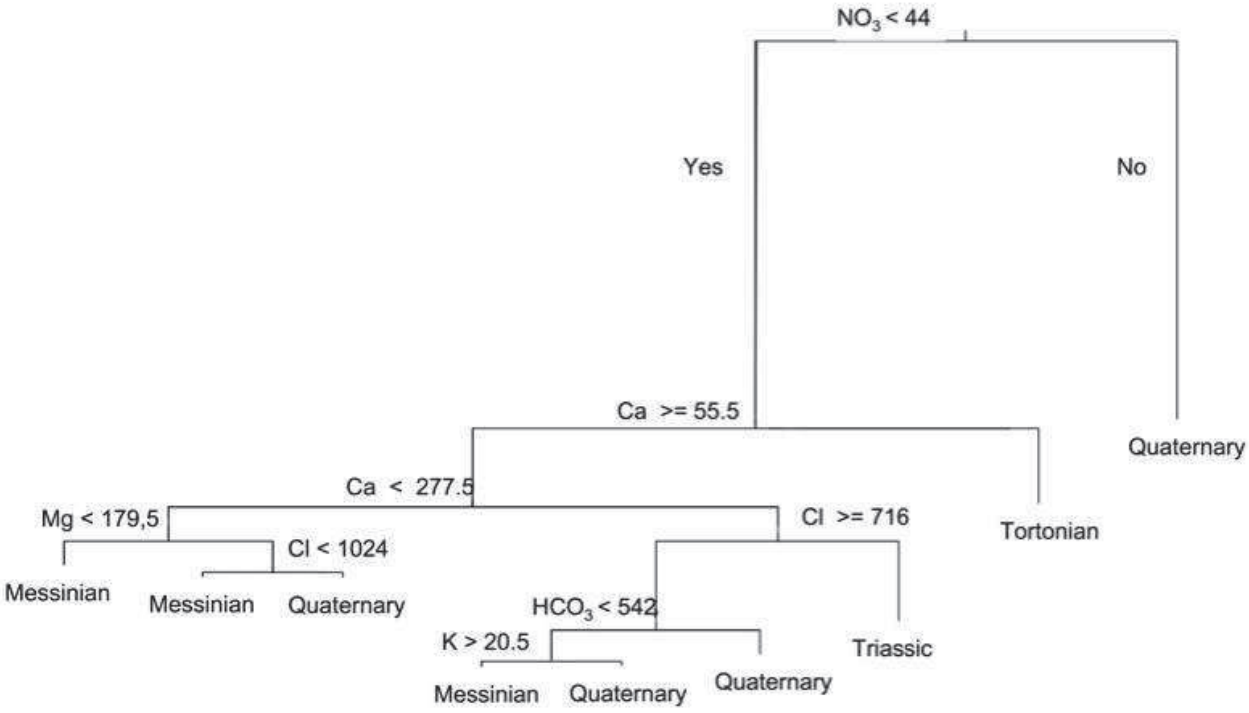

Figure 24 : Classification tree generated by CART

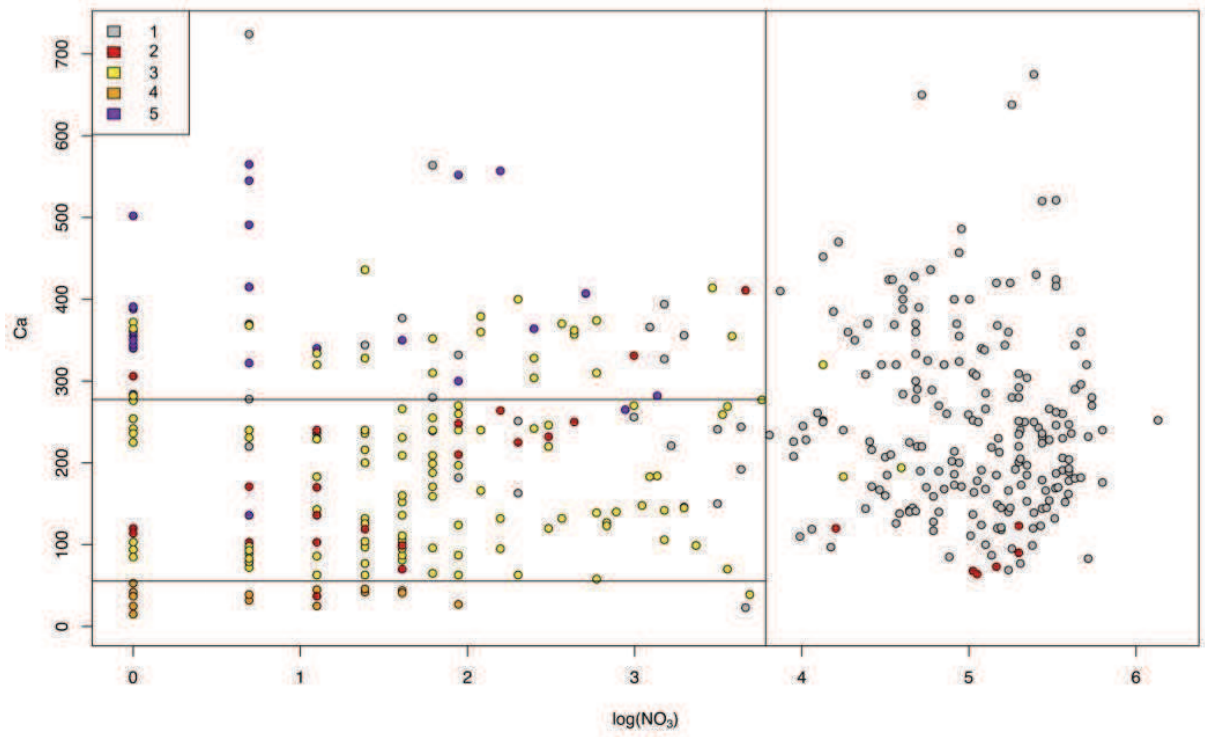

Figure 25: Plot of the NO_3^- < 44, Ca^{2+} >= 55.5 and Ca^{2+} < 277.5 nodes of the decision tree obtained by the CART model (values in $mg.l^{-1}$)

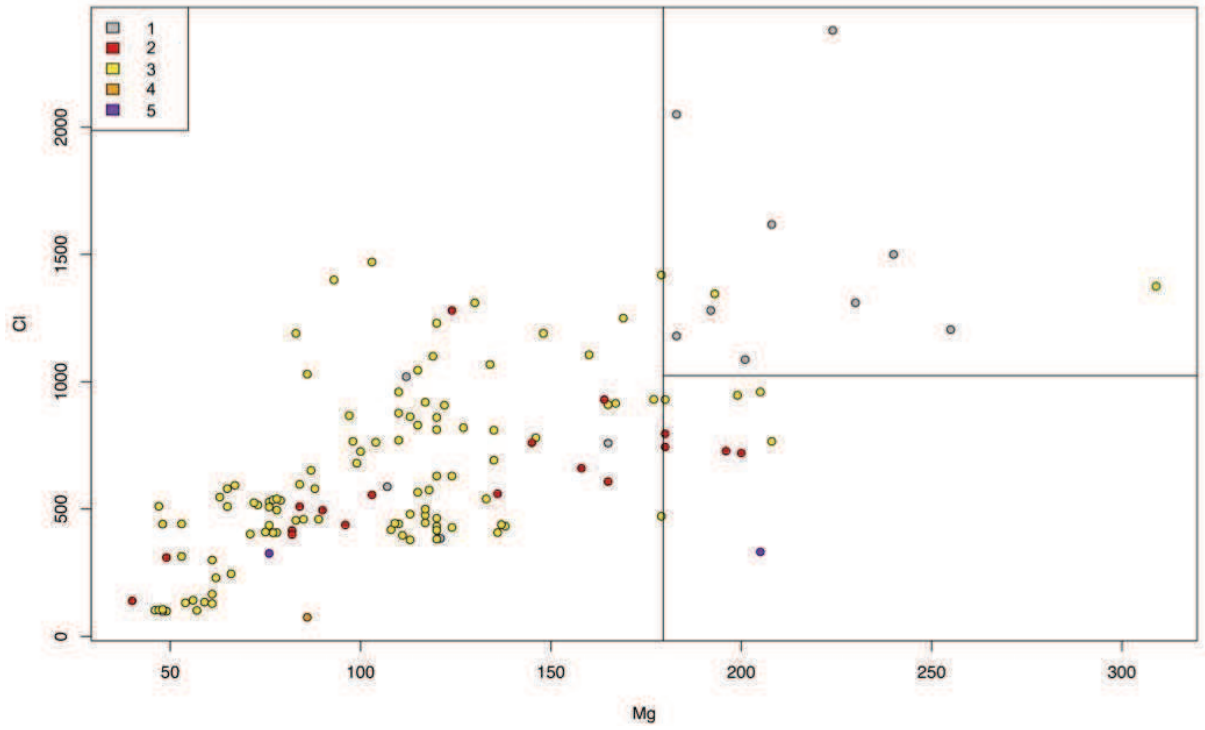

Figure 26: Plot of the Mg^{2+} < 179.5 and Cl^- < 1024 nodes of the decision tree (CART model) (values in $mg.l^{-1}$)

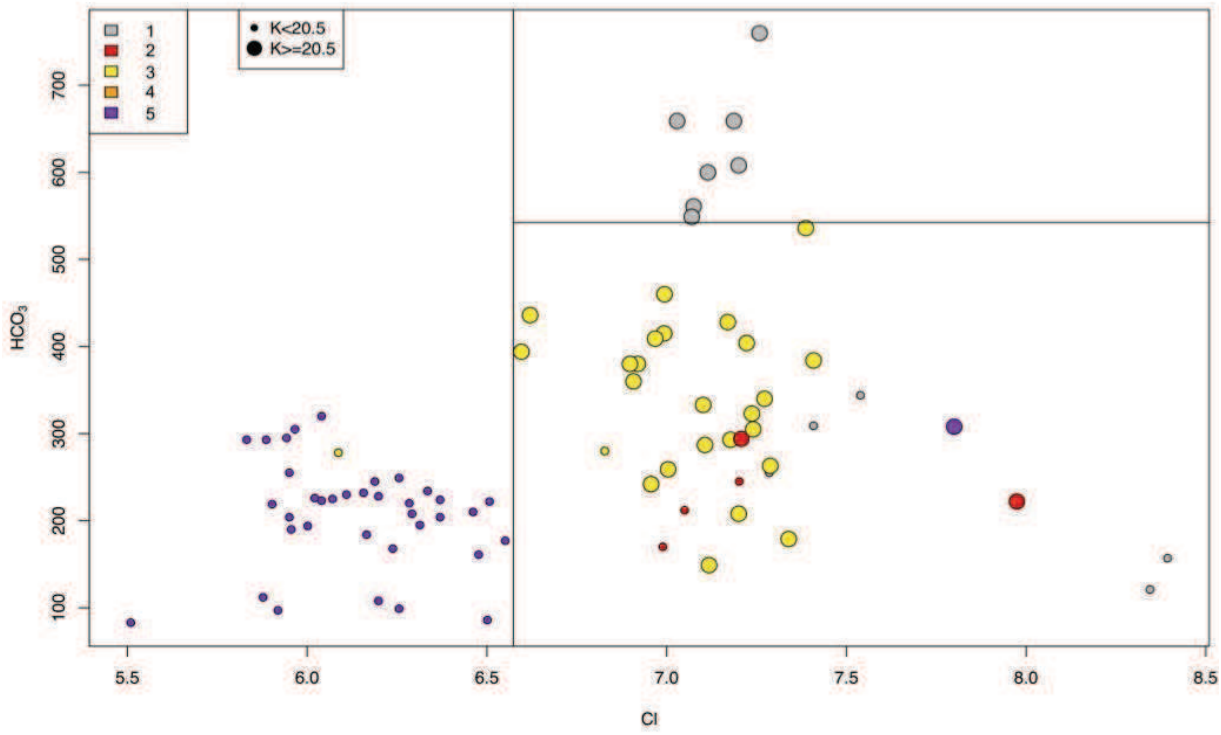

Figure 27: Plot of the Cl^- >= 716, HCO_3^- < 542.5 and K^+ >= 20.5 nodes of the decision tree (CART model). Note: values in mg/l

4.7.2.3 Random Forest (RF0)

The confusion matrix after applying Random Forest to the whole dataset and all the available variables is shown in Table 5 together with its analysis. Compared to the CART model, overall accuracy increased from 88.0% to 90.6%, i.e. 21.7% of the total scope of improvement. The omission error for the Pliocene aquifer decreased from 100% to 70.0%, showing a clear enhancement, although this value remains high. The commission error for the Pliocene is also high (40.0%).

Table 10: Confusion matrix of random forest

	Q	P	M	To	Tr
Quaternary	225	4	7	0	2
Pliocene	2	9	16	1	0
Messinian	6	16	129	0	1
Tortonian	0	1	0	25	0
Trias	0	0	1	0	36
Commission error	5.5	40	15.1	3.9	2.7
Omission error	3.43	70	7.86	0	10
κ=0.853 Overall accuracy = 90.6%					

4.7.2.4 Random Forest after elimination of unreliable samples (RF1)

Figure 28 shows the distribution of the ionic balance error (absolute values) for each result of the model. The actual and the estimated classes appear separated by a dot on the horizontal axis. Some of the well-classified samples (1.1, 2.2, 4.4) seem to have a lower ionic balance error than badly classified samples.

Nevertheless, overlapping areas between categories are very large, so no clear threshold can be assessed. As a general rule, it was decided to eliminate all samples above 5% of absolute ionic balance error (2 samples) for the calibration of the model. Anyway, there is a slight tendency to obtain better classifications in samples with a low error in the ionic balance. This seems supports the use of this classification method.

Depending on the borehole, the initial aquifer assigned to the samples is more or less reliable. The AR index expresses three levels of confidence: A (high), B (medium) and C (low). Figure 29 shows the distribution of AR for each one of the 25 possible classification cases (correct and incorrect).

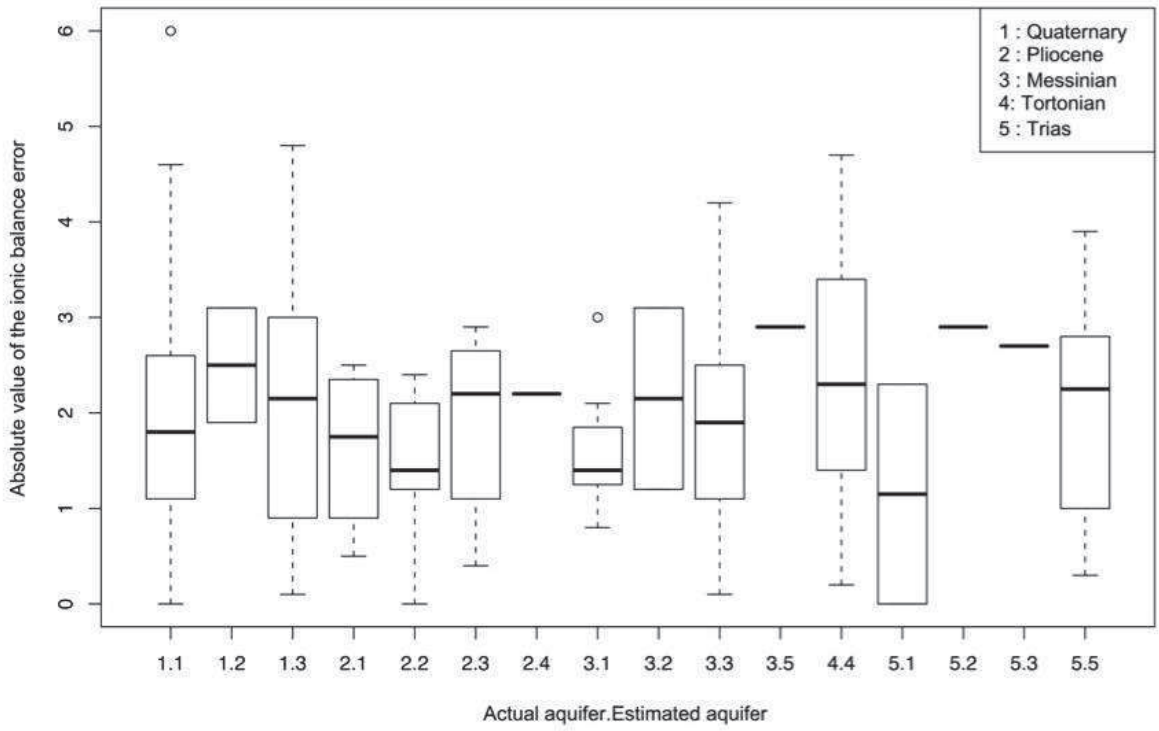

Figure 28: Absolute Ionic Balance Error

It is organised as a confusion matrix in which the elements are pie charts displaying, for each combination of real and estimated classes, AR distribution. Colours are chosen as follows: green (AR=”A”), yellow (AR=”B”) and red (AR=”C”) while the number between brackets indicates the number of cases. Nine combinations never occur (white circles); for example, samples from the Quaternary aquifer wrongly classified as Tortonian. In most cases of wrong classification, a predominance of low reliability initial aquifer assignment (AR=”C”) is found.

Specifically for Quaternary and Pliocene samples incorrectly classified as Messinian, most samples feature a highly reliable initial aquifer assignment (AR=”A”). In some cases (Pliocene, Messinian and Trias), well-classified samples present relatively high percentages of medium and low AR. In view of these results, it was decided to eliminate the samples featuring low AR. After eliminating all samples with AR=”C”, together with those with a ionic balance error higher than 5%, the classification accuracy increases (6). Especially relevant is the decrease from 70% to 48% in the omission error of the Pliocene aquifer. The commission error for the same layer reaches a reasonable value of 13.3%. Overall accuracy, increases from 90.6% to 93%.

Table 11: Confusion matrix of random forest eliminating doubtful samples (RF1)

	Q	P	M	To	Tr
Quaternary	210	3	6	0	0
Pliocene	0	13	2	0	0
Messinian	5	9	72	0	0
Tortonian	0	0	0	25	0
Trias	1	0	0	0	25
Commission error	4.1	13.3	16.2	0	3.8
Omission error	2.78	48	10	0	0
κ =0.882 Overall accuracy = 93%					

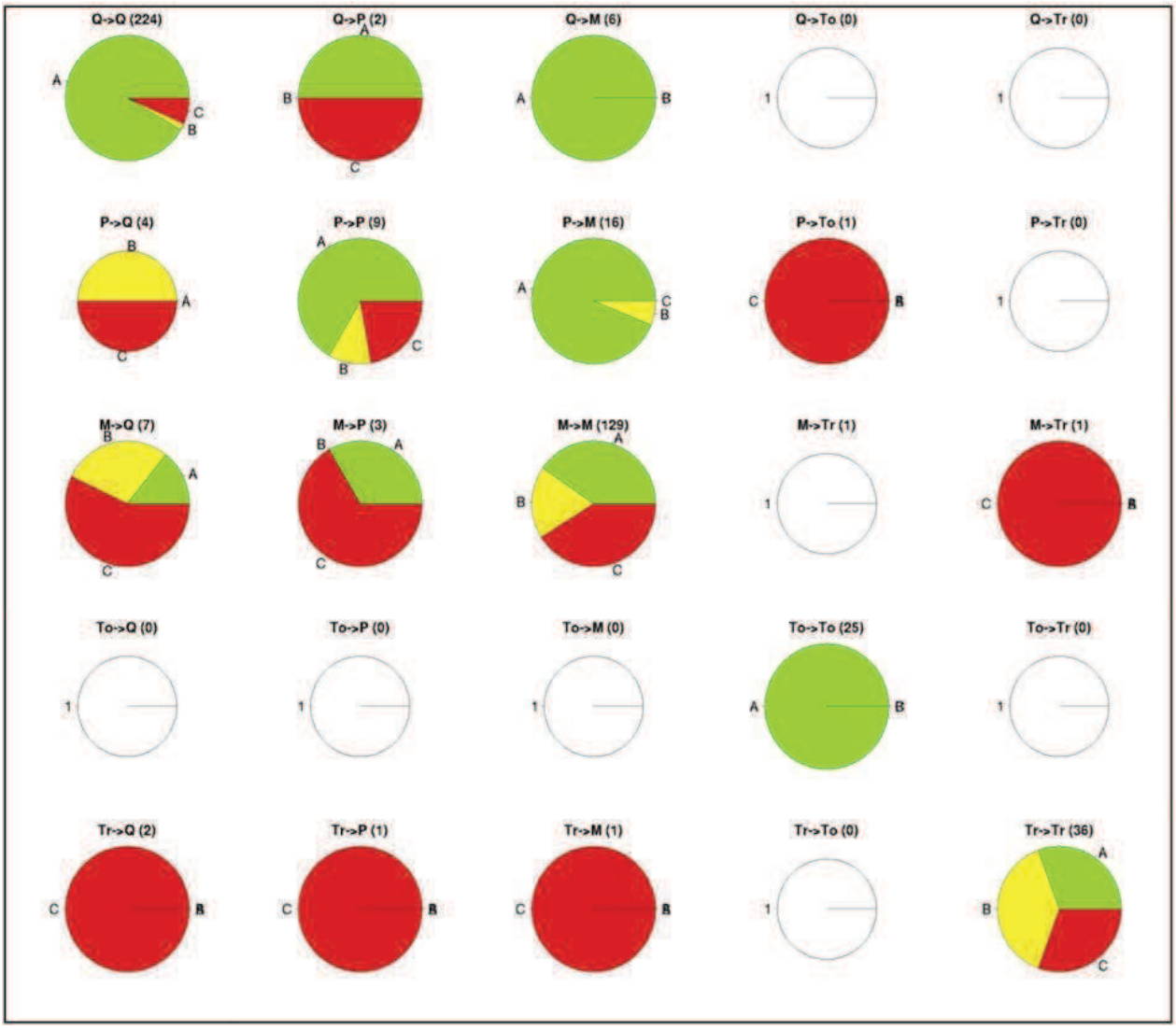

Figure 29: Distribution of aquifer reliability (AR) for the different combinations of actual and classified aquifers

4.7.2.5 Random Forest after elimination of variables (RF2)

To assess if any variable was producing a decrease in accuracy, different models were generated by adding and eliminating variables. The first model contained only NO_3^-, the variable that had obtained the higher importance in the RF0 model; it reached an accuracy of 71%. The highest increase in accuracy was obtained by adding Ca^{2+}; this two-variable model had an accuracy of 81%.

The same procedure of progressive increase in the number of variables was implemented step by step, up the total of all variables (Figure 30). Due to the random behaviour of Random Forest, the results can vary from one run to the other. Therefore, the protocol was repeated 50 times for each model. The accuracy results were obtained by out-of-bag cross-validation.

A decrease in accuracy was observed after adding the last variable (Cl^-). Eliminating chloride therefore improved the model (Table 7): a reliability of 94.3% was reached with a decrease of the commission error for all classes. Especially important is the decrease in the omission error of the Pliocene aquifer, from 48% to 40%. Removing Cl^- also seemed to reduce the confusion between Pliocene and Messinian aquifers.

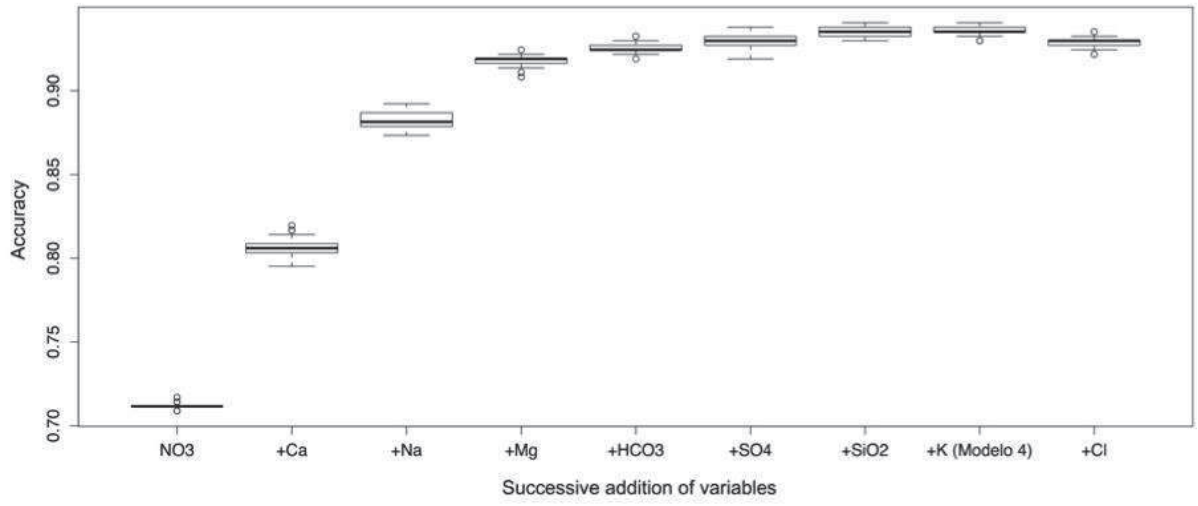

Figure 30: Accuracy of different models generated by adding and eliminating variables

Table 12: Confusion matrix of random forest eliminating Cl^-

	Q	P	M	To	Tr
Quaternary	211	3	4	0	0
Pliocene	0	15	2	0	0
Messinian	4	7	74	0	0
Tortonian	0	0	0	25	0
Trias	0	0	0	0	25
Commission error	3.2	11.8	12.9	0	3.9
Omission error	2.31	40	7.5	0	0
κ =0.905 Overall accuracy = 94.3%					

4.7.2.6 Comparison of statistical models

The similarity between water types was initially expected to be a strong limitation to the identification of the characteristic geochemical signatures of the three upper layers. Another problem is that artificial groundwater mixings between aquifers are cumulative over time, producing temporal variation in the geochemistry of groundwater samples. Despite such limitations, RF2 model reaches a high accuracy and a low omission error for the Pliocene compared to the other methods (Figure 31). Therefore, the RF2 model is selected as the best model.

Out of the 201 tubewells of unknown design featuring geochemical data, and based on the finally considered training set of 73 tubewells (those with a complete set of data), it succeeded to identify the aquifer corresponding to 47 tubewells (Figure 32), representing 107 samples. Regarding the samples that could not be identified, most of them had an incomplete dataset, making the classification impossible.

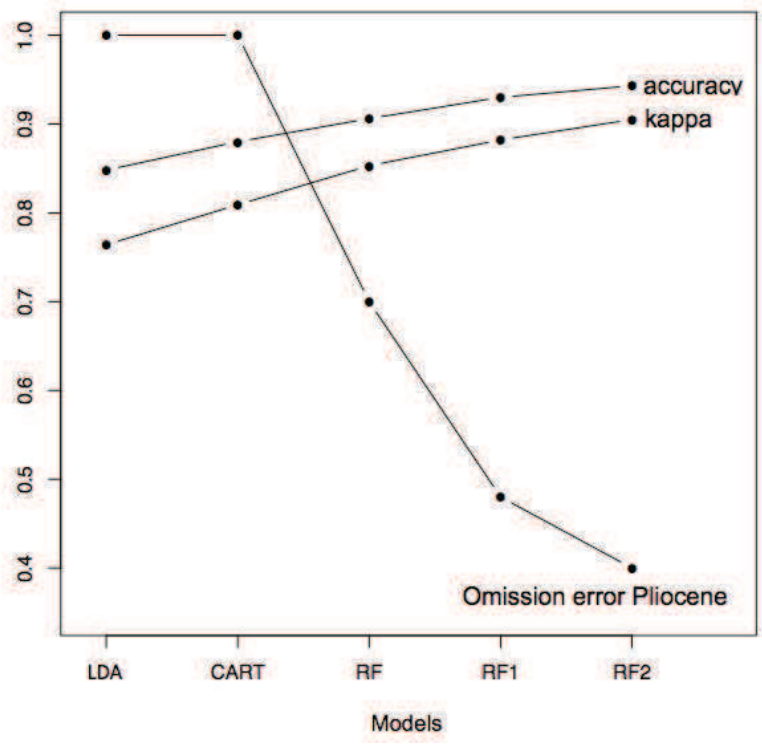

Figure 31: Accuracy indicators for the different models: LDA, CART, RF, RF1 and RF2.

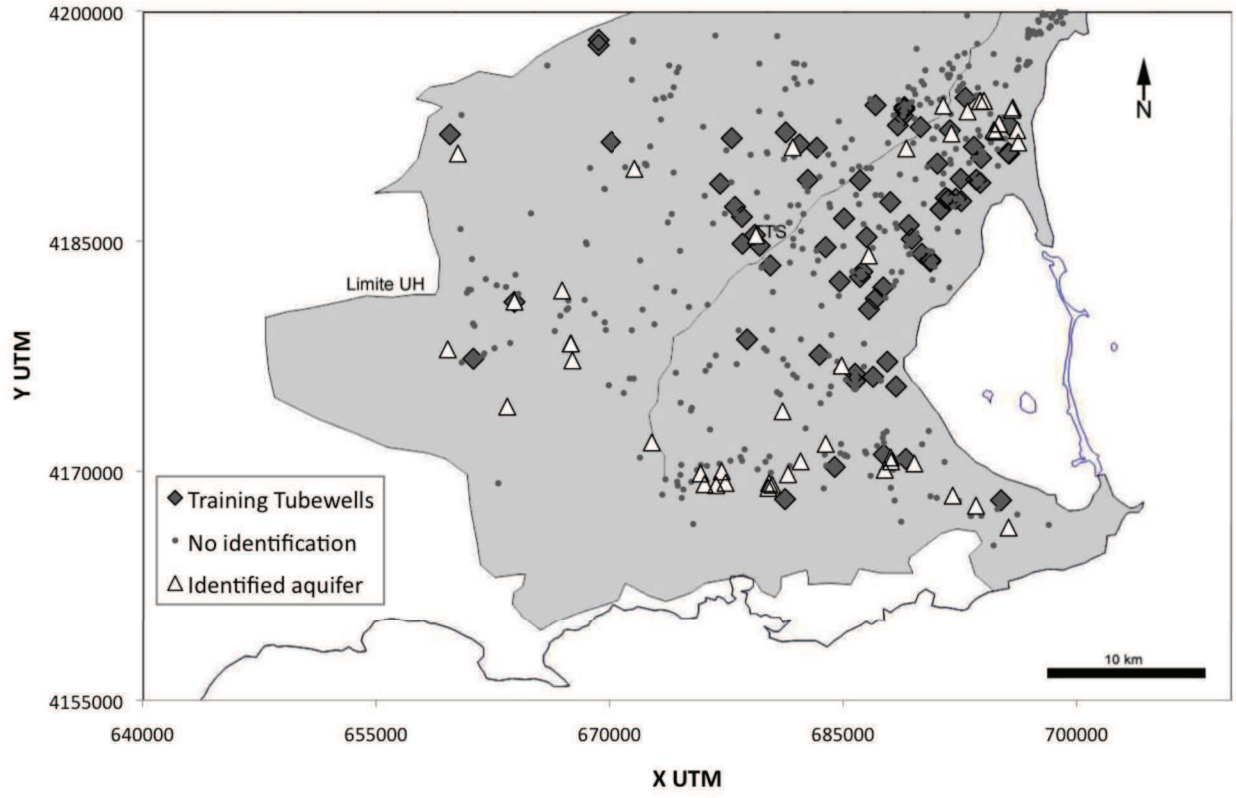

Figure 32: Map of the RF2 results

4.7.2.7 Predictive capacities of the model

The results of the RF2 model for unknown samples are represented in a Piper diagram (Figure 14). Piper diagrams use slightly different data than these used by Random Forest. First, data appear as percentages whereas the model is built on concentration values; secondly, some of the ions appear added.

Still, a Piper diagram of the classified samples was considered usable as a second validation approach and to check the predictive capacity of the model.

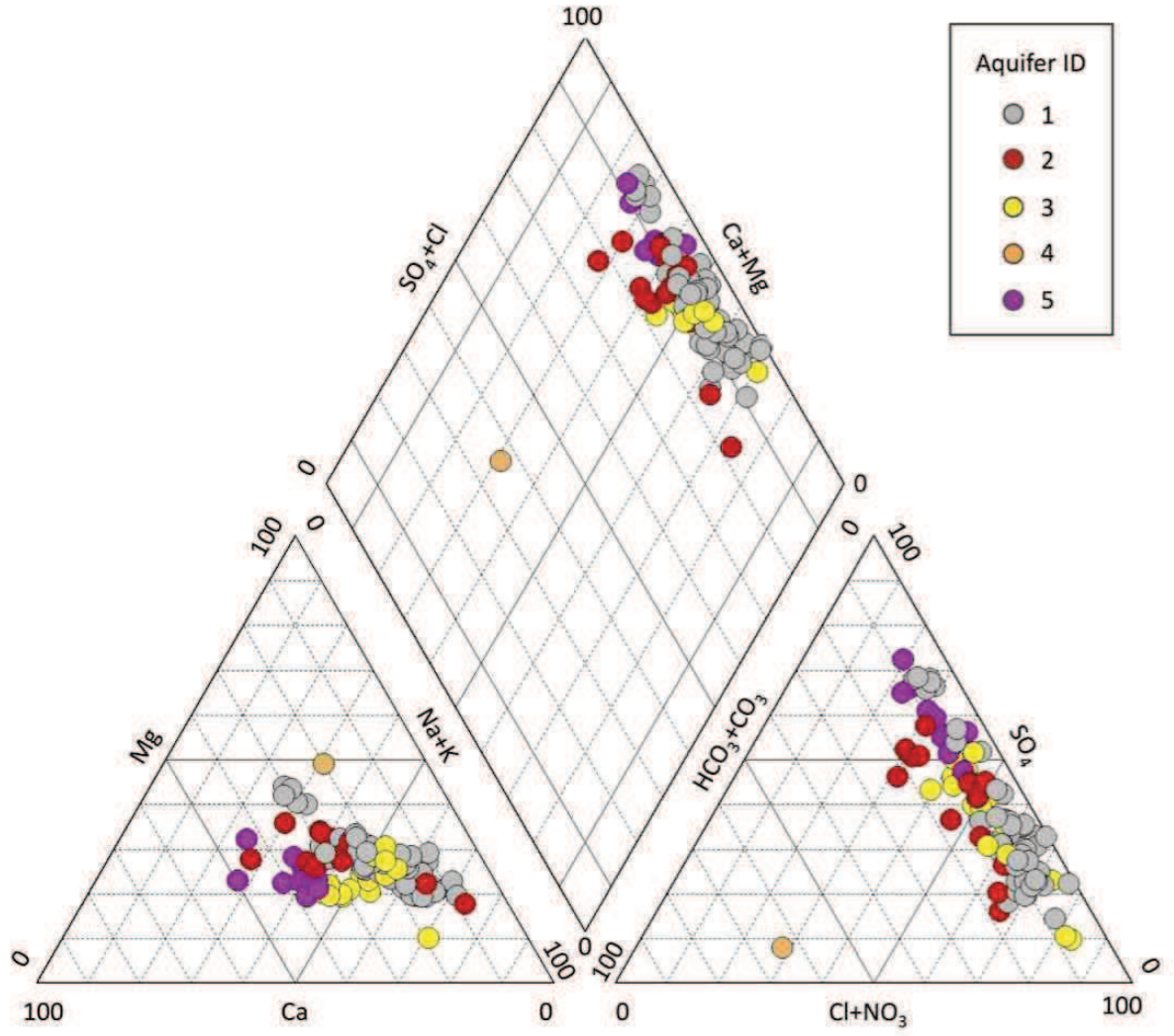

Figure 33: Piper diagram for samples of unknown origin featuring all variables and identified with the RF2 model. 1=Quaternary, 2=Pliocene, 3= Messinian, 4=Tortonian, 5=Triassic.

The water types displayed on Figure 33 (classified samples) are similar to those showed on Figure 3 (training samples), confirming the reliability of the method to identify the origin of groundwater samples.

Two problems, not directly attributable to the model, still appear. Some of the samples could not be identified because not all ion concentrations were measured, making the classification impossible. Secondly, some of the classified samples could actually represent a mixing between different aquifers layers; this already mentioned phenomenon is characteristic of the study area. Both problems, incomplete datasets and mixing samples, are to be dealt in future works.

Chapter 5

Evolution of recharge conditions and rates. Isotopic approach

5.1 Introduction

Isotopic methods were applied to estimate both i) the long-term pre-irrigation recharge and the ii) modern recharge, in relation with almost one century of various human perturbations. They were interpreted taking into account the complex groundwater flow patterns. As a complementary tool, high-resolution temperature logging was performed in several doubtful long-screened boreholes where artificial mixing between several aquifers may occur.

One advantage of this geochemical and isotopic approach using stable (^{2}H, ^{18}O, ^{13}C) and radio- (^{3}H, ^{14}C) isotopes of groundwater is to integrate the small-scale heterogeneity known to be common on the type of coastal carbonated and somehow over-exploited aquifers (Loosli et al., 2001).

5.2 Methodology

Fieldwork took place in February 2011. 24 groundwater samples were collected from boreholes (Figure 34) with electrical pumps reaching the shallow Quaternary and the confined Pliocene and Messinian aquifers. Additional samples (named Q+P) were taken from long-screened boreholes supposed to mix Quaternary and Pliocene waters.

Physical and chemical parameters, i.e. temperature, pH, electrical conductivity (EC), were measured in the field. Alkalinity was measured by titrimetry (Gran method) on the sampling day. The Total Dissolved Inorganic Carbon (TDIC) was calculated from pH and alkalinity (at 25ºC) using the equilibrium equation between the different carbonate species in solution.

Twenty-seven samples were selected for analysis of oxygen-18, deuterium, major ions and halogenide. Twenty samples were analysed for carbon-13/carbon-14 content of TDIC and twenty-four for tritium.

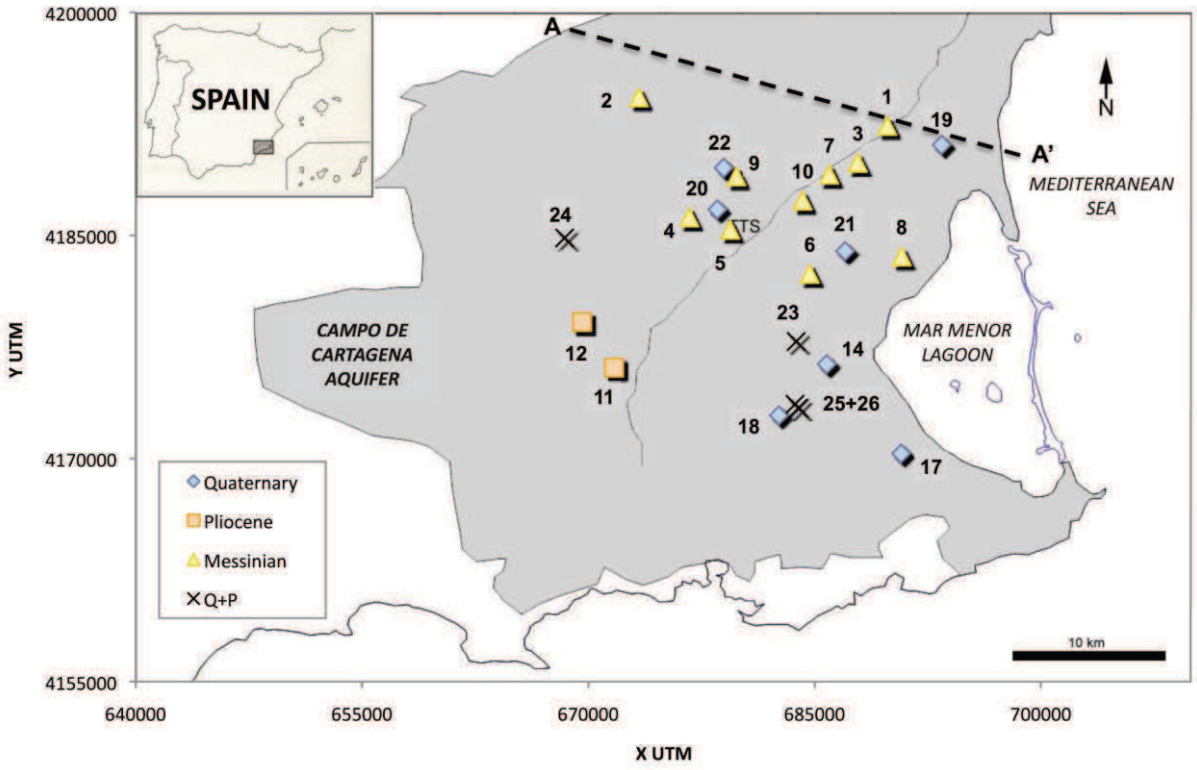

Figure 34: Location of the groundwater samples

Major elements contents were analysed by ion chromatography (MSE Montpellier). Br was analysed on a specific ion chromatography column (University of Avignon). Stable isotopes of water were analysed by mass spectrometry (MSE Montpellier). Results were reported using conventional δ (‰) notation, as a deviation from the VSMOW (Vienna Standard Mean Ocean Water). Tritium was analysed by liquid scintillation (University of Avignon) and reported as Tritium Units (TU).

The carbon species (i.e. CO_2, TDIC and carbonates) were converted into CO_2 by direct acidification, and the ^{13}C contents were measured by mass spectrometry (SIRA) at the IDES Laboratory (University of Paris Sud). The ^{13}C content is reported using δ (‰) notation, as a deviation from the V-PDB (Vienna-Belemnite from the Pee Dee formation, North Carolina, USA). Graphite sources for ^{14}C analyses were prepared from all carbon species (i.e. CO_2, TDIC and carbonates) in the IDES Laboratory, and measured using an accelerator mass spectrometry (UMS LMC14, Gif-sur-Yvette, France). The ^{14}C contents are expressed as a

percentage of modern carbon (pMC). Analytical errors, including laboratory errors, are of ± 0.2‰ vs V-PDB for the $\delta^{13}C$, and between 0.5 and 0.8 pMC for the $A^{14}C$.

Deep (up to 150 m) high-resolution temperature logs were performed inside boreholes where artificial mixing may occur every time it was possible. A temperature sensor with a resolution of 0.005 °C was used (Corcho Alvarado et al., 2009). In order to reduce measurement bias, the sensor was moved very slowly (around 0.5 m/s). The temperature measurements were performed i) before sampling, to represent undisturbed water columns and ii) during sampling, after a minimum of one hour of pumping. Each measurement was repeated after 15 min. This measurement also aimed at identifying groundwater flows inside tubewells when there is no pumping.

5.3 Results

5.3.1 Temperature logs

Temperature logs were performed before and during pumping inside five doubtful boreholes (15, 23, 24, 25, 26). The geothermal gradients observed in static conditions basically ranged between 4 ºC per 100 m and 5 ºC per 100 m. Thus, the mean value of 4.5 ºC per 100 m is considered as representative for the whole area. The intersection of the geothermal gradient with the ground level occurred at a mean temperature of 18.5°C, which was considered as representative of the mean ground temperature.. This geothermal gradient, higher than the common value of sedimentary basins (3 ºC per 100 m), is in agreement with other regional values (Fernández et al., 1990) and may be explained by the active tectonics, and especially the recent volcanic activity.

5.3.2 Temperature of the samples

The temperature measured in groundwater samples varied from 19.3 ºC to 34.5 ºC (Table 15). Shallow Quaternary wells are cool, from 19.3 to 21.9 ºC; Pliocene wells are between 24.7 and 25.0 ºC. Boreholes potentially mixing these two layers (called Q+P) present an intermediate and wide range of temperature (19.6 to 22.5 ºC). The deep Messinian wells are warmer, from 26.6 to 34.5 ºC. In the few cases where precise sampling depth could not be assessed, the mean depth of the screen was considered, with the associated error bars. The geothermal gradient obtained from groundwater samples (Figure 35) is in good agreement

with the one obtained from temperature logs. Two Quaternary samples (20 and 21) present excess in temperature compared to depth. A possible explanation could be a wrong estimate of the real depth of these two wells, defined from the owners' statements, but not confirmed by a precise technical description. As well in Well 1 (Messinian), the tubewell might be 100m less deep than expected from the owner's statements. Another explanation may be a deterioration of the cement ring isolating the upper aquifer, or even a still unidentified phenomenon affecting groundwater in this area. Both hypotheses are reasonably realistic. Additionally, a narrow anticline close to Well 1 was supposed by Jimenez-Martinez et al. (2012) and could lift up the aquifer formation. In the absence of more information, no hypothesis could be discarded.

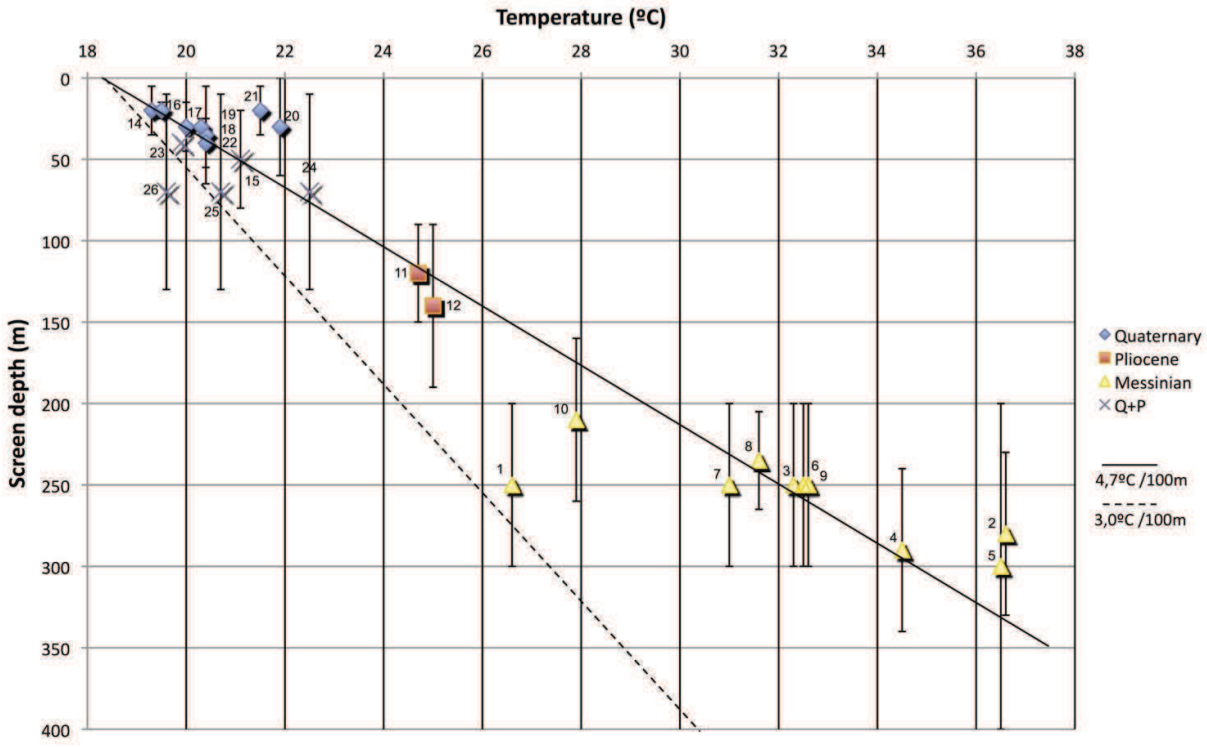

Figure 35: Groundwater temperature vs depth of the screen depth

5.3.3 TDS

The TDS values vary between 2604 and 6545 $mg.l^{-1}$ in the Messinian aquifer, 4008 and 4334 $mg.l^{-1}$ in the Pliocene, 3431 and 9176 $mg.l^{-1}$ in the Quaternary. The TDS values in the

Q+P samples (between 5527 and 8613 $mg.l^{-1}$) are higher than Pliocene values, and correspond to the mid-upper TDS Quaternary range, which reflects a variable but notable contribution of the Quaternary water. In the Quaternary aquifer, large differences in TDS exist even over a short distance: wells 20 and 22 are 2.8 km away and their TDS values are 6276 and 4094 $mg.l^{-1}$ respectively.

5.3.4 Majors ions

Whatever the wide range in TDS values, all groundwater samples belong to the same narrow Na-Ca-Cl water type in the Piper diagram (Figure 36). As a consequence, only a limited use can be made out of the major ion geochemistry for groundwater flow patterns, recharge or mixing processes. The same kind of limitations was found by other authors in multi-layer aquifers (e.g. Gassama et al. 2012).

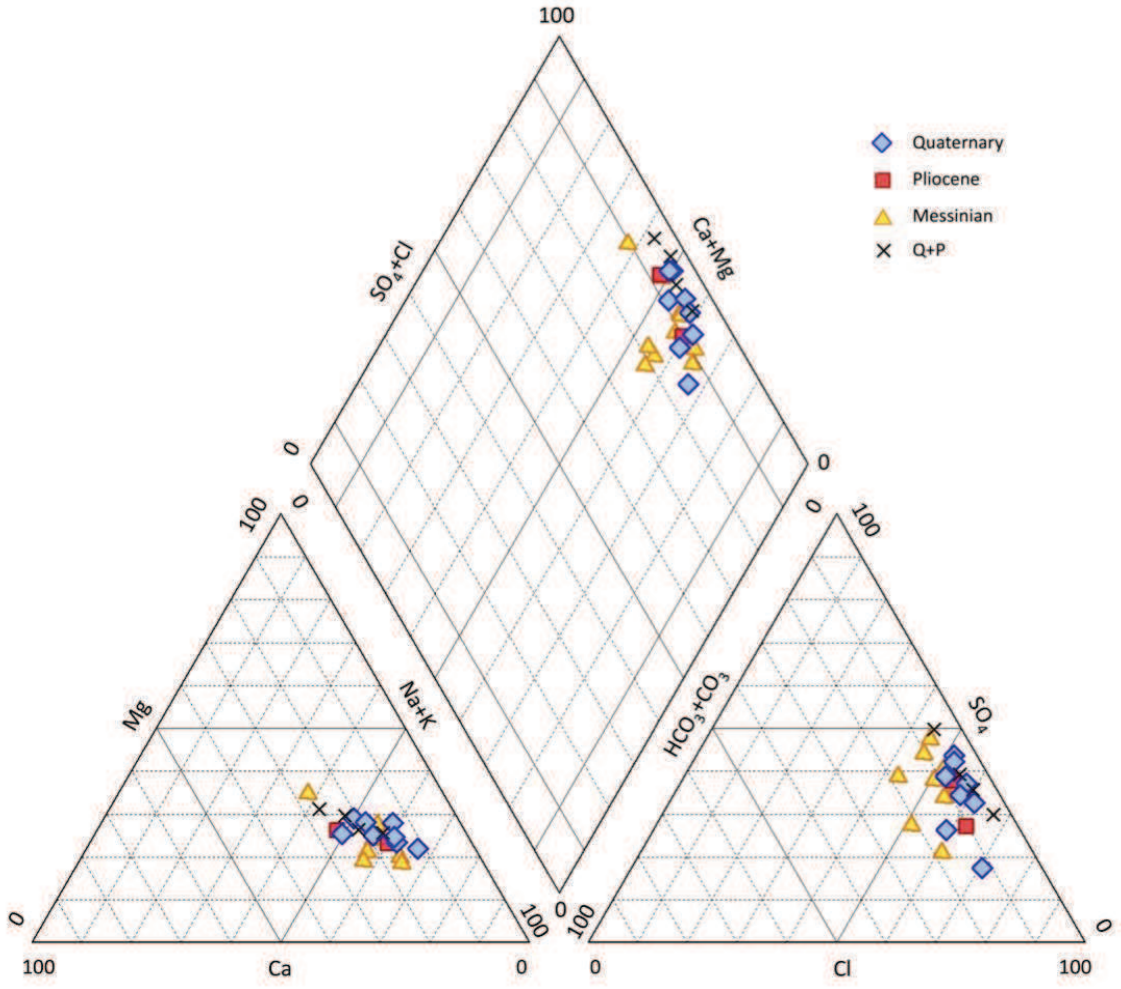

Figure 36: Piper diagram for the 27 samples

5.3.5 Isotopic data

5.3.5.1 ^{18}O and ^{2}H

Groundwaters have $\delta^{18}O$ isotopic contents between -6.66 and -4.08 ‰ vs VSMOW (Table 16). Except sample 10, the deep confined Messinian and Pliocene aquifers (-6.66 to -5.56 ‰ and –5.79 and –7.34 ‰, respectively) are well differentiated from the shallow Quaternary aquifer (-5.36 to -4.08 ‰), while Q+P samples have values between the two end-members (-6.18 to -4.97 ‰). $\delta^{2}H$ shows a similar distribution, with contents between -43.8 and -26.9 ‰ vs VSMOW. The deep Messinian and Pliocene aquifers (-43.8 to -37.1 and -43.2 to 34.4 ‰) differ from the Quaternary aquifer (-34.5 to -31.9 ‰), although Messinian samples n°3 and 1 are very close to Quaternary samples n°18 and 20. The Q+P samples still are between shallow and deep samples (-38.1 to -32.8 ‰). The average rainfall composition was provided by the six-year IAEA (International Atomic Energy Agency) dataset (2000-2006) at the San Javier Airport: -5.26 and -33.2 ‰ vs VSMOW for $\delta^{18}O$ and $\delta^{2}H$ respectively. The average TTS composition is obtained from a 2-year monthly sampling campaign (2007-2009) by Tovar Frutos (unpublished data): -5.63 for $\delta^{18}O$ and -38.8 ‰ vs VSMOW for $\delta^{2}H$. Nevertheless, a large scatter is observed (standard deviation of 0.74 and 4.28, respectively).

5.3.5.2 ^{3}H

Tritium was analysed in twenty-four samples: from the Quaternary aquifer (7), the Q+P mixing (5), the Pliocene (2) and Messinian aquifers (10). All Messinian samples are below the detection limit (0.5 TU), except the sample nº10 (0.9 TU). The Q+P sample nº15 is also below the detection limit. The Pliocene samples are below (n°12) or slightly above (n°11) the detection limit. Others (Q and most Q+P) are above the detection limit, in a wide range reaching the maximum value of 8.0 TU. Tritium value in rainfall is 5.21 TU, according to the IAEA data base. The TTS water transfer canal composition is obtained from potable water obtained from the TTS and considered representative for the TTS irrigation water reaching the study area. Nine years of sampling (1999-2008) provide stable values around 60 TU (ECT-03 in DePablo SanMartin, 2008).

5.3.5.3 ^{13}C

$\delta^{13}C$ content ranges from -16.9 to -4.7 ‰ vs PDB: -16.9 to -14.4‰ (Quaternary), -13.8 to -12.1‰ (Pliocene), -12.0 to -4.7‰ (Messinian). Two intermediate Q+P samples are inside the Quaternary range (-16.8 and -15.5‰) and the two others are between the Quaternary and Pliocene ranges (-13.9 and -14.1‰). The clear relation between the TDIC and the $\delta^{13}C$ content for the confined aquifer samples (Figure 37) is in agreement with the generalized calcite and dolomite saturation; pH increases with $\delta^{13}C$ and reveals evidence of C isotopic exchange between the carbonate matrix and groundwater (i.e. dissolution/precipitation of $CaCO_3$).

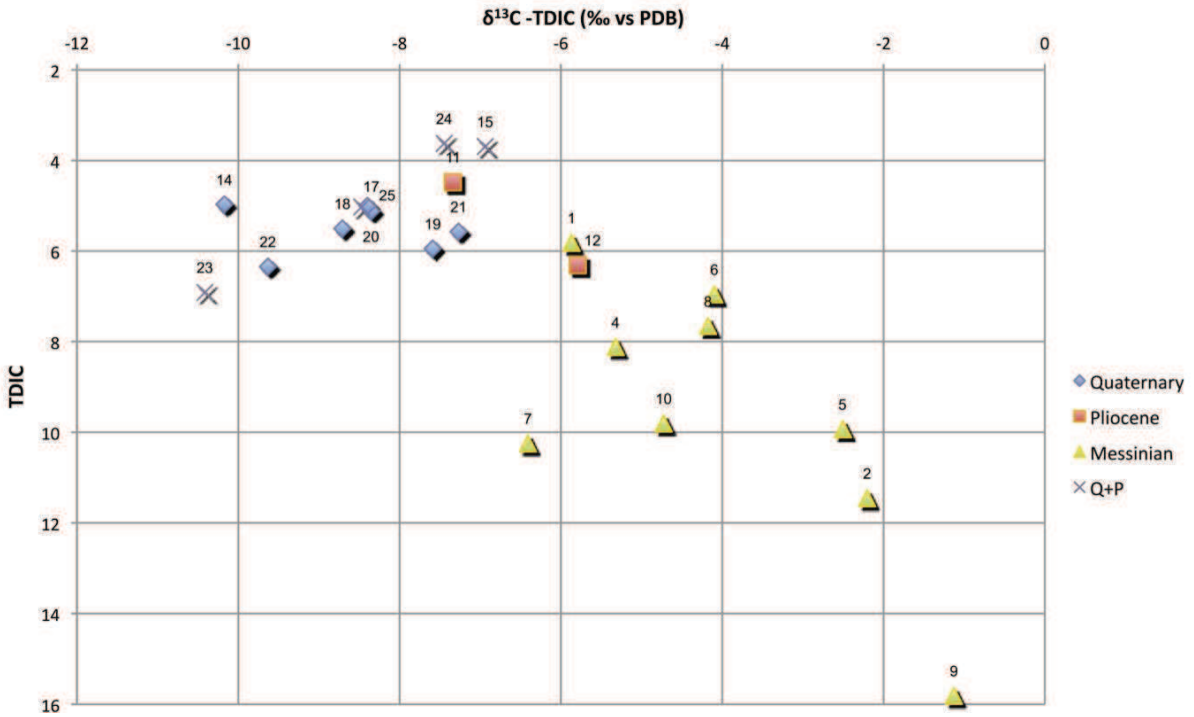

Figure 37: δ13C–TDIC vs TDIC of the groundwater samples, highlighting the C isotopic exchange between the carbonate matrix and the groundwater.

5.3.5.4 $A^{14}C$

The 23 radiocarbon analyses range from 0.3 to 76.1 percent of modern carbon (pMC): between 36.0 and 76.2 pMC in the Quaternary waters, 1.1 and 26.5 pMC in the Pliocene, 0.3 and 4.8 pMC in the Messinian (except sample n°10 at 15.3 pMC, discussed below).

5.4 Discussion

5.4.1 Mixing processes

Due to the high rates of pumping occurring for almost one century, the pre-anthropogenic groundwater hydrodynamics of each aquifer has been deeply modified. Quite uniformly distributed pumpings led to a global acceleration of groundwater flow. This first consequence of human activity is nonetheless of limited scope compared to the other human impacts, particularly, mixing processes, which take a variety of forms in the study area.

5.4.1.1 Irrigation water

The main source of recharge to the Quaternary aquifer is presently the irrigation return flow. Irrigation water results from a complex mixing, different for each farmer who combines his available water sources, in variable proportions depending on their respective availability and cost. At least nine sources are identified, the main ones being: the five aquifers, with their respective geochemical and isotopic signatures, the Tagus-Segura water transfer canal, desalinated groundwater, treated sewage water and desalinated seawater. As a consequence, the chemical and isotopic signals of recharge present a very high temporal and spatial variability. The wide scatter in the Quaternary data is representative for this spatial variability.

5.4.1.2 Inside borehole mixing

Temperature changes in borehole temperature profiles are often considered to be due to warmer or colder fluid inflows from permeable layers (e.g. Pehme et al., 2010; Klepikova, 2011), rather than differing thermal conductivity of the rocks. Borehole temperature profiles were used i) to confirm the sampling depth inside doubtful boreholes and ii) to assess vertical inside-borehole flow characteristics. It was considered that no one of the aquifers featured fractures that could lead to fast flow inside its formation matrix. In the contrary case, variations of the temperature gradient under no-pumping conditions could also be due to fast flows of water in the aquifer at close distance from the tube-well.

The results are illustrated for the well n°26, taken from a 140 m deep long-screened tubewell reaching both Quaternary and Pliocene aquifers (Figure 38 and Figure 39). The

local geothermal gradient (dashed line) is 5 ºC per 100 m, for a mean soil temperature of 19 ºC, close to the regional mean.

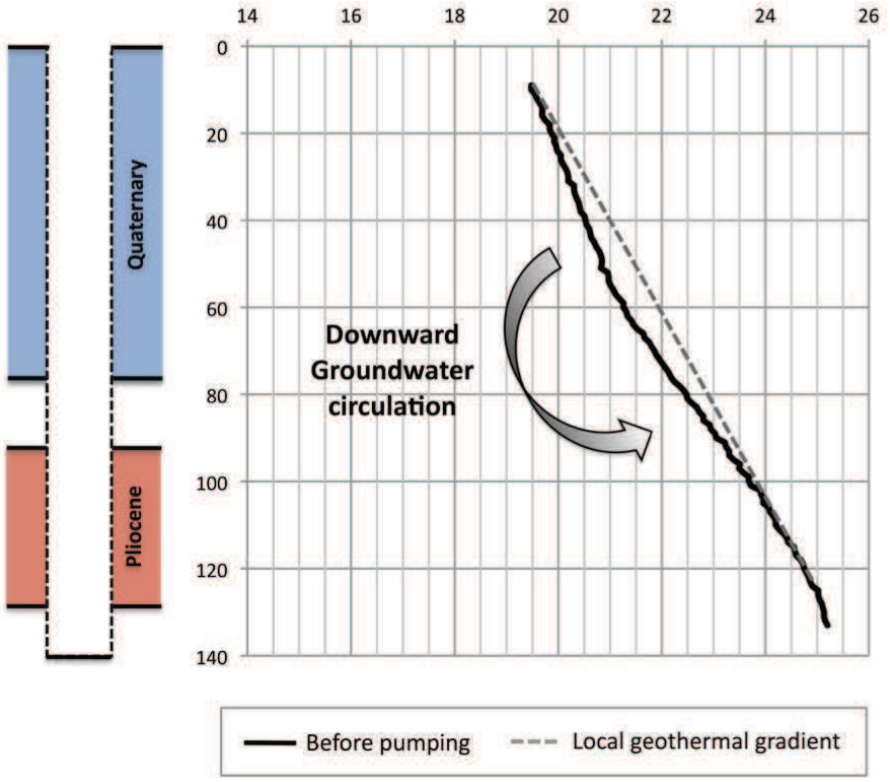

Figure 38: Temperature log showing downward groundwater circulation before sampling in the fully screened nº26 tubewell.

Prior to pumping (Figure 38), water temperature increases with depth, but remains slightly below the local geothermal gradient. A heat sink, with temperature below the local geothermal gradient, is localized at approximately 60 m. Moving away from this point in either direction (up to 8 m and down to 100 m), the temperature goes back to the local geothermal line. The cooler temperature is interpreted as an input of cooler water from the 10-60 m section, its downward movement inside the well and an output flow between 60 m and 100 m. Deeper, water temperature reaches the formation temperature and indicates an unaffected section. The exact shape of the curve depends on the localization and contribution of other inputs and on the flow velocity (Klepikova, 2011). A simple convective mixing due to density gradient in the water is discarded because of the break at 60 m. According to the geological profile indicated in Figure 38 and Figure 39, drawn from neighbouring tubewells, this movement of water would be driven by the hydraulic gradient between the Quaternary

and Pliocene aquifers layers. These observations prove that even unpumped boreholes act as a shortcut between water masses.

When the pump located at 80 m is turned on (Figure 39) the water temperature still increases with depth but remains, from point A (8 m) to point D (80 m), largely below the temperature prior to pumping. Below this section, i.e. from point D to the bottom of the tube-well (80 m), no change is observed compared to the pre-pumping conditions.

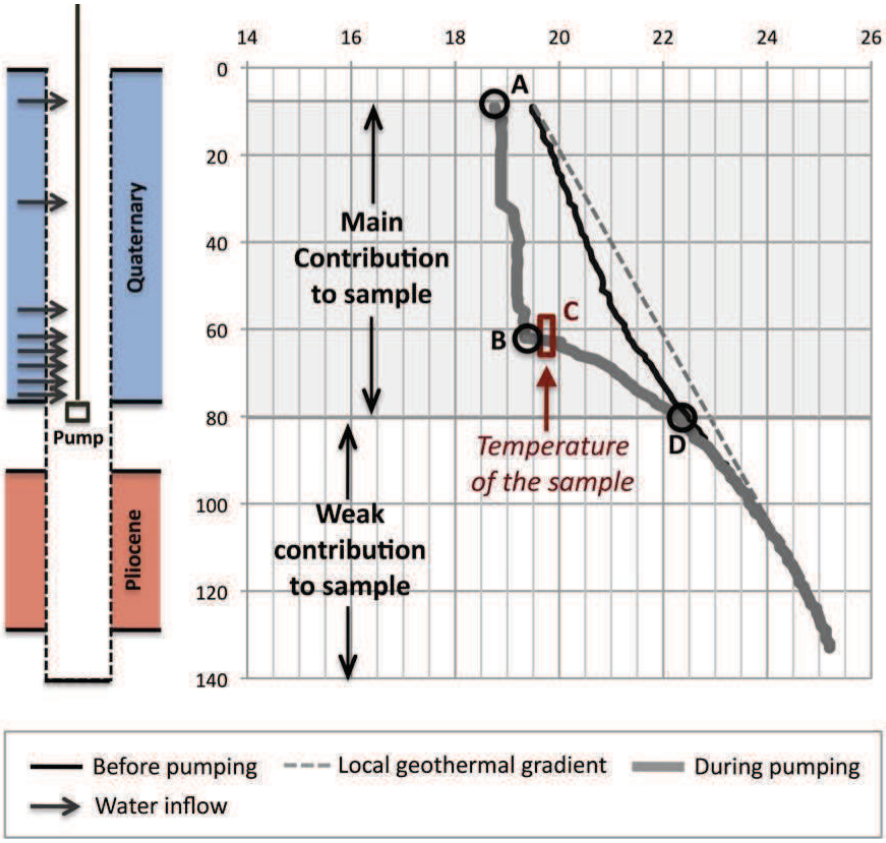

Figure 39: Temperature log showing downward groundwater circulation before sampling in the fully screened n°26 tubewell.

Therefore, the cooler water down to point D indicates a significant flow quickly coming downward to the pump, while the undisturbed water column below 80 m discards any important upward flow from below. The sample taken from this long-screened borehole can be considered as representative for the Quaternary aquifer, with very limited possibility of mixing with Pliocene groundwater.

In order to be even more precise on the origin of the sampled groundwater, the temperature of the sample (19.7° C, measured at the ground surface) was indicated on the

pumping-stage temperature profile in Figure 39 (point C). It intersects the temperature profile at approximately 62 m. The temperature measured at the surface is therefore necessarily the result of a mixing coming from the cooler above section (beginning at 18.6°C in point A) and the warmer section located below (ending at 22.4°C in point D).

Due to the conservative behaviour of temperature at the time scale of a stabilized pumping, this mixing can be considered as binary. Therefore, although the temperature rapidly reverts back to the pre-pumping conditions in the C-D section, half of the sampled water originated from there. This proportion might even be higher if the average air temperature of 10° C during the sampling campaign that might have led to a cooling of the sample is taken into account.

These facts illustrate the usefulness of the method for both aims: i) assessing the sampling depth of samples obtained from multi-layer aquifer systems and ii) understanding the groundwater flows between groundwater masses inside un-used long-screened tubewells (Figure 40).

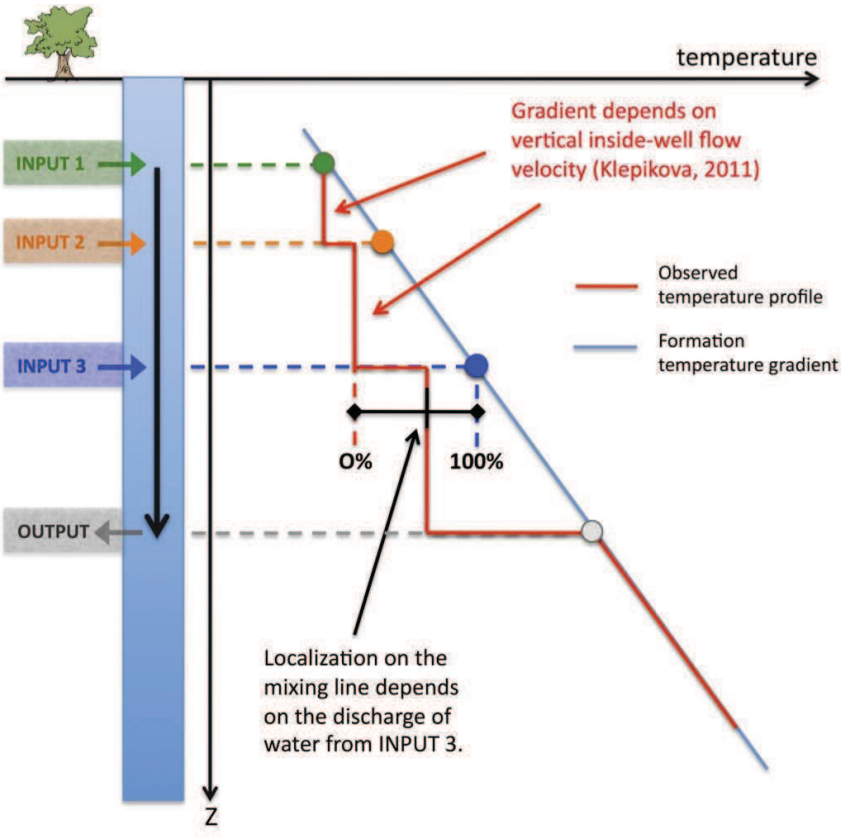

Figure 40: Scheme of the interpretation of inside boreholes temperature profiles

In addition to the temperature logs, the survey of physico-chemical parameters, chemical tracers and isotope tracers provides valuable indications of a possible mixing inside the borehole. For example, the intermediate position often observed for Q+P samples, between the Quaternary and Pliocene (Figure 35 to Figure 37, and Figure 41 to Figure 44) illustrates the different rates of mixing occurring inside the water column of Q+P boreholes.

Special focus will be set on tritium and nitrate, often considered as good indicators of recent recharge. These two tracers have elevated levels and are quite well correlated (Figure 41) in the Quaternary aquifer, where high variability reflects the spatial and temporal variability in the irrigation water quality.

In the confined aquifers, a value for "natural" NO_3 is hard to assess, and its origin can be discussed (Stadler et al., 2008), particularly in relation to redox conditions (see below). According to the few available time series (IGME), the maximum natural threshold would be around 10 $mg.l^{-1}$. In most deep samples (Figure 41), NO_3 is above this threshold, although the high thickness of the aquitard prevents vertical water fluxes at a one-century scale of time and no irrigation is developed on their outcrop areas.

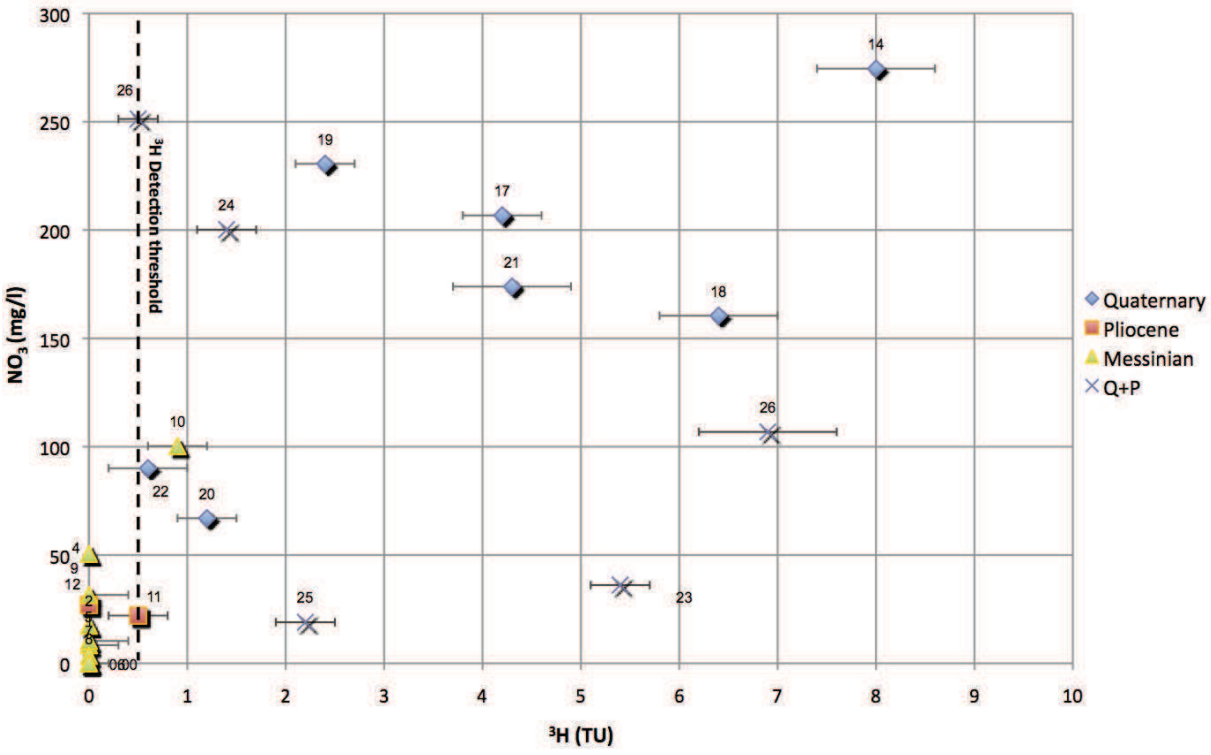

Figure 41: NO_3 vs ^3H

Here, an interesting consideration on nitrate as a tracer is the high reductive conditions indicated by the strong H_2S smell during sampling in Messinian wells, which should theoretically not be compatible with oxidized nitrogen (nitrate) to be found. As Messinian wells are screened along the entire Messinian thickness, the reductive conditions might not be present along the whole aquifer, but located only in some sections of the Messinian aquifer. Since the length of the Messinian tubewells do not allow performing full temperature loggings, no accurate assessment of the sampling depth(s) could be made. Still, another explanation could be a possible post-sampling oxidation process. In this context, at such concentrations, nitrate was not considered as a reliable tracer of downward movements of shallow groundwater into deep aquifers through long-screened boreholes.

Nonetheless, the above detection threshold ^{3}H in one Messinian well (n°10) and one Pliocene well (n°11) where the static potential heads is located tenths of meter below the lower Quaternary unit is considered to be representative of the local composition of the deep aquifer. Together with the combination of a very low ^{14}C activity ($A^{14}C$) with an above detection threshold ^{3}H (Figure 42), it confirms a local contamination of deep aquifers by Quaternary groundwater, exclusively found in these two boreholes.

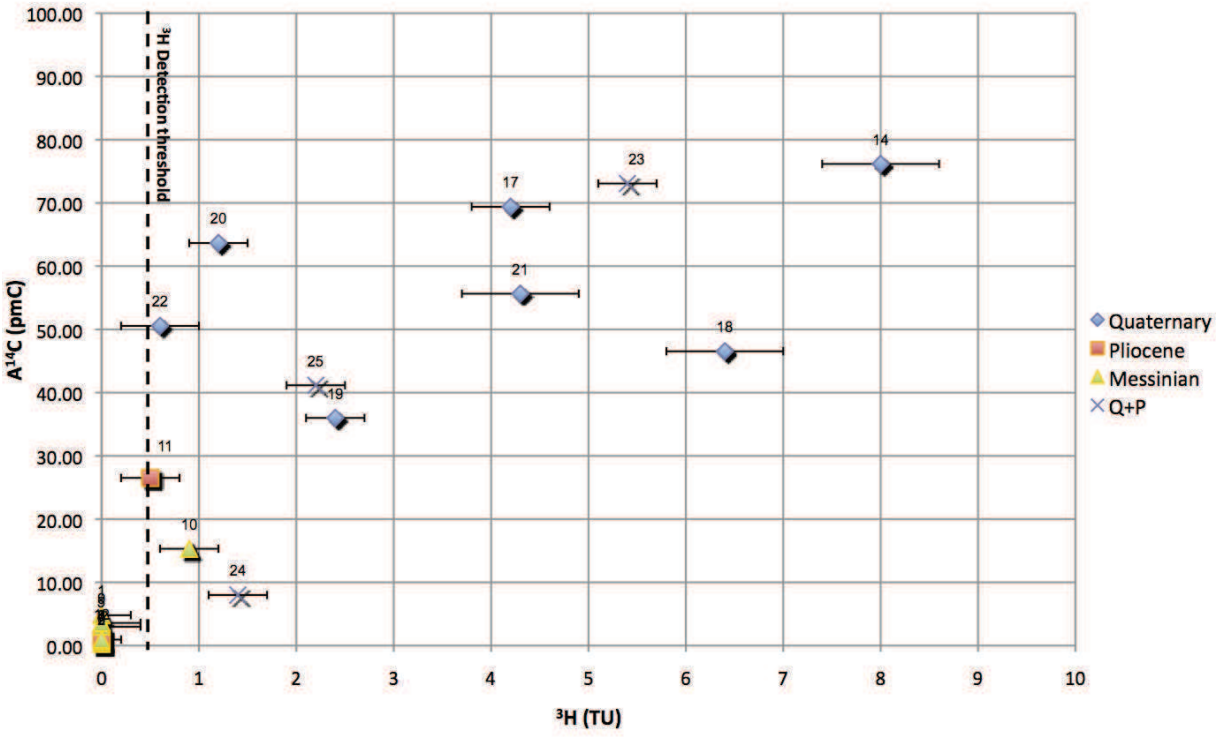

Figure 42: ^{3}H vs $A^{14}C$.

The combination of low $A^{14}C$, above detection level ^{3}H and high NO_3 was also observed at sample n°24, considered to be Q+P based on the available technical information and the comments of the owner. Nonetheless, a doubt remains on the origin of the sample, since no water level could be measured and the temperature profile gave surprisingly stable results. This may indicate i) problems inside the tube or ii) a water table deeper than 150m. In the second case, it would highlight a local contamination of deep aquifers, as for wells n°10 and n°11.

5.5 Groundwater mean residence time

Regarding radiocarbon mean residence time assessment (MRT), the isotopic exchange with the marine carbonate matrix is confirmed in Figure 43 by the evolution of radiocarbon and $\delta^{13}C$ (Gillon, 2009). For the deepest samples this progressive enrichment in ^{13}C continues despite almost 0 pMC ^{14}C activity, which implies a long residence time in the aquifer. The case of Messinian sample n°10 is clearly different, and highlights an evident mixing with shallow groundwater, as already assumed from ^{3}H (Figure 41). The limits of the radiocarbon method are almost reached for the deepest samples and increase the uncertainty of the dating evaluation (Le Gal La Salle, 1996).

The carbon isotopic composition (^{13}C, ^{14}C) of Total Dissolved Inorganic Carbon (TDIC) in groundwater is acquired mainly during transit in the unsaturated zone by exchanges with soil CO_2 and the carbonate matrix (Gillon et al., 2009). It is later affected by the equilibration with the carbonate matrix in the saturated zone (Fontes, 1992; Barbecot et al., 2000). Radiocarbon dating needs to assess the initial activity of the TDIC ($A^{14}C_0$). For assessing $A^{14}C_0$, the most common tools are adjustment models (Fontes, 1992). In adjustment models, a key parameter is the soil CO_2 radiocarbon activity ($A^{14}C_{soil\text{-}CO2}$), generally 100 pMC, i.e. the almost stable pre-bomb peak atmospheric state. But modern groundwater samples have radiocarbon activities higher than theoretical value of $A^{14}C_0$ (e.g. Bruce et al., 2006), preventing a direct MRT assessment. Such high values are explained by the influence of high atmospheric radiocarbon from the atmospheric nuclear tests.

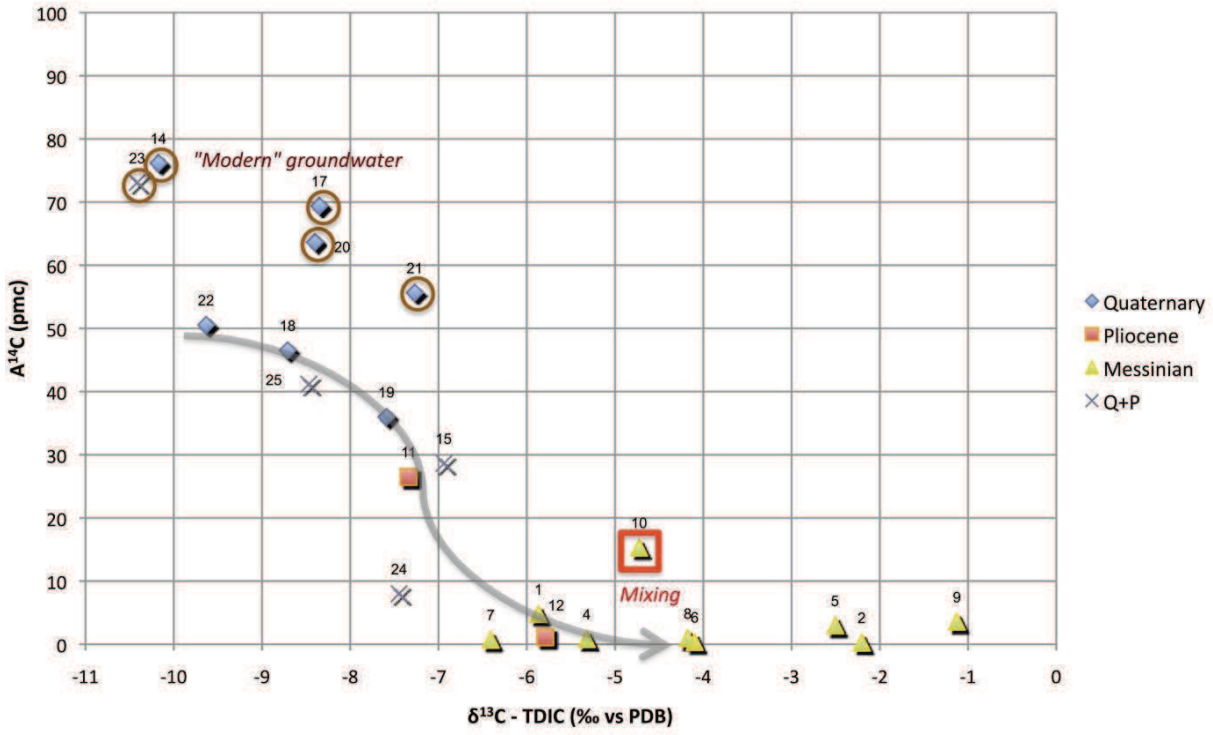

Figure 43: $A^{14}C$ vs $\delta^{13}C$. Brown circles identify the "modern pole" of Quaternary and Q+P samples

Considering root respiration to be the main source of radiocarbon in soils, $A^{14}C_{soil\text{-}CO2}$ should reflect the atmospheric radiocarbon ($A^{14}C_{atm}$). The $A^{14}C_{soil\text{-}CO2}$ that existed at the time of recharge of modern samples ($A^{14}C_{corr}$) was therefore assessed in order to identify modern and old groundwater samples. Radioactive decay of modern samples (a few tenths of years) is considered insignificant compared to the radiocarbon half-life (5730 years).

Thus, $A^{14}C_{mes}$ should be equal to $A^{14}C_0$, once corrected from exchange processes between TDIC and the carbonate matrix. The $A^{14}C_{soil\text{-}CO2}$ that allows this equality is $A^{14}C_{corr}$. Adjustment models like Mook (1980) were discarded because of the isotopic exchange with the carbonated matrix and the widely used Fontes & $Garnier_{equ}$ (Fontes, 1992) and IAEA methods (Fontes, 1992) were selected.

The isotopic contents for carbon end members were ones commonly applied in such environment: $\delta^{13}C$ = 0 ‰ and $A^{14}C$ = 0.8 pMC for marine carbonate and $\delta^{13}C_{soilCO2}$ = -23 ‰ for soil gas CO_2. All samples with $A^{14}C_{corr}$ > 100 pMC were considered as modern (Table 13), and their mean residence time to be 60 years (i.e. the elapsed time since atmospheric bomb tests).

Table 13: Calculation of the minimum atmospheric radiocarbon activity corresponding to Q and Q+P samples.

Sample ID	Aquifer ID	$A^{14}C_{mes}$ (pMC)	$A^{14}C_{corr}$ (pMC)			^{14}C age category	^{14}C MRT (years BP)
			$F\&G_{eq}$	IAEA	Average		
14	Q	76.2	116.7	98.8	107.8	Modern	60
17	Q	69.4	134.0	116.2	125.1	Modern	60
20	Q	63.7	119.7	107.4	113.6	Modern	60
21	Q	55.6	123.0	106.8	114.9	Modern	60
23	Q+P	73.1	121.5	99.7	110.6	Modern	60
18	Q	46.5	90.6	75.2	82.9	Old	1586
19	Q	36.0	72.5	65.9	69.2	Old	3054
22	Q	50.6	82.5	74.4	78.5	Old	2013
15	Q+P	28.6	68.2	57.1	62.7	Old	3894
25	Q+P	41.2	79.6	68.4	74.0	Old	2518

Using the same calculation for old groundwater samples ($A^{14}C_{corr}$ < 100 pMC), $A^{14}C_{corr}$ corresponds to the decayed value for $A^{14}C_{soil\text{-}CO2}$ in the atmosphere at the time of recharge. Indeed, the radiocarbon correction methods give mean residence time between 1500 and 3000 years for the "old" Quaternary samples (28, 19 and 22; Table 13).

These points are therefore considered as representative of the pre-anthropogenic pole, though a mixing with recent waters is evidenced by the presence of nitrate and tritium. Tritium is a tracer of recent recharge, but it has a low quantitative efficiency in the present case because of the numerous sources of water for irrigation, mixing deep groundwater (mostly below tritium detection limit), shallow Quaternary groundwater (0.6 to 8.0 TU), water from the TTS transfer canal (average value around 70 TU) and rainfall (5.2 TU). Multiple combinations could lead to the same final value.

5.5.1 Recharge conditions

The clear difference in the stable isotopic composition between the shallow Quaternary aquifer and the deep aquifers (Figure 44) can be explained by two hypotheses, or their

combination: i) the recharge water is isotopically depleted in the mountain range (between 300 and 400 m amsl) compared to the coastal range due to continental and altitude effects; ii) the recharge of the deep layers occurred under a past climate, with cooler temperatures than present (Jiráková et al., 2011).

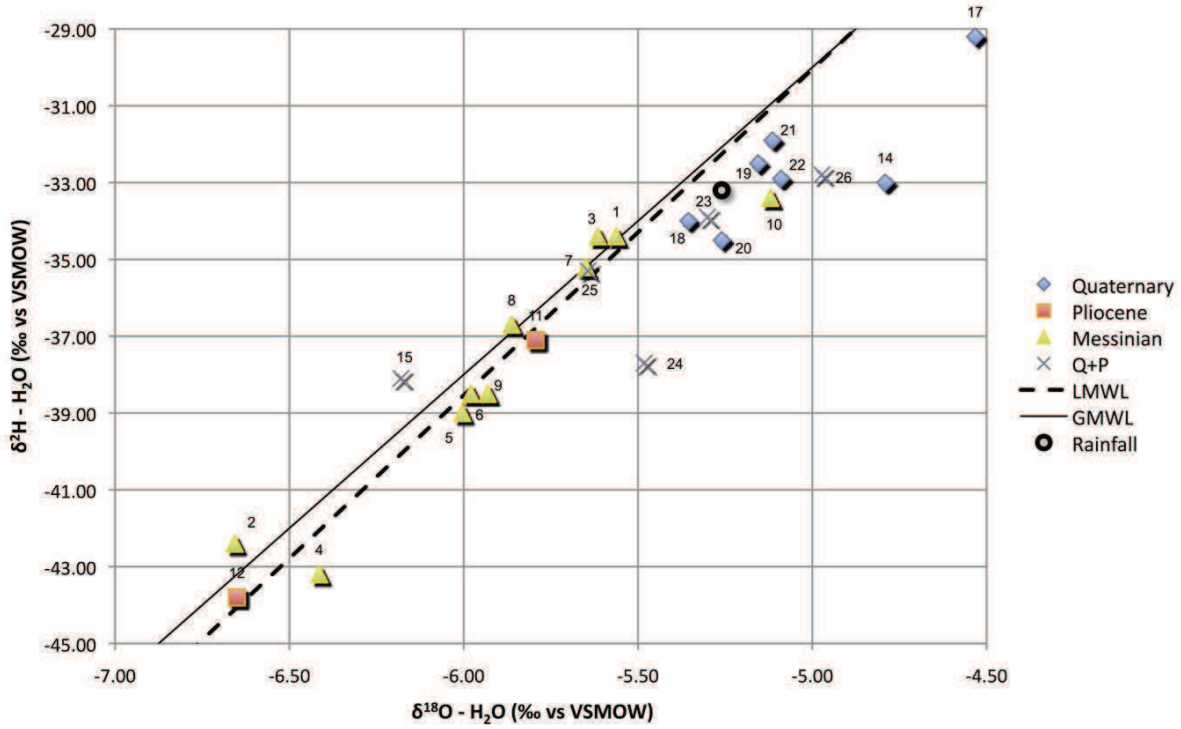

Figure 44: δ^2H vs $\delta^{18}O$.

The mean stable isotopic composition of rainfall matches quite well with the domain of the Quaternary aquifer, although some Quaternary samples are slightly enriched compared to rainfall. This is explained by the high variability in recharge water composition and by the high rate of evaporation of the irrigation water, before and during its application.

The assessment of the isotopic composition of rainfall at the mountain range relies on the right choice of the $\delta^{18}O$ altitudinal gradient. Diaz-Teijeiro et al. (2009) proposed -0.35 ‰ per 100 m for the Spanish Mediterranean area based on GNIP data, Fernández-Chacón et al. (2010) obtained -0.6‰ per 100 m in a local study in Southern Spain while commonly worldwide used gradients usually range around 0.2-0.3 ‰ per 100 m. Only the altitudinal $\delta^{18}O$ gradient from Diaz-Teijeiro et al. (2009) explains part of the isotopic composition of deep groundwater just by a continental and altitude effect, and therefore supports the first hypothesis.

Information supporting the second hypothesis is provided by the combination between stable isotope of water and ^{14}C MRT (Figure 45). A global enrichment in $\delta^{18}O$ is observed since 30 thousand years, and is interpreted as a global increase in temperature. This result is in good agreement with case studies in the Mediterranean: Portugal (Condesso de Melo et al., 2001; Galego Fernandes and Carreira, 2008), Spain (Manzano et al., 2001) and Southern France (Jiráková et al., 2009; Huneau et al., 2001).

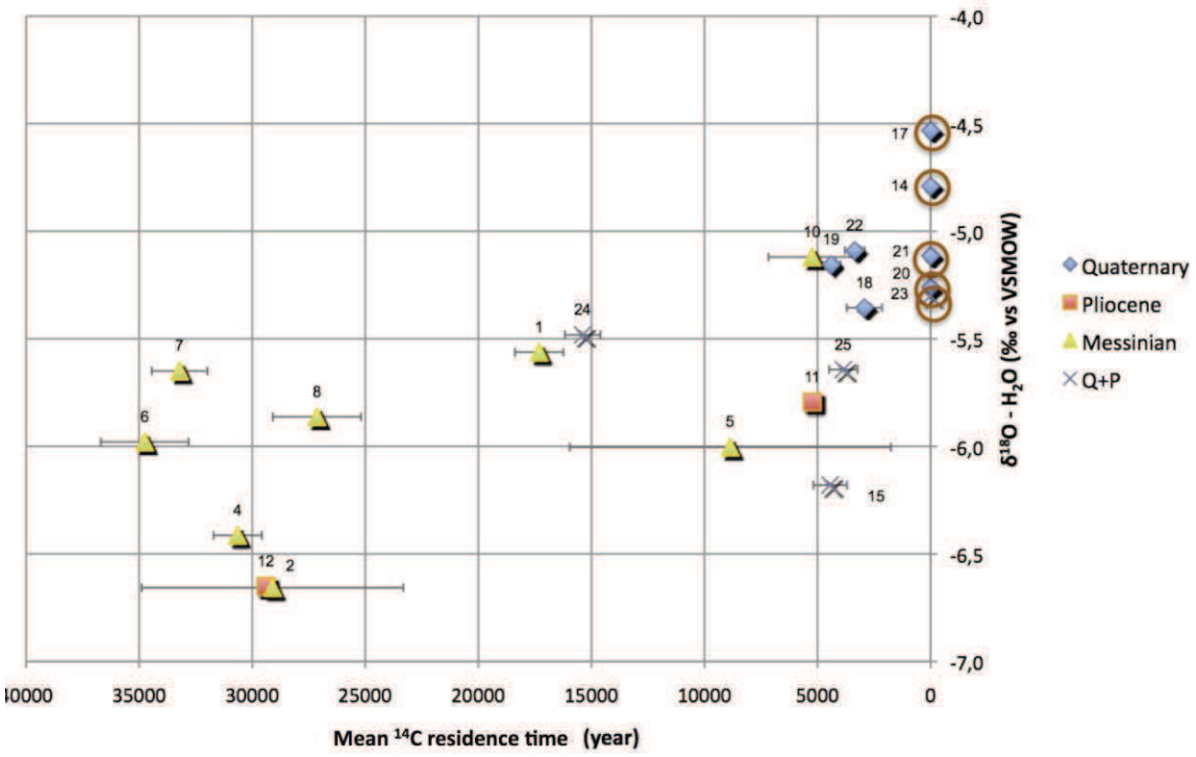

Figure 45: ^{14}C mean residence time vs $\delta^{18}O$ composition. Brown circles identify the "modern pole" of Quaternary and Q+P samples.

5.5.2 Recharge rates

Based on mean irrigation return flow rates and effective precipitation coefficients, the Spanish Geological Survey (IGME) proposed the first estimation of modern recharge rate to the Quaternary aquifer. The results integrated over the whole study area gave 50 $mm.year^{-1}$. Other studies were recently conducted to estimate recharge to the Quaternary aquifer, using a root zone modelling approach (Jimenez-Martinez et al., 2009) or the water balance in the soil, unsaturated and saturated zones (Jimenez-Martinez et al., 2010). A local recharge of 200 $mm.year^{-1}$ was then proposed for the irrigated area. Combining both approaches and

integrating data for the whole study area (irrigated and non-irrigated areas), a mean present recharge to the Quaternary aquifer of 80 mm.year^{-1} is obtained.

The absolute recharge contribution to the confined Pliocene and Messinian aquifers was calculated on the base of the radiocarbon absolute MRT computed against an exponential piston flow model. In order to lower the impact of mixing, confined samples issuing from mixing (particularly evidenced by the tritium content as in samples n°10 and 11) were discarded. For the confined Messinian and Pliocene aquifers, the equation from Cook and Herczeg (2000) for a purely advective transport in a confined aquifer of constant thickness were used:

where Rc is the recharge rate to the confined aquifers, n_{eM} is the effective porosity of confined aquifers, H is the thickness of the aquifer, and t is the radiocarbon MRT of the water. The distance to outcrop (x) varies for each sample, while the mean outcrop length (x_0) was considered as 800 m for the Messinian and 200 m for the Pliocene. Effective porosity range from 0.01 to 0.4 with a mean value of 0.19 for the Messinian aquifer and a mean value of 0.25 for the Pliocene aquifer (Jimenez-Martinez et al., 2012). From the same author, mean and maximum thickness values are 125 m and 240 m for the Messinian and 30 m and 110 m for the Pliocene (Table 14). The calculated mean recharge rate ranges from 1 to 99 mm.a^{-}1, with a mean value of 23 mm.a^{-1}.

The absolute recharge to the unconfined Quaternary aquifer was also calculated on the base of the radiocarbon absolute MRT, for both “old” and “modern” waters. An exponential mixing model was chosen to take into account the uniform recharge process, including all mixings. The equation from Cook and Herczeg (2000) corresponding to a purely advective transport in an unconfined aquifer of constant thickness was used:

where R_Q is the recharge rate to the unconfined aquifer, z is the saturated thickness and ne_Q is the effective porosity. ne_Q ranges from 0.1 to 0.4, with a mean value of 0.23; mean and maximum values for z are 55m and 150m, respectively (from Jimenez-Martinez et al., 2012). Using an exponential model in an unconfined aquifer with homogeneous recharge, recent recharge necessarily contributes to “old” groundwater samples representative for “natural

conditions". Thus, the high ^{3}H in samples 19 does not necessarily contradict its classification as an "old" Quaternary groundwater.

Considering a maximum MRT of 60 years for modern samples (14, 17, 20, 21), the minimum mean modern recharge rate for the Quaternary aquifer ranges from 92 to 1000 mm.year^{-1}, with a mean value of 210 mm.year^{-1} (Table 14), while the recharge rate for "old" Quaternary groundwater ranges from 2 to 26 mm.year^{-1} with an average value of 5 mm.year^{-1}. The accordance with the estimations made from hydrological and vadose zone approaches confirms the validity of the time-tracer approach.

Table 14: Sensitivity of recharge rates to thickness and porosity values

Sample ID	Aquifer	Mean MRT (year)	Effective porosity			Thickness (m)		Recharge rate (mm.a^{-1})		
			Min.	Mean	Max.	Mean	Max.	Min.	Mean	Max.
1	Messinian	16782	*0.01*	*0.19*	*0.40*	*125*	*240*	2	36	145
2	Messinian	28629	*0.01*	*0.19*	*0.40*	*125*	*240*	0	5	20
4	Messinian	30146	*0.01*	*0.19*	*0.40*	*125*	*240*	1	12	50
5	Messinian	8386	*0.01*	*0.19*	*0.40*	*125*	*240*	3	55	222
6	Messinian	34251	*0.01*	*0.19*	*0.40*	*125*	*240*	1	19	76
7	Messinian	32700	*0.01*	*0.19*	*0.40*	*125*	*240*	1	17	68
8	Messinian	26631	*0.01*	*0.19*	*0.40*	*125*	*240*	1	28	115
12	Pliocene	28861	--	*0.25*	--	*30*	*110*	--	9	--
14	Quaternary	60	*0.1*	*0.23*	*0.4*	*55*	*150*	92	210	1000
17	Quaternary	60	*0.1*	*0.23*	*0.4*	*55*	*150*	92	210	1000
20	Quaternary	60	*0.1*	*0.23*	*0.4*	*55*	*150*	92	210	1000
21	Quaternary	60	*0.1*	*0.23*	*0.4*	*55*	*150*	92	210	1000
18	Quaternary	1586	*0.1*	*0.23*	*0.4*	*55*	*150*	3	8	38
19	Quaternary	3054	*0.1*	*0.23*	*0.4*	*55*	*150*	2	4	20
22	Quaternary	2013	*0.1*	*0.23*	*0.4*	*55*	*150*	3	6	30

5.6 Conclusions

This two-step methodology with high precision temperature profiles and environmental tracers provides one of the first estimates of the evolution of recharge in relation to the development of irrigation in semiarid Spain. It shows that the multi-aquifer system of the Campo de Cartagena has had two distinct recharge regimes; the natural state before 1950 and the present artificial state, consequence of the heavy agricultural development in the whole region with a spectacular increase in the number of pumping wells.

The pre-anthropization recharge regime gave 23 mm.year^{-1} over the outcrops of the Pliocene and Messinian aquifers and 5 mm.year^{-1} in the plain (shallow Quaternary aquifer). The clear post-nuclear MRT of the modern Quaternary samples allowed to assess a modern recharge value of 210 mm.year^{-1}. Despite the unusual approach of determining modern recharge rates with radiocarbon, this approximation was confirmed by the results of local experiments in the unsaturated zone (Jímenez-Martinez et al., 2009; 2010). This chapter therefore evidences the recharge increase to the Quaternary aquifer by more than one order of magnitude as a consequence of irrigation. Tritium did not allow a reliable assessment of modern recharge because of the high variability of the recharge signal. Nevertheless, it remained a good qualitative indicator of modern recharge, more reliable than nitrate. Tritium evidenced the occurrence of a local contamination of deep layers by downward groundwater flows through long-screened boreholes, confirming the observations from undisturbed temperature loggings.

Table 15 : Results from the February 2011 groundwater sampling campaign. All geochemical species in $mg.l^{-1}$, temperature in °C, E.C. in mS/cm; Letters M, P and Q refer to the Messinian, Pliocene and Quaternary aquifers, respectively

Sample ID	Aquifer	Sampling date	pH	Temp.	E.C.	HCO_3^-	Cl^-	NO_3^-	SO_4^{--}	Ca^{++}	Mg^{++}	Na^+	K^+	Br
1	M	10/02/11	7,0	26,6	4,27	295	751	8	983	242	190	385	12	3
2	M	08/02/11	6,7	36,6	4,1	490	671	17	818	165	125	541	24	2
3	M	17/02/11	7,0	32,3	3,4	353	679	0	319	108	97	361	9	3
4	M	08/02/11	7,0	34,5	6,33	405	1435	51	1209	226	168	1001	38	6
5	M	16/02/11	6,6	36,5	6,15	391	1417	10	1516	330	191	956	27	5
6	M	14/02/11	6,8	32,5	5,8	328	1147	0	1626	345	213	753	21	4
7	M	07/02/11	6,8	31	3,43	485	680	4	488	115	116	433	14	2
8	M	08/02/11	6,8	31,6	6,19	361	1455	0	1240	326	158	885	24	6
9	M	16/02/11	6,4	32,6	6,8	560	1464	32	1476	279	222	1007	29	5
10	M	10/02/11	6,8	27,9	6,04	460	1283	100	1075	209	142	934	16	7
11	P	10/02/11	7,1	24,7	4,41	232	949	22	891	250	156	535	9	3
12	P*	10/02/11	7,0	25	4,59	323	1149	27	675	169	140	672	24	5
14	Q	14/02/11	7,0	19,3	7,73	256	1714	275	1951	396	335	1088	18	5
17	Q	17/02/11	7,2	20	5,07	275	957	207	955	203	181	636	20	3
18	Q	16/02/11	7,0	20,4	7,61	283	1676	160	1814	342	273	1150	19	5
19	Q	13/02/11	7,4	20,3	4,17	334	777	231	472	92	107	605	13	4
20	Q	18/02/11	7,3	21,9	6,79	275	1653	67	1186	202	253	998	14	6
21	Q	08/02/11	7,2	21,5	5,62	303	1258	174	1013	184	176	867	19	6
22	Q	16/02/11	7,2	20,4	4,96	347	1181	90	396	139	141	657	-	4
15	Q+P	09/02/11	7,1	21,1	5,92	197	1445	36	1155	350	247	640	-	5
23	Q+P	14/02/11	6,9	19,9	8,41	342	2045	200	1960	438	337	1245	21	6
24	Q+P	10/02/11	7,1	22,5	7,87	189	2180	19	1318	402	321	991	-	8
25	Q+P	18/02/11	7,1	20,7	7,13	267	1523	107	1463	295	243	960	14	5
26	Q+P	18/02/11	7,2	19,6	7,64	295	1456	251	2176	294	286	1249	21	5

Table 16: Results from the February 2011 groundwater sampling campaign. Stable and radiogenic isotopes. Letters M, P and Q refer to the Messinian, Pliocene and Quaternary aquifers, respectively

Sample ID	Aquifer	Sampling date	$\delta^2H - H_2O$ (‰ vs VSMOW)	$\delta^{18}O - H_20$ (‰ vs VSMOW)	^3H (UT)	^3H error (UT)	$\delta^{13}C$ (‰ vs PDB)	$A^{14}C$ (pMC)	$A^{14}C$ error (pMC)
1	M	10/02/11	-34,40	-5,56	0	0,3	-5,87	4,8	0,1
2	M	08/02/11	-42,40	-6,66	0	-	-2,20	0,3	0,1
3	M	17/02/11	-34,40	-5,62	0	-	-	-	
4	M	08/02/11	-43,20	-6,41	0	-	-5,32	0,8	0,1
5	M	16/02/11	-39,00	-6,00	0	0,4	-2,50	3,0	0,1
6	M	14/02/11	-38,50	-5,98	0	-	-4,10	0,4	0,1
7	M	07/02/11	-35,20	-5,65	0	-	-6,41	0,7	0,1
8	M	08/02/11	-36,70	-5,86	0	0,2	-4,18	0,9	0,1
9	M	16/02/11	-38,50	-5,93	0	0,4	-1,13	3,6	0,1
10	M	10/02/11	-33,40	-5,12	0,9	0,3	-4,73	15,3	0,1
11	P	10/02/11	-37,10	-5,79	0,5	0,3	-7,34	26,5	0,2
12	P*	10/02/11	-43,80	-6,65	0	-	-5,79	1,1	0,1
14	Q	14/02/11	-33,00	-4,79	8,0	0,6	-10,17	76,2	0,3
17	Q	17/02/11	-29,20	-4,53	4,2	0,4	-8,35	69,4	0,3
18	Q	16/02/11	-34,00	-5,36	6,4	0,6	-8,71	46,5	0,2
19	Q	13/02/11	-32,50	-5,16	2,4	0,3	-7,59	36,0	0,2
20	Q	18/02/11	-34,50	-5,26	1,2	0,3	-8,40	63,7	0,3
21	Q	08/02/11	-31,90	-5,11	4,3	0,6	-7,27	55,6	0,3
22	Q	16/02/11	-32,90	-5,09	0,6	0,4	-9,63	50,6	0,2
15	Q+P	09/02/11	-38,10	-6,18	0	-	-6,94	28,6	0,2
23	Q+P	14/02/11	-33,90	-5,30	5,4	0,3	-10,41	73,1	0,3
24	Q+P	10/02/11	-37,70	-5,48	1,4	0,3	-7,45	8,0	0,1
25	Q+P	18/02/11	-35,30	-5,64	2,2	0,3	-8,47	41,2	0,2
26	Q+P	18/02/11	-32,80	-4,97	6,9	0,7	-	-	

Chapter 6

Radon, Radium and hydrodynamic modeling for submarine groundwater discharge assessment

6.1 Introduction

In this chapter, a radon-radium mass balance was performed to quantify SGD to the Mar Menor. As the main surface water input (Rambla del Albujon) was known to carry water coming from groundwater drainage (García-Pintado et al., 2007), it was expected to be a non-negligible source of radionuclides to the lagoon. As well, hidden inputs of radionuclides originated by brines from groundwater desalination were expected, but without any idea on their location and flux. In order to i) understand the potential impact of surface water discharge to the lagoon, ii) localize additional undocumented inputs and iii) decipher surface inputs from SGD, the radionuclides survey was combined with a numerical simulation of the hydrodynamics of the lagoon. Reports of such combination are limited to the Venice lagoon (Ferrarin et al., 2008 and Rapaglia et al., 2008) but with different objectives: comparing estimates of residence times and estimating the seasonal and temporal variability of SGD.

Some authors tried to explain the origin of the radon and radium variability in groundwater (e.g. Dulaiova et al., 2008; Gonneea et al., 2008), but general guidelines cannot be drawn because of the complex behaviors of Ra and Rn in coastal aquifers. Moreover, radon and radium have recently been shown to be brought to coastal environments not only by "new water" carried by the regional subterranean hydrodynamics, but also by the recirculation of saline water in the sediments (e.g. Taniguchi et al., 2006; Gattacceca et al., 2011). These two processes trace two distinct components of SGD: fresh submarine groundwater discharge (FSGD) and recirculated saline groundwater discharge (RSGD). FSGD is driven by terrestrial hydraulic gradients and occurs at the freshwater/seawater interface, i.e. at the beach face. RSGD is the result of a series of mechanisms that force seawater to flow across the sediment-water interface, being "recycled" in the underlying sediments or at the beach face. The driving forces of both components of SGD were reviewed by Santos et al., (2012) and include tidal pumping, wave setup, wave pumping, ripple migration, bioturbation or gas bubble upwelling (Figure 46).

The correct characterization of the FSGD and RSGD groundwater end-member is crucial for a reliable SGD quantification with radon and radium, although only a limited number of authors attempted to separate both end-members (e.g. Taniguchi et al., 2006; Santos et al., 2012). In this chapter, FSGD and RSGD end-members were selected out a

detailed sampling of piezometers and sediments under the lagoon, combined with hydrodynamics calculations.

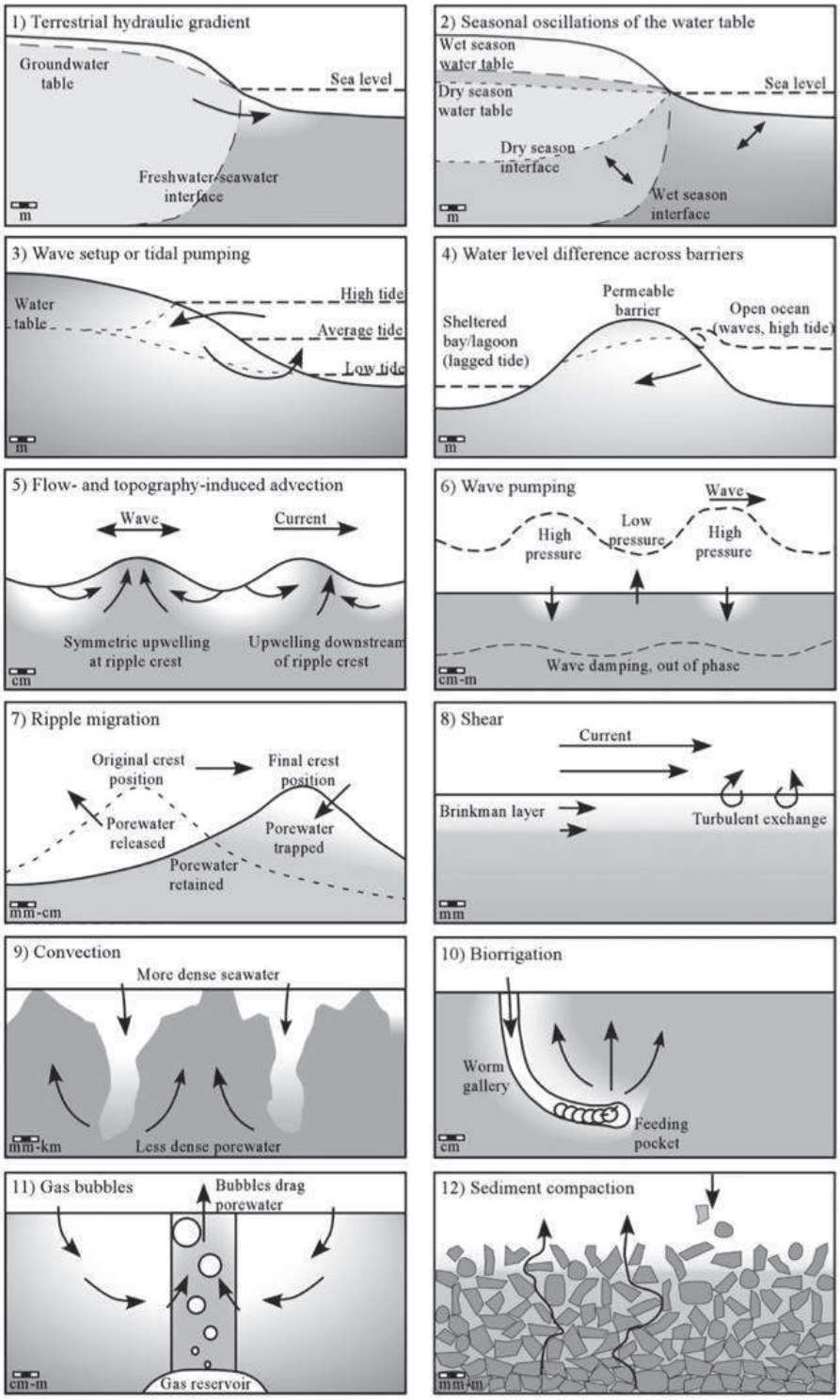

Figure 46: Drivers of porewater (or groundwater) advection in permeable sediments. From Santos et al. (2012).

6.2 Methods

6.2.1 Sampling

6.2.1.1 Groundwater and surface water

In order i) to define the SGD groundwater pole and ii) to assess the contribution of Quaternary groundwater through drainage to surface water streams, groundwater samples were collected in 2010, 2011 and 2012 from four Quaternary boreholes (A, G, I, J) located on the coastal border of Mar Menor (Figure 47).

Extraction from tubewells was made with an electric pump after stabilizing the physical and chemical parameters (pH, EC, temperature, eH). Although the Pliocene aquifer discharges neither into the lagoon nor to the surface water network, its groundwater is pumped and used for irrigation. When it is previously desalinated, brines are released to the Quaternary aquifer or to the ramblas network, as it is for the Quaternary aquifer. In order to trace the presence of these brines in surface water, one brine sample (D_{out2}) was collected at a reverse osmosis plant using Pliocene groundwater.

In addition, samples were collected before reverse osmosis (D_{in}) and in the final product (D_{out1}) to assess whether the desalination process modifies ^{222}Rn activities. Therefore, although no Quaternary desalination plant could be sampled, it was expected to get indications for estimating the composition of the brine that would be generated.

In order to characterize qualitatively and quantitatively the spatio-temporal variability of the surface water discharge to the lagoon, a series of key locations were selected and sampled along the Rambla del Albujón, in the main course of the river and in artificial releases (Figure 4). As aforementioned, R1 corresponds to the discharge point of the rambla into into the lagoon. It was sampled three times in 2011 and nine times in 2012, i.e. almost every day, starting 6 days before the lagoon-seawater sampling and with a last measurement one week after. R4 was collected once in 2011 and four times in 2012 (including one sample one week after the lagoon-seawater sampling). R2 and R3 were sampled twice in 2011 and five times in 2012.

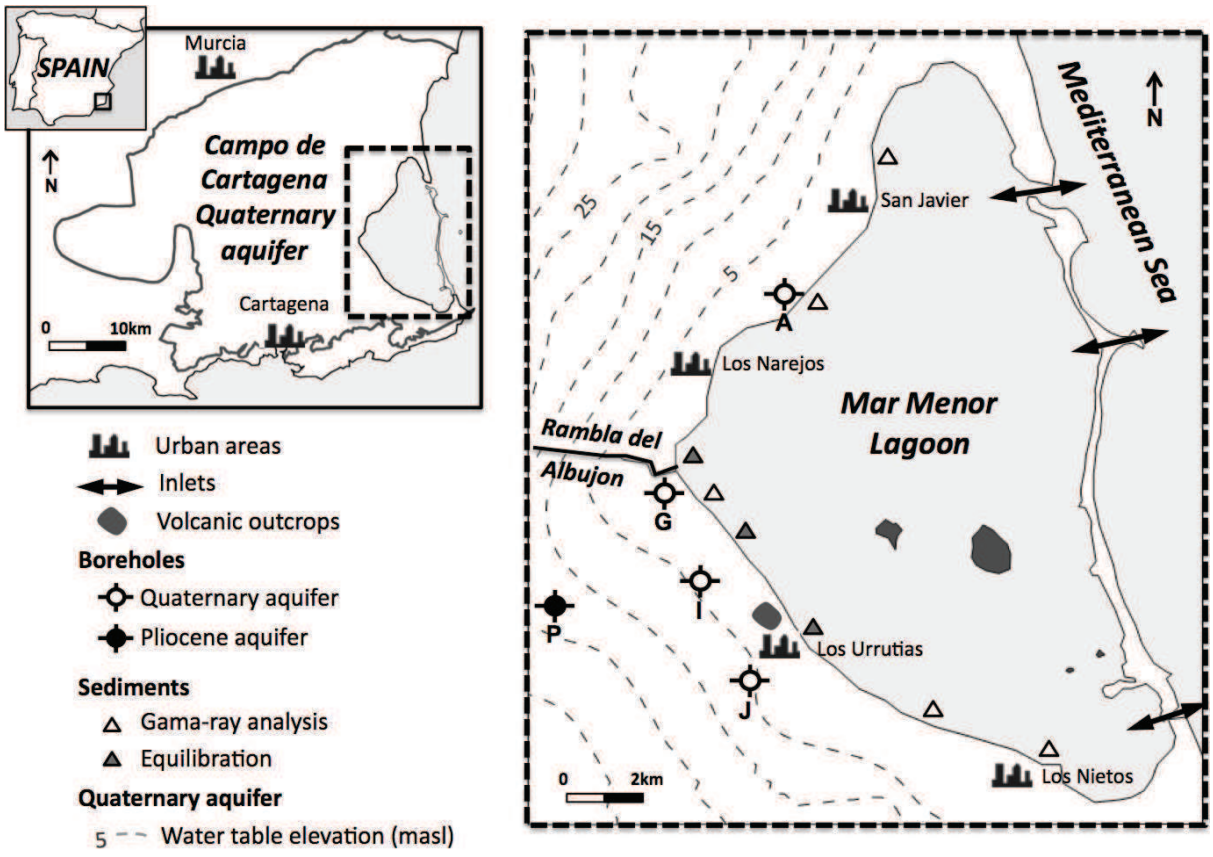

Figure 47: Location of the sampled boreholes, sampled sediments, inlets and water table elevation in the Quaternary aquifer (based on IEA, 2011).

Other surface samples (RO, R5, R7 and R9; Figure 4) also located upstream the rambla mouth, were collected once, in 2011, in order to provide a wider spatial resolution of the radionuclide activities in the watershed. Every time it was possible, discharge rates were measured during the sampling (Table 18).

Physical and chemical parameters were measured with a Hach multi parameter device. Samples were collected in 50 ml polypropylene bottles for anions. Samples for stable isotopes were collected in 30 ml glass bottles. Samples for Radon were collected in 250 ml glass bottles and samples for radium isotopes in 15 L containers.

6.2.1.2 Lagoon and seawater

The seasonal variations and the impact of climatic conditions (wind, temperature, salinity) on the distribution of Ra and Rn isotopes in the lagoon were characterized by three sampling campaigns in November 2010 (winter season), July 2011 (summer season) and January 2012 (winter season). The 2010 campaign mostly consisted in a ^{222}Rn survey along

the western coast of the Mar Menor (35 measurements), together with the collection of five samples for radium isotopes. In 2011, a wider area was sampled for ^{222}Rn, representing a total of 63 measurements, including the central part of the lagoon, the surroundings of an andesitic isle and the Mediterranean Sea, while ten samples were collected for radium inside the lagoon and one in the Mediterranean Sea. In 2012, a more complete definition of the lagoon and the Mediterranean Sea was obtained, with a total of 57 measurements, while fourteen samples in the lagoon and one in the Mediterranean Sea were collected for radium. In addition, a long-term (21h) sampling at a fixed location in an area sheltered from currents (the Los Urrutias harbour) was performed between 10 and 11 July 2011 to assess the temporal variability of the ^{222}Rn activity. It represents a total of 84 measurements.

Samples for ^{222}Rn were directly processed in the field, as detailed in the "Analytical techniques" section. Samples for radium isotopes were collected in 15 L containers. Turbidity, pH, temperature, electric conductivity, salinity and chlorophyll were continuously recorded by a YSI V6600 V2 multiparametric probe connected to a portable computer for data recording with the GPS location.

6.2.2 Sediments and pore water

In order i) to select the best end-member for the SGD pole (in addition to aforementioned groundwater sampling), ii) to quantify the diffusive production of radionuclides from the sediments underlying the lagoon and iii) to assess whether the release of radionuclides from resuspended sediments could be a significant source of radionuclides to the lagoon, a total of ten saturated sediments were collected from Mar Menor in July 2011 and January 2012. Their locations are shown in Figure 47.

6.2.3 Analytical techniques

6.2.3.1 Radium isotopes

Each sample passed by gravity through a PVC cartridge filled with 20 g dry weight “Mn-fibers” previously rinsed three times with Millipore water. The sample flow rate was checked to be less than 1 L per minute, in order to insure the retention capacity of the Mn fibers to be higher than 97% (Moore, 2008). Prior to process the sample, the water content of each fiber was kept between 0.4 and 1.1 g_{H2O}/g_{fiber} in order to get maximum emanation

efficiency (Sun and Torgersen, 1998). The samples were processed with either the RAD-7 for ^{224}Ra in November 2010 and July 2011 or the RaDeCC (Radium Delayed Coincidence Counting) system (Moore and Arnold, 1996) for ^{223}Ra and ^{224}Ra in January 2012.

^{223}Ra and ^{224}Ra activity measurement with the RaDeCC system was calibrated using in - house standards of ^{227}Ac and ^{232}Th prepared according to the technique of Scholten et al. (2010). Four standards were prepared, Th20a, Th20b, Ac10a, Ac10b standing for 20 and 10 dpm of ^{232}Th and ^{227}Ac respectively. Repeated measurements were performed over one week using three different detectors. Detection efficiencies for ^{224}Ra, ^{223}Ra and total dpm were very similar for the three detectors and similar to the values reported in Scholten et al. (2010). Their variations with time were within the error range, calculated according to Garcia-Solsona et al. (2008). ^{228}Th activity in water was measured with RaDeCC system ^{224}Ra supported and so in equilibrium with ^{228}Th in water samples, one month after collection. ^{227}Ac activity in water was measured with RaDeCC system ^{223}Ra supported and so in equilibrium with ^{227}Ac in water samples, 3 months after collection. Radium activities from November 2010 and July 2011 were measured using the RAD-7 as follows. Once impregnated with radium, the fibers were placed into in-house glass cartridge connected to the RAD-7 system. ^{224}Ra activity in the sample was estimated by measuring the decay of its daugther, ^{220}Rn or thoron by RAD-7. The RAD-7 detection efficiency for ^{224}Ra was calculated using two different standards. In 2006, a in-house sea water standard of ^{232}Th and ^{226}Ra (F3S, 4000 dpm) was used. The mother solution was shown to be in radioactive equilibrium with respect to ^{232}Th-^{228}Ra using independent estimations of ^{228}Ra by TIMS and PERALS techniques (Gattacceca et al., 2011). In 2012 the efficiency of RAD-7 was estimated using the Th20a standard of RaDeCC described above. RAD-7 detection efficiency for ^{224}Ra was similar using the two standards. Considering that the second standard was analyzed 6 years after the first one, the sensitivity of the RAD-7 system remained constant over time. ^{226}Ra activity in water was measured by radon emanation method with RAD-7 system in Mn-fiber placed in glass cartridge hermetically closed during 2 weeks. RAD-7 efficiency for ^{226}Ra was determined using F3S standard (^{232}Th and ^{226}Ra).

6.2.3.2 Radon isotopes

The ^{222}Rn activities of lagoon water and seawater were measured according to Dulaiova et al. (2005) by means of two radon-in-air detectors (RAD-7-Durridge, Co. Inc.) routed

simultaneously through one single air-water exchanger (RAD-Aqua, Durridge). Water was pumped at a constant flow rate of 2.5 L/min and filtered through a 80 mm cartridge. Data integration (run) was fixed to 15 minutes, and a typical equilibration time of 20-30 minutes was assumed for the system (Stieglitz et al., 2010). RAD-7 determines ^{222}Rn activity by measuring the decay of the daughter ^{218}Po, considered to be in equilibrium with ^{222}Rn after 5 *half-lives of ^{218}Po (= 15 min) (Stieglitz, 2005). The activity of one run therefore corresponds to the geographical position 15 minutes before. The longer equilibration time from high to low activity (Stieglitz et al., 2010) was not taken into account. For groundwater samples, ^{222}Rn activities were analyzed using a RAD-H20 extension of the RAD-7 using 250 ml samples. All ^{222}Rn activities were corrected from temperature and humidity effect (using the Durridge Capture software) as well as from salinity effect (according to Schubert et al., 2012).

6.2.3.3 Sediments and pore water

Five sediment samples (Figure 47) were analyzed by gamma ray spectrometry at CEREGE in order to assess their ^{226}Ra and ^{228}Ra activities (using the 295 and 911 KeV of ^{214}Pb and ^{228}Ac respectively). The mean Mar Menor sediment porosity was estimated by comparing the wet and dry weight (Corbett et al., 1998) of 4 sediment samples.

Sediment porewater radionuclides content (^{222}Rn, ^{223}Ra and ^{224}Ra) was estimated by processing equilibration experiments. 500 g of dry sediment was put in a hermetically closed glass bottles with 600mL of Ra-free seawater (previously passed through Mn-fiber to take away all radium isotopes) for enough time to allow the water overlying sediment in the bottle to be in equilibrium with porewater. For ^{222}Rn, the overlying waters of 5 equilibration experiments were analyzed 1 month after the bottle closing, i.e. more than 10 time the ^{222}Rn half-life, with RAD-7 system. For ^{223}Ra and ^{224}Ra, the water of 3 equilibration experiments were analysed 5 months after closing (more than 10 times the 224Ra and 223Ra half-lives) with RaDeCC system.

6.2.3.4 Other tracers

Nitrate for groundwater and surface water was analyzed by chromatography (UPCT, Cartagena) and was continuously recorded in lagoon and sea water by a SUNA V2 UV (Satlantic) equipment connected to a portable computer for data recording with the GPS

location. It had been previously calibrated with a standard solution of $NaNO_3$ prepared in the laboratory at the range of expected nitrate concentrations in the lagoon water. Results of SUNA measurements were similar to those measured by Ionic Chromatography in discrete samples. Stable isotopes of water were analyzed by mass spectrometry (MSE, Montpellier).

6.2.4 Hydrodynamic modeling of the lagoon

The hydrodynamic dispersion of the input of radionuclides generated by the rambla into the lagoon (thereafter called "plume") was modeled and compared to the radionuclide measurements. It was used as a diagnostic tool to locate point sources of radionuclides inside the lagoon by assessing the origin of high activities in areas not attained by the plume during the days of modeling: if such activities could not be explained by the plume, additional sources of radionuclides would be evidenced.

The introduction of the tracer in the model started 6 days before the days of sampling, i.e. approximately 1.5 half-life of decay for ^{222}Rn. This decay provided an additional criterion for evidencing the non-rambla origin of measured values, as no more than 25% of the input level of ^{224}Ra and ^{222}Rn was expected to persist at the time of sampling in the oldest parts of the plume.

The mean discharge and radon activity of the Rambla were the ones used in the balance, as well as the mean lagoon activity and Mediterranean Sea activity. In addition, previously to each simulation, the model ran for 6 days with all the hydrodynamics forcing in order to let it spin up before the river input was inserted into the model.

The hydrodynamic simulations of the lagoon were performed using ROMS-AGRIF (Debreu et al., 2011), the ROMS version developed by the Institut de Recherche pour le Développement (IRD) using the AGRIF grid refinement procedure developed at the LJK-IMAG (Laboratoire Jean Kuntzmann, Grenoble, France). The Mediterranean Sea grid (150 m resolution) was nested to the Mar Menor grid (40 m) and to the inlets grids (of 5 to 20 m). All nesting grids were bidirectional. The Mediterranean Sea model was forced with sea level fluctuations recorded by a sea level gauge in the Mediterranean Sea (northern part of the study area). The lagoon model was forced with hourly winds recorded at the meteorological station on the northwest coast of the lagoon in the San Javier Airport (run by the Spanish Meteorological Agency – AEMET).

Modelling results were validated against Acoustic Doppler Current Profilers (ADCP) (Aquadopp, Nortek) with data recorded at the NW lagoon coast, 500 m to the meteorological station at a 4 m depth. The validation parameters for a 15 days period simulation were: Bias, Root Mean Square error (RMS) and correlation coefficient.

6.3 Results

6.3.1 Geochemistry

Replicate analysis of water samples returned an external reproducibility of circa 30% (2s) (see Table 17 to Table 20). ^{224}Ra activities measured with the RAD7 (first and second campaigns) were cross calibrated to ^{224}Ra activities measured with the RaDeCC (third campaign) by measuring with both methods one standard fiber (Th20a) and three sample fibers with activities in the range 10 to 100 Bq/m^3. A constant bias of 35% was found between ^{224}Ra activities given by the RaDeCC with respect to the RAD-7. Although the origin of this systematic bias is not understood yet, all the ^{224}Ra data measured with the RAD-7 was standardized to the RaDeCC system, by multiplying RAD-7 data by 0.66 to compare data collected during the different campaigns.

6.3.1.1 Groundwater

Average temperature of 20.9 ± 0.9 °C was similar to the mean annual temperature of surface water (Fig. 2). Electrical conductivity (EC) ranged between 5.3 to 12.6 mS/cm and displayed minor change with time. δ^{18}O vs EC and δ^{18}O vs δD showed linear trends suggesting a two component mixing relationship where the salty one is isotopically depleted (Figure 48).

^{222}Rn activities in Quaternary groundwater ranged between 2100 and 26500 Bq/m^3 without any correlation with EC (Figure 49). Radon activities were rather homogenous, around 20000 Bq/m^3 with the exception of borehole A below 5000 Bq/m^3. ^{224}Ra activities in the Quaternary aquifer varied between 5 and 62 Bq/m^3 (Table 17 and Figure 49), with no significant ^{224}Ra changes in time.

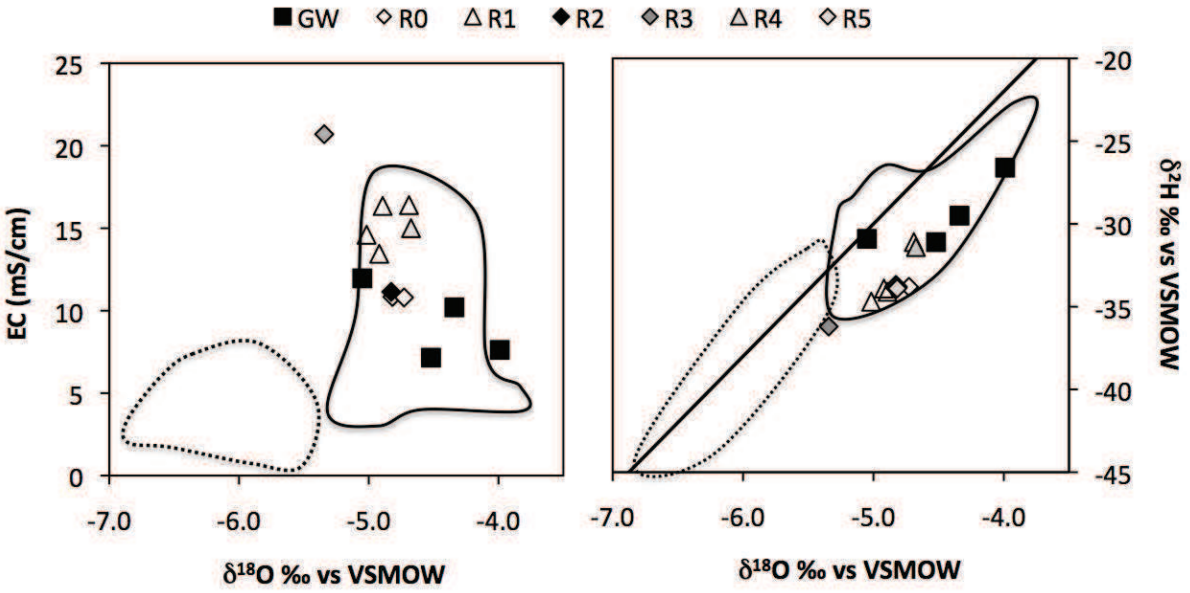

Figure 48: δ ^{2}H vs δ ^{18}O (left) and EC vs δ^{18}O (right) in Quaternary groundwaters, main streams (R1, R4) and tributaries (R0, R2, R3, R5). The black line indicates the CRAIG meteoric water line. The black dotted field stems for deep Miocene and Pliocene groundwater (from F-IEA, 2011) while the black line limits the field of the Quaternary aquifer.

The average ^{224}Ra in groundwater was 43 ± 10 Bq/m^3, dismissing borehole A that was characterized by lower radium activities like for ^{222}Rn. ^{223}Ra measured in two boreholes only varied by a factor of four (0.5 to 1.8 Bq/m^3), and ^{223}Ra/^{224}Ra activity ratio was 27 to 100.

Pliocene groundwater displayed much higher radon activities (about 75000 Bq/m^3, EC=5.7 mS/cm) than the maximum value of Quaternary samples (about 27000 Bq/m^3). The product of desalination by reverse osmosis of Pliocene groundwater had ^{222}Rn activities of approximately 59000 Bq/m^{3,} (EC=0.5 mS/cm) while the released brine reached approximately 69000 Bq/m^3 (EC=16.8 mS/cm).

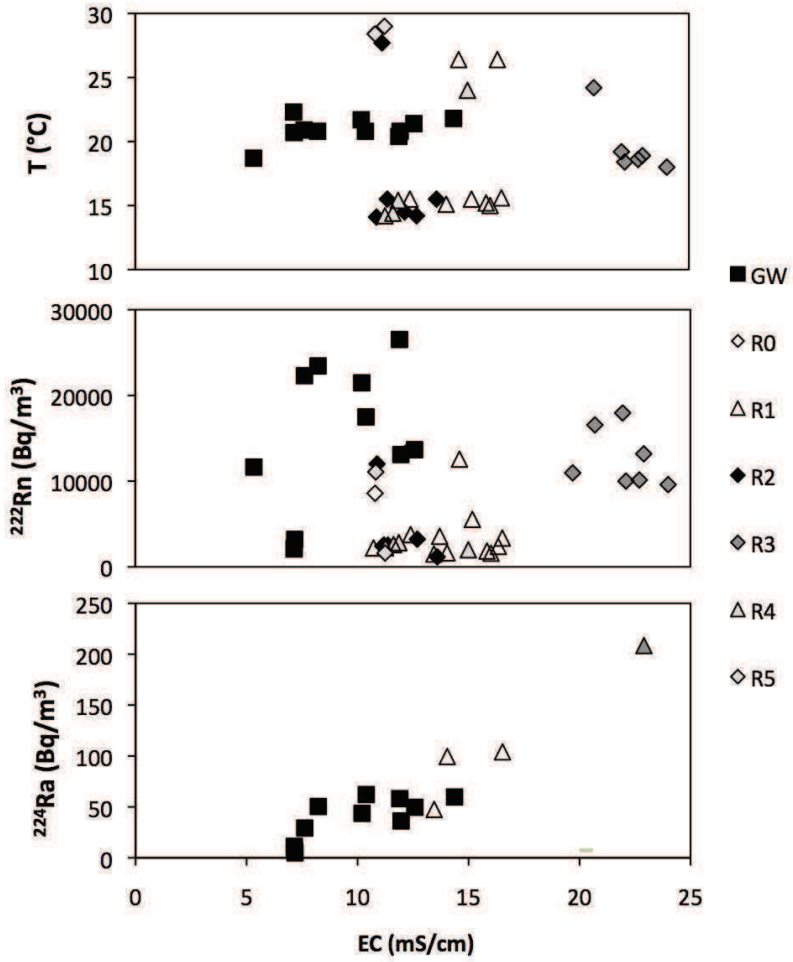

Figure 49: Temperature, ^{222}Rn and ^{224}Ra vs EC in Quaternary groundwaters, main streams (R1, R4) and tributaries (R0, R2, R3, R5).

6.3.1.2 Surface waters

Combining our physico-chemical results with the ones from IEA (2011), all tributaries (except R3) and main streams R1 and R4 showed a similar seasonal variability (winter/summer) for temperature: around 15°C in winter and between 24 and 28°C in summer (Figure 49). R3 appeared more specific since it displayed less variation in temperature (stable around 18°C, with a high value at 25°C), higher EC values (between 20 and 25 mS/cm) and more depleted stable isotopes composition (Figure 48). R1 was characterized by a large range of variation of EC (12.2 to 16.5 mS/cm) not correlated with the seasonality. Stable isotopes displayed a linear trend between R3 and deep groundwater. In addition, an increase of EC with the water discharge was observed simultaneously for R1 and R3.

Regarding ^{222}Rn, similar and almost constant activities were found in R1 and R4 with average values of 1950 and 2000 Bq/m^3 in July 2011 and 2950 and 2550 Bq/m^3 in January 2012 (Table 18). One high value was recorded in R1 in July 2011 (13000 Bq/m^3) but with some doubts on the analytical process. All these values were higher than those commonly found in literature for rivers (e.g. 4.4-11 Bq/m^3 in the Venice lagoon by Gattacceca et al., 2011). Indeed, activities were even higher in R2 and R3 pipes, especially R3 which ranged from 10000 to 18000 Bq/m^3.

Regarding radium, activities were especially elevated in R1, higher than groundwater. ^{224}Ra varied by a factor two between July 2011 and January 2012 but remained constant in January 2012 within a 3-day interval (102 ± 15 and 5.0 ± 1 Bq/m^3 for ^{224}Ra and ^{223}Ra respectively). R3 was characterized by twice more ^{224}Ra but similar ^{223}Ra activities than R1. As for radon, such high radium activities are very uncommon in surface waters (e.g. Beck et al., 2007).

For hydrodynamic modeling and mass-balance purposes, the mean ^{222}Rn activities in R1 and R4 are 1960 Bq/m^3 for July 2011 and 2860 Bq/m^3 for January 2012. The extreme value of 10 July 2011 is not taken into account because of the remaining doubt on the reliability of this first measurement. Together with mean ^{223}Ra (5.1 Bq/m^3 in 2012) and ^{224}Ra activities (47.0 and 100.9 Bq/m^3 in 2011 and 2012, respectively), they are combined to a mean discharge of 2.84 10^4 m^3/d (R1+R4) for both sampling campaigns in order to obtain river fluxes to the Mar Menor (Table 21).

6.3.1.3 Lagoon and Sea waters

The ^{222}Rn activities measured continuously during the three surveys are shown on Figure 50 to Figure 53. Radium activities in the Mar Menor lagoon ranged between 3 and 12, and 10 and 50 Bq/m^3 for ^{224}Ra and ^{222}Rn, respectively (Table 20, Figure 50 to Figure 53).

In comparison, activities measured in the Mediterranean Sea were lower than 3 Bq/m^3 (Table 20), similar to those reported for open Mediterranean Sea by Garcia-Solsona et al. (2010). ^{224}Ra and ^{222}Rn were clearly enriched along the western border of Mar Menor in a wide area starting from los Narejos to the North down to Los Nietos to the South.

Maximum values for both radium and radon isotopes were always found in front of the Rambla del Albujón discharge. The radiotracers, together with NO_3 contents and turbidity, are plotted as a function of the distance to the main surface water stream (positive to the North, negative to the South).

^{222}Rn and nitrate data collected in November 2010 show a well defined (15 km long) and symmetrical peak, slightly shifted to the South with respect to the main rambla (Figure 50). A tiny but significant peak in turbidity was also recorded. Nitrate ranged from 0.26 to 0.75 mg/L. ^{224}Ra activities were quite low too, but unfortunately no sample was taken at the location of the radon peak.

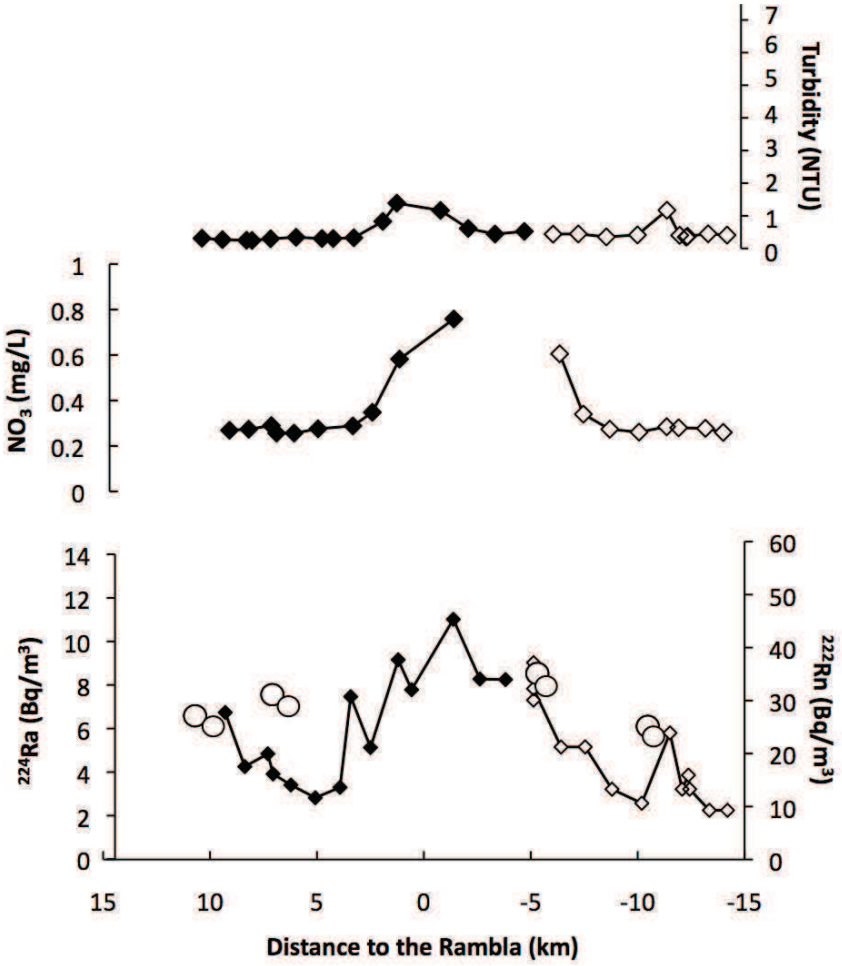

Figure 50: Turbidity, nitrate content, ^{224}Ra and ^{222}Rn activities along the western coastline of Mar Menor following a 2 m isobathymetry in November 2010. Negative distance refers to locations southwards from the Rambla del Albujón mouth. Black and white diamonds stem for 24 and 23 November respectively. White circles stem for 224Ra measurements.

In 2011, continuous measurements of ^{222}Rn, nitrate and turbidity were performed on 8 and 10 July (Figure 51). Two peaks in turbidity were observed each day: one large peak in front of the Rambla point of discharge and another one 6 km southward.

The peak was however higher on July, 8th. Nitrate ranged between 0.18 and 10.3 mg/L, which is 25% more than in November. A nitrate peak was also observed each day: narrow and strictly in front of the Rambla discharge on 8 July, it was wider and southward on July, 10th.

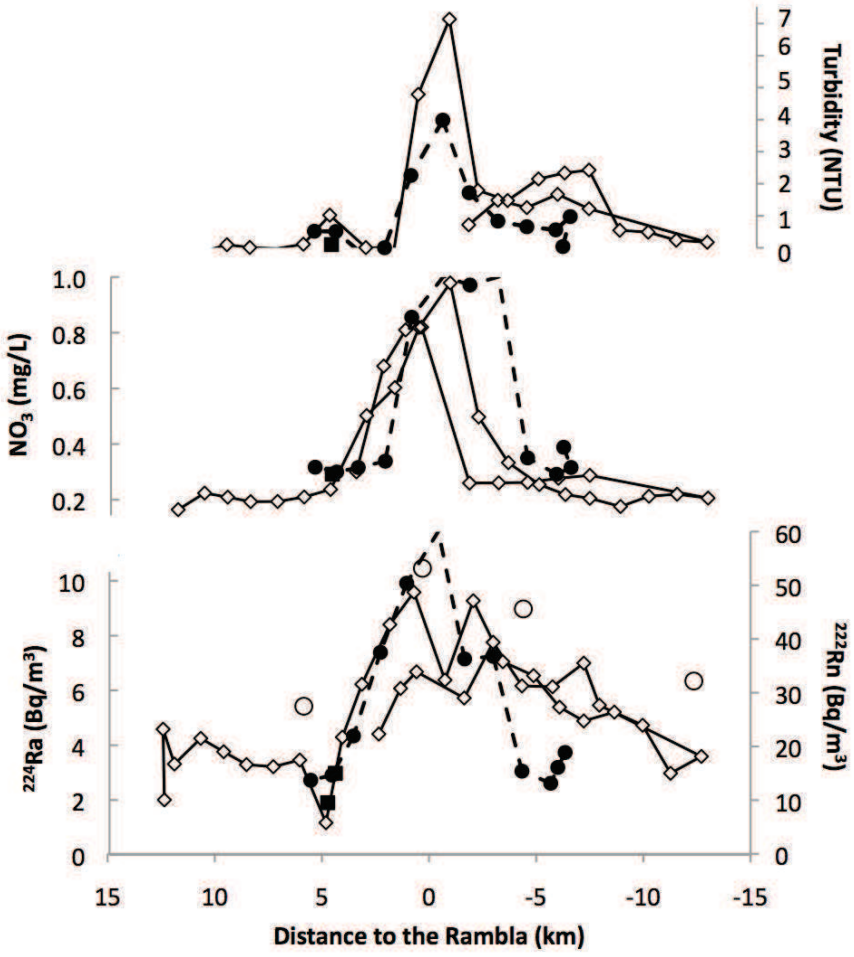

Figure 51: Turbidity, nitrate content, ^{224}Ra and ^{222}Rn activities along the western coastline of Mar Menor following a 2 m bathymetry. Negative distance refers to locations southwards from the Rambla del Albujón mouth. White diamonds stem for 8 July 2011; black squares and circles respectively stem for 9 and 10 July 2011. White circles stem for 224Ra measurements on 6 July 2011.

In terms of ^{222}Rn, the maximum values were measured in front of the Rambla but with a significant tailing southward (as for turbidity) on 8 July. On 10 July, the radon peak shape was symmetrical and located in front of the Rambla. ^{224}Ra activities ranged between 5 and 10 Bq/m^3 and showed the same peak shape of ^{222}Rn.

In January 2012, measurements were performed on the 23rd and 24th. The wind speed was very low (<1 m/s) and turbidity near zero. The lowest nitrate values ranged between 0.11 and 0.5 mg/L, with a narrow and well-defined symmetrical peak strictly in front of the Rambla. A similar feature was found for both ^{222}Rn and ^{224}Ra but the tail of the radon peak seems to be higher to the south. Radium and radon were very well correlated (Figure 52);

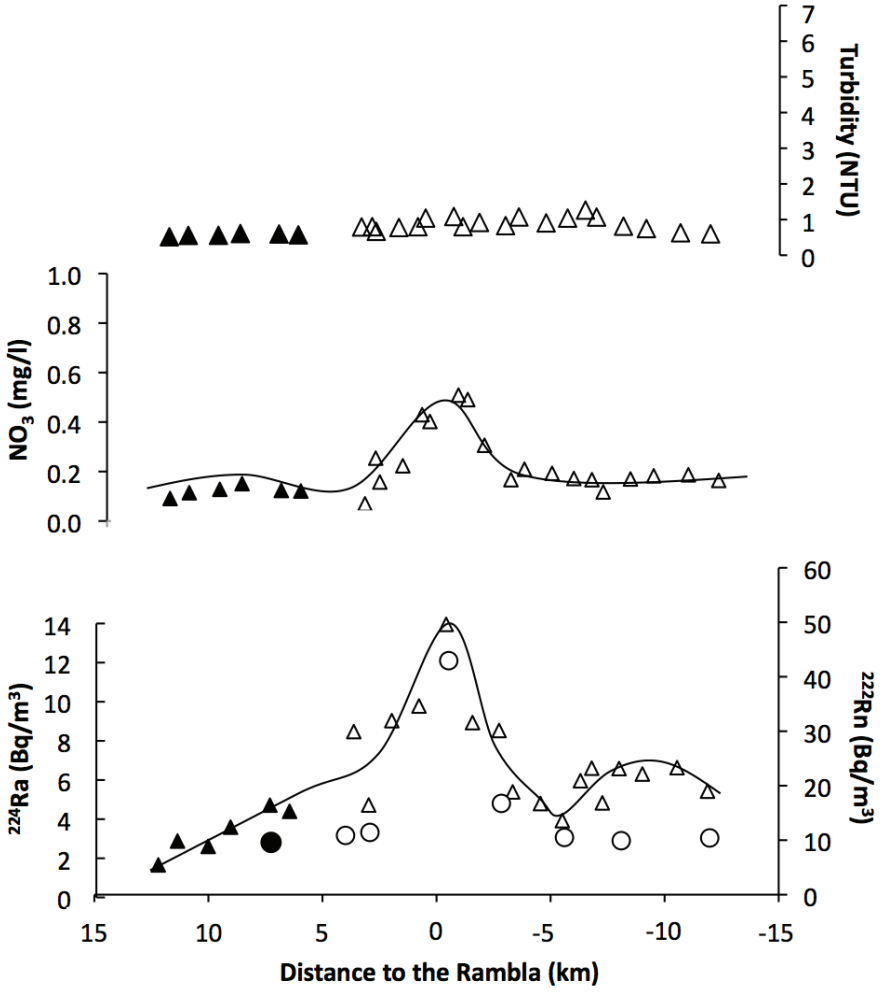

Figure 52: Turbidity, nitrate content, ^{224}Ra and ^{222}Rn activity along the western coastline of Mar Menor following a 2 m bathymetry in January 2012. Negative distance refers to locations southwards from the Rambla del Albujón mouth. Black and white triangles respectively stem for 23 and 24 January 2012; white circles stem for ^{224}Ra measurements.

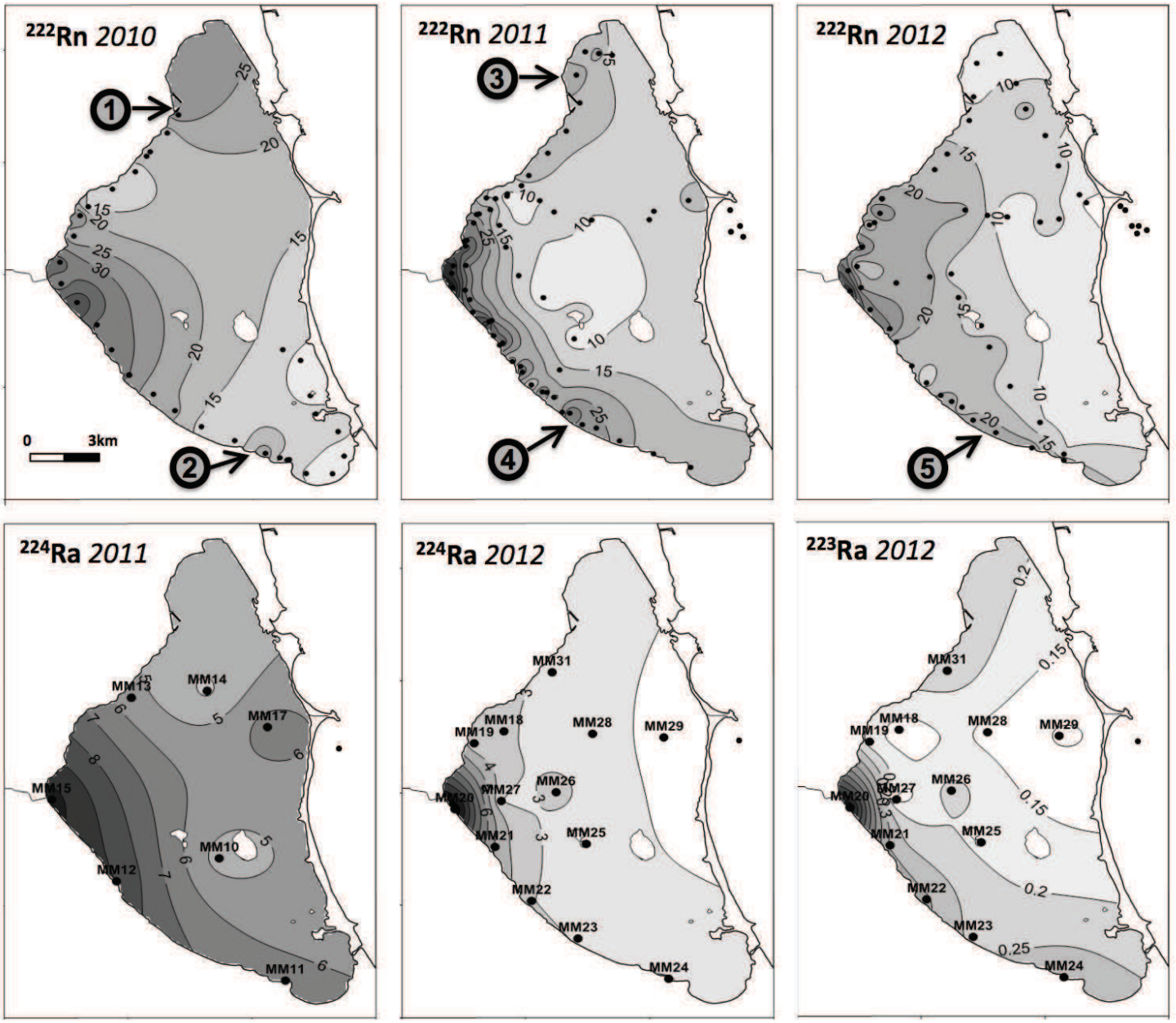

Figure 53: Interpolated maps of ^{222}Rn, ^{224}Ra and ^{223}Ra data from the lagoon (Bq/m^3). Black dots indicate the location of each sample. Values for Mediterranean Sea samples are not indicated (refer to Table 20).

As an attempt to provide a realistic overview of the distribution of radiotracers in the Mar Menor lagoon and the adjacent Mediterranean Sea, all results were interpolated by kriging on the base of 100 m by 100 m cells (Figure 53). Since the samples collected in November 2010 were all located on the western part of the Mar Menor, interpolation has a limited reliability for the central area. The three surveys revealed high ^{222}Rn spots further north and south from the Rambla mouth, as indicated by points 1 to 5 in Figure 53. Average activities for the lagoon were obtained by weighting the extrapolated value of each cell (Table 20) by the corresponding bathymetry. These values will be used for the radiotracers mass balance calculation.

The time series obtained from the long term ^{222}Rn sampling at the Los Urrutias port between 10 and 11 July 2011 is shown in Figure 54. A smooth repetitive oscillation similar to a sinusoid is observed, with a close to 12h periodicity and values ranging from 14 to 40 Bq/m^3. Combining these values with the variations of sea level recorded by an ADCP located less than 500m to Los Urrutias port, an inverse correlation is found. The amplitude of sea level variations is around 5cm.

^{228}Th, ^{227}Ac and ^{226}Ra are the radioactive parents of ^{224}Ra, ^{223}Ra, ^{222}Rn, respectively. In the lagoon, the activity of ^{228}Th is 0.54 Bq/m^3 while ^{227}Ac is negligible and ^{226}Ra gives 0.67 Bq/m^3.

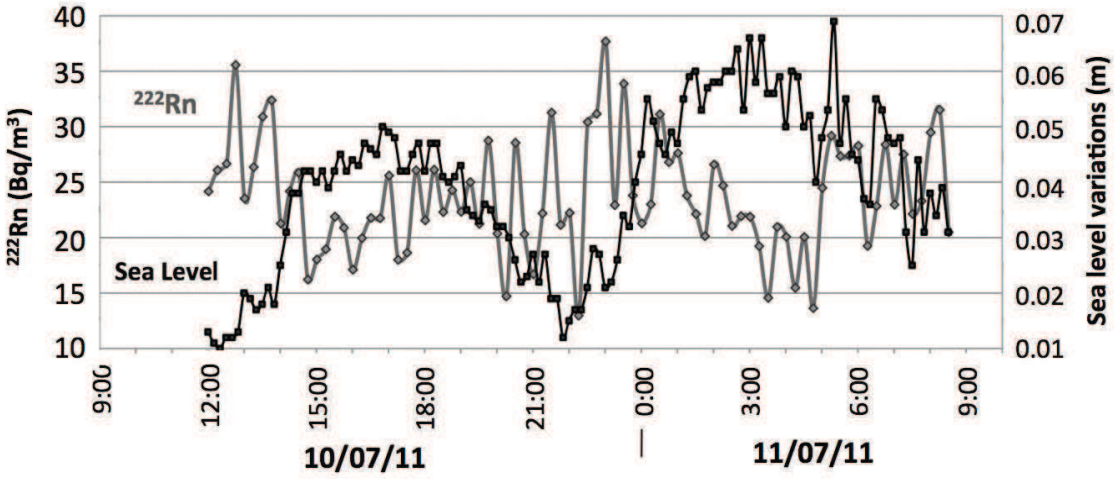

Figure 54: Time series for Radon and sea-level at the Los Urrutias harbour

6.3.1.4 Sediments and pore water

The ^{226}Ra activity in sediments ranged from 3.09 to 6.85 Bq/kg, with a mean value of 5.23 Bq/kg. The ^{228}Ra activity in sediments ranged from 3.43 to 11.34 Bq/kg, with a mean value of 6.56 Bq/kg. Regarding porous groundwater (i.e. sediment interstitial water), the results of equilibration experiments gave mean activities of 600 ± 225 Bq/m^3 for ^{222}Rn (four to forty times lower than the Quaternary piezometers), 34 ± 15 Bq/m^3 for ^{224}Ra (in the intermediate range of measured in groundwater from piezometers) and 3.3 ± 0.5 Bq/m^3 for ^{223}Ra (from three times to one order of magnitude higher than groundwater samples from piezometers). The mean porosity of Mar Menor sediment was 0.5.

6.3.2 Modeling of the currents

6.3.2.1 Hydrodynamic calibration

Regarding the hydrodynamic calibration of the model, sea level data showed the best correlation with an RMS of 1.2 cm and a correlation coefficient of 0.85 (bias of -0.0033). The ADCP speed currents in the lagoon were very slow (<0.1 m/s) giving a correlation coefficient of 0.70 for current at 2 m above the bottom and 0.72 at 0.5 m above the bottom layer with RMS of 1.1 (bias of 0.00056) and 0.1 cm/s (bias of 5.5639) respectively. Higher speed currents showed higher correlation coefficient reproducing correctly the main hydrodynamic patterns. The Bias results show that the model is not under- or over estimating the sea level variations and the speed currents.

6.3.2.2 Radionuclide dispersion

The key steps of the model for the dispersion of a ^{222}Rn plume originating from a continuous Rambla discharge during the 6 days before each campaign, including extreme southwards and northwards positions, are presented in Figure 55. The graphical step by step animations are available as online additional content. Basically, the modeled plume of the Rambla is found to be driven northwards or southwards by the currents, but always in a thick stripe (1 or 2 km max) along the coast. The radionuclide activities in the model naturally decrease with the distance from the output, because of both time elapsed and dilution. From top represented values of 60 Bq/m^3 (^{222}Rn) and 5 Bq/m^3 (^{224}Ra) in the close surroundings of

the discharge point, the plume of radionuclides from the Rambla reaches the mean lagoon value within a few kilometers.

In 2010, ^{222}Rn and radium tracers were injected in the model on 18/11 whereas data acquisition occurred on the 23 and 24/11. The modeled plume remained around the mouth until 20/11. After a slight displacement to the north on 21/11, and under the influence of west winds, the currents took the plume northwards and southwards over 3.5 km on 22 and 23/11. Finally, on 24/11, the currents quickly moved the southern part of the plume southwards down to a location between Los Urrutias and Los Nietos (7 km) while the northern part of the plume was dispersed.

In 2011, the injection started on 3/07. Very dynamic currents shifted the plume in the surroundings of the rambla's mouth from 4 to 5/07 then continuously northwards up to Los Narejos (6 km distance) until the evening of 9/07. No southwards displacement was produced by the model for this survey.

In 2012, the injection started on 17/01. The plume first moved southwards in relation to strong northern winds and it reached the town of Los Urrutias (5 km distance) on 19/01. As the currents decreased, a new plume was created around the mouth until 20/01 in mid-afternoon then it moved northwards. From 21 to 24/01 evening, the newly originated plume was shifted northwards, reaching Playa de la Hita (7 km), while the first plume had remained immobile in the south since 19/01.

6.4 Discussion

6.4.1 Quantification of SGD

A clear excess of radionuclide was observed in the Mar Menor lagoon compared to the Mediterranean Sea. Therefore, as in previous studies that investigate such settings around the world (e.g. Gattacceca et al., 2011) a radionuclide flux balance between input flux (F_{input}) and output flux (F_{output}) of tracers could be performed. Assuming a steady state, the excess of tracers is attributed to a SGD flux (F_{SGD}) as follows:

$$F_{input} + F_{SGD} = F_{output}.$$

The mass balance of the lagoon can therefore be performed using the following equations for radon and radium isotopes, respectively:

$$(F_{in} + F_R + F_{diff} + F_{resuspension} + F_{prod}) + F_{SGD} = F_{decay} + F_{out} + F_{atm} \text{ (radon)}$$

$$(F_{in} + F_R + F_{diff} + F_{resuspension} + F_{prod}) + F_{SGD} = F_{decay} + F_{out} \text{ (radium)}$$

where inputs are composed by the input flux from the Mediterranean Sea (F_{in}), the input flux from rivers (F_R), the diffusive flux from sediments (F_{diff}), the input flux from resuspended sediment ($F_{resuspension}$) and the production from parent in water (F_{prod}). Losses are composed by the natural decay of tracers (F_{decay}), the output flux to the Mediterranean Sea (F_{out}) and the radon atmospheric flux to the atmosphere (F_{atm}).

These different parameters are detailed and discussed in the following sections and summarized in Table 21 and Table 22, regarding the radionuclide budgets of July 2011 and January 2012. Special attention was dedicated to surface water and groundwater end-members, in addition to the input from resuspended sediments, not always considered in details in most studies, but whose role could be significant.

6.4.1.1 Assessment of ^{222}Rn and radium fluxes

6.4.1.1.1 Radon atmospheric flux (F_{atm})

The radon flux across the air-water interface (J_{atm}, in Bq/m^2/d) is generally calculated as:

$$F_{atm} = J_{atm} * Surface_{MM}$$

with

$$J_{atm} = k * (C_w - \alpha * C_{air})$$

where $Surface_{MM}$ is the surface area of the Mar Menor lagoon (in m^2), C_w and C_{air} are the radon activities in water and air, respectively (Bq/m^3). α is the Ostwald's solubility coefficient (dimensionless), i.e. the water–air partition coefficient of radon. It depends on both temperature and salinity and was calculated according to Schubert et al. (2012). The

variable k is the gas transfer velocity (cm/hr) which depends on kinematic viscosity, molecular diffusion and turbulence (principally due to wind speed). The empirical relationship between k and wind speed by Turner et al. (1996) was considered, as follows:

- for $u_{10} \leq 3.6$ m/s : $k = 0.45 * u_{10}^{1.6} * (Sc/600)^{-2/3}$
- for $u_{10} > 3.6$ m/s : $k = 0.45 * u_{10}^{1.6} * (Sc/600)^{-0.5}$

where u_{10} is the wind speed at 10 m height (m/s) and Sc is the Schmidt number for radon, i.e. the ratio of the kinematic viscosity to the molecular diffusion coefficient, calculated in the conditions of salinity and temperature.

The different conditions for wind speed and water temperature between the July (4.0 m/s and 28.9°C) and January surveys (1.0 m/s and 12.8°C) lead to important changes in the calculated atmospheric flux. The radon atmospheric loss was 12.3 Bq/m^2/d in July and 0.7 Bq/m^2/d in January.

6.4.1.1.2 Diffusive flux from sediments (J_{diff})

The equilibration experiments allowed estimating the diffusive flux from sediment J_{diff} assuming a steady state condition and no advective transport, according to Martens et al. (1980):

$$J_{diff} = \sqrt{(\lambda * D_S)} * (C_{eq} - C_0)$$

where J_{diff} is expressed in Bq/m^2/min, λ is the radon decay constant (min^{-1}), D_s is the effective radon diffusion coefficient in sediments (m^2/min), C_{eq} is the activity in pore water estimated with the equilibration experiments (Bq/m^3) and C_0 is the activity in the overlying water column during the field campaign (Bq/m^3). The effective radon diffusion coefficient was calculated according to Ullman and Aller (1981):

$$D_S = P * D_0$$

where P is the porosity, D_s is expressed in cm^2/s and D_0 is the molecular diffusion coefficient (cm^2/s), obtained according to Peng et al. (1974):

$$\log D_0 = \left(\frac{980}{T}\right) + 1.59$$

The radon diffusive fluxes estimated in July 2011 and January 2012 ranges from 1.27 to 3.27 Bq/m^2/d and 1.03 to 2.65 Bq/m^2/d, respectively. Rather similar mean values were therefore obtained: 1.99 and 1.61 Bq/m^2/d respectively. The empirical relationship of Burnett et al. (2003), based on the activity of ^{226}Ra in sediment were calculated using the following equation: Jdiff = 495 * ^{226}Ra + 18.2, where ^{226}Ra is expressed in dpm/g. It provided results in good agreement with the aforementioned ones: from 1.83 to 3.69, with a mean value of 2.89 Bq/m^2/d. Although much simpler, this second method provided very similar results that confirm the reliability of the approach and show that the choice of the method has a limited impact on the final balance of the lagoon. The equilibrium method was used for the radionuclide mass-balance.

To estimate the radium diffusive flux, a diffusion coefficient of 1.2 10^{-7} m^2/min (Moore et al. 2011) was used. The calculated diffusive fluxes for ^{224}Ra were very similar for July and January (0.17 and 0.18 Bq/m^2/d respectively) and 0.010 Bq/m^2/d for ^{223}Ra in January. These values are quite similar to the ones obtained by Garcia-Solsona et al. (2008) in the Venice lagoon (0.53 Bq/m^2/d and 0.018 Bq/m^2/d for ^{224}Ra and ^{223}Ra respectively) and Beck et al. (2007) in the Jamaica Bay (0.47 Bq/m^2/d and 0.019 Bq/m^2/d for ^{224}Ra and ^{223}Ra respectively).

6.4.1.1.3 Radioactive decay (F_{decay})

Radioactive decay was calculated using the following equation:

$$F_{decay} = activity_{MM} * V_{MM}$$

where $activity_{MM}$ is the mean activity of the tracer in Mar Menor and V_{MM} the volume of Mar Menor. As F_{decay} generally has a strong influence on the total budget, the mean activity used for the calculation needs to be very accurate. In order to give a limited weight to the large amount of data collected along the coastline, a 3D interpolation of the data was performed by krigging with 100m/100m cells taking in account the water depth of each one. As an example, in 2012, the arithmetic mean gives a mean ^{224}Ra $activity_{MM}$ of 3.7 Bq/m^3 compared to 2.5 Bq/m^3 with the interpolation.

F_{decay} for ^{222}Rn was similar in July and January (1.4 10^9 Bq/d, Table 20). Regarding ^{224}Ra, the mean value was almost double in July (2.9 10^8 and 4.9 10^8 Bq/d for January and July respectively, Table 20).

6.4.1.1.4 Inputs from resuspended sediment ($F_{resuspension}$)

The quantification of radium fluxes due to resuspension of sediment is not a routine task because of its difficulty. Indeed, this parameter is usually considered negligible compared to the other components of the radium budget. In the present study, an effort was made to assess whether it could have an influence or not on the radium budget.

Resuspension of sediment can add radium to the water by i) release of Ra-enriched pore water in the water column and ii) desorption of Ra from resuspended sediment. Assuming that turbidity is only due to daily resuspension, an estimation of the maximum amount of sediment that can be resuspended daily can be performed by combining the average concentration of total dissolved solids by the volume of the lagoon (Beck et al., 2007). Resuspension is not homogeneous in the whole lagoon, and the surveys were mostly performed where turbidity is higher, i.e. around 2 m depth and along the western coast. Average turbidity for the whole lagoon is therefore clearly overestimated in order to evidence whether $F_{resuspension}$ influences or not the global budgets.

Regarding the release of Ra-enriched pore-water (source i), the mean turbidity in July (1.1 NTU, i.e. ≈ 0.07 mg/L) provides a maximum estimation of the total resuspended sediment of 3.26 10^4 kg/d. Combining this result with the measured density of sediment (2350 kg/m^3) and the calculated porosity (0.5), a maximum amount of pore water daily released in the Mar Menor of 17.5 m^3/d was estimated.

Regarding desorption of Ra from resuspended sediments (source ii), the equilibration experiment gave a ^{224}Ra activity in pore water of 34 Bq/m^3, thus 594 Bq of ^{224}Ra can be released daily from pore water. Regarding desorption of ^{224}Ra from resuspended sediments, calculation can be performed based on the mean concentration of ^{228}Ra in sediment: 6.56 Bq/kg. According to the sediment leaching experiment by Moore et al. (2011), 7% of ^{224}Ra were considered to be desorbable from resuspended sediment. The total inventory of ^{224}Ra that could be leached daily from resuspended sediment to the Mar Menor is thus 1.91 10^4 Bq.

Summing both sources of radium to the water by resuspension (i and ii), a maximum input of ^{224}Ra by resuspension of 1.97 10^4 Bq/d. This value is two orders of magnitude lower than the ones obtained in Venice lagoon (3.3 10^6 Bq/d) by Garcia-Solsona et al. (2008) and in Jamaica bay (3.8 10^6 Bq/d) by Beck et al. (2007) due to a lower turbidity (up to 1 mg/L in Venice and 20 mg/L in Jamaica Bay).

For ^{222}Rn, which is not adsorbed on sediment, the input from resuspension is caused only by the release from pore water. 600 Bq/m^3 of ^{222}Rn was measured in pore water, that gives a maximum input of 1.05 10^4 Bq/d. In January 2012, as neither turbidity nor wind affected the survey, resuspension is assumed to be zero.

6.4.1.1.5 Production by parents decay (Fprod)

The activity of the tracer parents, ^{226}Ra, ^{228}Th, and ^{227}Ac in water in the Mar Menor were measured and multiplied by the radioactive decay constant of their respective daughter to estimate the production input in the water column. The production was 7.37 10^7 Bq/d and 6.14 10^7 Bq/d for ^{222}Rn and ^{224}Ra, respectively, and negligible for ^{223}Ra.

6.4.1.1.6 Surface water end-member

According to the mean discharge rate and radionuclide activities (see 6.3.1.2), the fluxes from the rambla to the lagoon in July 2011 and January 2012, respectively, are the following: 5.57 10^7 and 8.13 10^7 Bq/d for ^{222}Rn; 1.34 10^6 and 2.87 10^6 Bq/d for ^{224}Ra. Regarding ^{223}Ra, the value for January 2012 is 1.47 10^5 Bq/d.

The high changes in the ^{222}Rn composition of R1, R2 or R3 surface waters (Table 18) are linked to the high reactivity of the watershed to artificial discharges. Since ^{222}Rn is a non-conservative tracer, not all discharge rates could be measured and the presence of water along the watershed is discontinuous, a quantitative assessment of the contribution of each tributary to the final discharge cannot be carried out. Nonetheless, the good correlation between ^{222}Rn activities and discharge for R1 and R3 from 20 to 24 January 2012 and the very short distance between these two points (Figure 4) demonstrates that R3 has a major and direct impact on the ^{222}Rn signal discharged by R1 into Mar Menor. The same interpretation is suggested for the extreme R3 and R1 ^{222}Rn activities (close to 12000 Bq/m^3 for R1) measured on 2011 January 10th, although discharge was not quantified.

R3 presents the highest EC of all tributaries, together with δ^2H and $\delta^{18}O$ values close to Pliocene groundwater (Figure 48). Since reverse osmosis does not fractionate O and H stable isotopes ratios (Kloppman et al., 2008), R3 is the tributary that is most influenced by brines from desalinated water, of partly Pliocene origin. R3 also has the highest ^{222}Rn activities (close to 18000 Bq/m^3), but this tracer is not useful to identify brines since our dedicated sampling showed that reverse osmosis process do not modify consistently the ^{222}Rn activities between pumped groundwater, final product and brines.

The release from the Los Alcazares sewage water treatment plant was found to dilute the ^{222}Rn signal in the river, from 2200 to 900 Bq/m^3 (samples R9 and R7, Table 18). It therefore does not act as a notable source of ^{222}Rn for the watershed. Low activities in wastewater were also found for radium by Beck et al. (2007).

6.4.1.2 Groundwater end-member

The heterogeneity and temporal variability of radon and radium activities observed in groundwater samples collected from piezometers (Table 17) is a common feature in most SGD studies (e.g. Dulaiova et al., 2008; Gonneea et al., 2008). Since ^{222}Rn activities varied in a high range between potential groundwater end-members (between 2000 and 26500 Bq/m^3), the definition of the FSGD and RSGD end-members clearly has a large impact on the budget.

The characteristics of Mar Menor (shallow lagoon, gentle beach slope, almost uniform sediment cover of at least 10m thickness; Simonneau, 1973) combined with the very limited sea level variations (a few centimeters) lead to consider FSGD to occur through the underlying sediments of the lagoon. The corresponding radionuclide activity depends on the ratio "r" between the residence time of groundwater in the sediments and the equilibration time. If r<1, FSGD still reflects, at least partly, the activity of groundwater from the aquifer. If r>1, FSGD waters acquires the ^{222}Rn, ^{224}Ra and ^{223}Ra activity of the porous media underlying the lagoon.

The residence time of groundwater in the sediments can be calculated with local hydrodynamic data, assuming a continuous flow between the aquifer and the porous sediment underlying the lagoon. A rough idea of the velocity of groundwater in the Quaternary aquifer (v_{GW}) is provided by the following equation:

where k is the hydraulic conductivity, n_e is the effective porosity and i is the hydraulic gradient. We considered respective values of 1.5 m/d and 30% (according to Senent Alonso et al., 2009 and Jiménez Martinez et al., 2012) and 5 per mil (IEA, 2011). The mean velocity of groundwater in the Quaternary aquifer is therefore 2.5cm per day, i.e. lower than a tenth of meter (similar to the thickness of underlying sediments; Simonneau, 1973) per year.

The equilibration time (t_{eq}) required for the radionuclide activities of fresh groundwater entering the sediments to decay to the level of porous groundwater can be calculated as follows:

where λ is the decay constant (min^{-1}), $act_{initial}$ is the groundwater activity, considering the highest Quaternary values (26500 Bq/m3 and 62 Bq/m^3 for ^{222}Rn and ^{224}Ra, respectively); act_{final} is the porewater activity (600Bq/m^3 and 34Bq/m^3 for ^{222}Rn and ^{224}Ra, respectively). Calculated equilibration times are around 20 days for ^{222}Rn and 3 days for ^{224}Ra. Regarding ^{223}Ra, no decay has to be taken into account since activities in porous groundwater are higher than in groundwater. Meanwhile, the time needed for the new solution to get equilibrated with the porous media of underlying sediments is around 38 days (i.e. 10 half-lives of ^{222}Rn and ^{224}Ra).

In 38 days, continental groundwater covers a maximum distance of 1m in the sediments. “r” is therefore much higher than 1, demonstrating that continental groundwater does equilibrate with the underlying sediments before entering the lagoon. The composition of FSGD is therefore better represented by porous water from underlying sediments rather than by groundwater from the piezometers. The limited variability of ^{226}Ra of sediments and ^{222}Rn of porewater, even in front of the rambla where a continuous supply of sediment from different origins occurs, leads to consider a homogeneous sediment cover in the lagoon. This is in good accordance with the grain-size distribution mapping by Simonneau (1973).

As RSGD occurs along the sediment cover of the lagoon, it is reflected by the end-member obtained from equilibration experiments. A unique value for FSGD and RSGD end-members based on a mean value from equilibration experiments is therefore given: 600 Bq/m^3 for ^{222}Rn, 3.3 Bq/m^3 for ^{223}Ra and 34 Bq/m^3 for ^{224}Ra. Still, radionuclide-poor saline

water recirculation might induce a saline water recycling process shorter than 20 days (the time for radon equilibration). Seepage meter radon concentrations would then be slightly lower than the sediment equilibration results, as in Santos et al. (2009b). As a consequence, the value of 600 Bq/m^3 represents an upper limit for the radionuclides composition of RSGD, and the SGD rates will represent minimum values.

6.4.1.3 Radionuclide mass-balance

Ra and Rn mass balances of the lagoon were performed paying special attention to the atmospheric evasion and resuspension inputs, clearly different between summer (2011) and winter (2012) surveys due to various wind and temperature conditions.

The calculated SGD fluxes for ^{222}Rn are quite similar in 2011 and 2012, with 2.62 and 1.19 10^9 Bq/d respectively (Table 22). These values are 15 to 45 times higher than the influx from the Rambla del Albujón. The main fluxes influencing the radon balance of Mar Menor (Table 21 and Table 22) are the decay (F_{decay}), the atmospheric flux (F_{atm}) and the diffusive flux from sediments (F_{diff}). Resuspension flux has a very low impact (five orders of magnitude less than F_{decay}).

Controlled by wind speed and water temperature, the lower atmospheric flux in January 2012 (-1.5 10^9 Bq/d) explains most differences in the calculated SGD flux between both dates. The impact of other fluxes that were found to change between the two dates (sediment diffusion and rivers) is one or two orders of magnitude lower (Table 21 and Table 22). As wind speed and temperature have no control on the SGD process but only on total stock of ^{222}Rn in the lagoon, the SGD flux calculated for no-wind conditions (January 2012) is the value that is less affected by external processes.

The calculated SGD fluxes for ^{224}Ra are also very similar for 2011 and 2012 (4.16 and 2.04 10^8 Bq/d). The main term in this calculation is the radioactive decay (F_{decay}; Table 21 and Table 22), followed by the in-situ production from radioactive parents (F_{prod}) and the diffusive flux from sediments (F_{diff}). The difference in the SGD flux between the two dates is mostly due to the lower mean ^{224}Ra value in the lagoon in 2012 that induced a lower decay (F_{decay}, -2.07 10^8 Bq/d).

The other parameters that were notably different between both campaigns actually have a negligible impact on the ^{224}Ra balance: twice ^{224}Ra activity in the Rambla del Albujón (+1.53 10^6 Bq/d), lower exchanges with Mediterranean Sea (-2.47 and -5.29 10^6 Bq/d for input and output, respectively). As well as for ^{222}Rn, the contribution of resuspended sediments in 2011 has a very limited impact on the balance (1.97 10^4 Bq/d). As a consequence, the ^{224}Ra excess in the Mar Menor lagoon is directly driven by the mean ^{224}Ra value in the lagoon.

According to the ^{222}Rn mass-balance of the lagoon, SGD fluxes of water of 15.9 and 7.2 10^8 $m^3.a^{-1}$ are obtained, representative for summer and winter season, respectively. Regarding ^{224}Ra, SGD fluxes of water are 44.7 and 21.9 10^8 $m^3.a^{-1}$ A similar pattern is found for ^{223}Ra, with calculated SGD fluxes of water 2 to 3 times lower than with ^{224}Ra: 6.9 10^8 $m^3.a^{-1}$. As for radon, SGD is a more important source of radium than the Rambla del Albujón Table 21 and Table 22): from one order of magnitude (^{223}Ra) to two orders of magnitude (^{224}Ra).

6.4.1.4 Part of freshwater in total SGD

Radioisotopes mass-balances provide an integrated estimate of the total flux of groundwater to the lagoon (FSGD + RSGD). The fresh component is usually controlled by inland groundwater hydrodynamics (Santos et al., 2012) while the main driving force of RSGD is generally considered to be tidal pumping (Weinstein et al., 2007). Tidal pumping consists in a recirculation of saline water in the shore between high and low tides. A similar recirculation occurs during wave setup, although at a distinct time scale. In the particular case of the Mar Menor, as both tidal and non-tidal phenomenons are responsible for sea level variations (Gilabert, personal communication), the terms “sea-level effect” and “sea-level pumping” are preferred to “tidal effect” and “tidal pumping”. Indeed, the respective contribution of both phenomenons is highly variable in time.

Because of the limited amplitude of sea-level variations (a few centimeters), and the very narrow length of the shore (a few meters), sea-level effect was initially expected to have limited influence on the SGD fluxes to Mar Menor. Unexpectedly, data collected during the continuous ^{222}Rn and sea level sampling in the Los Urrutias port showed a negative correlation (Figure 54) between both. Despite the low amplitude of variation of sea-level, it highlights the influence of sea-level pumping on total SGD fluxes (e.g. Weinstein et al.,

2007) most probably through a modified proportion of FSGD and RSGD (e.g.; Santos et al., 2009a).

Since both fresh and saline SGD are Rn-rich, distinguishing between FSGD and RSGD solely based on ^{222}Rn activity is not an easy task, as observed in previous studies (e.g. Mulligan and Charette, 2006; Weinstein et al., 2007). Only a limited number of studies were published on this topic, based on different approaches: groundwater numerical modeling (Smith, 2004), mixing models (Santos et al., 2012; Tanuguchi et al., 2006), spatially distributed seepage meters (Michael et al., 2003) or comparison of different techniques (Santos et al., 2009b; Taniguchi and Iwakawa, 2004).

The radionuclide integrated estimates was compared with the Darcy's law and hydrogeological modeling. Taking the same parameters as used in the "Groundwater end-member" section, with a hydraulic conductivity of 1.5 m/d (60 m of mean saturated thickness), a hydraulic gradient of 5‰ and a total length of discharge between the Quaternary aquifer and the lagoon of 29.6 km (according to Senent et al., 2009), the Darcy's equation provides a FSGD of 5.10^6 $m^3.a^{-1}$. A mathematical model of the Quaternary aquifer performed by Senent et al. (2009) with the same parameters and calibrated on transmissivity provided a FSGD of $7.6.10^6$ $m^3.a^{-1}$. Comparing this last estimate with the integrated ones obtained with radionuclides (Table 22), FSGD would represent between 0.13% (^{224}Ra in July 2011) and 1.1% (^{223}Ra in January 2012) of the total SGD. These percentages are higher if considering the FSGD estimate by Martinez-Alvarez et al. (2011) who used a global salt balance in the lagoon and deduced a FSGD of 21.10^6 $m^3.a^{-1}$, i.e. between 0.5% (^{224}Ra in July 2011) and 3.0 % (^{223}Ra in January 2012) of the total SGD from radionuclides.

This percentage is lower than similar calculations in other locations: around 4% for Santos et al. (2009c) and below 80% for Mulligan and Charrette (2006). Compared to the rest of methodologies described above, it remains in the lower part of the usual range of values (only a few estimates below 1% in the review by Santos et al., (2012)).

6.4.2 Location of Radionuclide inputs

The model provides information on the shape of the plume originated by the discharge of the rambla to the lagoon. In the close surroundings of the mouth, the very high modeled activities (60 Bq/m^3 for ^{222}Rn and 5 Bq/m^3 for ^{224}Ra) are supported by the recorded ^{222}Rn and

^{224}Ra activities. Nonetheless, in this specific area, such high activities combined with the complex hydrodynamics do not allow a precise differentiation between SGD and surface water inputs. Farther from the Rambla output, in locations not reached by the plume in the previous 6 days (Figure 55) the highest measured ^{222}Rn values (points 1, 2, 3, 4, 5; Figure 53) cannot be explained by the contribution of the plume in this time-lapse. To justify the measured values, a previous plume that would have reached this area earlier than the 6 days of modeling would have needed the following initial radon activity (^{222Rn}initial):

$$^{222}Rn_{initial} = {}^{222}Rn_{measured} * \exp(\lambda * t_{elapsed})$$

where $^{222}Rn_{measured}$ is the measured radionuclide activity of the lagoon, $t_{elapsed}$ is the time elapsed since the considered position would have been reached by an earlier plume (i.e. 6 days, as a minimum value) and λ is radon decay constant.

The obtained initial activities range from 66 Bq/m^3 (point 5) to 129 Bq/m^3 (point 4), i.e. notably higher than the modeled range of values inside the plume. The discharge of the Rambla del Albujón into the lagoon is therefore not sufficient to explain these high measured ^{222}Rn activities. In addition, the measured values reflect 1.5 km of tracking and integrate both the "low" background activity of the lagoon and the "high" activity of the plume of the Rambla. For a same sampling location, the modeled values are therefore comparatively overestimated.

Apart from the generalized ^{222}Rn excess in the lagoon, point-sources ^{222}Rn independent from the Rambla are therefore highlighted around point 2, 4 and 5 (southern area) and points 1 and 3 (northern area). Since no other surface water course than the Rambla del Albujón was found to carry water during any of the three sampling campaigns, these high-^{222}Rn points cannot be explained by an additional river discharge. The southern point-source area was observed during each of the three campaigns, and has a considerable width (up to a tenth of km). This temporal regularity, together with the spatial extension, suggests a quite large diffuse ^{222}Rn-rich SGD zone.

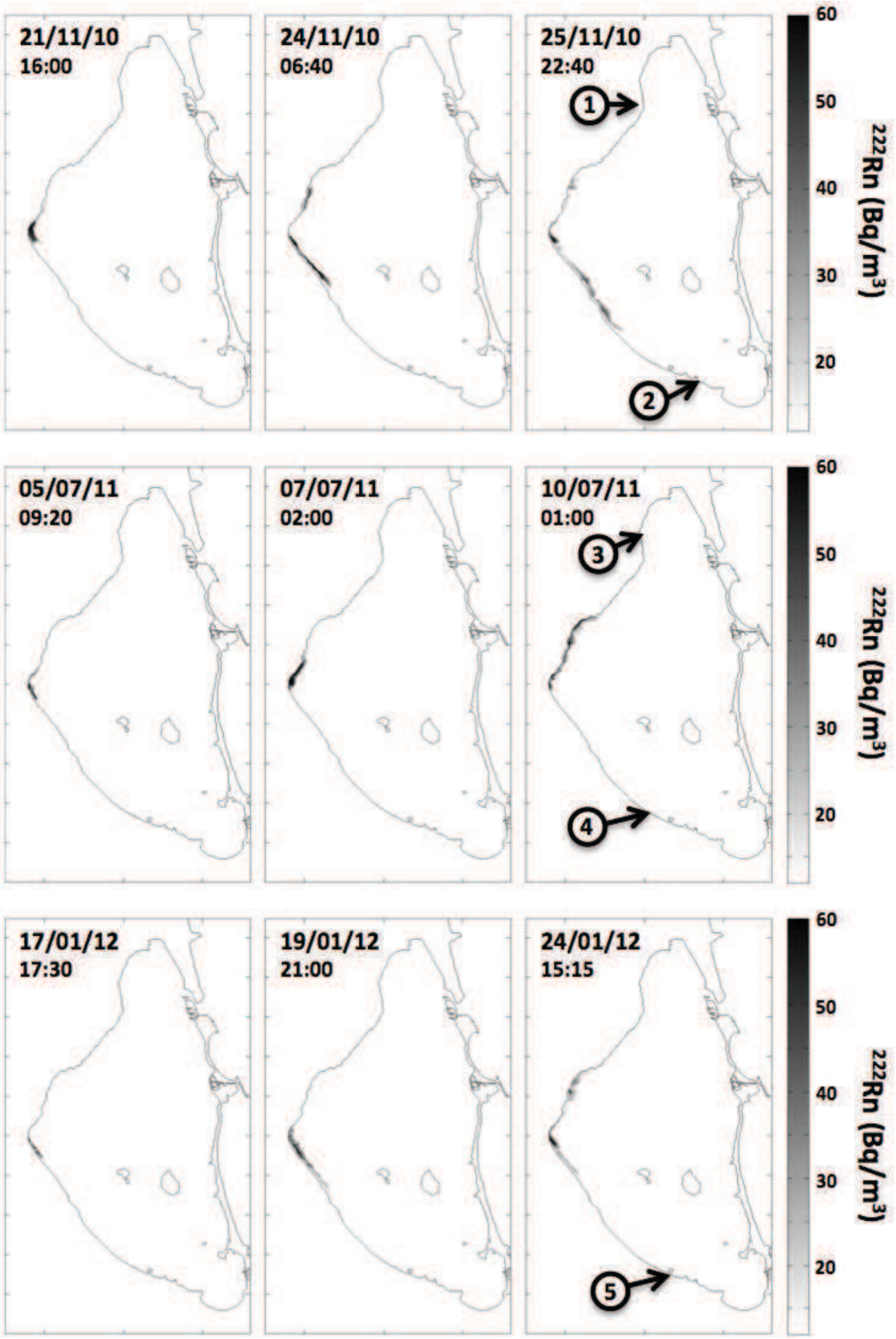

Figure 55: Extreme southwards and northwards displacement of the simulated Rambla del Albujón ^{222}Rn plume in the 6 days previous to the 2010, 2011 and 2012 sampling campaigns. Areas of high measured radionuclide activity out of the reach of this plume are indicated by number.

By contrast, the northern ^{222}Rn point source is narrower (covering one ^{222}Rn measurement only, i.e. less than 1.5 km), and was not measured in July 2012. The temporal variability and tightness of this signal might thus be explained by a hidden and undocumented submarine emissary, like brine release, that discontinuously discharges high ^{222}Rn in this area. Our knowledge of farmers desalination practices is coherent with a higher rate of desalination in January than July.

In terms of global mass balance of the lagoon, the impact of such "parasite" discharge is fortunately negligible (Figure 53) in comparison to the discharge from the Rambla del Albujón. Regarding the other radionuclides (^{223}Ra and ^{224}Ra) and although the modeling provided similar results, the more limited number of samples and the lower range of variation of the measured activities did not allow to evidence reliably any high activity point-source.

6.5 Conclusions

The coupling between ^{222}Rn, ^{224}Ra, ^{223}Ra and hydrodynamic modeling showed that the Rambla del Albujón wadi inputs have a considerable impact on the measured radionuclide in the lagoon. Very high values along the coast, a tenth of kilometers northwards and southwards from the mouth of the Rambla, were explained by the plume of the Rambla itself, hiding the possible contribution of other sources of radionuclide like Submarine Groundwater Discharge. In addition to the baseflow activities issued from groundwater drainage, the Ra-Rn peaks of the Rambla were controlled by the reject of groundwater desalination brines (Quaternary aquifers and deeper ones). High activities in a southern coastal zone not reached by the plume evidenced the location of diffuse SGD, as they covered a wide area and were found at all dates. As well, high activity in the northern part, observed during only two of the three campaigns and covering a very thick area, was explained by the local reject of brines or other rejects.

The best SGD pole was found to be the porous water from sediments for both fresh submarine groundwater discharge (FSGD) and recirculated saline groundwater discharge (RSGD). Yearly SGD fluxes of water obtained from the different tracers showed an excellent correlation, with 15.9 to 7.2 10^8 $m^3.a^{-1}$ (^{222}Rn), 44.7 to 21.9 10^8 $m^3.a^{-1}$ (^{224}Ra) for summer and winter, respectively, and 6.9 10^8 $m^3.a^{-1}$ (^{223}Ra) in winter. The variations between both dates could not be explained by high turbidity and the consequent increased diffusion from

sediments, but were consequences of meteorological conditions on the total budget. The impact of sea level effects was evidenced as a motor for Recirculated Saline Groundwater Discharge (RSGD) and the contribution of Fresh SGD to the total SGD was assessed to be around 1%.

Table 17: Physico-chemical parameters, stable isotopes and radionuclides data measured in groundwater. Coordinates are given in the Universal Transverse Mercator (UTM) geographic coordinate system. Errors on ^{224}Ra, ^{223}Ra and ^{222}Rn values are 2 σ. Errors on $\delta^{18}O$ data are ± 0.006‰ and errors on $\delta^{2}H$ are ± 0.001‰. $\delta^{18}O$ and $\delta^{2}H$ data are normalized to the VSMOW. * refers to ^{224}Ra values measured with RAD7 system and normalized to RaDeCC values using a ratio of 0.66 (see details in the text). [a] is desalinated water from D_{in} and [b] are brines from D_{in}.

ID	Aquifer	X (UTM)	Y (UTM)	Bore-hole depth (m)	Sampling Date	EC (mS/cm)	pH	Temp (°C)	^{224}Ra (Bq/m^3)	^{223}Ra (Bq/m^3)	^{222}Rn (Bq/m^3)	$\delta^{18}O$ (‰)	$\delta^{2}H$ (‰)	NO_3^- (mg/l)	Cl/Br
I	Quat.	688594	4173998	12	23-Nov-10	10.4	7.1	20.8	62.0*±16.0	-	17500±1900	-	-	223.8	307.0
				12	07-Jul-11	10.2	7.1	21.7	44.0*± 12.0	-	21500±2500	-4.34	-29.5	249.1	248.0
A1	Quat.	691755	4181757	25	20-Nov-10	7.2	7.4	20.7	4.9*± 1.0	-	3200±700	-	-	167.5	212.7
				25	07-Jul-11	7.2	7.5	22.3	11.3*± 3.0	-	2100±800	-4.52	-31.1	225.6	166.8
				25	21-Jan-12	5.3	7.6	18.7	-	-	11600±2000	-	-	144.4	145.5
A2		691755	4181757	7	21-Nov-10	7.2	7.6	20.7	8.1*± 2.0	-	2200±700	-	-	174.7	215.0
G	Quat.	687746	4176927	12	24-Nov-10	12.6	6.9	21.4	50.0*± 13.0	-	13700±1800	-	-	38.3	229.4
				12	07-Jul-11	12.0	6.9	20.8	36.0*± 10.0	-	13100±1900	-5.05	-30.9	29.0	229.8
				12	21-Jan-12	11.9	6.9	20.4	58.0*± 26.0	-	26500±1500	-	-	36.0	152.0
					duplicate				49.0 ± 5.0	1.80±0.80				36.0	
J	Quat.	689920	4170500	12	07-Jul-11	7.6	7.1	20.9	29.0*± 11.0	-	22300±2500	-3.99	-26.6	389.0	204.5
				12	21-Jan-12	8.2	7.1	20.8	50.0 ± 6.0	0.50±0.30	23400±5900	-	-	351.6	219.1
D_{in}	Plio.	683698	4173652	150	13-Feb-12	5.7	7.3	-	-	-	74900±3400	-	-	-	-
D_{out1}	[a]				13-Feb-12	0.5	6.5	-	-	-	58900±5600	-	-	-	-
D_{out2}	[b]				13-Feb-12	16.8	7.5	-	-	-	68700±4800	-	-	-	-

Table 18 : Physical-chemical parameters, stable isotopes and radionuclides measured in rivers (1/2). Coordinates are given in the Universal Transverse Mercator (UTM). Errors on ^{224}Ra, ^{223}Ra and ^{222}Rn values are 2 σ. Errors on $\delta^{18}O$ data are ± 0.006‰ and errors on $\delta^{2}H$ are ± 0.001‰. $\delta^{18}O$ and $\delta^{2}H$ data are normalized to the VSMOW. * refers to ^{224}Ra values originally measured with RAD7 system and normalized to RaDeCC values using a ratio of 0.66 (see details in the text).

ID	Sampling Date	EC (mS/cm)	pH	Temp (°C)	^{224}Ra (Bq/m^3)	^{223}Ra (Bq/m^3)	^{222}Rn (Bq/m^3)	$\delta^{18}O$ (‰)	$\delta^{2}H$ (‰)	NO_3^- (mg/l)	Cl/Br	Discharge (10^{-3} m^3/s)
R0	10-jul-11	10.8	-	28.5	-	-	8600±2700	-4.73	-33.8	-	-	-
R1	10-jul-11	14.6	-	26.4	-	-	12600±1500	-5.02	-34.7	-	-	-
	12-jul-11	13.5	-	-	47.0*± 13.0	-	1500±700	-4.92	-33.9	-	-	-
	13-jul-11	16.4	-	26.4	-	-	2400±2400	-4.89	-34.1	-	-	-
	17-jan-12	13.7	-	-	-	-	3600±1900	-	-	-	-	-
	18-jan-12	10.7	-	-	-	-	2200±1000	-	-	-	-	-
	19-jan-12	12.4	-	15.5	-	-	3800±1100	-	-	-	-	-
	20-jan-12	14.0	8.0	15.1	99.0*±13.0	-	1600±1300	-	-	159.6	-	275
	duplicate				99.0 ±16.0	5.6±1.1						
	21-jan-12	15.2	7.7	15.5		-	5500±3600	-	-	218.9	200.4	298
	22-jan-12	16.5	7.9	15.6	104.0 ±16.0	4.7±1.1	3400±900	-	-	114.0	-	-
	24-jan-12	15.8	7.9	15.2	-	-	1800±700	-	-	-	-	228
	25-jan-12	16.0	-	15.0	-	-	1600±1300	-	-	-	-	-
	1-feb-12	-	-	-	-	-		-	-	-	-	-
R2	10-jul-11	11.1	-	27.7	-	-	2400±400	-4.83	-33.8	-	-	-
	12-jul-11	11.2	-	-	-	-	2500±1500	-	-	-	-	-
	20-jan-12	11.4	7.9	15.5	-	-	2500±1400	-	-	138.8	-	14
	21-jan-12	10.9	7.5	14.1	-	-	12000±1700	-	-	167.5	218.8	20
	22-jan-12	12.2	7.6	14.5	-	-	13200±11000	-	-	-	-	17
	24-jan-12	13.6	8.1	15.5	-	-	1100±1000	-	-	239.0	227.0	-
	25-jan-12	12.7	-	14.2	-	-	3200±1900	-	-	-	-	13
R3	10-jul-11	20.7	-	24.2	-	-	16600±2500	-5.34	-36.2	-	-	-
	12-jul-11	19.7	-	-	-	-	11000±3100	-	-	-	-	-

Table 19 : Physical-chemical parameters, stable isotopes and radionuclides measured in rivers (2/2). Coordinates are given in the Universal Transverse Mercator (UTM). Errors on ^{224}Ra, ^{223}Ra and ^{222}Rn values are 2 σ. Errors on $\delta^{18}O$ data are ± 0.006‰ and errors on $\delta^{2}H$ are ± 0.001‰. $\delta^{18}O$ and $\delta^{2}H$ data are normalized to the VSMOW. * refers to ^{224}Ra values originally measured with RAD7 system and normalized to RaDeCC values using a ratio of 0.66 (see details in the text).

ID	Sampling Date	EC (mS/cm)	pH	Temp (°C)	^{224}Ra (Bq/m^3)	^{223}Ra (Bq/m^3)	^{222}Rn (Bq/m^3)	$\delta^{18}O$ (‰)	$\delta^{2}H$ (‰)	NO_3^- (mg/l)	Cl/Br	Discharge (10^{-3} m^3/s)
	20-jan-12	22.1	7.3	18.4	-	-	10000±2500	-	-	230.8	-	54
	21-jan-12	21.9	7.2	19.2	-	-	17900±2700	-	-	237.1	248.9	65
	22-jan-12	22.9	7.4	18.9	208.0±24.0	5.6±2.0	13200±4200	-	-	-	-	94
	24-jan-12	22.7	7.5	18.6	-	-	10100±3200	-	-	251.9	253.0	-
	25-jan-12	24.0	-	18.0	-	-	9600±3600	-	-	-	-	68
R4	12-jul-11	15.0	-	24.0	-	-	2000±800	-4.67	-31.4	-	-	-
	22-jan-12	11.3	8.1	14.2	-	-	2200±500	-	-	152.0	-	80
	24-jan-12	11.9	7.6	15.4	-	-	2800±400	-	-	223.0	261.5	-
	25-jan-12	11.6	-	14.4	-	-	2600±900	-	-	232.4	262.1	-
	1-feb-12	-	-	-	-	-	-	-	-	-	-	-
R5	10-jul-11	10.8	-	28.4	-	-	11100±2900	-4.82	-33.9	-	-	-
	12-jul-11	11.3	-	29.0	-	-	1600±1200	-	-	-	-	-
R7	12-jul-11	11.4	-	27.4	-	-	900±400	-	-	-	-	-
R9	12-jul-11	14.5	-	26.8	-	-	2200±800	-	-	-	-	-

Table 20: Physico-chemical parameters, stable isotopes and radionuclides data measured in Mar Menor and Mediterranean Sea waters. Coordinates are given in the Universal Transverse Mercator (UTM) geographic coordinate system. Errors on ^{224}Ra, ^{223}Ra and ^{222}Rn values are 2 σ. * refers to ^{224}Ra values measured with RAD7 system and normalized to RaDeCC values using a ratio of 0.66 (see details in the text).

ID	SAMPLE TYPE	Sampling Date	Depth (m)	EC (mS/cm)	Temp (°C)	^{224}Ra (Bq/m^3)	^{223}Ra (Bq/m^3)	^{222}Rn (Bq/m^3)	NO_3^- (mg/l)
LO PAGAN	MAR MENOR	23-nov-10	2	-	-	-	-	19.0±5.0	
MM1	MAR MENOR	24-nov-10	2	68.6	14.4	3.40*±1.30	-	15.0±6.0	0.26
MM2	MAR MENOR	24-nov-10	2	68.4	14.4	3.00*±1.00	-	23.0±8.0	0.27
MM3	MAR MENOR	25-nov-10	2	67.8	14.1	2.40*±0.80	-	14.0±5.0	0.28
MM4	MAR MENOR	25-nov-10	2	68.6	14.2	3.90*±1.10	-	35.0±7.0	-
Spatial integration		November 2010				2.4		19.4	0.34
MM10	MAR MENOR	6-jul-11	6	65.6	28.4	4.60*±1.30	-	-	-
MM11	MAR MENOR	6-jul-11	4	65.7	28.4	6.30*±1.90	-	-	-
MM12	MAR MENOR	6-jul-11	2	65.7	28.7	9.00*±2.60	-	-	-
MM13	MAR MENOR	6-jul-11	2	64.6	28.9	5.40*±1.70	-	-	-
MM14	MAR MENOR	6-jul-11	6	64.3	28.9	3.20*±1.10	-	-	-
MM14 duplicate	MAR MENOR	6-jul-11				3.10*±1.00			
MM14 triplicate	MAR MENOR	6-jul-11				5.10*±1.60			
MM15	MAR MENOR	6-jul-11	2	63.7	29.4	10.50*±2.90	-	-	-
MM16	MEDITERRANEAN SEA	9-jul-11	8	56.8	25.7	0.80*±0.30	-	3.0±3.0	-
MM17	MAR MENOR	9-jul-11	6	63.5	28.9	6.50*±1.90	-	11.0±6.0	-
Spatial integration	MAR MENOR	July 2011				4.3		12.6	0.30
MM18	MAR MENOR	23-jan-12	3	67.1	12.3	3.20±0.30	0.13±0.04	-	0.05
MM19	MAR MENOR	23-jan-12	3	66.9	12.3	3.30±0.50	0.18±0.08	17.0±9.0	0.16
MM20	MAR MENOR	23-jan-12	2	66.7	12.3	11.00*±3.30	-	50.0±17.0	0.50
MM20 duplicate	MAR MENOR					12.10±1.40	0.70±0.17		
MM21	MAR MENOR	23-jan-12	2	67.2	12.1	4.80±0.40	0.29±0.09	31.0±13.0	0.17
MM22	MAR MENOR	23-jan-12	2	67.2	12.5	3.10±0.40	0.31±0.15	13.0±8.0	0.17
MM23	MAR MENOR	23-jan-12	2	67.2	12.8	2.90±0.40	0.23±0.08	23.0±11.0	0.17
MM24	MAR MENOR	23-jan-12	3	66.9	13.1	3.10±0.50	0.29±0.13	19.0±10.0	0.16
MM25	MAR MENOR	23-jan-12	5	67.0	12.7	2.50±0.30	0.19±0.08	12.0±8.0	0.20
MM26	MAR MENOR	23-jan-12	5	67.1	12.6	3.30±0.20	0.23±0.12	13.0±8.0	0.23
MM27	MAR MENOR	23-jan-12	4	67.1	12.7	3.00±0.30	0.14±0.04	22.0±11.0	0.26
MM28	MAR MENOR	24-jan-12	6	67.0	12.5	2.60±0.40	0.14±0.06	15.0±9.0	0.12
MM29	MAR MENOR	24-jan-12	6	66.6	12.4	1.60±0.20	0.09±0.03	11.0±7.0	0.08
MM30	MEDITERRANEAN SEA	24-jan-12	6	58.8	15.2	0.34±0.06	0.04±0.03	3.0±2.0	0.04
MM31	MAR MENOR	24-jan-12	3	66.8	13.5	2.80±0.30	0.24±0.11	16.0±9.0	0.12
Spatial integration	MAR MENOR	January 2012				2.5	0.2	13.1	0.15

Table 21 : Definition and values for each terms of the Ra-Rn mass balance: Inputs.

definition	July 2011 ^{222}Rn	July 2011 ^{224}Ra	January 2012 ^{222}Rn	January 2012 ^{224}Ra	January 2012 ^{223}Ra	Units
Inputs						
F_{in} : input flux from the Mediterranean Sea ($activity_{SW}$*Q_{in})	**$1.56\ 10^7$**	**$4.30\ 10^6$**	**$1.40\ 10^7$**	**$1.83\ 10^6$**	**$2.15\ 10^5$**	**Bq/d**
$activity_{Sw}$: tracer (^{222}Rn, ^{224}Ra or ^{223}Ra) activity in the Mediterranean Sea	2.9	0.8	2.6	0.34	0.04	Bq/m^3
Q_{in} : water inflow from the Med. Sea into Mar Menor	$5.37\ 10^6$	$5.37\ 10^6$	$5.37\ 10^6$	$5.37\ 10^6$	$5.37\ 10^6$	m^3/d
F_R : input flux from rivers ($activity_R$*Q_R)	**$5.57\ 10^7$**	**$1.34\ 10^6$**	**$8.13\ 10^7$**	**$2.87\ 10^6$**	**$1.47\ 10^5$**	**Bq/d**
$activity_R$: tracer activity in rivers (rambla)	1960	47.0	2860	100.9	5.16	Bq/m^3
Q_R : water inflow from rivers into Mar Menor	$2.84\ 10^4$	$2.84\ 10^4$	$2.84\ 10^4$	$2.84\ 10^4$	$2.84\ 10^4$	m^3/d
F_{diff} : Diffusive flux from sediment (J_{diff}*S_{MM})	**$2.59\ 10^8$**	**$2.21\ 10^7$**	**$2.09\ 10^8$**	**$2.34\ 10^7$**	**$1.30\ 10^6$**	**Bq/d**
J_{diff} : see in the text	1.99	0.170	1.61	0.180	0.010	$Bq/m^2/d$
S_{MM} : surface area of Mar Menor	$1.3\ 10^8$	$1.3\ 10^8$	$1.3\ 10^8$	$1.3\ 10^8$	$1.3\ 10^8$	m^2
$F_{resuspension}$: input of tracer from resuspended sediment	**$1.05\ 10^4$**	**$1.97\ 10^4$**	**0**	**0**	**0**	**Bq/d**
F_{prod} : production from parent in water (λ*$activity_P$)	**$7.37\ 10^7$**	**$6.14\ 10^7$**	**$7.37\ 10^7$**	**$6.14\ 10^7$**		**Bq/d**
$activity_P$: activity of the parent in water	0.67	0.54	0.67	0.54	Negligible	Bq/m^3
TOTAL INPUTS	$4.04\ 10^8$	$8.92\ 10^7$	$3.78\ 10^8$	$8.95\ 10^7$	$1.66\ 10^6$	Bq/d

Table 22: Definition and values for each terms of the Ra-Rn mass balance: Output and SGD water flux.

definition	July 2011 ^{222}Rn	July 2011 ^{224}Ra	January 2012 ^{222}Rn	January 2012 ^{224}Ra	January 2012 ^{223}Ra	Units
Outputs						
F_{decay} : decay of tracers in the studied volume ($activity_{MM}*V_{MM}*\lambda$)	**1.38 10^9**	**4.93 10^8**	**1.44 10^9**	**2.86 10^8**	**7.33 10^6**	**Bq/d**
$activity_{MM}$: mean activity of the tracer in Mar Menor	12.6	4.3	13.1	2.5	0.2	Bq/m^3
V_{MM} : water volume in Mar Menor	6.05 10^8	6.05 10^8	6.05 10^8	6.05 10^8	6.05 10^8	m^3
λ : decay constant of the tracer	1.81 10^{-1}	1.89 10^{-1}	1.81 10^{-1}	1.89 10^{-1}	6.06 10^{-2}	d^{-1}
F_{out} : output flux to the Mediterranean Sea ($activity_{MM}*Q_{out}$)	**3.70 10^7**	**1.26 10^7**	**3.85 10^7**	**7.35 10^6**	**5.88 10^5**	**Bq/d**
Q_{out} : water outflux from Mar Menor to the Med. Sea	2.94 10^6	2.94 10^6	2.94 10^6	2.94 10^6	2.94 10^6	m^3/d
F_{atm} : Radon atmospheric flux to the atmosphere ($J_{atm}*S_{MM}$)	**1.60 10^9**		**9.2 10^7**			**Bq/d**
J_{atm} : radon atmospheric loss to the atmosphere per unit area per day	12.3		0.7			
TOTAL OUTPUTS	3.02 10^9	5.05 10^8	1.57 10^9	2.94 10^8	7.92 10^6	Bq/d
F_{SGD}: Submarine Groundwater Discharge flux of tracers, estimated by difference between output terms and input terms	**2.62 10^9**	**4.16 10^8**	**1.19 10^9**	**2.04 10^8**	**6.26 10^6**	**Bq/d**
$activity_{GW}$: tracer activity in groundwater endmember	600	34	600	34	3.3	Bq/m^3
SGD WATER FLUX : F_{SGD} / $activity_{GW}$	**1.59 10^9**	**4.47 10^9**	**7.24 10^8**	**2.19 10^9**	**6.92 10^8**	$m^3.a^{-1}$

Chapter 7

Conclusions and future research

7.1 General conclusions

The three approaches developed in this research were i) the review of historical data, including the use of a Random Forest statistical tool to optimize geochemical datasets; ii) the assessment of the evolution of recharge using environmental tracers and iii) the assessment of submarine groundwater discharge coupling radon and radium isotopes with hydrodynamic modeling. These approaches prove their relevance by providing a series of advances.

The review and the combination of historical various sources of information (archaeological data, newspapers from the XIXth century, modern reports, etc.) was the base of a new interpretation. This heavy work was essential for reconstructing the evolution of groundwater resources during the last century. Indeed, it provided novel insights into the long-term groundwater level evolution, revealing the inversion of vertical hydraulic gradient between aquifer layers in the last century, and cumulated levels decrease by more than 500 m in the Triassic aquifer since 1850. Without such an approach, the understanding of the evolution of the system would have remained limited and partly mistaken, as in the case of the apparent stabilization of water table levels at more than 100m below sea level. These interpretations validated the choice of the case study as an extreme case for the anthropization of groundwater in the Mediterranean region.

The borehole inventory highlighted the lack of reliable data for assessing the aquifer of origin of groundwater samples. Nonetheless, it also provided a series of reference tubewells that could be reliably used for the interpretation of geochemical and piezometric information. Part of the boreholes officially considered as representative of one aquifer actually came from another layer, or even mixed water from various layers. This means that several previous studies had mistaken interpretation.

The Random Forest method allowed identifying the aquifer of origin of groundwater samples based on commonly available major ion geochemistry, even when the different aquifers had similar geochemical water types. Random Forest also provided a more accurate classification than LDA or CART. The identification of the aquifer of origin of unknown samples optimized the hydrogeochemical dataset, enhancing the possibilities of further geochemical interpretations. More generally, the Random Forest method showed potential for

a wide range of hydrological, hydrogeological and geochemical applications, and offered novel prospects in this field.

Independently, low cost but high resolution temperature profiles allowed the in-situ assessment of the origin of groundwater samples during sampling. They also provided precious information on intraboreholes vertical groundwater flows occurring in no-pumping conditions. They strengthened the interpretation of environmental tracers.

Stables isotopes of water were very efficient for distinguishing between the shallow unconfined Quaternary aquifer and the two deeper aquifers, counterbalancing their very similar geochemistry. They highlighted the combined effects of evaporation, altitude and climate. Combining various geochemical and isotopic tracers, mixing could be described at several scales. The high variability of the composition of Quaternary groundwater was explained by the variety of water sources for irrigation (more than 8 identified sources). As well, the tracers confirmed the intra-boreholes mixings observed with temperature profiles and occurring in both pumping and no-pumping conditions.

Both pre-anthropization and post-anthropization samples could be identified by applying a simple correction factor to radiocarbon measurements. Mean residence times were then calculated in both cases. Recharge signal was shown to have been continuous since 35.000 years, with no influence of the Last Glacial Maximum. Tritium did not give good quantitative results for mean residence rate assessment because of the high variability of the recharge signal. Nonetheless, it remained an excellent indicator of recent recharge.

Quantifying recharge rates based on absolute radiocarbon mean residence times was made possible by the continuous recharge signal, and could be done for both pre-anthropization and post-anthropization regimes. Before the development of agriculture, recharge varied from 17 $mm.a^{-1}$ at the mountain ranges to 6 $mm.year^{-1}$ in the plain. In response to the increase of agricultural activity, recharge fluxes to the plain were amplified up to modern rates of 210 $mm.a^{-1}$ in irrigated areas.

The impacts that surface water tributaries and undocumented emissaries potentially carrying high quantities of these tracers can have on the radionuclides distribution of the Mar Menor lagoon were assessed by integrating ^{222}Rn, ^{224}Ra and ^{223}Ra with the hydrodynamic modeling of the lagoon. Values measured in the lagoon were compared with the simulated

displacement of the plume of radionuclide originated by the mouth of the river. The areas of influence of the plume of radionuclides from the river could be located, together with the main areas of SGD and the existence of a possible submarine emissary.

The tricky choice of the fresh groundwater end-member in such radionuclide mass-balance was solved by a simple calculation comparing its residence time inside the sediments underlying the lagoon with the equilibration time of the radionuclides in this porous media. Finally, although porous water from underlying sediments is usually not considered as a possible groundwater end-member, it was found to be more representative than groundwater from piezometers for the mass balance and therefore selected for the calculation.

Finally, mass balances in winter and summer seasons provided yearly SGD fluxes of water of 7.2-15.9 10^8 m^3/a^{-1} (^{222}Rn), 21.9-44.7 10^8 m^3/a^{-1} (^{224}Ra) and 6.9 10^8 m^3/a^{-1} (^{223}Ra, measured in winter only). The difference between values for ^{222}Rn was explained by the different temperature and wind conditions. Water level effect, rather than tidal pumping, was identified as the main driver for recirculated saline groundwater, while fresh submarine groundwater discharge from the aquifer represented about 1% of total SGD.

Part of the data collected during this thesis was not interpreted because the focus was finally set on the three main investigations, although it could provide the opportunity of additional research. For example, the large scale stable isotope sampling in groundwater performed in 2009-2010, consisting in more than 100 analyses in boreholes corresponding to unique aquifers or to mixings, and including small time series. The first analysis of this data, in 2010, did not evidence useful information on mixing and recharge processes, and motivated the use of specific time tracers. Nonetheless, a new analysis could benefit from the knowledge acquired through the analysis of chapter 5. Another example is the detailed sampling, discharge measurements and observations that were performed all along the surface watershed during the two first years of this thesis, and after all strong rain events. Finally, surface hydrology was not detailed in the thesis, but it was not possible to foresee that this data would not have a central interest.

7.2 Limits and possible enhancements

A particularly abundant instrumentation was developed during this thesis. This research represents an important step beyond in the knowledge of the Campo de Cartagena, and a

novel example for the adaptation of approaches to such highly anthropized areas. Still, further work on these subjects may still be developed.

The Random Forest classification model could be improved. Firstly, a strategy to identify water samples produced by the mixing of groundwater from different layers inside long-screened boreholes would improve the results. A possibility would be to use a new training dataset integrating the different samples identified for each mixing possibility. Secondly, several samples were not used to calibrate the model because some of the nine predictor variables had not been measured. It would be necessary to check the accuracy of the method with samples with less information. Thirdly, temporal variation in the geochemistry of samples can introduce noise in the models. A possibility could be to investigate new classification models calibrated with data from the first official campaigns only. Finally, the spatial variability is not taken into account, although it could also affect the model, as for the agricultural activity and the introduction of NO_3^- in the aquifers, which has not followed the same pattern in the whole area. Additional investigations considering sub-areas of the system could provide interesting developments. In future works, all these tracks should be investigated. Then, a new geochemical interpretation of the times series could be performed.

Regarding temperature profiles, some points could be enhanced. A specific sampling campaign on a much larger number of boreholes would provide complementary dataset to enhance the method, since only a limited number of boreholes were surveyed up to now. Apart from the authorization of the field owners, the limiting factors were i) the length of the monitoring cable (150 m), that allowed to reach in most cases the Quaternary and Pliocene aquifer, but not the deepest ones (Messinian, Tortonian, Triassic) and ii) the thickness of the cable, that induced troubles with the extraction equipment installed inside the boreholes (cables, tubes). The design of the device will be adapted, using a longer, thinner and lighter cable in order to reach depths up to 400 m.

For water with a relatively short residence time, a comparison with specific tools like SF6 and CFCs could provide more precision on the variability inside the modern period. The combination of these two types of tracers, together with the other ones, could then be inserted into a 3D hydrogeological model based on the geological one developed during this investigation, in order to simulate various realistic hydrodynamic scenarios, in addition to the (piston-)exponential groundwater flow models considered here.

Another interesting added value of the 3D hydrogeological model would be to simulate the seawater salinization hazard of the deep Messinian aquifer, where water table levels are between 100 m and 200 m below sea level. At the moment, no evidence of such process is observed in the Campo de Cartagena area, probably due to the fact that the Messinian formation extends much further below the Mediterranean Sea on the continental shelf, up to 11 km eastwards.

Regarding the SGD assessment, further investigation should be developed to enhance the hydrodynamic model as a steady state model of a lagoon that would account for all external sources and be centered on the following points: i) increase of the number of sampling points for radium (degasing-free) in order to obtain a spatial resolution comparable with radon enough to compare with modeling data and ii) integration of the radioactive decay of tracers.

In parallel, a more precise assessment of the proportion of FSGD in relation to total SGD will be obtained when an estimation of FSGD only could be assessed with radionuclides. To achieve this, a possibility will be to perform salinity mixing models in seepage chambers that require a large number of seepage meters to compensate the very small spatial representativeness of such devices.

In any case, this investigation represents a considerable step forward for the application of the radon and radium method in hypersaline environments such as Mar Menor. Indeed, some of the problems we experimented during the boat survey had never been observed by the device manufacturer of the equipment, who had no solution to propose. As an example, when the level of water in the air-water exchanger suddenly increased, posing risks of a complete filling of the RAD-7 with water, we could save the material by improvising a device with a gardening tool.

7.3 Interest for other Mediterranean studies

All these results present a wide interest that is not limited to the Murcia region or to the Campo de Cartagena aquifer. Around the semiarid Mediterranean Sea, most hydrosystems have been heavily disturbed by human activities and many aquifers are already overexploited. In addition to these anthropogenic and climatic patterns, a similar geological and geomorphological background is found all around the Mediterranean coast. It explains the

large number of multi-layer coastal aquifers, a classical feature in most Mediterranean countries, e.g. Spain (e.g. Manzano et al., 2001), Morocco (e.g. Vias et al., 2007) or France (e.g. Aunay et al., 2006), among many others. In most cases, these multi-layer aquifers contain mostly Pliocene and Quaternary sediments, although deeper layers may also appear, including Messinian deposits (e.g. Manzano et al., 2001). It also explains the existence of a large number of coastal lagoons, from the Nile delta to the French or Tunisian coasts. Thus, many Mediterranean multi-layer aquifer systems could benefit from the approaches developed in the Campo de Cartagena to provide a better identification of the evolution of their resources, a better knowledge of the regional water balance and a better understanding of the representativeness of the different measurements.

For further investigations of such anthropized groundwater systems of the Mediterranean, the following guidelines are proposed: i) searching for all measurements and all data that can be found, even in datasets and archives that have nothing to do with hydrogeology, as their interpretation might provide the key information for a global understanding; ii) considering large temporal scales, as situations constantly evolve and the main drivers of hydrological changes are not persistent over time and iii) crossing as much hydrodynamic and geochemical approaches as possible in order to strengthen the understanding of complex situations, even though their respective results would not be completely coherent.

The present investigation linked several French, Spanish and Canadian research teams on a common study area and through three main projects. The most important of them, the CARTAG-EAU project funded by the French "SICMED-MISTRALS" initiative, should allow further developments in the next future. One of the main objectives is the comparison with similar cases in the Mediterranean focussing both on the research domains treated in the Campo de Cartagena and on additional societal aspects. The Campo de Cartagena case study should be considered as an extreme case of what could happen to groundwater resources in areas where its use is still being developed, such as northern Africa.

In addition, it would be an excellent laboratory for the integrated management of water resources, between intensively exploited groundwater and large distance water transfer channel. The potential of the inter-annual groundwater storage capacity for water resources regulation has not been yet considered in due form. Once obtained the mathematical

groundwater flow model, strategies of integrated management of water will be possible to design. The lessons learnt from such investigations could then be applied to similar cases in the Mediterranean.

Chapter 7 (bis)

Conclusions and future research

- French -

Conclusions générales

Cette recherche s'est basée sur trois approches principales. Elle a débuté par une réinterprétation de données historiques, incluant le développement d'un outil statistique pour optimiser les bases de données géochimiques. Ensuite, l'évolution de la recharge des aquifères a été caractérisée quantitativement et qualitativement à l'aide de traceurs environnementaux. Finalement, la décharge sous-marine d'eau souterraine a été quantifiée en combinant les isotopes du radon et du radium à une modélisation hydrodynamique. La pertinence de ces approches est démontrée par les avancées détaillées ci-après.

La révision et la combinaison de divers sources d'information (données archéologiques, journaux du XIX^{ème} siècle, études modernes etc.) a été la base d'une nouvelle interprétation. Cette lourde tâche était essentielle pour permettre la reconstitution de l'évolution des ressources en eau souterraine durant le siècle dernier. En effet, elle a permis une vue d'ensemble inédite de l'évolution à long terme des niveaux piézométriques, en révélant une inversion des gradients hydrauliques verticaux entre les aquifères ainsi qu'une baisse cumulée des niveaux de plus de 500 m dans l'aquifère du Trias depuis 1850. En l'absence d'une telle approche, la compréhension du système aurait été limitée et en partie erronée, comme dans le cas de l'apparente stabilisation de certains niveaux piézométriques à plus de 100 m sous le niveau de la Mer. Ces interprétations ont validé le choix de la zone d'étude comme un cas extrême de l'anthropisation des eaux souterraines dans les régions méditerranéennes.

L'inventaire des forages a mis en évidence le manque d'informations fiables permettant de déterminer l'origine d'échantillons d'eau souterraine, tout en fournissant une série de forages de référence pouvant être utilisés de manière fiable pour l'interprétation de données piézométriques et géochimiques. De même, il a été découvert qu'une partie des forages officiellement considérés comme représentatifs d'un aquifère correspondaient en réalité à un autre aquifère, voire à un mélange entre les eaux de plusieurs nappes. Les interprétations d'études antérieures sont donc en partie potentiellement erronées.

La méthode Random Forest a permis d'identifier l'aquifère d'origine d'échantillons d'eau souterraine en se basant sur les données disponibles de géochimie des ions majeurs, même lorsque différents aquifères avaient des faciès géochimiques similaires. Elle a

également permis une classification plus précise que les méthodes LDA ou CART. L'identification de l'aquifère d'échantillons d'origine inconnue a permis d'optimiser la base de données hydrogéochimique, augmentant ses possibilités d'interprétation. Plus généralement, cette première application du Random Forest en hydrogéologie a démontré son potentiel pour une large gamme d'applications hydrologiques, hydrogéologiques et géochimiques.

Indépendamment, bien que basés sur une instrumentation peu onéreuse, les profils de température de haute résolution ont permis la détermination in-situ de l'origine d'échantillons d'eau souterraine durant un échantillonnage. Ils ont également apporté des informations précieuses sur les mouvements verticaux d'eau souterraine lorsque les forages sont au repos. Ainsi, ils ont renforcé l'interprétation des traceurs environnementaux.

Les isotopes stables de l'eau ont démontré leur efficacité pour distinguer les eaux de l'aquifère libre Quaternaire de celles des nappes plus profondes, contrebalançant des géochimies similaires. Ils ont mis en évidence les effets combinés de l'évaporation, de l'altitude et du climat. En croisant plusieurs traceurs géochimiques et isotopiques, les phénomènes de mélange ont pu être décrits à plusieurs échelles. La grande variabilité de composition des eaux du Quaternaire a été expliquée par la variabilité des sources d'eau pour l'irrigation (plus de 8 sources identifiées). De même, les traceurs ont confirmé les mélanges intra-forages observés avec les profils de température et ayant lieu autant en condition de pompage et au repos.

Les échantillons pré-anthropisation et post-anthropisation ont pu être distingués en appliquant un simple facteur de correction aux mesures de radiocarbone. Les temps de résidence ont été calculés dans les deux cas. Il a ainsi été démontré que le signal de recharge a été continu au cours des derniers 35000 ans, sans influence du Dernier Maximum Glaciaire. Le tritium n'a pas donné de bons résultats quantitatifs en termes de temps de résidence à cause de la grande variabilité du signal de recharge. La quantification des taux de recharge à partir des temps de résidence moyens donnés par le radiocarbone a été permise par la continuité du signal de recharge, et a pût être réalisée autant pour le régime pré-anthropisation que pour le régime post-anthropisation. Avant le développement de l'agriculture, le taux de recharge variait entre 17 $mm.an^{-1}$ dans les zones montagneuses et

moins de 10 mm.an^{-1} en plaine. Puis, en réponse à la mise en place de l'activité agricole dans la plaine, les flux de recharge ont augmenté jusqu'à atteindre aujourd'hui 210 mm.an^{-1}.

L'impact que les fortes activités apportées par la Rambla del Albujón et par les potentiels rejets non contrôlés pourraient avoir sur la distribution des traceurs dans la lagune a été étudié en intégrant ^{222}Rn, ^{224}Ra et ^{223}Ra avec la modélisation hydrodynamique de la lagune. Les valeurs mesurées ont été comparées avec le déplacement simulé du panache de radionucléïdes de la Rambla del Albujón, permettant de localiser les zones d'influence de ce panache, de même que les zones principales de SGD et des rejets de saumures.

Difficulté récurrente dans cette approche, la détermination de la composition de l'eau souterraine douce issue de la nappe a été résolue par un calcul simple: comparer le temps de résidence de cette eau dans les sédiments avec le temps nécessaire pour y atteindre l'équilibre radioactif. Ainsi, l'eau porale contenue dans les sédiments a montré qu'elle était bien plus représentative que l'eau souterraine prélevée dans des forages de la frange côtière. Cette approche est inédite, étant donné que la majorité des auteurs considèrent arbitrairement les valeurs issues de forages pour le calcul.

Finalement, des flux de SGD de l'ordre de 7.2 à 15.9 10^8 m^3.an^{-1} (^{222}Rn) et 21.9-44.7 10^8 m^3.an^{-1} (^{224}Ra) ont été obtenus par le bilan de masse pour l'été et l'hiver, respectivement, tandis que le ^{223}Ra, mesuré en hiver seulement, a donné 6.9 10^8 m^3.an^{-1}. Des conditions de température et de vent différentes sont responsables de la différence entre les deux valeurs obtenues avec ^{222}Rn. L'effet de la variation du niveau de la mer a été identifié comme le moteur de la recirculation d'eau salée, tandis que la décharge d'eau douce souterraine issue de la nappe a été évaluée à 1% des SGD totales.

Centrée sur ces trois principaux axes, cette thèse propose une partie des données recueillies comme opportunités pour de futures recherches. Par exemple, les isotopes stables de l'eau ont été déterminés dans plus de 100 échantillons prélevés en 2009-2010 dans des forages représentant un seul aquifère ou associés à un mélange. Une première analyse de ces données, en 2010, n'avait pas mis en évidence d'informations utiles pour l'étude des mélanges ou des processus de recharge, mais elle avait motivé l'utilisation de traceurs de temps spécifiques. Un nouvel examen de ces données pourrait désormais bénéficier des avancées réalisées au long du chapitre 5. Un autre exemple est lié aux campagnes effectuées durant les deux premières années de thèse pour mesure de débit, échantillonnage et

observations diverses dans le réseau hydrographique mensuellement et après chaque forte pluie, tandis que l'hydrologie de surface n'a finalement pas justifié une étude détaillée dans cette thèse.

Limites et possibles améliorations

Une instrumentation particulièrement abondante a été mise en place durant cette thèse. Les recherches qui ont été développées représentent un important pas en avant dans la connaissance du Campo de Cartagena mais également un exemple novateur pour l'adaptation d'approches à une zone aussi anthropisée. Par ailleurs, de nouveaux développements pourraient encore être réalisés.

Le modèle de classification Random Forest pourrait être amélioré. Premièrement, une stratégie pour l'identification d'échantillons provenant du mélange d'eau souterraine issue de différents niveaux aquifères à l'intérieur de forages entièrement crépinés devrait améliorer les résultats. Une possibilité est d'utiliser une nouvelle base de données d'entraînement qui intégrera les échantillons correspondant aux différentes possibilités de mélange. Deuxièmement, un certain nombre d'échantillons n'a pas pu être utilisé pour caler le modèle, en l'absence de certains ions majeurs. Il serait intéressant de tester la précision de la méthode en intégrant ces échantillons ayant une information moindre dans un modèle à 3, voire 4 variables. Troisièmement, les variations temporelles de la géochimie des échantillons peuvent introduire du bruit dans les modèles. Une possibilité serait d'essayer de nouveaux modèles de classification calés uniquement sur les données des premières campagnes. Finalement, la variabilité spatiale n'est pas prise en compte, alors qu'elle pourrait affecter les modèles, comme pour l'activité agricole et l'introduction de NO_3^- dans les nappes, qui n'a pas suivi un même schéma dans toute la zone. Des travaux complémentaires considérant des sous-zones du système pourraient apporter des développements intéressants à ce propos. Finalement, une nouvelle interprétation géochimique des séries temporelles pourrait être réalisée.

Concernant les profils de température, certains points pourraient être améliorés. Une campagne de prélèvement spécifique sur un nombre de forages plus importants pourrait apporter des données complémentaires pour améliorer la méthode, étant donné qu'un nombre limité de forages ont été étudiés pour le moment. Hormis l'autorisation des propriétaires des champs, les facteurs limitant étaient i) la longueur du câble de contrôle (150 m), qui a permis d'atteindre les niveaux Quaternaire et Pliocène dans la majorité des cas, mais pas les

compartiments les plus profonds (Messinien, Tortonien, Trias) et ii) l'épaisseur du câble de contrôle, qui a induit des complications avec l'équipement d'extraction installé dans les forages (câbles électriques, tuyaux). La conception de l'appareil devra être adaptée en utilisant un câble plus long, plus fin et plus léger afin d'atteindre des profondeurs de 400 m.

Pour des eaux au temps de résidence relativement court, la comparaison avec des outils plus spécifiques tels que les SF_6 ou CFC_s permettrait d'obtenir plus de précision sur la variabilité au sein de la période moderne. La combinaison de ces deux types de traceurs avec les autres pourrait ensuite être insérée dans un modèle hydrogéologique 3D basé sur le modèle géologique mis au point durant cette recherche, afin de simuler différents scénarios hydrodynamiques, en plus du modèle (piston-)exponentiel considéré ici.

Un autre apport du modèle hydrogéologique 3D serait de simuler le risque d'intrusion saline dans l'aquifère Messinien, où les niveaux piézométriques se situent entre 100 m et 200 m au-dessous du niveau de la Mer. Bien qu'aucune preuve d'un tel processus n'ait pour le moment été observée, l'étendue sous-marine de la formation messinienne, à plus de 11 km sur la plateforme continentale, ne permet pas d'en négliger le risque futur.

En ce qui concerne la détermination de la décharge sous-marine d'eau souterraine, des travaux futurs devraient être développés pour obtenir un modèle hydrodynamique de la lagune en régime permanent, qui prendrait en compte tous les apports externes et serait centré sur les points suivants : i) augmentation du nombre d'échantillons de radium afin d'obtenir une résolution spatiale comparable à celle du radon qui permette la comparaison avec les données modélisées et ii) intégration de la décroissance radioactive des traceurs.

En parallèle, une meilleure précision quant à la proportion d'eau douce issue de l'aquifère (FSGD) dans la décharge sous-marine totale (SGD) pourrait être obtenue à l'aide des radionucléïdes. Une possibilité serait d'insérer des dispositifs de type « seepage-meter » dans les sédiments avec un prélèvement à courte échelle de temps (par ex. chaque heure) afin de distinguer la proportion du pôle FSGD via un modèle de mélange de salinités. Dans tous les cas, les recherches développées sur la caractérisation de SGD représentent un considérable pas en avant pour l'application de cette méthode dans un environnement hypersalin tel que la Mer Mineure. En effet, certains des problèmes expérimentaux auxquels il a fallu faire face n'avaient jamais été portés à la connaissance du constructeur de l'équipement, qui n'avait donc pas de solution à proposer. Ainsi, par exemple, lorsque le

niveau d'eau dans l'échangeur air-eau est soudainement monté, risquant de remplir complètement les RAD-7 d'eau, l'appareil put être mis hors de danger en improvisant un dispositif à l'aide d'éléments provenant de matériel de jardinage.

Intérêt pour d'autres études en Méditerranée

Tous ces résultats présentent un large intérêt qui va bien au-delà du système aquifère multicouche du Campo de Cartagena ou de la région de Murcie. En effet, sur le pourtour méditerranéen semi-aride, la plupart des hydrosystèmes sont lourdement impactés par les activités humaines et de nombreux aquifères sont d'ores et déjà surexploités. En plus de ces caractéristiques anthropiques et climatiques, un contexte géologique et géomorphologique similaire se retrouve tout autour de la côte méditerranéenne. Il explique le grand nombre d'aquifères multicouche, un trait classique de la plupart des pays méditerranéens, comme par exemple en Espagne (p.e. Manzano et al., 2001), au Maroc (p.e. Vias et al., 2007) ou en France (p.e. Aunay et al., 2006), entre de nombreux autres. Dans la plupart des cas, ces aquifères multicouches contiennent principalement des sédiments d'âge Pliocène ou Quaternaire, bien que d'autre niveaux plus profonds tels que le Messinien apparaissent parfois (p.e. Manzano et al., 2001). Cela explique également l'existence d'un grand nombre de lagunes côtières, depuis le delta du Nil jusqu'aux côtes tunisiennes ou françaises. Ainsi, de nombreux systèmes aquifères méditerranéens multicouches pourraient bénéficier des approches mises en œuvre dans le Campo de Cartagena afin d'arriver à une meilleure identification de l'évolution de leurs ressources, une meilleure connaissance du bilan hydrique régional et une meilleure compréhension de la représentativité des différentes mesures.

Pour de nouvelles recherches sur des milieux aquifères anthropisés du pourtour méditerranéens, les principaux résultats méthodologiques de cette thèse amènent à formuler les recommandations suivantes: i) nécessité de rechercher et exploiter toutes les mesures anciennes possibles, y compris dans des archives qui ne soient pas ni hydrologiques ni hydrogéologiques, étant donné que leur interprétation peut apporter les informations clés pour une compréhension globale ; ii) nécessité de se placer dans des perspectives temporelles longues, étant donné que les situations ne cessent d'évoluer et que les principaux moteurs du changement hydrologique ne sont pas toujours persistants dans le temps et iii) nécessité de croiser un maximum de méthodes hydrodynamiques et géochimiques afin de renforcer les

interprétations et améliorer la compréhension des situations complexes, même si les résultats ne sont pas tous parfaitement cohérents.

Cette recherche s'est inscrite dans un cadre multi-institutionnel entre divers partenaires de recherche français, espagnols et canadiens sur un même objet d'étude et au travers de trois projets principaux. Le plus important d'entre eux, le projet CARTAG-EAU financé par l'initiative française « SICMED-MISTRALS », devrait permettre des développements dans le futur proche. L'un de ses principaux objectifs est la comparaison avec d'autres cas similaires en Méditerranée, en se centrant sur les domaines de recherche traités dans le Campo de Cartagena mais en s'ouvrant également vers des dimensions sociétales plus larges. Le Campo de Cartagena doit être considéré comme un cas extrême pouvant servir d'exemple de ce qui pourrait arriver aux ressources d'eau souterraine dans des zones où leur usage est en plein essor, tel qu'au Maghreb.

De plus, le Campo de Cartagena ferait un excellent laboratoire pour la gestion intégrée des ressources en eau, entre eaux souterraines intensivement exploitées et canal de transfert d'eau de surface à longue distance. Le potentiel en capacité de stockage inter-annuelle de l'eau souterraine pour la régulation des ressources en eau n'a pas encore été considéré en due forme. Une fois que le modèle mathématique de flux souterrains sera mis en place, il permettra de tester et de définir des stratégies de gestion de l'eau. Les leçons tirées d'une telle recherche pourront à leur tour être appliquées à des cas similaires en Méditerranée.

Chapter 7 (ter)

Conclusions and future research

- Spanish -

Conclusiones generales

Las tres aproximaciones implementadas en esta investigación han sido: i) la reinterpretación de datos históricos, incluyendo el desarrollo de una herramienta estadística para optimizar las bases de datos hidrogeoquímicas: ii) el estudio de la evolución temporal de la recarga con trazadores ambientales y iii) la cuantificación de la descarga submarina de agua subterránea combinando los isótopos del radón y del radio con una modelización hidrodinámica. Estas metodologías han demostrado su pertinencia y permitido una serie de avances.

La revisión y la combinación de varias fuentes de información (datos arqueológicos, búsqueda en hemeroteca, estudios recientes, etc.), ha sido la base de una nueva interpretación de la conceptualización previa del sistema. Esta tarea laboriosa ha sido esencial para permitir la reconstrucción de los flujos de agua subterránea a la largo del siglo pasado. De hecho, ha proporcionado una visión de conjunto inédita de la evolución a largo plazo de los niveles piezométricos, que revela una inversión de los gradientes hidráulicos verticales entre acuíferos así como una bajada acumulada de los niveles de más de 500 m en el acuífero triásico desde el 1850. En ausencia de tal enfoque, la comprensión previa del sistema ha sido limitada y en parte errónea, como en el caso de la estabilización aparente de ciertos niveles piezométricos a más de 100 m bajo el nivel del mar, que implica entre otros la extensión de los límites de los acuíferos inferiores (al menos el acuífero Messiniense) más allá del borde costero. Estas interpretaciones han validado la elección de la zona de estudio como un caso extremo de efectos antrópicos en el derivados del uso de las aguas subterráneas en regiones mediterráneas.

El inventario puntos de agua ha puesto en evidencia la falta de información fiable para determinar el origen de muestras de agua subterránea, y ha proporcionado además una serie de captaciones de referencia que si pueden ser utilizadas de manera fiable para la interpretación de datos piezométricos e hidrogeoquímicos. Asimismo, se ha puesto de manifiesto que una parte de los puntos de la red previa de calidad consideradas como representativa de un acuífero correspondían en realidad a un otro acuífero, o incluso a una mezcla entre las aguas de varios acuíferos en la vertical.

El método Random Forest ha permitido identificar el acuífero de origen de muestras de agua subterránea a partir de los datos disponibles de hidroquímica con iones mayoritarios, aun cuando diferentes acuíferos presentan hidrofacies similares. También ha permitido una clasificación más precisa que los métodos LDA o CART. Esta identificación del acuífero para las muestras de origen desconocido permitió ha permitido optimizar la base de datos hidrogeoquímica y por tanto, aumentan las posibilidades de interpretación. A nivel más general, se trata de una de las primeras aplicaciones de Random Forest en hidrogeología y demuestra su potencial para una amplia de problemáticas que pueden surgir en este campo científico. Por otro lado, los perfiles de temperatura de alta resolución, de bajo coste de ejecución, han permitido la determinación in situ del origen de muestras de agua subterránea durante un muestreo, y han aportado información interesante sobre los flujos verticales de agua subterránea cuando las captaciones están en reposo. Todo ello, ha reforzado la interpretación de los trazadores ambientales.

La investigación con isótopos estables del agua ha demostrado su eficacia para distinguir las aguas del acuífero libre Cuaternario de las de los acuíferos más profundos, a pesar de sus características hidroquímicas similares. Se han podido observar los efectos combinados de la evaporación, la altitud y las variaciones climáticas. Asimismo, al cruzar los algunos trazadores geoquímicos e isotópicos, se han podido identificar los fenómenos de mezcla a varias escalas. La gran variabilidad de composición de las aguas del Cuaternario se explica por la variabilidad de las fuentes de agua empleadas para riego (más de 8 fuentes identificadas). Además, los trazadores han confirmado las mezclas observadas dentro las las propias captaciones que fueron registradas con los perfiles de temperatura tanto en condición de bombeo como de reposo.

Las muestras correspondientes a los estados de pre y post-antropización se han distinguido a partir de la aplicación de un factor simple de corrección sobre las medidas de radiocarbono, y los tiempos de residencia han sido calculados en ambos casos. Se ha demostrado que la señal de recarga ha sido continua en los últimos 35000 años, sin influencia del Último Máximo Glaciar. La intepretación de los análisis de tritio no ha dado buenos resultados cuantitativos en cuanto al tiempo de residencia dada la gran variabilidad de la señal de recarga. La cuantificación de la tasa de recarga a partir de los tiempos de residencia medios dados por el radiocarbono se tuvo por la continuidad de la señal de recarga, y pudo ser obtenida tanto para el régimen pre-antropización como para el régimen post-

antropización. Antes del desarrollo de la agricultura, la tasa de recarga variaba entre 17 mm $año^{-1}$ en las zonas elevadas a menos de 10 mm $año^{-1}$ en llanura. En respuesta al desarrollo de la actividad agrícola en la llanura, los valores de recarga aumentaron hasta alcanzar los 210 mm $año^{-1}$.

El impacto de las aportaciones de la rambla del Albujón y los supuestos rechazos de salmuera no controlados sobre la distribución de los trazadores en la laguna fue estudiado integrando ^{222}Rn, ^{224}Ra y ^{223}Ra con la modelización hidrodinámica de la laguna. Los valores medidos se compararon con el desplazamiento simulado del penacho de radionucleidos de Rambla del Albujón, lo que ha permitido localizar las zonas de influencia de tal penacho, al igual que con las zonas principales de SGD y los rechazos de salmueras. Una dificultad recurrente en el uso de este método, ha sido la determinación de la composición del agua subterránea dulce originada por el acuífero que se resolvió por un cálculo simple consistente en la comparación del tiempo de residencia de esta agua en los sedimentos con el tiempo necesario para alcanzar el equilibrio radiactivo. De esta manera, el agua en poro contenida en los sedimentos mostró que era mucho más representativa que el agua subterránea tomada en captaciones de la franja costera. Este enfoque es inédito, dado que la mayoría de los autores considera arbitrariamente para el cálculo los valores obtenidos a partir de captaciones.

Finalmente, flujos de SGD del orden de 7.2 - 15.9 10^8 $m^3.año^{-1}$ (^{222}Rn) y 21.9-44.7 10^8 $m^3.año^{-1}$ (^{224}Ra) se obtuvieron por el balance de masa para el verano e invierno, respectivamente, mientras que el 223Ra, medido en invierno solamente, dio 6.9 10^8 $m^3.año^{-1}$. Las diferentes condiciones de temperatura y de viento son los responsables de la diferencia entre ambos valores obtenidos con 222Rn. El efecto de la variación del nivel del mar se ha considerado como el motor de la recirculación del agua salada, mientras que la descarga de agua subterránea dulce originada por el acuífero (FSGD) se ha evaluado en el 1 % del SGD total.

Conviene señalar que dado que esta Tesis finalmente se centró sobre los citados tres ejes principales de investigación, una parte de los datos recogidos no ha sido interpretada. Sin embargo, estos representan una fuente de oportunidad para futuras investigaciones. Por ejemplo, los isótopos estables del agua fueron determinados en más de 100 muestras tomadas en 2009-2010 en perforaciones que representan un solo acuífero o asociadas con una mezcla. Un primer análisis de estos datos, en 2010, no puso en evidencia informaciones útiles para el

estudio de las mezclas o de los procesos de recargo, sino que motivó la utilización de trazadores de tiempo específicos. Un nuevo examen de estos datos podría gozar de los avances realizados expuestos en el capítulo 5. Otro aspecto que puede dar lugar a líneas de trabajo posteriores está relacionado con las campañas efectuadas durante dos primeros años de Tesis para medida de flujo, muestreo y observaciones diversas en la red hidrográfica, con carácter mensual y después de cada episodio de lluvias importantes. Asimismo, la hidrología de superficie no fue detallada en esta Tesis, pero no era posible prever, en la época, que estos datos no tendrían un interés central. Finalmente, se ha realizado un tratamiento muy intenso de los aspectos geométricos tendentes a la elaboración de un completo modelo de flujo subterráneo, cuyos resultados se muestran sucintamente en esta Memoria.

Límites y posibles mejoras

Una instrumentación particularmente abundante ha sido implementada durante esta Tesis. Las investigaciones desarrolladas representan un importante paso adelante en el conocimiento de este caso de estudio (Campo de Cartagena), pero sobre todo un ejemplo novedoso de adaptación de enfoques a una zona extremadamente antropizada. No obstante, nuevos desarrollos podrían todavía ser realizados.

El modelo de clasificación Random Forest puede ser mejorado, lo que es deseable al abrir un nueva línea de investigación en hidrogeología. En primer lugar, la mejora de resultados puede obtenerse según la estrategia para la identificación de muestras que provienen de la mezcla del agua subterránea de diferentes niveles acuíferos dentro de perforaciones totalmente ranuradas. Una posibilidad sería utilizar una nueva base de datos de entrenamiento que integraría las muestras que corresponden a las diferentes posibilidades de mezcla. En segundo lugar, un cierto número de muestras no pudo ser utilizado para calibra el modelo, en ausencia de ciertos iones mayores, y por ello sería interesante probar la precisión del método integrando estas muestras que tienen una información menor en un modelo de 3 o incluso 4 variables. En tercer lugar, las variaciones temporales de la hidrogeoquímica de las muestras pueden estar introduciendo ruido en los modelos, por lo que convendría ensayar nuevos modelos de clasificación calados únicamente a partir de los datos de las primeras campañas. Finalmente, no se ha tenido en cuenta la variabilidad espacial y ellos puede afectar como la actividad agrícola y la introducción de nitratos en los acuíferos que no sigue el

mismo esquema en toda la zona; los trabajos complementarios en este aspecto deben considerar subzonas del sistema que podrían aportar desarrollos interesantes.

En cuanto a los perfiles de temperatura de precisión con equipamiento experimental, ciertos puntos podrían ser mejorados. Una campaña de medidas específica sobre un número de perforaciones más importantes podría aportar datos complementarios para mejorar el método, dado que un número limitado de perforaciones ha sido estudiado por el momento. Además de la obvia necesidad de disponer de la autorización de los propietarios de las captaciones, los factores limitantes han sido i) la longitud del cable de control (150 m), que permitió alcanzar los niveles Cuaternario y Plioceno en la mayoría de los casos, pero no los tramos más profundos (Messiniense, Tortoniense, Triásico), y ii) el espesor del cable de control, que indujo complicaciones con equipo de extracción instalado en las perforaciones (cables eléctricos, tubos). El diseño del aparato experimental con el que se ha efectuado esta investigación deberá ser adaptado utilizando un cable más largo, más fino y más ligero con el fin de alcanzar profundidades de 400 m.

En el caso de aguas subterráneas con un tiempo de residencia relativamente corto, la comparación con herramientas más específicas tales como el SF_6 o CFC_s permitiría obtener más precisión sobre la variabilidad reciente. La combinación de estos dos tipos de trazadores con otros podría luego ser insertada en un modelo hidrogeológico 3D basado en el modelo geológico puesto a punto durante esta investigación, con el fin de simular diferentes escenarios hidrodinámicos, además del modelo (pistón-)exponencial considerado en esta investigación. Otra aportación del modelo hidrogeológico 3D está relacionada con la simulación del riesgo de intrusión marina en el acuífero Messiniense, para el que los niveles piezométricos se sitúan entre 100 m y 200 m bajo del nivel del mar en el borde costero. A pesar de no disponer de pruebas de que tal proceso se esté produciendo, dada la extensión submarina de la formación Messiniense, más de 11 km sobre la plataforma continental, no se puede eliminar la posibilidad de un riesgo futuro.

En cuanto a la determinación de la descarga submarina de agua subterránea al lagoon costero, los trabajos futuros deberían ser desarrollados para obtener un modelo hidrodinámico de la laguna en régimen permanente, que tomaría en consideración todas las aportaciones externas y debería estar centrado sobre los puntos siguientes: i) aumento del número de muestras de isótopos de radio con el fin de obtener una resolución espacial comparable a las

del radón, lo que permitiría la comparación con los datos modelizados; ii) integración de la desintegración radioactiva de los trazadores.

En paralelo a lo anterior, se requiere una mejor precisión en cuanto a la proporción de agua dulce originada por el acuífero (FSGD) en la descarga submarina total (SGD), que podría ser obtenida con la ayuda del radón y del radio. Una posibilidad para resolver este aspecto sería insertar dispositivos de tipo "seepage-meter" en los sedimentos con una toma de muestra a escala temporal corta (por ejemplo, datos horarios), con el fin de distinguir la proporción de FSGD a través de un modelo de mezcla de salinidades. En todos los casos, las investigaciones desarrolladas sobre la caracterización de SGD representan un paso adelante considerable para la aplicación de este método en un entorno hipersalino tal como el Menor Mar. En efecto, algunos de los problemas experimentales que surgieron durante el muestreo nunca habían sido puestos en conocimiento del constructor del equipo, el cual no tenía solución técnica que proponer. Así, por ejemplo, cuando subió repentinamente el nivel de agua en el intercambiador aire-agua, y se puso en peligro de llenar completamente de agua el equipo RAD-7, se consiguió eliminar tal peligro improvisando un dispositivo de bricolaje.

Interés para otros estudios en el Mediterráneo

Los resultados obtenidos pueden ser de interés en otros lugares más allá del sistema acuífero multicapa de Campo de Cartagena o de la región de Murcia. En efecto, en la región mediterránea semiárida, la inmensa mayoría de los hidrosistemas presentan un importante impacto por las actividades humanas con frecuentes casos de explotación intensiva e incluso minera. Además de estas características antrópicas y climáticas, un contexto geológico y geomorfologico similar se encuentra por toda la costa mediterránea. Eso explica el gran número de acuíferos multicapa, un aspecto clásico en la mayoría de los países mediterráneos, como por ejemplo en España (p.e. Manzano y al., 2001), en Marruecos (p.e. Vias y al., 2007) o en Francia (p.e. Aunay y al., 2006), entre otros. En la inmensa mayoría de los casos, estos acuíferos multicapa contienen principalmente sedimentos de edad pliocena o cuaternaria, aunque otros niveles más profundos tales como el Messiniense a veces también está presente (p.e. Manzano y al., 2001). El contexto geomorfologico explica también la existencia de un gran número de lagunas costeras, desde el delta del Nilo hasta las costas tunecinas o francesas. Así, los numerosos sistemas acuíferos mediterráneos multicapa podrían gozar de los enfoques desarrollados e implementados en el caso estudiado, con el fin de llegar a una

mejor identificación de la evaluación de sus recursos, un mejor conocimiento del balance hídrico regional y una mejor comprensión de la representatividad de las diferentes mediciones.

Para nuevas investigaciones sobre medios acuíferos antropizados de regiones mediterráneas, los avances metodológicos de esta Tesis permiten ofrecer la siguiente guía de recomendaciones : i) necesidad de recopilar y explotar todos los datos antiguos posibles, incluidos los archivos de todo tipo, dado que su interpretación puede aportar las informaciones claves para una comprensión global; ii) necesidad de posicionarse desde perspectivas temporales largas, dado que las situaciones no dejan de evolucionar y que los principales motores del cambio hidrológico no son siempre persistentes en el tiempo e iii) necesidad de cruzar un máximo de métodos hidrodinámicos y geoquímicos con el fin de reforzar las interpretaciones y mejorar la comprensión de las situaciones complejas, aunque los resultados no sean total o perfectamente coherentes.

Esta investigación está inscrita en un marco multi-institucional entre diversos socios de investigación franceses, españoles y canadienses sobre el mismo objeto de estudio y a través de tres proyectos principales. El más importando de ellos, el proyecto CARTAG-EAU financiado por la iniciativa francesa " SICMED-MISTRALS ", debería permitir desarrollos en el futuro próximo. Uno de sus principales objetivos es la comparación con otros casos similares en el Mediterráneo, con un foco especial en las líneas de investigación aplicadas en el Campo de Cartagena pero también desea incorporar la dimensión social del agua. El Campo de Cartagena debe ser considerado como un caso extremo que puede servir de ejemplo de lo que previsiblemente ocurrirá con los recursos de agua subterránea en zonas donde su uso está en auge, tales como el norte de África.

Además, el Campo de Cartagena es un laboratorio excelente para la gestión integrada de los recursos en agua subterránea intensivamente explotada, el canal del trasvase Tajo-Segura y los nuevos recursos adicionales procedentes de la desalación y reutilización. El potencial que presenta en terminos de capacidad de almacenamiento interanual del agua subterránea para la regulación de los recursos hídricos todavía no ha estado considerado en su debida forma. La implementación futura del modelo matemático de flujo subterráneo permitirá probar y definir estrategias de gestión del agua, y los resultados cualitativos obtenidos podrán ser extrapolados en casos similares del área circunmediterránea.

Chapter 8

References

Adams, S., Titus, R., Pietersen, K., Tredoux, G., Harris, C., 2001. Hydrochemical characteristics of aquifers near Sutherland in the Western Karoo, South Africa. *Journal of Hydrology* **241**, 91–103.

Adar, E.M., Rosenthal, E., Issar, A.S., Batelaan, O., 1992. Quantitative assessment of the flow pattern in the southern Arava Valley (Israel) by environmental tracers and a mixing cell model. *Journal of Hydrology* **136**, 333–352.

Adiaffi, B., Marlin, C., Oga, Y.M.S., Massault, M., Noret, A., Biemi, J., 2009. Palaeoclimatic and deforestation effect on the coastal fresh groundwater resources of SE Ivory Coast from isotopic and chemical evidence. *Journal of Hydrology* **369**, 130-141.

Alcamo, J., Flörke, M., Märker, M., 2007. Future long-term changes in global water resources driven by socio-economic and climatic changes. *Hydrological Science Journal* **49**(4), 549–562.

Arévalo, L. 1988. El Mar Menor como sistema forzado por el Mediterráneo. Control hidráulico y agentes fuerza. *Boletín del Instituto Español de Oceanografía* **5**(1):63-95.

Aunay B., Duvail C., Giordana G., Dorfliger N., Le Strat P., Montginoul M., Pistre S., 2006. A pluridisciplinary methodology for integrated management of a coastal aquifer: Geological, hydrogeological and economic studies of the Roussillon aquifer (Pyrénées-Orientales, France). *Life and Environment* **56**(4), 275-285.

Babovic, V., 2005. Data Mining in Hydrology. *Hydrological Processes* **19**, 1511-1515.

Barbecot, F., Marlin, C., Gibert, E., Dever, L., 2000. Hydrochemical and isotopic characterisation of the Bathonian and Bajocian coastal aquifer of the Caen area (northern France). *Applied Geochemistry* **15**, 791–805.

Baudron, P., Barbecot, F., Taupin, J.-D., Leduc, C., Garcia-Arostegui, J.-L., Pinti, D., Travi, Y., Leduc, C., Martinez-Vicente, D., 2011a. Use of environmental tracers to assess the impact of intense agricultural activity on a semi-arid aquifer: case study in Campo de Cartagena (Spain). Oral presentation at the *9th International Symposium on Applied Isotope Geochemistry, AIG9*, Barcelone (Spain). September 2011.

Baudron, P., Garcia-Arostegui, J.-L., Leduc, C., Senent, M., Jimenez-Martinez, J., Martinez, D., 2011b. Impact of human activities on groundwater flow and quality in a coastal Mediterranean semi-arid aquifer system. Case study of the Campo de Cartagena (S.E. Spain). Oral presentation at the *CIREDD4 Conference*, Alger (Algeria). February 2011.

Baudron, P., Leduc, C., Garcia-Arostegui, J-L., 2011c. Incertitudes liées à la caracterisation geochimique du systeme aquifere multicouche du Campo de Cartagena (SE Espagne). Oral presentation at the *International Groundwater Conference*, Orléans (France), March 2011.

Baudron, P., Alonso Sarriá, F., García Aróstegui, J-L., Moreno Brotóns, J., Cánovas García, F., Molina, J-L., 2012a. Identifying the origin of groundwater samples in a Multi-layer Aquifer system affected by long-screen boreholes using Random Forest Classification. Oral presentation at the *39th IAH Congress*, Niagara Falls (Canada), September 2012.

Baudron, P., Martinez-Vicente, D., Garcia-Arostegui, J-L., Cabezas Calvo-Rubio, F., Senent Alonso, M., 2012b. Contribucion de las tecnicas hidroquimicas e isotopicas al estudio del impacto de los cambios de uso del suelo en el funcionamiento del acuifero multicapa del Campo de Cartagena (SE Spain). Oral presentation at the *Congreso internacional sobre uso sostenible del suelo*. Murcia (Spain). February 2012.

Baudron, P., Garcia-Arostegui, J.-L., Barbecot, F., Martinez-Vicente, D., Travi, Y., Leduc, C., Noret, A., 2012c. Multi-isotopic approach to assess groundwater flow pattern in a stressed multi-layer coastal aquifer (Campo de Cartagena, Southeastern Spain). Oral presentation at the *IV International Conference on Technology Seawater Intrusion in Coastal Aquifers (TIAC)*, Alicante (Spain). April 2012.

Baudron, P., Barbecot, F., Garcia-Arostegui, J.L., Martinez-Vicente, D., Noret, A., Travi, T., Leduc, C., 2012d. Assessing groundwater recharge in a complex multi-layer aquifer in transitory conditions. Poster presented at the *21st International Radiocarbon Conference*, Paris (France), July 2012.

Baudron, P., Alonso Sarriá, F., Garcia-Arostegui, J-L., Canovas Garcia, F., Moreno Brotons, J., Martinez Vicente, D., 2013a. Identifying the origin of groundwater samples in a multi-layer aquifer system with Random Forest classification. Under review by Journal of Hydrology.

Baudron, P., Barbecot, F., García-Aróstegui, J.L., Leduc, C., Travi, Y., Martinez-Vicente, D., 2013b. Impacts of human activities on recharge in a multilayered semiarid aquifer (Camp de Cartagena, SE Spain). *Hydrological Processes*. DOI: 10.1002/hyp.9771

Baudron, P., Barbecot, F., Gillon, M., Aróstegui, J.L.G., Travi, Y., Leduc, C., Castillo, F.G., Martinez-Vicente, D., 2013. Assessing Groundwater Residence Time in a Highly Anthropized Unconfined Aquifer Using Bomb Peak 14C and Reconstructed Irrigation Water 3H. *Radiocarbon* **55**, in press.

Baudron, P., Cockenpot, S., Lopez, F., Claude, C., Gilabert, J., Mayer, A., Garcia-Arostegui, J.-L., Radakovitch, O., Leduc, C., 2013d. Combining Radon, Radium and hydrodynamic modeling to assess submarine groundwater discharge from an anthropized semiarid watershed to a Mediterranean lagoon (Mar Menor, SE Spain). In preparation for Estuarine, Coastal and Shelf Science.

Beck, A.J., Rapaglia, J.P., Cochran, J.K., Bokuniewicz, H.J., 2007. Radium mass-balance in Jamaica Bay, NY: Evidence for a substantial flux of submarine groundwater. *Marine Chemistry* **106**, 419–441.

Ben Hamouda, M., Tarhouni, J., Leduc, C., Zouari, K., 2011. Understanding the origin of salinization of the Plio-quaternary eastern coastal aquifer of Cap Bon (Tunisia) using geochemical and isotope investigations. *Environmental Earth Sciences* **63**, 889–901.

Ben Kabbour, B., Zouhri, L., Mania, J., 2005. Overexploitation and continuous drought effects on groundwater yield and marine intrusion: considerations arising from the modelling of Mamora coastal aquifer, Morocco. *Hydrological Processes* **19**, 3765-3782.

Berrocal Caparrós, M.C., Vidal Nieto, M., Andreo Martínez, M.A., 1999. Excavación arqueológica de urgencia en el paraje de El Raal. Las Palas, Fuente Álamo. *Memorias de Arqueología* **9**, 359-386.

Breiman, L., 1994. Bagging predictors. *Department of Statistics, University of California, Berkeley, California Technical Report* **421**, 1-19.

Breiman, L., 2001. Random Forests. *Machine Learning* **45**(1), 5–32.

Breiman, L., Friedman, J.H., Olshen, R.A., Stone, C.J., 1984. Classification and regression trees. Wadsworth and Brooks/Cole, Monterey, California, USA. 368 pp.

Burnett, W.C., Taniguchi, M., Oberdorfer, J., 2001. Measurement and significance of the direct discharge of groundwater into the coastal zone. *Journal of Sea Research* **46**, 109–116.

Burnett, W. C., Cable, J. E., Corbett, D. R., 2003. Radon tracing of submarine groundwater discharge in coastal environments. *In* Land and Marine Hydrogeology, Taniguchi, M., Wang, K., Gamo, T. (Eds.). Elsevier Publications, pp. 25-43.

Cabezas Calvo-Rubio, F., 2009. Balance hídrico del Mar Menor (Murcia), *In* El Mar Menor: Estado Actual Del Conocimiento Científico. *F-IEA Publications*. Murcia, pp. 167–206.

Cable, J.E., Burnett, W.C., Chanton, J.P., Weatherly, G.L., 1996. Estimating groundwater discharge into the northeastern Gulf of Mexico using radon-222. *Earth and Planetary Science Letters* **144**, 591-604.

Cable J.E., Burnett W.C., Chanton J.P., Corbett D.R., Cable P.H., 1997. Field evaluation of seepage meters in the coastal marine environment. *Estuarine Coastal and Shelf Science* **45**, 367–75.

CARM, 2000. Estudio para un plan de gestión de las aguas subterráneas del Campo de Cartagena. Report for the Murcia region. Unpublished.

Celle-Jeanton, H., Huneau, F., Travi, Y., Edmunds, W.M.. 2009. Twenty years of groundwater evolution in the Triassic sandstone aquifer of Lorraine: Impacts on baseline water quality. *Applied Geochemistry* **24**, 1198–1213.

Cloutier, V., Lefebvre, R., Therrien, R., Savard, M.M., 2008. Multivariate statistical analysis of geochemical data as indicative of the hydrogeochemical evolution of groundwater in a sedimentary rock aquifer system. *Journal of Hydrology* **353**, 294–313.

Condesso De Melo, M.T., Carreira Paquete, P.M.M., Marques Da Silva, M.A., 2001. Evolution of the Aveiro Cretaceous aquifer (NW Portugal) during the Late Pleistocene and present day: evidence from chemical and isotopic data. *In* Palaeowaters in coastal Europe:

evolution of groundwater since the last Pleistocene. Geological Society, London, Special publications. pp. 139–154.

Conesa-García, C., 1990. El Campo de Cartagena. Clima e hidrología de un medio semiáárido. Universidad de Murcia, Ayuntamiento de Cartagena. Comunidad de Regantes del Campo de Cartagena. Technical report.

Congalton, R.G., Green, K., 2008. Assessing the Accuracy of Remotely Sensed Data. Principles and Practices. CRC Press. 200 pp.

Corbett, D.R., Burnett, W.C., Cable, P .H., Clark, S.B., 1998. A multiple approach to the determination of radon fluxes from sediments. *Journal of Radioanalytical and Nuclear Chemistry* **236**, 247-252.

Cook, P.G., Herczeg, A.L., 2000. Environmental Tracers in Subsurface Hydrology. Springer.

Corcho Alvarado, J., Barbecot, F., Purtschert, R., 2009. Ambient vertical flow in long-screen wells: a case study in the Fontainebleau Sands Aquifer (France). *Hydrogeology Journal* **17**, 425–431.

Cronin, A.A., Barth, J.A.C., Elliot, T., Kalin, R.M., 2005. Recharge velocity and geochemical evolution for the Permo-Triassic Sherwood Sandstone, Northern Ireland. *Journal of Hydrology* **315**, 308–324.

Cudennec, C., Leduc, C., Koutsoyiannis, D., 2007. Dryland hydrology in Mediterranean regions-a review. *Hydrological Sciences Journal* **52**(6), 1077-1087.

Currell, M.J., Cartwright, I., Bradley, D.C., Han, D., 2010. Recharge history and controls on groundwater quality in the Yuncheng Basin, north China. *Journal of Hydrology* **385**, 216–229.

Cutler, A., Stevens, R.J., 2006. Random forests for microarrays. *Methods in Enzymology* **411**, 422–432.

Cutler, D.., Edwards, T.C., Beard, K.H., Cutler, A., Hess, K.T., Gibson, J., Lawler, J.J., 2007. Random Forest for Classification in Ecology. *Ecology* **88**(11), 2783–2792.

Dahan, O., McGraw, D., Adar, E., Pohll, G., Bohm, B., Thomas, J., 2004. Multi-variable mixing cell model as a calibration and validation tool for hydrogeologic groundwater modeling. *Journal of Hydrology* **293**, 115–136.

Daughney, C., Raiber, M., Moreau-Fournier, M., Morgenstern, U., van der Raaij, R., 2012. Use of hierarchical cluster analysis to assess the representativeness of a baseline groundwater quality monitoring network: comparison of New Zealand's national and regional groundwater monitoring programs. *Hydrogeology Journal* **20**, 185–200.

De'ath, G., Fabricius, K., 2000. Classification and regression trees: a powerful yet simple techn ique for ecological data analysis. *Ecology* **81**, 3178-3192.

Debreu, L., Marchesiello, P., Penven, P., Cambon, G., 2012. Two-way nesting in split-explicit ocean models: Algorithms, implementation and validation. *Ocean Model* **49-50**, 1–21.

DePablo SanMartin, M.A., 2008. Vigilancia radiológica del agua (I). *Ingeniería Civil* **152**, 77–83.

Diaz-Teijeiro, M.F., Rodríguez-Arévalo, J., Castaño, S., 2009. La Red Española de Vigilancia de Isótopos en la Precipitación (REVIP): distribución isotópica espacial y aportación al conocimiento del ciclo hidrológico. *Ingeniería Civil* **155**, 87–97.

Dulaiova, H., Peterson, R., Burnett, W.C., Lane-Smith, D., 2005. A multi-detector continuous monitor for assessment of 222Rn in the coastal ocean. *Journal of Radioanalytical and Nuclear Chemistry* **263**(2), 361-365.

Dulaiova, H., Gonneea, M.E., Henderson, P.B. and Charette, M.A., 2008. Geochemical and physical sources of radon variation in a subterranean estuary - Implications for groundwater radon activities in submarine groundwater discharge studies. *Marine Chemistry* **110**(1-2), 120-127.

Dupuy de Lome, E., Gorostízaga, J. y Novo y Chicarro, P., 1917. Informe del Instituto Geológico sobre alumbramientos de aguas subterráneas por cuenta del estado. *Boletín Oficial de Minas y Metalurgia* **1917**, 55-68.

Efron, B., Tibshirani, R., 1997. Improvements on Cross-Validation: The 632+ Bootstrap Method. *Journal of the American Statistical Association* **92**, 548–560.

Elçi, A., Flach, G.P., Molz, F.J., 2003. Detrimental effects of natural vertical head gradients on chemical and water level measurements in observation wells: identification and control. *Journal of Hydrology* **281**, 70–81.

Favreau, G., Leduc, C., Marlin, C., Dray, M., Taupin, J.-D., Massault, M., Le Gal La Salle, C., Babic, M., 2002. Estimate of Recharge of a Rising Water Table in Semiarid Niger from 3H and 14C Modeling. *Ground Water* **40**, 144–151.

Fernández, M., Torné, M., Zeyen, H., 1990. Modelling of thermal anomalies in the NW border of the Valencia Trough by groundwater convection. *Geophysical Research Letters* **17**, 105-108.

Fernández-Chacón, F., Benavente, J., Rubio-Campos, J.C., Kohfahl, C., Jiménez, J., Meyer, H., Hubberten, H., Pekdeger, A., 2010. Isotopic composition (δ18O and δD) of precipitation and groundwater in a semi-arid, mountainous area (Guadiana Menor basin, Southeast Spain). *Hydrological Processes* **24**, 1343–1356.

Ferrarin, C., Rapaglia, J., Zaggia, L., Umgiesser, G., Zuppi, G.M., 2008. Coincident application of a mass balance of radium and a hydrodynamic model for the seasonal quantification of groundwater flux into the Venice Lagoon, Italy. *Marine Chemistry* **112**, 179–188.

Fontes, J.C. 1992. Chemical and isotopic constraints on 14C dating of groundwater. *In* Radiocarbon after four decades, Taylor E.D., Long A., and Kra R.S. (Eds). Springer-Verlag; pp. 242–261.

Galego Fernandes, P., Carreira, P.M., 2008. Isotopic evidence of aquifer recharge during the last Ice age in Portugal. *Journal of Hydrology* **361**, 291–308.

García-Aróstegui, J.L., Jiménez-Martinez, J., Baudron, P., Martinez-Vicente, D., M., Guerra, J., 2012. Geometría del Campo de Cartagena e implicaciones en el funcionamiento hidrogeológico. *In* Nuevas Aportaciones Al Conocimiento De Los Acuíferos Costeros, Serie Hidrogeología y Aguas Subterráneas. Instituto Geologico y Minero de España, Madrid, Vol. I, pp. 439–449.

García-Pintado, J., Martínez-Mena, M., Barberá, G.G., Albaladejo, J., Castillo, V.M., 2007. Anthropogenic nutrient sources and loads from a Mediterranean catchment into a coastal lagoon: Mar Menor, Spain. *Science of the Total Environment* **373**, 220–239.

Garcia-Solsona, E., Masqué, P., Garcia-Orellana, J., Rapaglia, J., Beck, A. J., Cochran, J.K., Bokuniewicz, H.J., Zaggia, L., Collavini, F., 2008. Estimating submarine groundwater discharge in the Isola La Cura, northern Venice Lagoon (Italy), by using the radium quartet. *Marine Chemistry* **109**, 292–306.

Garcia-Solsona, E., Garcia-Orellana, J., Masqué, P., Garcés, E., Radakovitch, O., Mayer, A., Estradé, S., Basterretxea, G., 2010. An assessment of karstic submarine groundwater and associated nutrient discharge to a Mediterranean coastal area (Balearic Islands, Spain) using radium isotopes. *Biogeochemistry* **97**, 211–229.

Gassama, N., Dia, A., Violette, S., 2012. Origin of salinity in a multilayered aquifer with high salinization vulnerability. *Hydrological Processes* **26**, 168–188.

Gattacceca, J.C., Mayer, A., Cucco, A., Claude, C., Radakovitch, O., Vallet-Coulomb, C., Hamelin, B., 2011. Submarine groundwater discharge in a subsiding coastal lowland: A 226Ra and 222Rn investigation in the Southern Venice lagoon. *Applied Geochemistry* **26**, 907–920.

Ghimire, B., Rogan, J., Miller, J., 2010. Contextual land-cover classification: incorporating spatial dependence in land-cover classification models using random forests and the Getis statistic. *Remote Sensing Letters* **1**(1), 45–54.

Gilabert J, 2008. Modelado hidrodinámico del Mar Menor. Aproximación al cálculo de la tasa de renovación de la laguna. Scientific report for the Foundation Instituto Euromediterraneo del Agua, Murcia.

Gillon, M., Barbecot, F., Gibert, E., Corcho Alvarado, J.A., Marlin, C., Massault, M., 2009. Open to closed system transition traced through the TDIC isotopic signature at the aquifer recharge stage, implications for groundwater 14C dating. *Geochimica et Cosmochimica Acta* **73**, 6488–6501.

Gillon, M., Renard, F., Crancon, P., Aupiais, J., 2012. Kinetics of incongruent dissolution of carbonates in a Chalk aquifer using reverse flow modelling. *Journal of Hydrology* **420**, 329–339.

Gislason, P.O., Benediktsson, L.A., Sveinsson, J.R., 2006. Random Forests for land cover classication. *Pattern Recognition Letters* **27**, 294–300.

Gómez, J.M., Castejón, G., Zubillaga, E.G., 2012. Un modelo de captación y conducción de aguas en medios semiáridos: El Canal del Sifón en Fuente Álamo de Murcia. *In* Proceedings of the International Conference "Patrimonio hidráulico y cultura del agua en el Mediterráneo". *Fundación Séneca. Murcia*. pp. 227-248.

Gosnold, W.D., Todhunter, P.E., Schmidt, W., 1997. The borehole temperature record of climate warming in the mid-continent of North America. *Global and Planetary Change* **15**, 33–45.

Guardiola, F., 1927. Estudio metalogenético de la Sierra de Cartagena. *Memorias del Instituto Geológico de España,* **33**. 331 pp.

Guhimre, B., Rogan, J., Miller, J., 2010. Contextual land-cover classification: incorporating spatial dependence in land-cover classification models using random forests and the Getis statistic. *Remote Sensing Letters* **1**(1), 45–54.

Guler C., Kurt M.A., Alpaslan M., Akbulut C., 2012. Assessment of the impact of anthropogenic activities on the groundwater hydrology and chemistry in Tarsus coastal plain (Mersin, SE Turkey) using fuzzy clustering, multivariate statistics and GIS techniques. *Journal of Hydrology* **414**, 435–451

Hastie, T., Tibshirani, R., Friedman, J., 2003. The Elements of Statistical Learning: Data Mining, Inference, and Prediction. Springer.

Herczeg, A., Leaney, F., 2011. Review: Environmental tracers in arid-zone hydrology. *Hydrogeology Journal* **19**, 17–29.

Horst A., Mahlknecht J., Merkel B., Aravena R., Ramos-Arroyo Y., 2008. Evaluation of the recharge processes and impacts of irrigation on groundwater using CFCs and

radiogenic isotopes in the Silao-Romita basin, Mexico. *Hydrogeology Journal* **16**, 1601–1614.

Hughes, G.F., 1968. On The Mean Accuracy Of Statistical Pattern Recognizers. *IEEE Transactions on Information Theory* **14**(1), 55–63.

Huneau F., Blavoux B., Bellion Y., 2001. Différence entre vitesses hydrauliques et vitesses radiométriques des eaux d'un réservoir profond : proposition d'explication pour l'aquifère miocène du bassin de Valréas (Sud-Est de la France). *Comptes Rendus de l'Académie des Sciences - Series IIA - Earth and Planetary Science* **333**, 163–170.

IEA Fundation, 2011. Modelacion hidrologica en zonas semiaridas - Subproject Modelizacion Hidrogeologica. Final report. Fundación Instituto Euromediterráneo del Agua, Murcia. 470 pp.

Iglesias, A., Garrote, L., Flores, F., Moneo, M., 2007. Challenges to manage the risk of water scarcity and climate change in the Mediterranean. *Water Resources Management* **21**, 775–788.

IGME, 1982. Investigación geotérmica en el Campo de Cartagena. IGME, Technical report (unpublished).

IGME, 1990. Mapa Geológico de la plataforma continental española y zonas adyacentes a escala 1:200.000 Hojas 79-79E. Murcia.

IGME, 1994. Las aguas subterráneas del Campo de Cartagena (Murcia). IGME, Madrid, Spain, 62 pp.

IGME, 2005. Estudio de la información geológica y geofísica del subsuelo (sísmica de reflexión y sondeos) en el sector SE de la Provincia de Murcia. Consejería de Industria y Medio Ambiente de la Región de Murcia, IGME Murcia, Technical report (unpublished).

IGME-IRYDA, 1978. Plan Nacional de Investigación de aguas subterráneas. Investigación hidrogeológica de la cuenca baja del Segura. Tomos 8 y 9: Campo de Cartagena. Technical report (unpublished).

INC, 1962. Informes de sondeos del INC-IRYDA en España. IGME, Technical report (unpublished).

ITGE, 1989. Geometría de los acuíferos del Campo de Cartagena (Murcia). IGME, Technical report (unpublished).

Israelsen, O.W., Reeve, R.C., 1944. Canal lining experiments in the delta area, Utah. *UAES Bulletin Paper* **313**. 52 pp.

Jiménez-Martínez, J., Skaggs, T.H., van Genuchten, M.T., Candela, L., 2009. A root zone modelling approach to estimating groundwater recharge from irrigated areas. *Journal of Hydrology* **367**, 138–149.

Jiménez-Martínez, J., Candela, L., Molinero, J., Tamoh, K., 2010. Groundwater recharge in irrigated semi-arid areas: quantitative hydrological modelling and sensitivity analysis. *Hydrogeology Journal* **18**, 1811–1824.

Jiménez-Martínez, J., Aravena, R., Candela, L., 2011. The role of leaky boreholes in the contamination of a regional confined aquifer. A case study: the Campo de Cartagena region, Spain. *Water Air and Soil Pollution* **215**, 311–327.

Jiménez-Martinez, J., Candela, L., García-Aróstegui, J.L., Aragón R., 2012. A 3D geological model of Campo de Cartagena, SE Spain: Hydrogeological implications. *Geologica Acta* **10**, 49–62.

Jiráková, H., Huneau, F., Celle-Jeanton, H., Hrkal, Z., Le Coustumer, P., 2009. Palaeorecharge conditions of the deep aquifers of the Northern Aquitaine region (France). *Journal of Hydrology* **368**, 1–16.

Jirakova, H., Huneau, F., Celle-Jeanton, H., Hrkal, Z., Le Coustumer, P., 2011. Insights into palaeorecharge conditions for European deep aquifers. *Hydrogeology Journal* **19**, 1545–1562.

Klaus, J., Külls, C., Dahan, O., 2008. Evaluating the recharge mechanism of the Lower Kuiseb Dune area using mixing cell modeling and residence time data. *Journal of Hydrology* **358**, 304–316.

Klepikova, M.V., Le Borgne, T., Bour, O., Davy, P., 2011. A methodology for using borehole temperature-depth profiles under ambient, single and cross-borehole pumping conditions to estimate fracture hydraulic properties. *Journal of Hydrology* **407**, 145–152.

Kloppmann, W., Van Houtte, E., Picot, G., Vandenbohede, A., Lebbe, L., Guerrot, C., Millot, R., Gaus, I., Wintgens, T., 2008. Monitoring Reverse Osmosis Treated Wastewater Recharge into a Coastal Aquifer by Environmental Isotopes (B, Li, O, H). *Environmental Science and Technology* **42**, 8759–8765.

Kundzewicz, Z. W., Mata, L. J., Arnell, N. W., Döll, P., Kabat, P., Jiménez, B., Miller, K. A., Oki, T., Sen, Z., Shiklomanov, 2007. Freshwater resources and their management. *In* Climate Change 2007: Impacts, Adaptation and Vulnerability. Contribution of Working Group II to the Fourth Assessment Report of the Intergovernmental Panel on Climate Change M. L. Parry, O. F. Canziani, J. P. Palutikof, P. J. van der Linden & C. E. Hanson (Eds), Cambridge University Press, Cambridge, UK, pp. 173–210.

Kurtulus, B., Razack, M., 2007. Evaluation of the ability of an artificial neural network model to simulate the input-output responses of a large karstic aquifer: the La Rochefoucauld aquifer (Charente, France). *Hydrogeology Journal* **15**, 241–254.

Lacombe, S., Sudicky, E.A., Frape, S.K., Unger, A.J.A., 1995. Influence of Leaky Boreholes on Cross-Formational Groundwater Flow and Contaminant Transport. *Water Resources Research* **31**, 1871.

Lambrakis, N., Antonakos, A., Panagopoulos, G., 2004. The use of multi-component statistical analysis in hydrogeological environmental research. *Water Research* **38**, 1862–1872.

Le Gal La Salle, C., Marlin, C., Savoye, S., Fontes, J.C., 1996. Geochemistry and 14C dating of groundwaters from Jurassic aquifers of North Aquitaine Basin (France). *Applied Geochemistry* **11**, 433–445.

Le Gal La Salle, C., Marlin, C., Leduc, C., Taupin, J.D., Massault, M., Favreau, G., 2001. Renewal rate estimation of groundwater based on radioactive tracers (3H, 14C) in an unconfined aquifer in a semi-arid area, Iullemeden Basin, Niger. *Journal of Hydrology* **254**, 145–156.

Leduc C., Favreau G., Schroeter P., 2001. Long-term rise in a Sahelian water-table: the Continental Terminal in South-West Niger. *Journal of Hydrology* **243**, 43–54.

Lempitsky, V., Verhoek, M., Noble, J.A., Blake, A., 2009. Random Forest Classification for Automatic Delineation of Myocardium in Real-Time 3D Echocardiography, *In* Functional Imaging and Modeling of the Heart, Lecture Notes in Computer Science. Ayache, N., Delingette, H., Sermesant, M. (Eds.),. Springer Berlin Heidelberg, pp. 447–456.

Levin I., Kromer B., 2004. The tropospheric $^{14}CO2$ level in mid-latitudes of the Northern Hemisphere (1959-2003). *Radiocarbon* **46**, 1261–1272.

Li, L., Barry, D.A., Stagnitti, F., Parlange, J.-Y., 1999. Submarine groundwater discharge and associated chemical input to a coastal sea. *Water Resources Research* **35**, 3253–3259.

Liaw, A., Wiener, M., 2002. Classication and regression by Random Forest. *R News* **2**(3), 18–22.

Lillo Carpio, M., 1978. Geomorfología litoral del Mar Menor. *Universidad de Murcia. Papeles del Departamento de Geografía* **8**, 9–48.

Liu, S.M., Li, R.H., Zhang, G.L., Wang, D.R., Du, J.Z., Herbeck, L.S., Zhang, J., Ren, J.L., 2011. The impact of anthropogenic: activities on nutrient dynamics in the tropical Wenchanghe and Wenjiaohe Estuary and Lagoon system in East Hainan, China. *Marine Chemistry* **125**, 49–68.

Loos, M., Elsenbeer, H., 2011. Topographic controls on overland flow generation in a forest – An ensemble tree approach. *Journal of Hydrology* **409**, 94–103.

Loosli, H.H., Aeschbach-Hertig W., Barbecot F., Blaser P., Darling W.G., Dever L., Edmunds W.M., Kipfer R., Purtschert R., Walraevens K., 2001. Isotopic methods and their hydrogeochemical context in the investigation of palaeowaters. *Geological Society, London, Special Publications* **189**, 193 –212.

Lorenzen, G., Sprenger, C., Baudron, P., Gupta, D., Pekdeger, A., 2012. Origin and dynamics of groundwater salinity in the alluvial plains of western Delhi and adjacent territories of Haryana State, India. *Hydrological Processes* **26**, 2333–2345.

Ma, R., Zheng, C., Tonkin, M., Zachara, J.M., 2011. Importance of considering intraborehole flow in solute transport modeling under highly dynamic flow conditions. *Journal of Contaminant Hydrology* **123**, 11–19.

Manzano, M., Custodio, E., Loosli, H.H., Cabrera, M.C., Riera, X., Custodio, J., 2001. Palaeowater in coastal aquifers of Spain. *In* Palaeowaters in coastal Europe: evolution of groundwater since the last Pleistocene. *Geological Society, London. Special publications* **189,** 107–138.

Margat, J., Vallée, D., 2000. Water Resources and Uses in the Mediterranean Countries: Figures and Facts. Blue Plan for the Mediterranean. Regional Activity Centre, Sophia-Antipolis, France, 224 pp.

Margat, J., Treyer, S., 2004. L'eau des Méditerranéens: situation et perspectives. PNUE-PAM. Plan Bleu, Technical Report Series no. 158, Athens, Greece.

Marín, A., 1925. Informe acerca de la ejecución de sondeos artesianos del Campo de Cartagena. IGME. Technical report, unpublished.

Martens, C., Kipphut, G., Klump, J., 1980. Sediment-water chemical exchange in the coastal zone traced by in situ radon-222 flux measurements. *Science* **208**, 285-288.

Martin-Hayden, J.M., 2005. Controlled laboratory investigations of wellbore concentration response to pumping. *Groundwater* **38**, 121–128.

Martínez-Alvarez, V., Gallego-Elvira, B., Maestre-Valero, J.F., Tanguy, M., 2011. Simultaneous solution for water, heat and salt balances in a Mediterranean coastal lagoon (Mar Menor, Spain). *Estuarine, Coastal and Shelf Science* **91**, 250–261.

Mayo, A., 2010. Ambient well-bore mixing, aquifer cross-contamination, pumping stress, and water quality from long-screened wells: What is sampled and what is not? *Hydrogeology Journal* **18**, 823–837.

Mesa y Ramos, J., 1909. Pozos artesianos. Tordesillas, Madrid, 238 pp.

Michael, H.A., Lubetsky, J.S., Harvey, C.F., 2003. Characterizing submarine groundwater discharge: A seepage meter study in Waquoit Bay, Massachusetts. *Geophysical Research Letters* **30**, 1297.

Mitchell, M., 2011. Bias of Random Forest Out-of-Bag (OOB) Error for Certain Input Parameters. *Open Journal of Statistics* **1**, 205–211.

Molina, L., Vallejos, A., Pulido-Bosch, A., Sánchez-Martos, F., 2002. Water temperature and conductivity variability as indicators of groundwater behaviour in complex aquifer systems in the south-east of Spain. *Hydrological Processes* **16**, 3365–3378.

Molina, J.L., García-Aróstegui, J.L., Bromley, J., Benavente, J., 2011. Integrated Assessment of the European WFD Implementation in Extremely Overexploited Aquifers Through Participatory Modelling. *Water Resources Management* **25**, 3343–3370.

Moore, W.S., 1996. Large groundwater inputs to coastal waters revealed by 226Ra enrichments. *Nature* **380**, 612–614.

Moore, W.S., Arnold, R., 1996. Measurement of 223Ra and 224Ra in coastal waters using a delayed coincidence counter. *Journal of Geophysical Research* **101**, 1321–1329.

Moore, W.S., 2008. Fifteen years experience in measuring 224Ra and 223Ra by delayed-coincidence counting. *Marine Chemistry* **109**, 188–197.

Moore, W.S., Beck, M., Riedel, T., Rutgers van der Loeff, M., Dellwig, O., Shaw, T.J., Schetger, B., Brumsack, H.-J. 2011. Radium-based pore water fluxes of silica, alkalinity, manganese, DOC, and uranium : A decade of studies in the German Wadden Sea. *Geochimica and Cosmochimica Acta* **75**, 6535-6555.

Mulligan, A.E., Charette, M.A., 2006. Intercomparison of submarine groundwater discharge estimates from a sandy unconfined aquifer. *Journal of Hydrology* **327**, 411–425.

Oberdorfer, J.A., Valentino, M.A., Smith, S.V., 1990. Groundwater contribution to the nutrient budget of Tomales Bay, California. *Biogeochemistry* **10**, 199–216.

Olson, J.R., Hawkins, C.P., 2012. Predicting natural base-flow stream water chemistry in the western United States. *Water Resources Research*. **48**. DOI: 10.1029/2011WR011088

Pal, M., 2005. Random forest classifier for remote sensing classification. *International Journal of Remote Sensing* **26**, 217–222.

Pehme, P.E., Parker, B.L., Cherry, J.A., Greenhouse, J.P., 2010. Improved Resolution of Ambient Flow through Fractured Rock with Temperature Logs. *Ground Water* **48**, 191–205.

Peng, T.H., Takahashi, T., Broecker, W., 1974. Surface radon measurements in the north Pacific station Papa. *Journal of Geophysical Research* **79**, 1772-1780.

Peñuelas, L., 1851. Sobre los pozos artesianos en la provincia de Murcia. *Revista Minera* **2**, 717-724.

Pérez-Ruzafa, A., Fernández, A.I., Marcos, C., Gilabert, J., Quispe J.I., García-Charton J.A., 2005. Spatial and temporal variations of hydrological conditions, nutrients and chlorophyll α in a Mediterranean coastal lagoon (Mar Menor, Spain). *Hydrobiologia* **550**, 11–27.

Perni, A., Martínez-Carrasco, F., Martínez-Paz, J.M., 2011. Economic valuation of coastal lagoon environmental restoration: Mar Menor (SE Spain). *Ciencias marinas* **37**, 175–190.

Peters, J., Baets, B.D., Samson, R., Verhoest, N.E.C., 2008. Modelling groundwater-dependent vegetation patterns using ensemble learning. *Hydrological Earth Systems Science* **12**, 603–613.

Prasad, A.M., Iverson, L.R., Liaw, A., 2006. Newer classification and regression tree techniques: bagging and random forests for ecological prediction. *Ecosystems* **9**, 181–199.

Prieto, C., Destouni, G., 2005. Quantifying hydrological and tidal influences on groundwater discharges into coastal waters. *Water Resources Research* **41**. W12427.1-W12427.12.

Pulido-Bosch, A., Bensi, S., Molina, L., Vallejos, A., Calaforra, J.M., Pulido-Leboeuf P., 2000. Nitrates as indicators of aquifer interconnection. Application to the Campo de Dalias (SE - Spain). *Environmental Geology* **39**, 791–799.

Pulido-Bosch, A., Delgado, J., Sola, F., Vallejos, A., Vicente, F., Lopez-Sanchez, J.M., Mallorqui, J.J., 2012. Identification of potential subsidence related to pumping in the Almeria basin (SE Spain). *Hydrological Processes* **26**, 731–740.

Qin, D., Qian, Y., Han, L., Wang, Z., Li, C., Zhao, Z., 2011. Assessing impact of irrigation water on groundwater recharge and quality in arid environment using CFCs, tritium and stable isotopes, in the Zhangye Basin, Northwest China. *Journal of Hydrology* **405**, 194–208.

R Development Core Team, 2010. R: A language and environment for statistical computing. R Foundation for Statistical Computing, Vienna, Austria. ISBN 3-900051-07-0.

Ramos, G., 2003. Posibilidades de aplicación de la inyección mediante sondeos profundos a la gestión de salmuera de rechazo de plantas desaladoras en España. PhD thesis. Polytechnical University of Madrid, 352 p.

Ramos, G., Sánchez, J., 2003. Estructura geológica profunda "Murcia Sur-I". Definición geológica, geométrica y confinamiento. In Tecnología de la Intrusión de Agua de mar en Acuíferos Costeros (TIAC'03). López Geta, J.A., de la Orden, J.A., de Dios Gómez, J., Ramos, G., Mejías, M., Rodríguez, L. (Eds.). IGME, Madrid, pp. 691-700.

Rapaglia, J., Ferrarin, C., Zaggia, L., Moore, W.S., Umgiesser, G., Garcia-Solsona, E., Garcia-Orellana, J., Masque, P., 2010. Investigation of residence time and groundwater flux in Venice Lagoon: comparing radium isotope and hydrodynamical models. *Journal of Environmental Radioactivity* **101**, 571–581.

Rey, J., Martínez, J., Barberá, G.G., García-Aróstegui, J.L., García-Pintado, J., Martínez-Vicente, D., 2013 Geophysical characterization of the complex dynamics of groundwater and seawater exchange in a highly stressed aquifer system linked to a coastal lagoon (SE Spain). *Environmental Earth Science*. In press. DOI: 10.1007/s12665-013-2472-2

Robinson, C., Li, L., Barry, D.A., 2007. Effect of tidal forcing on a subterranean estuary. *Advances in Water Resources* **30**, 851–865.

Rodriguez Estrella, T., 2004. Decisive influence of neotectonics of the water connection between the Mediterranean Sea, Mar Menor and the Campo de Cartagena aquifers (South-East of Spain). *In* Groundwater and saline intrusion: selected papers from the 18th Salt Water Intrusion Meeting, *18 SWIM*, Cartagena (Spain). IGME. Madrid.

Román, C., 1996. Uso y explotación de la tierra en la comarca del Campo de Cartagena (siglos XIX y XX). MAPA (Ed.), Madrid, 587 p.

Rosenzweig, C., Casassa, G., Karoly, D.J., Imeson, A., Liu, C., Menzel, A., Rawlins, S., Root, T.L., Seguin, B., Tryjanowski, P., 2007. Assessment of observed changes and responses in natural and managed systems. *In* Climate Change 2007: Impacts, Adaptation and Vulnerability. Contribution of Working Group II to the Fourth Assessment Report of the Intergovernmental Panel on Climate Change. M. L. Parry, O. F. Canziani, J. P. Palutikof, P. J. van der Linden & C. E. Hanson (Eds), Cambridge University Press, Cambridge, UK. pp. 79–131.

Rubio, J. M., 1928. La cuenca artesiana del Campo de Cartagena. *Revista Minera, Metalúrgica y de Ingeniería*, **LXXIX**: 229-231, 433-444 y 457-460.

Ruzafa, A. 1998. Estudio ecológico y bionomico de los poblamientos bentónicos del Mar Menor (Murcia, SE de España). PhD thesis. University of Murcia.

Santos, I.R., Burnett, W.C., Dittmar, T., Suryaputra, I.G.N.A., Chanton, J., 2009a. Tidal pumping drives nutrient and dissolved organic matter dynamics in a Gulf of Mexico subterranean estuary. *Geochimica and Cosmochimica Acta* **73**, 1325–1339.

Santos, I.R., Dimova, N., Peterson, R.N., Mwashote, B., Chanton, J., Burnett, W.C., 2009b. Extended time series measurements of submarine groundwater discharge tracers (222Rn and CH4) at a coastal site in Florida. *Marine Chemistry* **113**, 137–147.

Santos, I.R., Burnett, W.C., Chanton, J., Dimova, N., Peterson, R.N., 2009c. Land or ocean? Assessing the driving forces of submarine groundwater discharge at a coastal site in the Gulf of Mexico. *Journal of Geophysical Research* **114**, C04012.

Santos, I.R., Eyre, B.D., Huettel, M., 2012. The driving forces of pore water and groundwater flow in permeable coastal sediments: A review. *Estuarine, Coastal and Shelf Science* **98**, 1–15.

Scanlon, B.R., Keese, K.E., Flint, A.L., Flint, L.E., Gaye, C.B., Edmunds, W.M., Simmers, I., 2006. Global synthesis of groundwater recharge in semiarid and arid regions. *Hydrological Processes* **20**, 3335–3370.

Scholten, J.C., Pham, M.K., Blinova, O., Charrette, M.A., Dulaiova, H., Eriksson, M., 2010. Preparation of Mn-fiber standards for the efficiency calibration of the delayed coincidence counting system (RaDeCC). *Marine Chemistry* **121**, 206-214.

Schubert, M., Paschke, A., Lieberman, E., Burnett, W.C., 2012. Air-Water Partitioning of 222Rn and its Dependence on Water Temperature and Salinity. *Environmental Science and Technology* **46**, 3905-3911.

Senent Alonso, M., Martinez-Vicente, D., Cabezas Calvo-Rubio, F., García-Aróstegui, J.L., Baudron, P., 2009. Aproximación mediante modelización matemática a la evaluación de las descargas del acuífero cuaternario del Campo de Cartagena al Mar Menor (Murcia), in: El Mar Menor: Estado Actual Del Conocimiento Científico. Murcia, pp. 109–130.

Servat, E., Najem, W., Leduc, C., Shakeel, A., 2003. Hydrology of Mediterranean and Semiarid Regions. *IAHS Publications* **278**.

Simonneau, J. 1973. Mar Menor. Evolution sédimentologique et géochimique récente du remplissage. PhD thesis. Paul Sabatier University. Toulouse.

Smith, A.J., Turner, J.V., 2001. Density-dependent surface water-groundwater interaction and nutrient discharge in the Swan-Canning Estuary. *Hydrological Processes* **15**, 2595 – 2616.

Smith, A.J., 2004. Mixed convection and density-dependent seawater circulation in coastal aquifers. *Water Resources Research* **40**, W08309.

Smith, A., Sterba-Boatwright, B., Mott, J., 2010. Novel application of a statistical technique, Random Forests, in a bacterial source tracking study. *Water Research* **44**, 4067–4076.

Stadler. S., Osenbrück; K., Knöller; K., Suckow, A., Sültenfuß, J., Oster, H., Himmelsbach, T., Hötzl, H., 2008. Understanding the origin and fate of nitrate in groundwater of semi-arid environments. *Journal of Arid Environments* **72**, 1830–1842.

Stieglitz, T. 2005. Submarine groundwater discharge into the near-shore zone of the Great Barrier Reef, Australia. *Marine Pollution Bulletin* **51**, 51-59.

Stieglitz, T.C., Cook, P.G., Burnett, W.C., 2010. Inferring coastal processes from regional-scale mapping of 222Radon and salinity: examples from the Great Barrier Reef, Australia. *Journal of Environmental Radioactivity* **101**, 544-552.

Sun, Y., Torgersen, T., 1998. The effects of water content and Mn-fiber surface conditions on 224Ra measurement by 220Rn emanation. *Marine Chemistry* **62**, 299–306.

Svetnik, V., Liaw, A., Tong, C., Wang, T., 2004. Application of Breiman's Random Forest to Modeling Structure-Activity Relationships of Pharmaceutical Molecules. *In* Multiple Classifier Systems, Lecture Notes in Computer Science. Roli, F., Kittler, J., Windeatt, T. (Eds.), Springer Berlin Heidelberg, pp. 334–343.

Taniguchi, M., Iwakawa, H., 2004. Submarine groundwater discharge in Osaka Bay, Japan. *Limnology* **5**, 25–32.

Taniguchi, M., Ishitobi, T., Shimada, J., 2006. Dynamics of submarine groundwater discharge and freshwater-seawater interface. *Journal of Geophysical Research* **111**, C01008.

Therneau, T.M., Atkinson, B.R. port by Ripley, B. (2008). rpart: Recursive Partitioning. R package version 3.1 -41. Software package available at http://mayoresearch.mayo.edu/mayo/research/biostat/splusfunctions.cfm

Trigueros, E., Navarro-Alvargonzales, A., Núñez, V. y García de la Barrera, A., 1962. Estudio hidrogeológico de la Provincia de Murcia. IGME, Technical report (unpublished).

Turner, S.M., Malin, G., Nightingale, P.D., Liss, P.S., 1996. Seasonal variation of dimethyl sulphide in the North Sea and an assessment of fluxes to the atmosphere. *Marine Chemistry* **54**, 245-262.

Ullman, W., Aller, R., 1981. Diffusion coefficients in nearshore marine sediments. *Limnology and Oceanography* **27**, 552-556.

Valder, J.F., Long, A.J., Davis, A.D., Kenner, S.J., 2012. Multivariate statistical approach to estimate mixing proportions for unknown end members. *Journal of Hydrology* **460–461**, 65–76.

Vaselli, O., Buccianti, A., Siena, C.D., Bini, C., Coradossi,N., Angelone,M, 1997. Geochemical characterization of ophiolitic soils in a temperate climate: a multivariate statistical approach. *Geoderma* **75**, 117-133.

Vengosh, A., Kloppmann, W., Marei, A., Livshitz, Y., Gutierrez, A., Banna, M., Guerrot, C., Pankratov, I., Raanan, H., 2005. Sources of salinity and boron in the Gaza strip: Natural contaminant flow in the southern Mediterranean coastal aquifer. *Water Resources Research* **41**. 1- 19

Vías, J.M., Draoui, M., Andreo, B., Maate, A., Stitou, J., Carrasco, F., Perles, M.J., 2007. Vulnerability mapping in two coastal detrital aquifers in South Spain and North Morocco. *In* Groundwater Vulnerability Assessment and Mapping: Selected Papers from the Groundwater Vulnerability Assessment and Mapping International Conference: Ustrón, Poland, 2004, 11. Taylor & Francis. pp. 166-175.

Weinstein, Y., Burnett, W.C., Swarzenski, P.W., Shalem, Y., Yechieli, Y., Herut, B., 2007. Role of aquifer heterogeneity in fresh groundwater discharge and seawater recycling: An example from the Carmel coast, Israel. *Journal of Geophysical Research* **112**, C12016.

Villasante, F., 1913. Criaderos de hierro en España, Tomo I, Criaderos de la Provincia de Murcia. Memorias del Instituto Geológico de España, Madrid, 26, 316 pp.